GFZ
POTSDAM
Helmholtz-Gemeinschaft

TRACE Tree Rings in Archaeology, Climatology and Ecology

Edited by:
Didzis Elferts
Guntis Brumelis
Holger Gärtner
Gerd Helle
Gerhard Schleser

Proceedings of the DENDROSYMPOSIUM 2007
May 3rd – 6th 2007, Riga, Latvia

Scientific Technical Report STR08/05

DOI:10.2312/GFZ.b103-08056

Preface

This volume contains extended abstracts from talks and posters presented at the sixth TRACE (Tree Rings in Archaeology, Climatology and Ecology) conference, held in Riga (Latvia) May 3rd – 6th, 2007. The annual TRACE conference seeks to strengthen the network and scientific exchange between scientists and students involved in the study of tree rings. This annual conference is an initiative of the 'Association for Tree-Ring Research' (ATR). A high scientific level was maintained at the conference as at previous TRACE conferences, but simultaneously an informal forum was provided for young scientists and students to discuss concepts and ongoing or completed projects.

The conference was organized by the Latvian Dendroecologist Society and Faculty of Biology, University of Latvia. There were more than 80 participants at the conference from Australia, Austria, Belgium, Chile, Czech Republic, Estonia, Finland, France, Germany, Latvia, Lithuania, Poland, Romania, Slovenia, Spain, Sweden, Switzerland, and the United Kingdom. Outstanding oral and poster presentations were given by participants. In total, 36 talks were presented, covering the fields of Archaeology (5), Climatology (9), Ecology (7), Geomorphology (3), Isotopes (6), Methods (1), and Wood anatomy (5). In addition, 39 posters were displayed to the audience.

Two talks were given by invited speakers. Dr. Alar Läänelaid (University of Tartu, Estonia) presented an overview of dendrochronological studies in the three Baltic countries (Estonia, Latvia, Lithuania) to introduce the audience to the region, including ongoing and finished work as well as future perspectives for dendrochronological studies in the area. Dr. Hans Linderholm (Göteborg University, Sweden) presented a Summer North Atlantic Oscillation variability reconstruction over the last five centuries.

The editors of TRACE proceedings 2007 are delighted to present 25 short papers of tree-ring studies that were presented during the conference. We would like to thank the reviewers for their valuable comments on the first versions of these manuscripts. The organisers of the conference would like to thank sponsors (Administration of Latvian Environmental Protection Fund, State Stock Company „Latvia's State Forests", Regent Instruments Inc.), whose contribution helped support the conference. Appreciation is also given to all participants for their valuable work, discussions, and exchange of ideas.

Didzis Elferts
Guntis Brumelis
Holger Gärtner
Gerhard Schleser

DOI:10.2312/GFZ.b103-08056

CONTENTS

SECTION 1 CLIMATOLOGY

SECTION 2 DENDROECOLOGY

DOI:10.2312/GFZ.b103-08056

SECTION 3 ISOTOPES

SECTION 4 GEOMORPHOLOGY

SECTION 5 WOOD ANATOMY

DOI:10.2312/GFZ.b103-08056

SECTION 6 ARCHAEOLOGY

SECTION 7 NEW APPLICATIONS

TRACE 2007 Conference, May 3rd – 6th 2007, organized by the Latvian Dendroecologist Society and Faculty of Biology, University of Latvia, Riga, Latvia.

SECTION 1

CLIMATOLOGY

Reconstructing Summer North Atlantic Oscillation (SNAO) variability over the last five centuries

H.W. Linderholm[1], C.K. Folland[2]& J.W. Hurrell[3]

[1] Department of Earth Sciences, Göteborg University, Göteborg, Sweden
[2] Hadley Centre for Climate Prediction and Research, Met Office, Exeter, UK
[3] National Center for Atmospheric Research, Boulder, Colorado, USA

Introduction

The North Atlantic Oscillation

The climate over the North Atlantic region exhibits considerable variability on a wide range of timescales, manifested as coherent fluctuations in ocean and land temperature, rainfall and surface pressure (Hurrell et al. 2002). Without doubt, the North Atlantic Oscillation (NAO) is the most widely known example of such variability. The NAO is a major source of interannual variability in the atmospheric circulation, and is associated with changes in the westerlies across the North Atlantic Sector (Hurrell 1995). The NAO can be described as an oscillation of atmospheric mass between the Arctic and the subtropical parts of the Atlantic, usually defined through changes in surface pressure. These oscillations produce changes in wind speed (and direction) over the North Atlantic, which affects heat and moisture transport over land adjacent to the ocean, as well as frequency and intensity of storms (Hurrell et al. 2003). Furthermore, the NAO strongly affects the heat and freshwater exchange at the ocean surface of the Atlantic Ocean itself by inducing changes in surface wind patterns (Hurrell et al. 2001). Such changes affect the strength and character of the overturning in the North Atlantic and could thus have influence on the thermohaline circulation (Delworth & Dixon 2000). Perhaps the main reason for the recent focus on the NAO is the strong positive trend in the index of the winter NAO from the 1980s and onwards. Hurrell & van Loon (1997) noted that *t*he recent cooling over the northwest Atlantic and the warming across Europe since the early 1980s was related to the decadal variability of the NAO. Furthermore, they showed that since the early 1980s, circulation changes over the Atlantic was linked to coherent large-scale anomalies in precipitation (e.g. dry conditions over southern Europe and the Mediterranean and wetter-than-normal conditions over northern Europe and parts of Scandinavia). Also, Hurrell et al. (2001) suggested a link between the Northern Hemisphere warming and the positive trend in the NAO. In addition to the direct effects of the NAO on, mainly winter-time, climate, a vast number of papers have shown a correspondence between the NAO and a number of ecological features, such as phenology, terrestrial and marine ecosystems, agriculture etc. (see Drinkwater et al. 2003, Mysterud et al. 2003).

Defining the NAO

NAO indices can be derived in different fashions; either from the simple difference in surface pressure anomalies between various northern and southern locations (e.g. Iceland and Azores/Portugal/Gibraltar), or from the principal component (PC) time series of the leading empirical orthogonal function (EOF) of sea level pressure (SLP). In the past, the former approach has been most widely used (e.g. Hurrell 1995, Jones et al. 1997, Visbeck et al. 2001). However, a disadvantage of station-based indices is that they are fixed in space. As shown by e.g. Barnston & Livezey (1987), the NAO centers of action shifts throughout the year, and consequently, such indices can only adequately capture the NAO variability for parts of the year (Hurrell et al. 2003, Allan & Ansell 2006). The advantage of using PC analysis on SLP is that such indices provide more optimal representations of the NAO spatial pattern, but since they are based on gridded SLP data, they usually provide shorter time series than those based on station data (Hurrell et al. 2003). However, recently Allan & Ansell (2006) provided an upgraded version of the Hadley Centre's monthly historical hemispheric mean SLP (MSLP) data set and Ansell et al. (2006) a daily MSLP reconstruction for the European-North Atlantic region, both going back to 1850.

The summer NAO (SNAO)

Because the winter months are dynamically the most active, the largest amplitude anomalies in SLP occur during the cold season. Consequently, most focus has been on winter-time NAO. However, Barnston & Livezey (1987) noted that the NAO pattern was found throughout the year, but that it showed pronounced seasonal variation in location. In winter, they found a Greenland center near 70°N and an Atlantic center at 30°-35°N. In summer, the action centers had moved further to the north: a Greenland center near 70°-75° N and an Atlantic center at 40°-50°N. Although the NAO is most pronounced in the cold season, strong climate anomalies can be detected outside winter. This is especially true for summer, when variability is particularly important from the perspective of droughts and heat waves (Hurrell et al. 2002). Taking the leading eigenvector of SLP during July-August, over a large domain centered over the North Atlantic, Hurrell & Folland (2002) found a dipole pattern much like that of Barnston & Livezey, where the southern center extending over the northeast Atlantic across western Europe into Scandinavia. Their SNAO time series revealed strong variations on interannual to multi-decadal time scales (see Fig. 1 in Hurrell & Folland 2002). The most significant characteristic of this time series is the transition from an extended period of below average SLP anomalies since about 1967 to above average SLP anomalies, indicating a change toward persistent anticyclonic flow during high summer in recent decades. The SNAO index increase corresponded to an increase in mean central England temperatures (CET), and Greatbatch & Rong (2006) found that a strong correlation between SNAO and CET holds for much of the twentieth century. Also, this increase in SNAO corresponds to a lowering of precipitation over much of Northern Europe. In fact, some of the driest summers over the UK in recorded history have occurred during this most recent period (Hurrell et al., 2002). Strong associations between SNAO and temperature/precipitation are found over large parts of Europe, but also elsewhere in the northern hemisphere, e.g. over the Sahel in Africa (Hurrell & Folland 2002, Folland et al. submitted).

NAO and tree rings

Previous reconstructions of the NAO, using different kinds of proxies including tree rings, have focused on the winter NAO (e.g. Appenzeller et al. 1998, Cook et al. 1998, Cullen at al.

DOI:10.2312/GFZ.b103-08056

2001, Glueck & Stockton, 2001, Cook et al. 2002). From a tree-ring point of view, it means that trees respond to conditions of the winter prior to the year of growth. This is certainly true for trees sensitive to precipitation variability, e.g. in arid/semi-arid regions. But also tree growth at higher latitudes seems to be influenced by the winter NAO (see e.g. D'Arrigo et al. 1993, Linderholm et al. 2003). Trees growing in regions surrounding the North Atlantic Ocean could be useful for SNAO reconstruction, considering the links between SNAO and climate in these regions and the strength of tree growth/climate relationships in the growing season. In a first attempt, tree-ring data (tree-ring widths (TRW) as well as maximum latewood density (MXD)) from Great Britain and western Scandinavia were used to reconstruct the SNAO back to 1706, showing promising results (Folland et al. submitted). Here an extension of that reconstruction, based on tree-ring data from a wider geographical area is presented.

Material and Methods

Reconstructing the SNAO

The definition of the SNAO used here is a covariance eigenvector analysis of July-August MSLP anomalies for 25°N-70°N, 70°W-50°E, for 1850-2003. The data derive from the new daily MSLP analysis by Ansell et al. (2006) where EOF1 is defined as the summer NAO (Fig. 1).

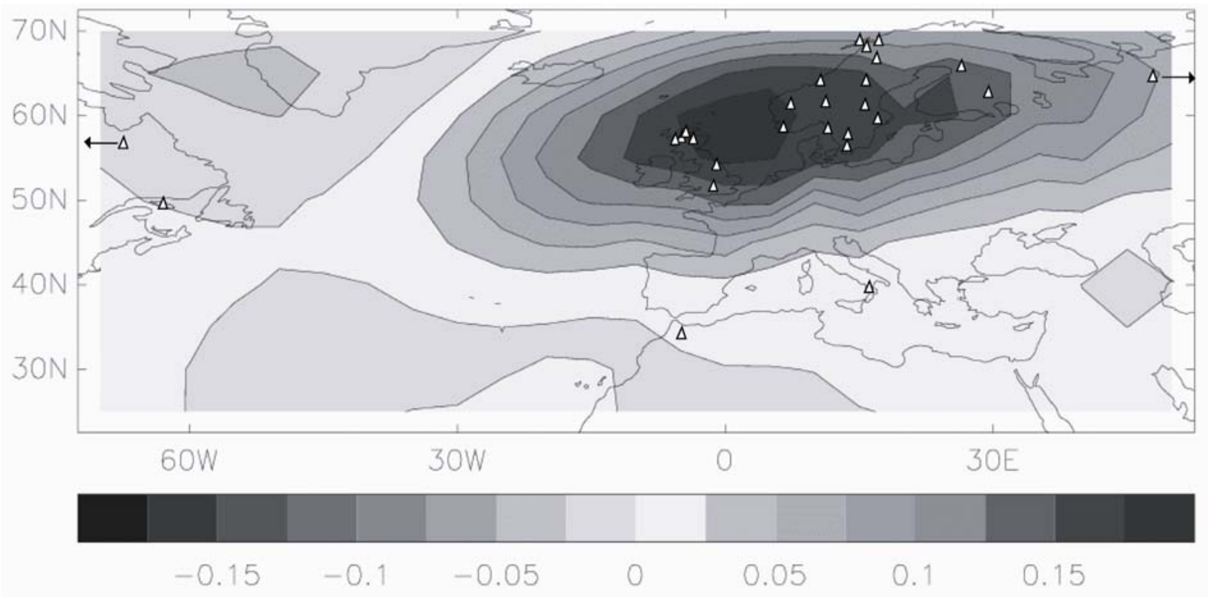

Figure 1: The definition of the SNAO used here is first area weighted covariance EOF of daily pressure at mean sea level over the region 70W-50 °E, 25N-70°N for July-August, 1850-2003, based on the new daily EMSLP data set by Ansell et al. (2006). Shown in this figure is the pattern of the SNAO, with its southern action centre located over the British Isles and southern Scandinavia. White triangles indicate locations of the tree-ring chronologies used in the reconstruction (Note: some sites provided both TRW and MXD).

Folland et al. (submitted), show that SNAO is positively correlated to temperatures over north western Europe and eastern North America, and negative over the eastern Mediterranean/Middle East. Strong negative correlations between SNAO and precipitation are found over north western Europe and moderate positive correlations over the Mediterranean. Consequently, although it is likely that the strongest SNAO signal is found in trees close to the southern node, tree-ring data from all around the North Atlantic sector may be suitable as SNAO predictors. In order to extend the reconstruction as far back in time as possible, we concentrated on chronologies approaching (or exceeding) 500 years, but shorter records from areas with strong SNAO/climate relationships (mainly north-western Europe) were also chosen. Most tree-ring data were obtained from the International Tree-Ring Data Bank (http://www.ncdc.noaa.gov/paleo/treering.html), while the remaining data (mainly for Sweden) was provided by Keith Briffa and the first author. All available long tree-ring chronologies (TRW and MXD) from different species from the area within the 25ºN-70ºN; 70ºW-50ºE boundary were extracted, as well as some long chronologies further east and west in the higher latitudes (western North America and eastern Siberia). The chronologies were standardized, using negative exponential or lines of zero or negative slope on individual tree-ring series to remove the age effect and to strengthen the common climate signel. This process results in loss of century scale variability in the data, but since we were mainly interested in the interannual to interdecadal variability, the standardization method was sufficient. Initially, 168 tree-ring chronologies were screened. To select chronologies suitable for reconstructing SNAO, we chose those showing significant ($p<0.05$, two-tailed test) moderate to strong correlations ($r >0.2$ or <-0.2) over the 1850-2000 period (with the end date of the correlations depending on the length of the individual chronology lengths) with observed SNAO index. Thirty seven chronologies passed that criterion. Since start years varied among the accepted chronologies, the number of available chronologies decreases back in time. In addition, a large number of the chronologies end in the late 1970s or early 1980s. Using only the common overlapping period would give a very time-restricted reconstruction, so instead we used the method previously used to reconstruct Fennoscandian summer temperatures (Gouriand et al. 2007). The thirty seven chronologies were divided into five subsets, where each subset consisted of those chronologies going back to (at least) some specific year. The first subset contained all thirty seven chronologies (1850-1976), the second subset included those chronologies covering the period 1706-1976 (17 chronologies), etc. (Tab. 1).

Table 1: Correlations (annual/decadal) between the subgroup SNAO reconstructions and observed SNAO in the period 1850-1976 (1978-1995 for subgroup 5). In the final reconstruction, each subgroup represents the time given in the first column, but all reconstructions were calibrated over the same period (except subgroup 5). Number of PCs indicates the number of predictors used in the regression models to reconstruct SNAO.

Subgroups	Corr recon vs obs (1850-1995)	Number of PCs	Number of tree-ring chronologies
1: 1441-1499	0.46/0.73	1	8
2: 1500-1705	0.50/0.68	3	10
3: 1706-1849	0.69/0.90	4	17
4: 1850-1976	0.72/0.93	6	37
5: 1977-1995	0.42/0.66	3	9

DOI:10.2312/GFZ.b103-08056

Subsequently, SNAO was reconstructed for each subset. EOF/PC decomposition was performed on the tree-ring chronologies in each of the five subsets and the PCs with eigenvalues >1 were regressed against observed SNAO and significant (0.05 level) PCs retained for further analysis. To make the five separate reconstructions, the significant PCs were set as predictors into a multiple linear regression analysis, where the SNAO was the predictand. The models were initially calibrated using half of the data (e.g. 1915-1978), and then verified over the other half (e.g. 1850-1914). The procedure was then reversed to assess the stability in time of the relationship between observed SNAO and tree-ring PCs. The final model for each subset was calibrated using the full common period. The full reconstruction of SNAO was obtained by combining the six individual reconstructions into one single reconstruction. This combined reconstruction is constructed by using the reconstruction based on subgroup one for the period AD 1441-1499, subgroup two for AD 1500-1705, etc., and subgroup five for the period 1978-1995 (Tab. 1).

Results

SNAO evolution over the last 550 years

The reconstruction is quite skilful in reproducing the interannual variability in observed SNAO and very skilful on decadal timescales. However, it fails to provide the full high-frequency variability evident in the observed data (Fig. 2).

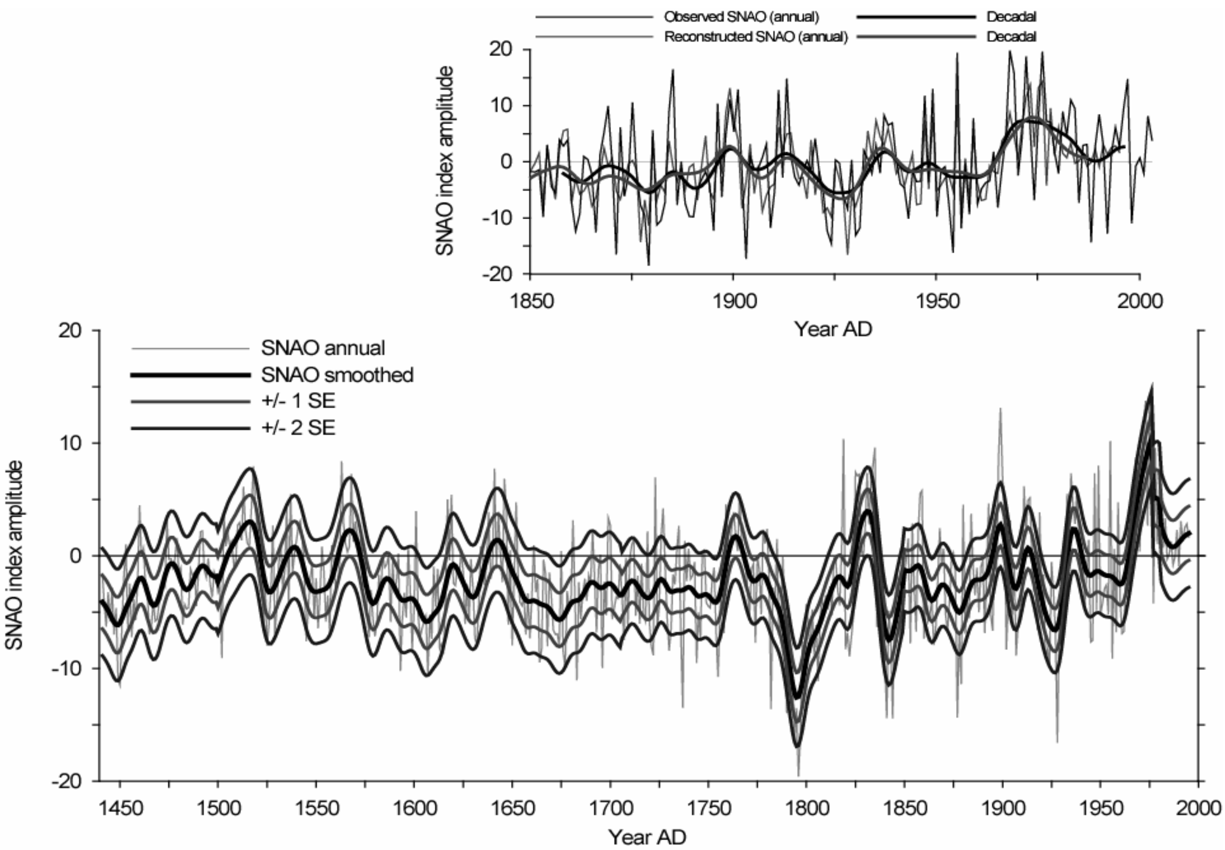

Figure 2: Reconstruction of the SNAO. Upper figure shows reconstructed vs. observed SNAO 1850-1995. Lower figure shows the full reconstruction, with 1 and 2 standard errors (SE). Note that SE is based on the decadal values. Thick black lines represents smoothed (Gaussian filtered, σ=3) values, highlighting variability on timescales longer than 10 years.

DOI:10.2312/GFZ.b103-08056

The lack of correlation between observed and reconstructed SNAO in the early twentieth century corresponds to a period of zero correlation between SNAO and CET noted by Greatbatch & Rong (2006), a feature that has yet to be explained. The highest correlations between observed and reconstructed SNAO were found in the subgroup four reconstruction (1850-1978), which includes the maximum number of tree-ring chronologies, although the subgroup three reconstruction (1706-1849) is similar in strength of correlation. Quite naturally, the correlation weakens with lower number of chronologies (PCs) in the other subgroups (especially subgroup five, see table 1). This is due to the lack of long tree-ring chronologies in the immediate area of the southern action centre of the SNAO. Consequently, there is a large increase in the uncertainty of the reconstructions back in time. On decadal timescales, there is better agreement, suggesting that tree-rings are useful in capturing the SNAO variability on those timescales. Throughout the last 550 years the SNAO has been, in general, in a negative phase, with occasional short term excursions into positive phases (Fig. 3).

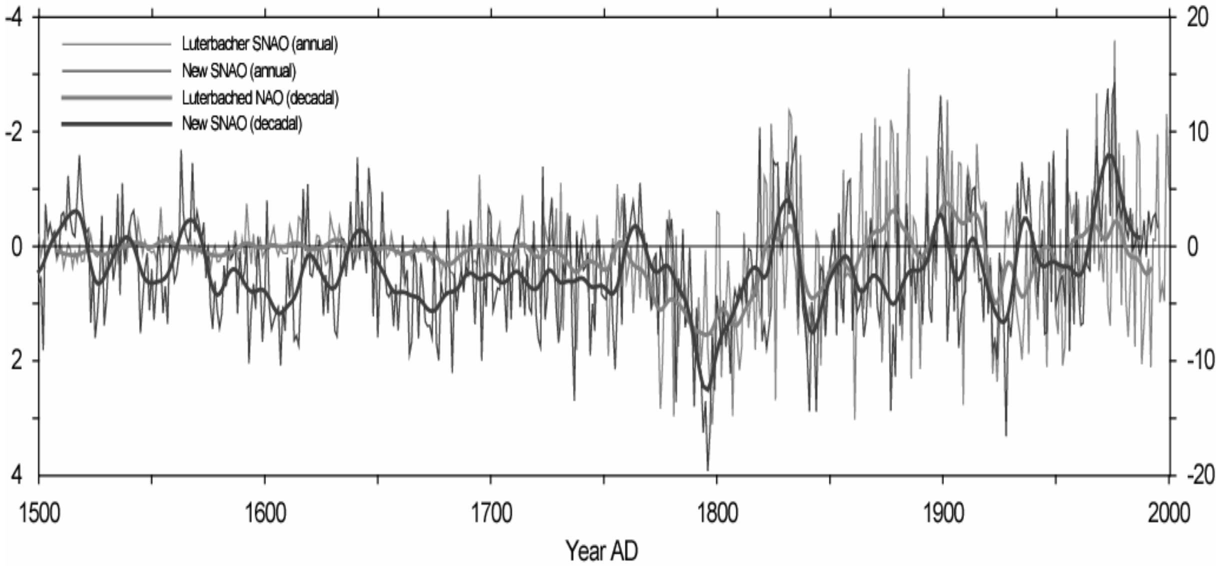

Figure 3: The new SNAO reconstruction compared to average July-August NAO reconstructed by Luterbacher et al. (2002b). Note that before 1659, the Luterbacher reconstruction gives seasonal values (June-August).

Only a handful of positive phases are found beyond 1850, but no coherent positive phases exceed 20 years (decadally smoothed data, see Fig. 3). On the contrary, the longest coherent period of negative SNAO lasts for a century between ca 1650 and 1750, a period which is also characterized by low interannual and decadal variability. The strongest negative phase was found in the late eighteenth century, while the high positive values in the late 1960s to early 1980s seems anomalous within the 550 years. Overall, there is a slight positive trend in the SNAO over the reconstructed period.

Discussion

Since previous studies have mostly focused on reconstructing past winter NAO variability, only few SNAO records are available for comparison with our reconstruction. However, Luterbacher et al. (2002a) reconstructed the NAO back to AD 1500, with monthly resolution from 1659 and seasonal estimates 1500–1658. This reconstruction was developed using principal component regression analysis based on the combination of early instrumental station series (pressure, temperature and precipitation) and documentary proxy data from Eurasian sites, but no tree-ring data (Luterbacher et al., 2002a, 2002b). The NAO index was defined as the standardized (1901–1980) difference between SLP average of four grid points on a 5×5 longitude-latitude grid over the Azores and over Iceland. In the comparison (Fig. 3), the Luterbacher SNAO is based on July-August averages from 1659 and June-August averages prior to that. In general there is quite good agreement between the two reconstructions, although disagreements are found in the last halves of the nineteenth and twentieth centuries. The low SNAO values just before 1800 are found in both records, as well as low values in the period between 1650 and 1750. The lack of correspondence prior to 1650 is mainly caused by the significant drop in proxies used to reconstruct the Luterbacher SNAO. Despite the obvious differences (which in part are due to the Luterbacher record being "station based"), the similarities of the two records between approximately 1650 and 1850, suggests that our new reconstruction captures some of the "true" variability in SNAO back in time.

Since the relationship between NAO and climate using the traditional definition (see above) is much weaker in summer than in winter, previous attempts to reconstruct NAO with tree-ring data have focused on the winter season (Cook et al. 1998, Cullen at al. 2001, Glueck & Stockton, 2001, Cook et al. 2002). Additionally, the relationship between tree growth and station-based NAO during summer in Scandinavia was previously found to be quite weak (e.g. Linderholm et al. 2003). However, here we show that tree-ring data are indeed useful for inferring past SNAO variability, especially on decadal timescales. Furthermore, the spatial distribution of the tree-ring chronologies we used in our reconstruction suggests that SNAO is more than a feature influencing the immediate surroundings of the North Atlantic Ocean. The tree-ring data indicate that it also affects climate down to the Mediterranean as well as further west and east over North America and Eurasia.

Conclusion

We have shown that using tree-ring data from a large geographical region, the SNAO can be reconstructed with some skill on interannual to interdecadal timescales. Extending the SNAO record back in time will be of importance for increasing the understanding of the influence of summer atmospheric circulation on climate, ocean-atmosphere coupling, as well as global teleconnections and their role in climate variability and change.

Acknowledgements

We would like to acknowledge the valuable comments from an anonymous reviewer which led to an improved manuscript. This work was initiated in the EMULATE project, funded by the European Commission under contract EVK2.CT2002-00161, and was also supported by the Swedish Research Council (grant to Hans Linderholm). Chris Folland was also funded by the United Kingdom Joint Defra and MoD Programme, (Defra) GA01101 (MoD) CBC/2B/0417_Annex C5. We are grateful for all who have provided tree-ring data for the analysis, especially the ITRDB and Keith Briffa.

References

Allan, R. J., Ansell, T. J. (2006): A new globally complete monthly historical gridded mean sea level pressure data set (HadSLP2):1850-2003. *Journal of Climate 19*: 5816-5842.

Ansell, T.J., and co-authors (2006): Daily mean sea level pressure reconstructions for the European-North Atlantic region for the period 1850-2003. *Journal of Climate 19*: 2717-2742.

Appenzeller, C., Stocker, T.F., Anklin, M. (1998): North Atlantic Oscillation Dynamics Recorded in Greenland Ice Cores. *Science 282*: 446 – 449.

Barnston, A.G., Livezey, R.E. (1987): Classification, seasonality and persistence of low-frequency atmospheric circulation patterns. *Monthly Weather Review 115*: 1083-1126.

Cook, E.R., D'Arrigo, R.D., Briffa, K.R. (1998): A reconstruction of the North Atlantic Oscillation using tree-ring chronologies from North America and Europe. *The Holocene 8*: 9-17.

Cook, E.R., D'Arrigo, R.D., Mann, M.E. (2002): A well-verified, multiproxy reconstruction of the winter North Atlantic Oscillation index since AD 1400. *Journal of Climate 15*: 1754-1764.

Cullen, H.M., D'Arrigo, R.D., Cook, E.R., Mann, M.E. (2001): Multiproxy reconstructions of the North Atlantic Oscillation. *Paleoceanography 16*: 27-39.

D'Arrigo, R.D., Cook, E.R., Jacoby, G.C., Briffa, K.R. (1993): NAO and sea surface temperature signatures in tree-ring records from the North Atlantic sector. *Quaternary Science Reviews 12*: 431-440.

Delworth, T.L., Dixon, K.W. (2000): Implications of the recent trend in the Arctic/North Atlantic Oscillation for the North Atlantic thermohaline circulation. *Journal of Climate 13*: 3721-3727.

Drinkwater, K.F., Belgrano, A., Borja, A., Conversi, A., Edwards, M., Greene, C.H., Ottersen, G., Pershing, A.J., Walker, H. (2003): The response of marine ecosystems to climate variability associated with the North Atlantic Oscillation. The North Atlantic Oscillation – Climatic Significance and Environmental Impact. *Geophysical Monograph 134*: 211-234.

Folland, C.K., Linderholm, H.W., Knight, J., Hurrell, J.W., Fereday, D., Ineson, S., Scaife, A., Eastman, R., Warren, S. (submitted): The Summer North Atlantic Oscillation: past, present and future. *Journal of Climate*.

Glueck, M.F., Stockton, C.W. (2001): Reconstruction of the North Atlantic Oscillation, 1429-1983. *International Journal of Climate 21*: 1453-1465.

Greatbatch, R.J., Rong, P.P. (2006): Discrepancies between different Northern Hemisphere summer atmospheric circulation data products. *Journal of Climate 19*: 1261-1273.

Gouirand, I., Linderholm, H.W., Moberg, A., Wohlfarth, B. (2007): On the spatiotemporal characteristics of Fennoscandian tree-ring based summer temperature reconstructions. *Theoretical and Applied Climatology*. DOI 10.1007/s00704-007-0311-7

Hurrell, J.W. (1995) Decadal trends in the North Atlantic Oscillation: regional temperatures and precipitation. *Science 269*: 676-679.

Hurrell, J.W., van Loon, H. (1997): Decadal variations in climate associated with the North Atlantic Oscillation. *Climatic Change 36*: 301-326.

Hurrell, J.W., Kushnir, Y. Visbeck, M. (2001): The North Atlantic Oscillation. *Science 291*: 603-604.

Hurrell, J.W., Folland C.K. (2002): The relationship between tropical Atlantic rainfall and the summer circulation over the North Atlantic. *CLIVAR Exchanges 25*: 52-54.

Hurrell, J.W., Hoerling, M.P., Folland C.K. (2002): Climatic variability over the North Atlantic. Meteorology at the Millennuim: 150th Anniversary of the Royal Meteorological Society, Academic Press, London. 143-151.

Hurrell, J.W., Kushnir, Y. Ottersen, G., Visbeck, M. (2003): An overview of the North Atlantic Oscillation. The North Atlantic Oscillation – Climatic Significance and Environmental Impact. *Geophysical Monograph 134*: 1-35.

Jones, P.D., Jonsson, T., Wheeler, D. (1997): Extension to the North Atlantic Oscillation using early instrumental pressure observations from Gibraltar and south-west Iceland. *International Journal of Climatology 17*: 1433-1450.

Linderholm, H.W., Solberg, B.O., Lindholm, M. (2003): Tree-ring records from central Fennoscandia: The relationship between tree growth and climate along an east west transect. *The Holocene 13*: 887-895.

Luterbacher, J., Xoplaki, E., Dietrich, D., Rickli, R., Jacobeit, J., Beck, C., Gyalistras, D., Schmutz, C., Wanner, H. (2002a): Reconstruction of sea-level pressure fields over the eastern North Atlantic and Europe Back to 1500. *Climate Dynamics 18*: 545–561.

Luterbacher, J., Xoplaki, E., Dietrich, D., Jones, P.D., Davies, T.D., Portis, D., Conzalez-Rouco, J.F., von Storch, H., Gyalistras, D., Casty, C., Wanner, H. (2002b): Extending North Atlantic Oscillation reconstructions back to 1500. *Atmospheric Science Letters 2*: 114–124.

Mysterud, A., Stenseth, N.C., Yoccoz, N.G., Ottersen, G., Langvatn, R. (2003): The response of terrestrial ecosystems to climate variability associated with the North Atlantic Oscillation. The North Atlantic Oscillation – Climatic Significance and Environmental Impact. *Geophysical Monograph 134*: 235-262.

Visbeck, M.H., Hurrell, J.W., Polvani, L., Cullen, H.M. (2001): The North Atlantic Oscillation: Past, present, and future. *PNAS 98*: 12876-12877.

Growth responses to NAO along a Central European west - east transect

J. Schultz, B. Neuwirth, D. A. Friedrichs, J. Löffler & M. Winiger

[1]*Institute of Geography, University of Bonn; Meckenheimer Allee 166, 53115 Bonn, Germany;*

Email: schultz@giub.uni-bonn.de

Dendroclimatology investigates the relation between tree-ring growth and climate on a regional and supraregional scale. Especially temperature and precipitation are two of the dominant factors influencing tree-ring growth (Schweingruber 1996, Fritts 1976). Tree-rings are widely used proxy to reconstruct past climate elements like precipitation or temperature (Treydte et al. 2006, Esper et al. 2002). Despite the strong influence of precipitation and temperature, they do not represent the whole climate impact on tree-ring growth. Many studies have been carried out during the last decade to reconstruct large scale circulation conditions, particularly in the North Atlantic sector (Pauling et al. 2006, D'Arrigo et al. 2003, Cook et al. 2002). For instance, the typical circulation pattern over the North Atlantic sector expressed by the position and the air-pressure differences between the Islandic Low and Azores High is quite important for the weather conditions in Central Europe. These circulation modes are described as the North Atlantic Oscillation (NAO). Various indices (NAOI) have been developed to describe such variations in the air pressure fields over the North Atlantic sector (overview see Hurrell et al. 2003). For a better understanding of the influences of NAO on tree-ring growth, this study investigates growth responses to NAO along a Central European west-east transect from the Eifel (Germany) to the Ore Mountains (Czech Republic).

Data

Tree-ring data

The 430 km long transect from the Eifel (W-Germany) to the Ore Mountains (NW-Czech Republic) (area between 6-14°E and 50-51°N) consists of 37 dendrochronological sites (Fig. 1) with the following tree species*: Fagus sylvatica*, *Larix decidua*, *Picea abies*, *Pinus sylvestris, Pseudotsuga menziesii, Quercus petraea,* and *Quercus robur*.

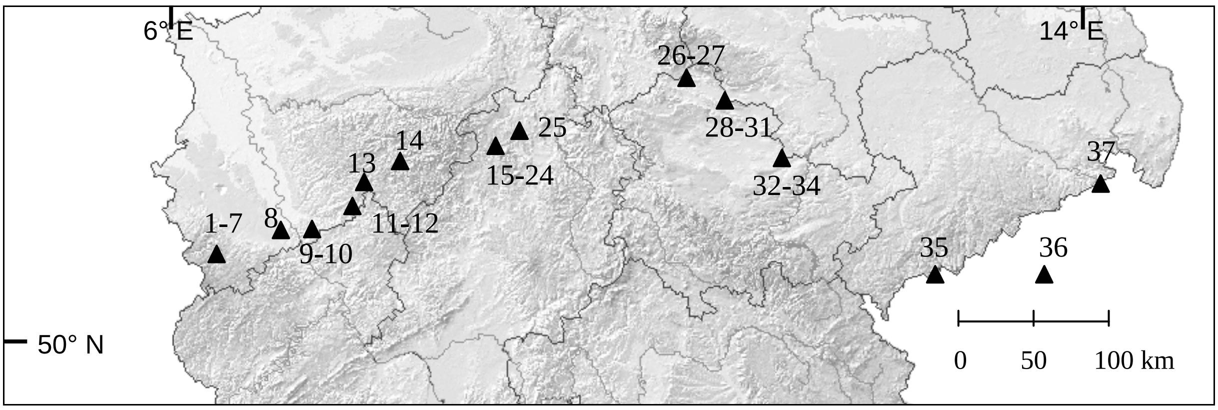

Figure 1: Spatial distribution of the dendrochronological sites (▲).

A dendrochronological site consists of at least 10 dominant trees for each tree species. Therefore, two or more dendrochronological sites can be found at the same spatial location. The elevations of the sites in the transect vary from 150 m a.s.l. in the Sieg valley near Bonn to 1030 m a.s.l. in the Ore Mountains (Tab.1). The sites represent a varying ecological spectrum regarding exposition, altitude, inclination, and forest community. All selected trees are dominant trees and at least older than AD 1890.

Table 1: Characteristics of dendrochronological sites. *Abbreviations of the tree species see figure 2.*

code	number	species	latitude / longitude	altitude	exposition	region
dre11	1	QUPE	50,5708 / 6,3603	500	150	Rureifel
dre12	2	FASY	50,5717 / 6,3611	480	150	
dre09	3	QUPE	50,6244 / 6,3992	400	300	
dre03	4	FASY	50,6086 / 6,4569	530	315	
dre04	5	PSME	50,6097 / 6,4639	525	135	
dre05	6	FASY	50,6061 / 6,4900	470	60	
dre13	7	PCAB	50,6056 / 6,4917	470	60	Eifel
drb13	8	QURO	50,6700 / 7,0472	185	15	Kottenforst-Ville
drb05	9	FASY	50,6689 / 7,2489	360	320	Siebengebirge
drb06	10	QUPE	50,6694 / 7,2492	370	320	
drs02	11	FASY	50,8039 / 7,5906	150	250	Siegtal
drs03	12	QURO	50,8036 / 7,5908	165	245	
drl02	13	QUPE	50,9825 / 7,7169	385	270	Oberbergisches Land
dro01	14	FASY	51,1022 / 8,0222	455	130	Olpe
dhk05	15		51,1672 / 8,9583	420	345	Kellerwald
dhk02	16		51,1703 / 8,9669	310	150	
dhk03	17	QUPE	51,1708 / 8,9681	290	135	
dhk04	18	FASY	51,1936 / 9,0117	280	180	
dhk11	19	QUPE	51,1561 / 9,0761	400	215	
dhk12	20		51,1556 / 9,0769	390	150	
dhk07	21	LADE	51,1567 / 9,0836	360	180	
dhk08	22	QUPE	51,1564 / 9,0842	350	180	
dhk10	23		51,1581 / 9,0842	380	180	
dhk06	24	PISY	51,1569 / 9,0844	360	180	
dhb01	25	FASY	51,3167 / 9,1833	300	270	Hessisches Bergland
dtt01	26		51,5361 / 10,5556	440	180	Mitteldeutsches Trias Bergland
dtt02	27	QURO	51,5361 / 10,5556	440	180	
dtk02	28	FASY	51,4125 / 11,0611	480	315	Kyffhäuser
dtk03	29		51,4083 / 11,0861	460	180	
dtk01	30		51,4194 / 11,1083	425	-	
dtk04	31	QUPE	51,4194 / 11,1083	425	-	
dtj02	32	FASY	51,0017 / 11,6442	320	-	Jena
dtj01	33		51,0014 / 11,6444	320	-	
dtj03	34	QUPE	51,0014 / 11,6444	320	-	
tkp01	35	PCAB	50,4000 / 12,7500	870	330	Ore Mountains
tkk01	36		50,4086 / 12,9669	1030	30	
tul01	37	PISY	50,8681 / 14,3672	300	120	

There are 16 beech and 14 oak sites concentrated in the west and in the middle of the transect, respectively. Two spruce sites are found in the eastern part of the transect, whereas one site is located in the western area, the Eifel. The easternmost site of the

DOI:10.2312/GFZ.b103-08056

transect is represented by pine. Further a pine site is located in the Kellerwald region near Kassel. There are only one larch site, which is located in the Kellerwald (site No. 21), and one site of douglas fir, which is located in the Eifel (site No. 5).
Table 1 and figure 2 illustrate that the 7 different tree species are not represented by the same number of sites. With 16 beech and 14 oak sites more than 80% of the investigated sites represent deciduous forests. This distribution does not reflect the natural distribution of tree species in the research area. In fact, there exist clearly more spruce sites, but especially in the western part of the transect most of them are cultural forest and not old enough, to use them in this study.
Corresponding to the natural situation, the spatial distribution of the tree species is inhomogenuous; coniferous forests are concentrated to the eastern parts and deciduous forests to the middle and western parts of the transect (Tab. 1, Fig. 1).

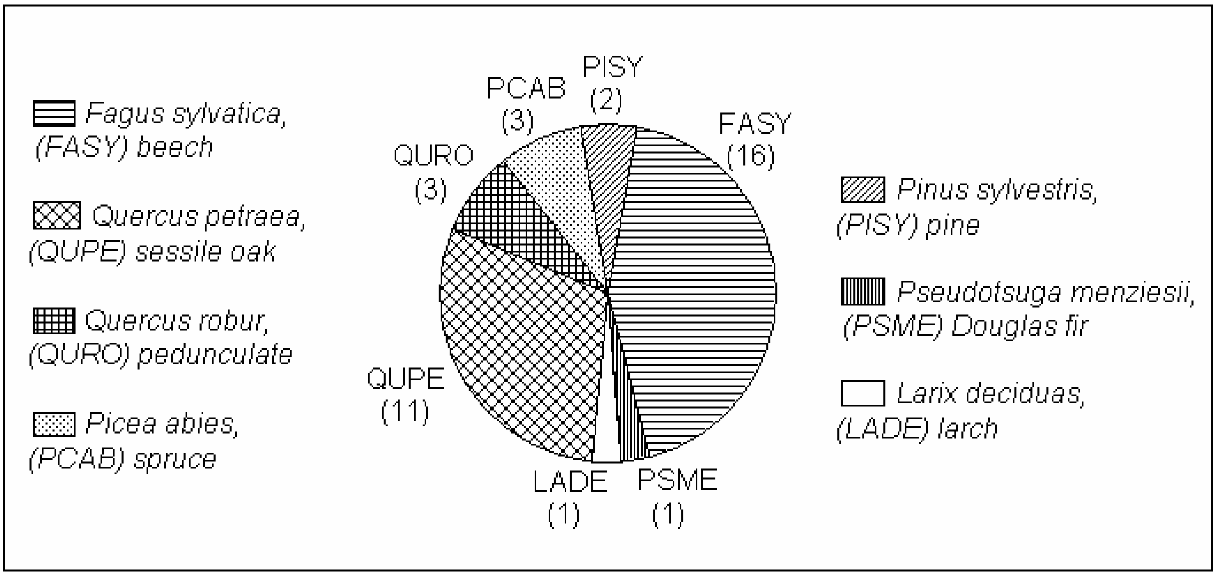

Figure 2: Number of tree species and sites.

NAO data

The NAOI is the normalised surface pressure difference between the Islandic Low and the Azores High. There are two basic ways to compute the NAOI. The first is to calculate the air pressure difference between two stationary points. The second is a zonal index, which takes into consideration that the atmospheric control centres can change their position (Glowienka-Hense 1990). In this study three different NAOI for the time period from 1901 to 1990 are used. They are derived from the climatic stations Akureyri on Iceland (65,7°N/18.1°W) and Ponta Delgada on the Azores (37.7°N/25.7°W) (Rogers 1990, van Loon and Rogers 1978) and from Stykkisholmur on Iceland (65.0°N/22.8°W) and Gibraltar (36.1°N/25.7°W) in Southern Spain (Jones et al. 1997). We abbreviate these two indices as PON and GIB, respectively. The third index is named ZON, because it is a more zonal index describing the zonal air pressure mean minima and maxima values between 20° to 70°N over the North Atlantic (Paeth 2000, Glowienka-Hense 1990).

The strongest impact of the NAO on the weather conditions in Europe and North America is observable in winter. The NAO alternates between a positive and a negative phase. A negative NAOI is associated with a weak Azores High and a weak Islandic Low. The reduced pressure differences cause fewer and weaker winter storms on a west-eastern pathway corresponding with cold and dry conditions in the North of Europe and wet conditions in the Mediterranean region. A positive NAO phase is characterised by a strong Azores High and a deep Islandic Low and yields to wet and warm winter conditions in Northern Europe (Hurrell et al. 2003).

Methods

Two increment cores from opposite directions of each tree were sampled. Using Lintab V measurement tables (resolution 1/100 mm) in combination with the software package TSAPWIN-Scientific 0.53 (Rinn 2005) the tree-ring widths were measured. Synchronization and cross-dating were carried out with TSAPWin (Rinn 2005) and Cofecha (Holmes 1983). All tree ring width (TRW) series were detrended calculating ratios from a 13-year moving average. Afterwards for each site the tree series were averaged to site chronologies and shortened to the research period from AD 1901 to AD 1990.
Using Pearson's correlation coefficients r (Bahrenberg et al. 1999) and their confidence intervals expressed as 1.6-time standard deviation (white bars in Fig. 3) around the mean values, the connection between the 37 chronologies and the various NOAI series were computed. Therefore, the NAOI data were separated into 18 monthly series, from April of the previous year to September of the growth year. Further 9 averaged series for the year, two growing seasons (April to September and May to August), for the seasons winter, spring, summer, autumn and for the seasons of the prior year summer and autumn, were separated. To aggregate all histograms species specific chronologies and a mean chronology for all sites were calculated. Correlations will be classified to significant if the r-values exceed the thresholds for the 90% level. For the 90 year long investigation period (89 degrees of freedom), the critical value is r = ±0.18 (Bahrenberg et al. 2000). Significant correlations will be devided into weak and strong signals if the significance level is lower or higher than 95%, respectively. Therefore the threshold is r = ±0.22.

Results and Discussion

In total 222 charts were analysed. Figure 3 illustrates the correlations and corresponding confidence intervals between the mean chronology derived from all sites and the three NAO indices. No bar rises up above the thresholds for the levels of significance. Thus, neither on a monthly nor on a seasonal scale a significant NAO effect to the mean growth over the whole dataset exists, regardless which NAO index is chosen. However, concerning the statistical spread of the correlations (white bars in Fig. 3) around the mean values, the values reach the level of significance and document the existence of significant correlations.
Figure 3 shows two foci of significant reactions: first a negative correlation to the beginning of the growing season, especially to March and consequently to spring, and second a positive correlation to the end of the growing season in August and/or September.

Comparing the histograms of the three NAOI some differences are obvious. While for autumn ZON and PON show positive correlations, the GIB index has a negative correlation.

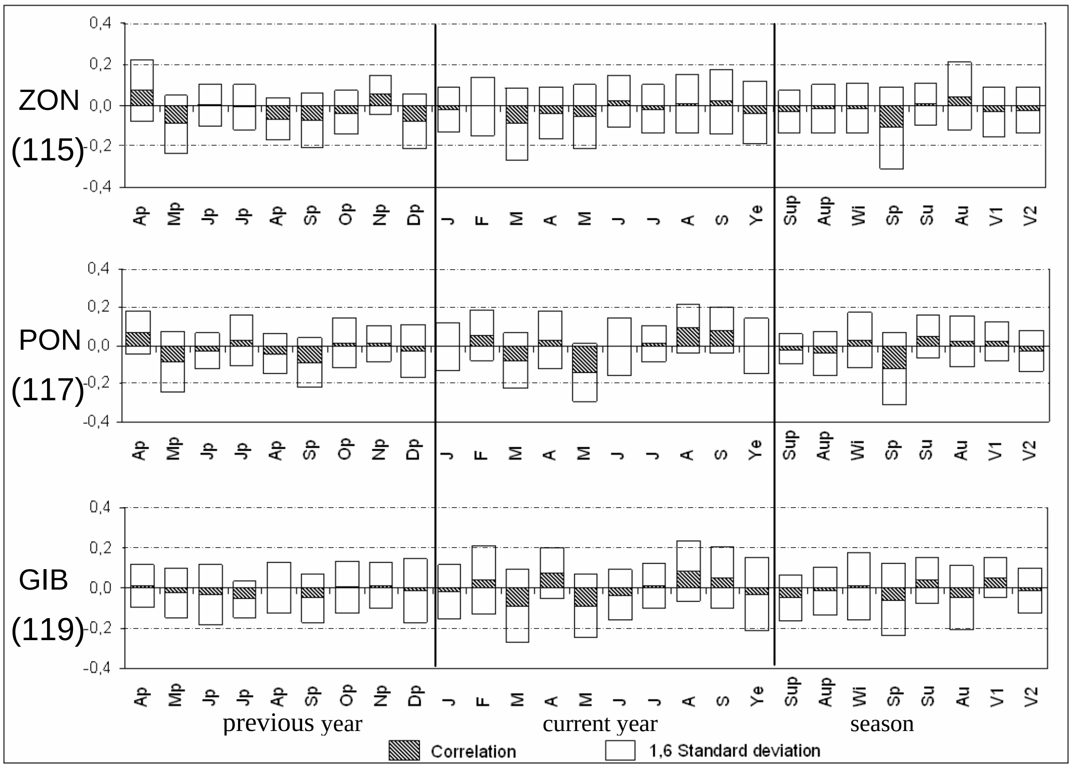

Figure 3: Monthly and seasonal correlations between the three NAO indices ZON, PON, and GIB and the chronology averaged over all sites (grey bars) and the corresponding scatter over the single sites expressed as 1.6-time standard deviation (white bars) around the mean values. Additionally the total number of significant positive and negative correlations of all 37 sites in the 27 time windows is noted below the NAOI name. The threshold for the 90% significant level is ± 0,18 and for the 95% significant level ± 0,22. Short cuts: p =previous, Sp = Spring, Su = Summer, Au = Autumn, Wi = Winter, V1 = April-September, V2 = May-August.

In most cases however, especially regarding the strongest signals in spring/March/May and in August/September, the directions of the reaction are the same, only the values are different. Calculating the total number of all significant positive or negative correlations between the single sites and the three NAO indices, the GIB NAOI shows most significant correlations (numbers in Fig. 3). This might serve as an indicator for the fact, that for each of the three NAOI various combinations of sites and/or time periods significant correlations can be observed. This is especially amazing because of the fact, that all three indices intend to describe the same phenomena – the air pressure difference between the Azores High and the Islandic Low. Hence, the differences of the correlation values are caused by the different calculation techniques of the three NAO indices.
Therefore, in the following specifications for each case the index with the most significant correlating sites will be shown. Regarding the investigated aspects the March/spring signal will be discussed by using the GIB index and the summer/autumn signal will be discussed by using the PON index.

DOI:10.2312/GFZ.b103-08056

Specification of the spring signal

The examination of the site specific correlations from the GIB NAOI in March (Fig. 4) involves the finding, that only the beech sites (circles) show significant correlations.

All the other species have correlations near by zero. Therefore, according to the westerly distribution of the beech sites, the apparent gradient with a decreasing March signal from West to East is explainable by the species specific reactions. Because of the fact, that the 4 non-significant beech sites are located in the western part as well as in the middle and eastern part of the beech distribution, decreasing correlations within the beech sites cannot be detected.

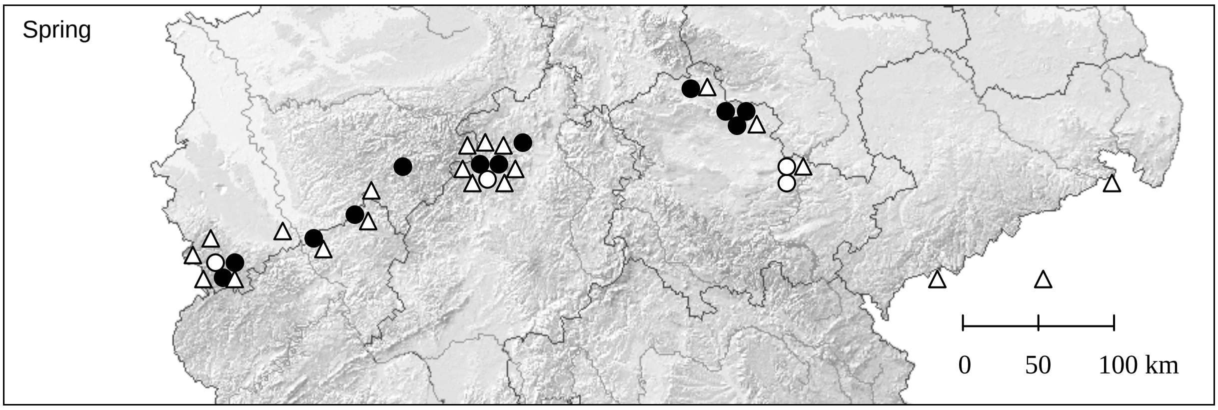

Figure 4: Spatial distribution of beech (circles) and non beech sites (triangles) with significant negative correlations (black) and without significant correlations (white) in March against the GIB index (level of significance: 90%).

Specification of the summer/autumn signal

In total, for 11 sites of the transect a positive significant correlation exists in months or seasons of the second half of the growing season, including the species oak, beech, spruce and pine (Fig. 5). The strong signals are located in the Eifel (r = 0.29 for the beech site 6 and 0.25 for the oak site 3) and in the Ore Mountains (r = 0.24 for the oak site 31). In the middle of the transect only weak correlations can be observed. Thus, from the signal strength a gradient from West to East cannot be deduced.

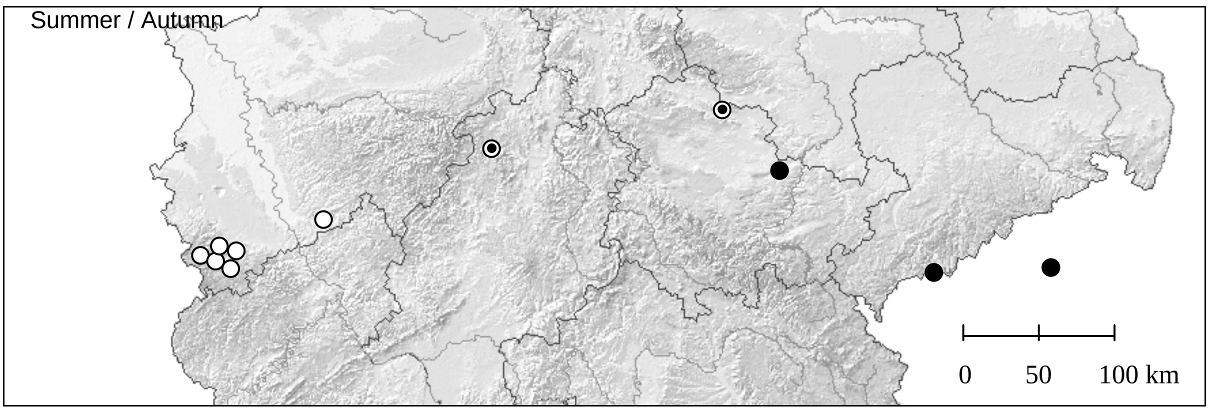

Figure 5: Spatial distribution of sites with significant positive correlations (90% significance level) to the PON NAOI at the end of the growing season. The sites are differentiated as follows: positive significant correlations a) in June, July or summer ● ; b) in August and additionally in summer ⦿, and c) in August, September or autumn ○.

Focusing the view on the correlations for the investigated time periods (Fig. 3), a clear gradient from West to East is apparent. In the western part of the transect all correlations appear in the months August or September or for the autumn season (white circles in Fig 4). In contrast, in the eastern part the correlations are dated in June or July or in the summer season (black circles). In the middle of the transect two sites show significant correlations in both the summer season and additionally in august. These sites represent a transition and show the strongest reaction in late summer. In consequence, the specification of the summer/autumn signal results in a movement of the positive NAO - TRW correlation from autumn in the West to early summer in the East.

An additional investigation of the effect of the exposition of the tree sites on the NAO-signals in the TRW series did not lead to a clear result (not shown). There are no systematic differences in the results by dividing the dataset into two groups - a so called Luv-group with southern to eastern expositions and a Lee-group with western to northern expositions.

Conclusion and Perspectives

The first results of this study concerning the effects of the NAO on tree-ring growth in a West-East transect from the Eifel (W-Germany) to the Ore Mountains (Czech Republic) can be summarized as follows:

On an interannual scale the NAO has only a small effect on tree-ring growth with highest correlations around r = 0.3. The strongest correlations appear as a negative relation at the beginning of the growing season and a positive relation at the end of the growing season. The spring signal is only caused by the beech sites and does not underline any variations within the transect. In contrast, the weaker summer/autums signal is caused by many species and describes a movement from West to East according to a decreasing length of the growing season.

Both findings yield to the conclusion that especially for NAO-TRW investigations a species specific and a meridional separation of the dataset is advisable.

The next step, is to investigate the NAO signals in tree-ring chronologies on a decadal and multi-decadal scale – the scale of the strongest NAO modifications (Hurrell et al. 2003). Additionally, according to the findings of Friedrichs et al. (submitted) we have to examine the timely stability of these signals.

Acknowledgments

Thanks to following colleagues and institutes for providing tree-ring data: Čejková, A. (CZ), Mácová, M. (CZ), Bonn, S. (Dendro-Institut Tharandt) and the members of the Dendro Group Bonn.

References

Bahrenberg, G., Giese, E., Nipper, J. (1999): Statistische Methoden in der Geographie. Bd. 1: Univariate und bivariate Statistik. BG Teubner, Stuttgart. 234 p.

Cook, E.R., D'Arrigo R.D., Mann, M.E. (2002): A well-verified, multiproxy reconstruction of the winter North Atlantic Oscillation index since AD 1400. *Journal of Climate* 15:1754-1764.

D'Arrigo, R.D., Cook E.R., Mann, M.E., Jacoby, G.C. (2003): Tree-ring reconstructions of temperature and sea-level pressure variability associated with the warm-season Arctic Oscillation since AD 1650. *Geophysical Research Letters* 30(11): 1549.

Esper, J., Cook, E.R., Schweingruber, F.H. (2002): Low-frequency signals in long tree-ring chronologies for reconstructing past temperature variability. *Science* 295: 2250-2253.

Friedrichs, D. A., Neuwirth, B., Löffler, J., Winiger, M. (2007): Effects of different statistical on site classifications in a homogeneous tree-ring network. *Dendrochronologia* (in review).

Fritts, H.C. (1976): Tree rings and climate. Academic Press, London. 567pp.

Glowienka-Hense, R. (1990): The North Atlantic Oscillation in the Atlantic-European SLP. *Tellus* 42(A): 497-507.

Holmes, R.L. (1983): Computer-assisted quality control in tree-ring dating and measurement. *Tree-Ring Bulletin* 43: 69-78.

Hurrell, J.W., Kushnir, Y., Ottersen, G., Visbeck M. (2003): The North Atlantic Oscillation. Climatic significance and environmental impact. Washington D.C. 279pp.

Jones, P.D., Jonsson, T., Wheeler, D. (1997): Extension of the North Atlantic Oscillation using early instrumental pressure observations from Gibraltar and South-West Iceland. *International Journal of Climatology* 17(13-15): 1433-1450.

Loon, v.H. Rogers, J.C. (1978): The seesaw in winter temperatures between Greenland and Northern Europe. Part I: General Description. *Monthly Weather Review* 106: 296-310.

Paeth, H. (2000): Anthropogene Klimaänderungen auf der Nordhemisphäre und die Rolle der Nordatlantik-Oszillation. *Bonner Meteorologische Abhandlungen* 51. 168pp.

Pauling, A., Luterbacher, J., Casty, C., Wanner, H. (2006): Five hundred years of gridded high-resolution precipitation reconstructions over Europe and the connection to large-scale circulation. *Climate Dynamics* 26(4): 387-405.

Rinn, F. (2005): TSAPWin – Time Series Analysis and Presentation for Dendrochronology and Related Applications, Version 0.53, User Reference. Heidelberg 91pp.

Rogers, J. C. (1990): Patterns of low-frequency monthly sea level pressure variability (1899-1986) and associated wave cyclone frequencies. *Journal of Climate* 3 (12): 1364-1379.

Schweingruber, F.H. (1996): Tree rings and environment – Dendroecology. Haupt, Bern, Stuttgart, Wien. 609pp.

Treydte, K.S., Schleser, G.H., Helle, G., Frank, D.C., Winiger, M., Haug G.H., Esper, J. (2006): The twentieth century was the wettest period in northern Pakistan over the past millennium. *Nature* 440 (7088): 1179-1182.

DOI:10.2312/GFZ.b103-08056

SOI and NAO impacts on *Pinus pinaster* Ait. growth in Spanish forests

S. Bogino[1,2] & F. Bravo[1]

[1] *Departamento de Producción Vegetal y Recursos Forestales. Universidad de Valladolid, Avda. de Madrid 44. 34004 Palencia. Spain. TE. 34 979108427.*

[2] *Departamento de Ciencias Agropecuarias. Facultad de Ingeniería y Ciencias Económico-Sociales. Universidad Nacional de San Luis. Argentina. Email: sbogino@fices.unsl.edu.ar*

Introduction

Global change provides an extraordinary research opportunity and challenges for dendroclimatologists and other scientists who investigate the natural variability in the Earth's system (Hughes 2002). Climate has been used as a source of explanation for changes in the size and state of the tree-ring and it should be used to predict future tree-ring growth (Hughes 2002). The North Atlantic Oscillation (NAO) is traditionally defined as the normalized pressure difference between the Azores and Iceland. The NAO pattern is most pronounced both, in intensity and area coverage, during the winter. This phenomena is considered to be the most important source of climate variability in Europe, northern Africa and eastern North America; affecting temperature, precipitation and atmospheric circulation (Hurrell 1995, Hurrel & van Loon 1997). The Southern Oscillation Index (SOI) refers to the pressure variation between Darwin (Australia) and Tahiti. This pressure variation defines the cyclic warming and cooling of the equatorial Pacific Ocean, commonly known as El Niño phenomena (Bjerknes 1966). The impact of the SOI is felt mainly in the Pacific, however, its effect seems to influence climatic variability on a global scale (Trenberth et al. 1998).

The NAO and SOI should be considered as the major sources of the inter-annual variability of weather and climate around the world (Hurrell 1995, Hurrell & van Loon 1997). Over the last five centuries the connection between the mean winter precipitation over the Mediterranean and the NAO has turned out to be stable, with highly negative correlations throughout the period (Cook et al. 2001). *Pinus pinaster* Ait. occurs naturally in the western Mediterranean Basin, in the northern rim (France, Italy, Portugal and Spain) and in the southern rim (Algeria, Morocco and Tunisia). It is a characteristic species of the Mediterranean forests and its main distribution area is across the Iberian Peninsula where it covers about 2.4 million hectares (Blanco et al. 1997). It is adapted to different environments and, consequently, shows a wide ecological variety of adaptations: it survives under high or low temperatures, under regular or variable rainfall as well as under sever droughts; it is also adapted to the extremely cold winter in the centre of the peninsula and to the mild temperature next to the Atlantic ocean coast (Blanco et al. 1997).

There are no previous studies made on the impact of the SOI and NAO indexes on conifers growing in the Iberian Peninsula. Because of many scientists arguing about both indexes global impact on the earth's surface, it could be an excellent opportunity to analyse the relationship between these indexes and the growth of woody species. The aim of this study was to analyze the relation between the *Pinus pinaster* 's tree-ring width and the NAO and

DOI:10.2312/GFZ.b103-08056

SOI atmospheric indexes in Eastern Spain. This objective was addressed analyzing sixty trees cored at four different sites. Correlation analysis, bootstrapped response function and Kalman filter analysis were applied to study both, time-independent and time-independent growth responses to atmospheric indexes.

Material and Methods

Study sites and laboratory methods

Four sampling sites were selected In Central Spain. The sites were located between 920 and 1,437 m a.s.l. (Fig.1, Tab. 1).

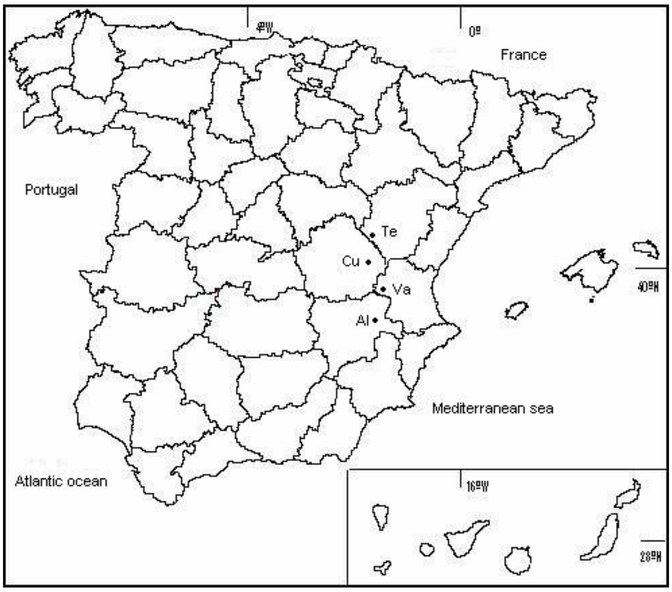

Figure 1: Geographical location of P. pinaster sampling sites in the Iberian Peninsula. The round points indicate the sampling sites. Sites codes: Te: Teruel; Cu: Cuenca; Va: Valencia; Al: Albacete.

The climate of the area is Mediterranean with sever droughts during the summer and precipitation from autumn to spring. Mediterranean Maritime pine grows on permeable soils, generally rich in organic matter, which have developed on calcareous or siliceous substrates. At each sampling site, in the summer of 2006, from fifteen dominant and co-dominant trees, two cores were extracted at a hight of 1.30 meter. Cores were polished and subsequently dated under a binocular microscope following standard dendrochronological techniques (Stokes & Smiley 1968). Sections were scanned at high resolution (2,000 dpi) with an Epson Expression 1640 XL scanner with a 0.01 mm accuracy. Tree-rings were measured using WinDENDRO© (Regent Instruments).

Statistical analysis

The NAO and SOI values were obtained from www.cru.uea.ac.uk/cru/data/nao.htm and www.cru.uea.ac.uk/cru/data/soi.htm (Jones et al. 1997). The COFECHA program 6.06P version (Grissino-Mayer 2001 available at: www.ltrr.arizona.edu) was applied to assess the data accuracy. This program calculates the correlation indices between the ring width series and also identifies errors such as missing or false rings. To eliminate the growth biological tendency and to minimise growth variation which was not present in all trees (Fritts 1976),

DOI:10.2312/GFZ.b103-08056

the ARSTAN program, 2.07 version (Cook & Holmes 1984 available at: www.ltrr.arizona.edu) was used. To obtain a master chronology at each study site, the standardised series were averaged. These temporal series or master chronologies expressed the annual variations in radial growth of *P. pinaster* at each sampling place. The quality of the chronologies was evaluated using the mean sensitivity (MS) (Schweingruber 1996), the signal-to-noise ratio (SNR) (Fritts & Swetnam 1989) and the expressed population signal (EPS) (Wigley et al. 1984). A chronology is considered to be confident with a higher than 0.85 EPS value. The common growth signal between residual chronologies was analysed using the Pearson correlation coefficient (Sokal & Rohlf 1995).

To determine the climatic variables that control the growth of *Pinus pinaster*, atmospheric indexes were compared with residual chronologies from June previous to the growing season to September of the current growth year during the period 1950-2005. The PRECON program version 5.17 (Fritts 1999 available at: www.ltrr.arizona.edu) was used. This is a statistical model for analysing the tree-ring response to variations in climate using a stepwise multiple regression analysis. The coefficients are considered significant at a 95% level of confidence. The program also includes a bootstrapped response function to improve the statistical significance of the regression coefficient ($p < 0.05$). In this analysis 999 interactions were made. To analyse the time dependent relationship between these atmospheric indexes and radial growth, Kalman filter analysis was applied (Visser & Molenar 1988).

Results

An evaluation of climate atmospheric indexes impact on radial growth of Mediterranean Maritime pines has been carried out. This evaluation was based on a dendrochronological analysis of dominant and co-dominant trees in four stands in Eastern Spain.

The descriptive statistic of all the chronologies showed that the mean sensitivity varied from 0.2571 to 0.3779, and the standard deviation varied from 0.2555 to 0.3179, according to the sampling site. The SNR fluctuated from 29.087 to 68.444, and the EPS values varied from 0.967 to 0.986. The total period covered by the chronologies varied from 120 in the shortest chronologies, to 162 years in the longest ones (Tab. 1).

Table 1: Coordinates, altitude, basal area (BA) and descriptive statistic of the four Pinus pinaster chronologies in Eastern Spain. SD: standard deviation; MS: mean sensibility; SNR: Signal to noise ratio; EPS: Expressed population signal. Te: Teruel; Cu: Cuenca; Va: Valencia; Al: Albacete.

	Te	Cu	Va	Al
UTM_X	639753	638858	648053	645583
UTM_Y	4464496	4467569	4411314	4411593
Altitud (m)	1437	1364	970	1090
BA($m^2.ha^{-1}$)	40.17	45.73	36.66	34.74
Time span	1844-2005	1847-2005	1879-2005	1886-2005
Core number	26	29	26	30
Ring number	3757	4128	2723	3043
Age range	124-162	124-158	72-127	72-120
SD	0.2589	0.3179	0.2555	0.2764
MS	0.2992	0.3708	0.2571	0.2978
SNR	29.087	68.444	38.528	36.254
EPS	0.967	0.986	0.975	0.973
Variance in first eigenvector	54.85	71.41	62.78	59.62
Mean correlation among trees	0.528	0.702	0.606	0.573

DOI:10.2312/GFZ.b103-08056

The four chronologies showed high SNR (over 29.087) and EPS (over 0.967), and the percentage of the variance accounted for the first eigenvector (over 54.85) reflected a strong common signal related to climatic-environmental factors. The Pearson correlation coefficient between all residual chronologies varied from 0.37 to 0.76 in the 1887-2005 common growth period (DF = 111 and p*< 0.05). The association between radial growth and monthly climatic atmospheric indexes is shown in figure 2. The total variance explained by atmospheric indexes varied from 8.95 to 37.46%.

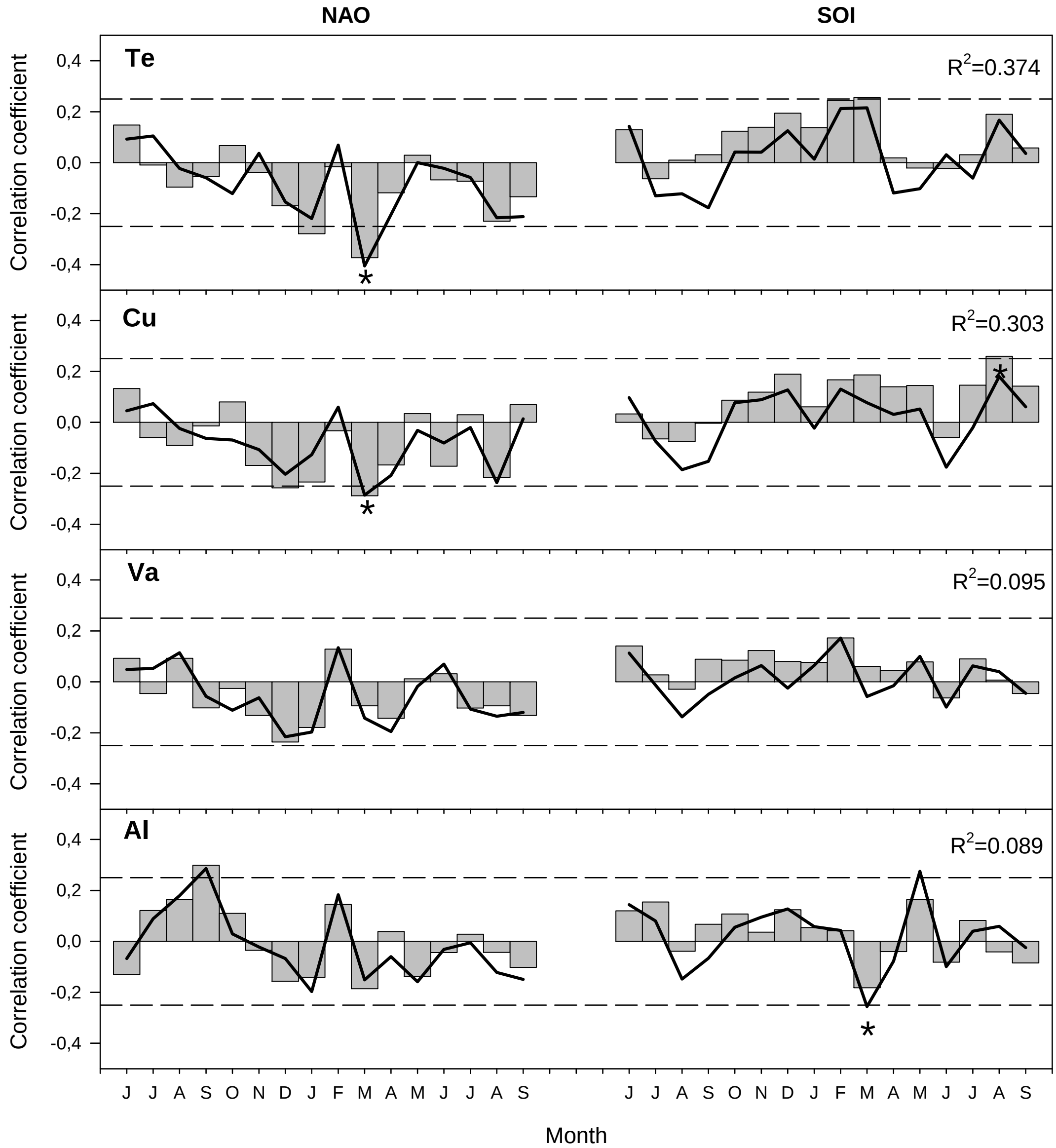

Figure 2: Regression coefficients (bars) and bootstrapped response function (lines) which relate the effect of climatic atmospheric indexes and growth of Pinus pinaster during the 1950-2005 period. The analysed period is from June to the previous growing season to September of the current growing season. Bars higher than the dashed lines show significant coefficient at the 0.05 level. Asterisks point the months where the bootstrapped response function coefficients are significant at the 0.05 level. R^2 values show the total variance explained by both indexes. Sites codes: Te: Teruel; Cu: Cuenca; Va: Valencia; Al: Albacete

The total variance explained by the NAO and SOI indexes is higher in the sites at higher positions (chronologies Te and Cu). In these places there is a significant negative

DOI:10.2312/GFZ.b103-08056

association between the NAO index and growth during January and March (site Te) and December and March (site Cu), but only March is significant in the bootstrapped analysis. Only one place showed a positive association with NAO values during September prior to the growing season (Site Al), but this association was not significant in the bootstrapped analysis. The association with the SOI was positive in all the analysed sites, but it was only significant, in the correlation coefficient and the in the bootstrapped response function, in place Cu. Only site Al showed a negative association with the SOI, shown by the bootstrap coefficient during March previous to the growing season.
The Kalman filter showed that no place showed a changing association through time with NAO index. Only place Te showed a changing association with SOI, statistically significant in February, from 1982 to 1987. This significant association was coincident with the strongest El Niño phenomena recorded during the last century.

Discussion

It is difficult to find a simple linear correlation between radial growth and atmospheric indexes because their global effects and their impact on regional climatic variables are not yet completely understood.
In these results, the total variance explained by NAO and SOI indexes suggested that the signal is weak if it is compared with regional climatic variables. However, the negative correlation with NAO during winter in two sites, and the changing effect of SOI index through time in one site, offer new information about the association between atmospheric indexes and coniferous species growing in the Iberian Peninsula.
Although atmospheric indexes explain less variability than other regional climatic variables, these results emphasis that these indexes effects could be recorded on tree-ring and they could have a sensible effect in growth of woody species, even if their action centres are located too far away from the analysed sites.
Previous studies have determined an opposite relation between winter NAO index and precipitation on the Iberian Peninsula (Esteban Parra et al.1998) and in this study two sites showed a negative winter correlation with the NAO index, consequently, these results suggest that these negative relation between NAO and growth could be associated with a moisture availability that could affect growth. Also, NAO effect is related to altitudinal position: the highest sites showed a significant relation with NAO during winter but there was no association with NAO values at the lowest analysed sites.
The association between growth and the NAO index was different from *Pinus sylvestris* across Northern Fennoscandia where this species had a positive correlation between early winter NAO indexes previous to the growing season and late spring NAO (Macias et al. 2004). In our study, only one place showed a positive association with the NAO during the autumn previous to the growing season. The positive correlation these authors found in Fennoscandia between the NAO winter index and growth does not exist in Spanish Mediterranean Maritime pine forests at any sampling site. This difference could be explained by the fact that the effect of the NAO index on Northern Europe is opposite to the effect in Southern (Hurrel 1995).

DOI:10.2312/GFZ.b103-08056

In Spain, the relation between the SOI and plant growth has only been previously analysed on annual crops (Gimeno et al. 2002). As far as we know, there is no study focused on forest growth related to the SOI in our region. According to Trenberth et al. (1998) the SOI index mainly affects the Pacific area, but they consider that its effect might also influence climatic variability on a global scale. In this study a positive association was found between the index named above and growth in August in one of the highest sites, and negative in March in one of the lowest altitudinal position sites. Unfortunately, previous studies on the SOI effect in Spain are contradictory, as a consequence of that, future studies have to be made in order to understand better the opposite effect, according to the site and the changing impact through time. Modelling the impact of climate change on the distribution of species on a European scale under future climatic scenarios, Spain's environment will become unsuitable for *Pinus pinaster* by 2080 (Harrison et al. 2006). This would be coherent if growth were associated with precipitation, but the comprehensive general circulation models used for future climate projections leave us with an indeterminate picture of ENSO's future. Some observers predict more ENSO activity, others less, with the highly uncertain forecast consensus indicating little change (Cane 2005). Considering that this index shows a peculiar association with growth, which changes through time, future studies will have to be carried out.
Results can serve both, to understand climate/forest growth associations, and to determine which climatic variables can be useful for improving empirical models in order to help forest managers to adopt decisions in the future within the context of an extremely unpredictable climatic scenario.

Acknowledgements
The authors thank Cristobal Ordóñez for field assistance.This study was supported by the Research project from Junta de Castilla y León (Spain) Code: AGL 2004-07094-CO2- and by the Programme Alβan, the European Union Programme of High Level Scholarships for Latin America, scholarship # E05D049920AR.

References

Bjerknes, J. (1966): A possible response of the atmospheric Hadley circulation to equatorial anomalies of ocean temperature. *Tellus 18:* 820–829.

Blanco, E., Casado, M., Costa, M., Escribano, R., Gracía Antón, M., Génova, M., Gómez Manzaneque, G., Gómez Manzanaque, F., Moreno, J., Morla, C., Regato, P., Sainz Ollero, H. (1997): Los bosques ibéricos. Editorial Planeta.

Cane, M. (2005): The evolution of El Niño, past and future. *Earth and Planetary Science Letters 230*: 227-240.

Cook, E.R., Holmes, R.L. (1984): Program ARSTAN users manual. Lab. Tree Ring. Res. Univ. of Arizona, Tucson, Arizona, EUA.

Cook, E.R., Glitzenstein, J.S., Krusic, P.J., Hracombe, P.A. (2001): Identifying functional groups of trees in west Gulf Coast forests USA: a tree-ring approach. *Ecological applications 11*: 883-903.

Esteban-Parra, M., Rodrigo, F., Castro Diéz, Y. (1998): Spatial and temporal patterns of precipitation in Spain for the period 1880-1992. *Int. Journal of Climatology 18*: 1557- 1574.

Fritts, H.C. (1976): Tree Ring and Climate, Academic Press Inc, London.

Fritts, H.C. (1999): PRECON vers. 5.17, http://www.arizona.edu/webhome/hal/dlprecon.html

Fritts, H.C., Swetnam, T. (1989): Dendroecology: a tool for evaluating variations in past and present forest environments. *Advances in Ecological Research 19:* 111-188.

Gimeno, L., Ribera, P., Iglesias, R., de la Torre, L., García, R., Hernández, E. (2002): Identification of empirical relationships between indices of ENSO and NAO and agricultural yields in Spain. *Climate research 21*: 165-172.

Grissino-Mayer, H.D. (2001): Assessing crossdating accuracy: a manual and tutorial for the computer program COFECHA. *Tree-Ring Res. 57*: 205–221.

Harrison, P., Berry, P., Butt, N., New, M. (2006): Modelling climate change impacts on species' distributions at the European scale: implications for conservation policy. *Environmental Science & Policy 9:* 116-128.

Hughes, M. (2002): Dendrochronology in climatology – the state of the art. *Dendrochronologia 20:* 95-116.

Hurrell, J.W. (1995): Decadal trends in the North Atlantic Oscillation and relationships to regional temperature and precipitation. *Science 269:* 676-679.

Hurrel, J., Van Loon, H. (1997): Decadal variations in climate associated with the North Atlantic Oscillation. *Clim. Change 36:* 301-326.

Jones, P.D., Jonsson, T., Wheeler, D. (1997): Extension to the North Atlantic Oscillation using early instrumental pressure observations from Gibraltar and South-West Iceland. *Int. J. Climatol. 17:* 1433-1450.

Macias, M., Timonen, M., Kirchhefer, A., Lindholm, M., Eronen, M., Gutiérrez, E. (2004): Growth variability of Scots pine (*Pinus sylvestris* L.) along a west-east gradient across northern Fennoscandia: a dendroclimatic approach. *Arct. Antart. Alpine Res. 36*: 565-574.

Schweingruber, F.H. (1996): Tree rings and environment: Dendroecology, Haupt, Berne.

Sokal, R.R., Rohlf, F.J. (1995): Biometry: the principles and practice of statistics in biological research, 3rd edition, WH Freeman and Co., New York, UEA.

Stokes, M.A., Smiley, T.L. (1968): An Introduction to Tree-Ring Dating, University of Arizona Press, Tucson, UEA.

Trenberth, K., Branstator, G., Karoly, D., Kumar, A., Lau, N., Ropelewski, C. (1998): Progress during TOGA in understanding and modelling global teleconnections associated with tropical sea surface temperatures. *Journal of Geophysical Research 103*: 14291–14324.

Visser, H., Molenaar, J. (1988): Kalman filter analysis in dendroclimatology. *Biometrics 44:* 929-940.

Wigley, T.M.L., Briffa, K.R., Jones, P.D. (1984): On the average value of correlated time series, with applications in dendroclimatology and hydrometeorology. *J. Clim. Appl. Meteorol. 23:* 201-213

Seasonal growth dynamics and its climate forcing in a tropical mountain rain forest in southern Ecuador

A. Bräuning, P. von Schnakenburg, F. Volland-Voigt & T. Peters

Institute of Geography, University of Erlangen-Nuremberg, Kochstr. 4/4, D-91054 Erlangen, Germany

Email: abraeuning@geographie.uni-erlangen.de

Introduction

Tree ring series are a well established data source to derive urgently needed long-term palaeoclimate information. In contrast to formerly widely accepted assumptions, even in the humid tropics trees do not grow continuously. Irrespective of the formation of clearly distinguishable ring boundaries, many tropical tree species show pronounced growth variations triggered by fluctuations in temperature, water availability and phenology (Bauch et al. 2006; Bräuning & Burchardt 2006; Détienne 1989; Devall et al. 1995; Dünisch et al. 2002; Sass et al. 1995; Verheyden et al. 2004). An understanding of the linkage between growth dynamics and seasonal climatology is fundamental to derive climate reconstructions from tree-ring analysis. Stem diameters can vary on diurnal (day-night cycle), short-term (water shortage) and long-term (stem growth by cambial activity) time scales. Long-term variations are the result of radial growth, whereas short-term stem diameter variations reflect changes of the internal water status. This study sheds light on seasonal and short-term growth variations of tropical trees and relates them to climate and local site conditions.

Material and Methods

The study area is located at ca. 4°S at the northern rim of Podocarpus National Park in Southern Ecuador. The three sites A, B and C are located on a slope with northern exposure at an altitude of 2030 m, 1970 m and 1980 m a.s.l., respectively. Sites A and B are located in straight slope positions, whereas site C is located in a small valley. Electronic dendrometers were attached to a total number of 11 trees in the three sites. Among the many species present, trees from the species *Prumnopitys montana* (Podocarpaceae), *Cedrela cf. montana* (Meliaceae), *Inga acreana* (Mimosaceae) and *Nectandra laevis* (Lauraceae) were selected because of their wood anatomy that allows the detection of more or less distinct growth boundaries (Fig. 1). The studied species belong to different life forms: While *Inga* and *Nectandra* are evergreen broadleaved species, *Cedrela* is deciduous broadleaved and *Prunmopitys* is an evergreen conifer.

The use of dendrometers is a standard approach to register growth rates of trees inside and outside tropical climate zones (e.g. Biondi et al. 2005; Hauser 2003). Band dendrometers that measure changes in the circumference of a tree stem are not able to detect short-term variations in the stem size as a result of fluctuations in the water status of the tree. Therefore, they integrate the long-term water status of a stem and long-term growth rates, but they are not suited to study the process of real xylem growth and short-term growth rhythms of trees (Homeier 2004; Kuroda & Kiyuno 1997). In March 2006, we installed point dendrometers in a

DOI:10.2312/GFZ.b103-08056

height of ca. 1.5 m of the stems at a position parallel to the slope to avoid a possible influence of reaction wood. Measurements of stem radius changes were taken in 30 min. intervals and stored in a data logger.

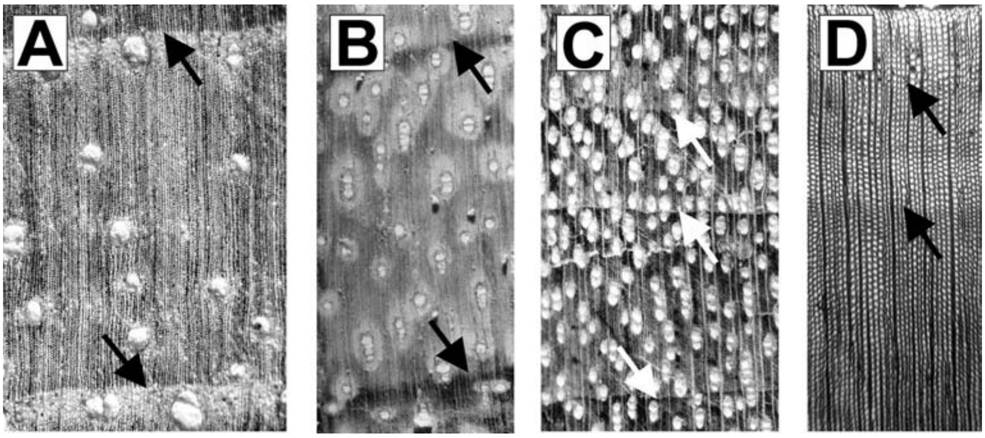

Figure 1: Macroscopic images of Cedrela montana (A), Inga acreana (B), Nectandra laevis (C) and Prumnopitys montana (D). Growth boundaries are marked with arrows.

Climate data were collected from a climate station in ca. 1 km horizontal distance of the study plots in an altitude of 1950 m a.s.l. Mean annual temperature is around 16°C and shows only marginal seasonal variations (Bendix et al. 2006). Annual mean rainfall amounts to 2176 mm, in addition ca. 120 mm of available water from cloud and horizontal rain water deposition have to be considered. Maximum rainfall amounts are registered during March to July. Between August to February, average monthly rainfall amounts between ca. 110-160 mm. However, even in the relatively drier months, monthly sums of rainfall exceed evaporation, so that climate conditions are humid in all months of the year (Bendix et al. 2006). However, it becomes clear that rainless periods of more than two consecutive weeks may occur (Fig. 2).

Results

Figure 2 shows the dendrometer curves for 2006. Unfortunately, some missing values occurred after several weeks of measurement. Nevertheless, the growth curves reveal several interesting facts:

- Different tree individuals of the same species but from different study plots show widely varying absolute growth increment rates during the studied period.
- Despite differences in absolute growth rates, short-term stem diameter fluctuations are astonishingly synchronous among all trees. This applies not only for individuals of the same species, but for all trees of all studied species and live forms.
- Periods of stem shrinkage can be attributed to time periods without rainfall. After only several days without precipitation, growth increments stop or stem diameters even start to shrink. The degree of stem diameter shrinkage is different between individual trees and probably depends on the water storage capacity of the local soils.

DOI:10.2312/GFZ.b103-08056

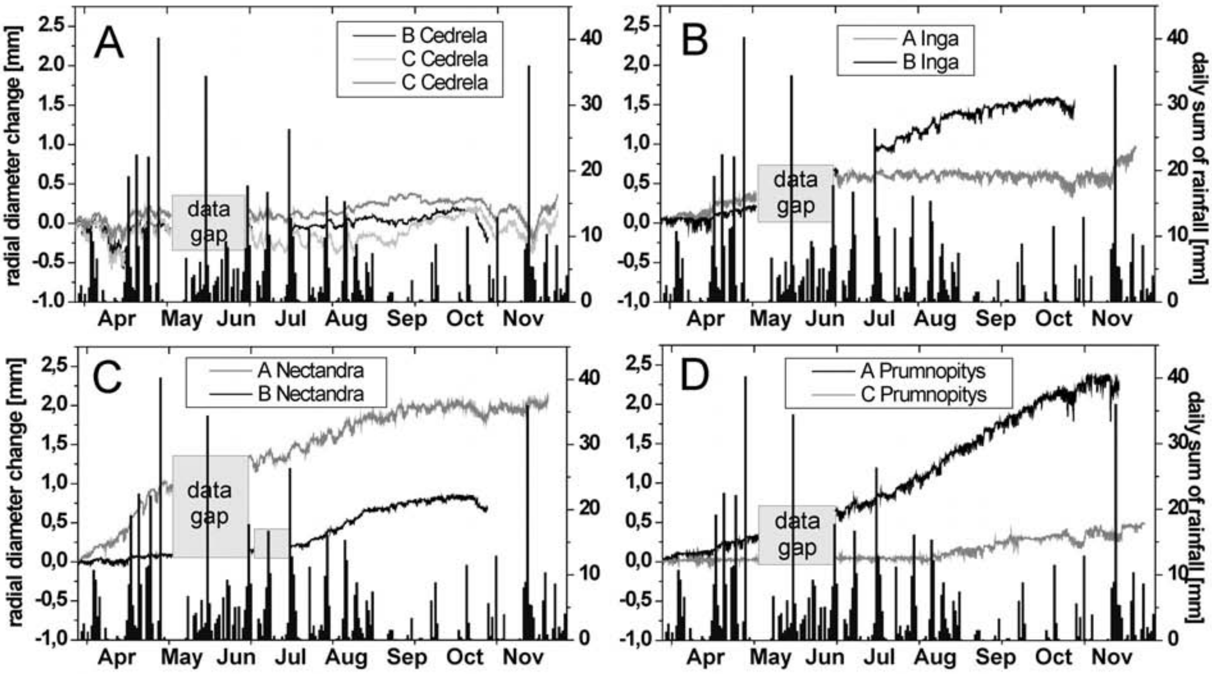

Figure 2: Dendrometer growth curves for Cedrela montana (A), Inga acreana (B), Nectandra laevis (C) and Prumnopitys montana (D).Capital letters A, B and C in the legend point to the trees' location in the respective study plot.

Discussion

We found that even in an environment with very humid average climatic conditions, tree growth is limited by water availability. Cambial activity reacts very sensitively to moisture supply and after only several days without rain, increment rates drop and stem diameters start to shrink since transpiration rates probably exceed water uptake. Absolute growth rates are strongly influenced by the local soil conditions and probably also by crown competition and social tree status (Bräuning et al. 2007). Further investigations shall combine growth increment measurements with wood anatomical studies to study the interrelation between water shortage, growth increment and the formation of visible growth boundaries (Bräuning & Burchardt 2006). This will be the basis for an interpretation of tree-ring series derived from increment cores and for the climatological interpretation of ring width chronologies.

Acknowledgements

The authors are indebted to the German Research Foundation (DFG) for financial support of the projects BR 1895/8-1-2 (FOR 402) and BR 1895/14-1 (FOR 816).

References

Bauch, J., Quiros, L., Noldt, G., Schmidt, P. (2006): Study on the wood anatomy, annual wood increment and intra-annual growth dynamics of Podocarpus oleifolius var. macrostachyus from Costa Rica. *Journal of Applied Botany and Food Quality* 80: 19-24.

Bendix, J., Homeier, J., Cueva Ortiz, E., Emck, P., Breckle, S.-W., Richter, M., Beck, E. (2006): Seasonality of weather and tree phenology in a tropical evergreen mountain rain forest. *International Journal of Biometeorology* 50: 370-384.

Biondi, F., Hartsough, P. C., Estrada, I. G. (2005): Daily weather and tree growth at the tropical treeline of North America. *Arctic, Antarctic and Alpine Research* 37 (1): 16-24

Bräuning, A., Burchardt, I. (2006): Detection of growth dynamics in tree species of a tropical mountain rain forest in southern Ecuador. *TRACE - Tree Rings in Archaeology, Climatology and Ecology,* Vol. 4: 127-131.

Bräuning A, Homeier J, Beck E, Günter S (2007): Growth dynamics of trees in tropical mountain ecosystems. *Ecological Studies, in press.*

Détienne P. (1989): Appearance and periodicity of growth rings in some tropical woods. *IAWA Bulletin* 10: 123-132.

Devall, M. S., Parresol, B. R., Wright, S. J. (1995): Dendroecological analysis of Cordia alliodora, Pseudobombax septenatum and Annona spraguei in central Panama. *IAWA Journal* 16 (4): 411-424.

Dünisch, O., Bauch, J., Gasparotto, L. (2002): Formation of increment zones and intraannual growth dynamics in the xylem of Swietenia macrophylla, Carapa guianensis, and Cedrela odorata (Meliaceae). *IAWA Journal* 23: 101-119.

Hauser, S. (2003): Dynamik hochaufgelöster radialer Schaftveränderungen und des Dickenwachstums bei Buchen (*Fagus sylvatica* L.) der Schwäbischen Alb unter dem Einfluss von Witterung und Bewirtschaftung. *Dissertation Universität Freiburg.*

Homeier, J. (2004): Baumdiversität, Waldstruktur und Wachstumsdynamik zweier tropischer Bergregenwälder in Ecuador und Costa Rica. *Dissertationes Botanicae* 391: 207 p.

Kuroda, K., Kiyono, Y. (1997): Seasonal rhythms of xylem growth measured by the wounding method and with a band-dendrometer: an instance of Chamaecyparis obtusa. *IAWA Journal* 18: 291-299.

Sass, U., Killmann, W., Eckstein, D. (1995): Wood formation in two species of Dipterocarpaceae in peninsular Malaysia. *IAWA Journal* 16: 371-384.

Verheyden, A., Kairo, J. G., Beeckman, H., Koedam, N. (2004): Growth rings, growth ring formation and age determination in the mangrove Rhizophora mucronata. *Annals of Botany* 94: 59-66.

A challenge for spatially explicit reconstructions: the climate response of trees is a function of climate

D. Frank[1], O. Bouriaud[2], R. Wilson[3], G. Battipaglia[1], U. Büntgen[1], P. Fonti[1], K. Treydte[1], V. Trouet[1] & J. Esper[1]

[1] Swiss Federal Research Institute WSL, 8903 Birmensdorf, Switzerland

[2] Forest Research and Management Institute, 725100 Câmpulung Moldovonesc, Romania

[3] School of Geography & Geosciences, University of St. Andrews, St. Andrews, Scotland, United Kingdom

Email: frank@wsl.ch

Introduction

It is well known that ambient climate conditions, modulated by site ecology, place limitations on tree growth (Fritts 1976). Year-to-year variations in local climate result in more or less severe growth constraints that typically are reflected as narrower or wider annual rings. Accordingly, dendroclimatic investigations target sampling locations where the limitation from one climatic element -- the reconstruction target -- is dominant. Thus skillful temperature reconstructions from tree-ring width (TRW) require data from trees growing near the theoretical thermal limit sufficient for survival, i.e., the elevational or latitudinal treeline. For these reasons, local, regional, and hemispheric temperature reconstructions are weighted towards the high latitudes or mountainous areas. These biogeographic and plant physiological constraints may hinder efforts to develop spatial reconstructions seeking to utilize data well distributed over the earth's land surface.

Within the European region, significant progress has been made in understanding longer-term, spatially-resolved, climate variations via multi-proxy studies (Luterbacher et al. 2004). Such efforts rely heavily upon long-instrumental series (Auer et al. 2007) and documentary evidence (Brazdil et al. 2005; Pfister 1999), which are either non-existent or increasingly scarce prior to about 1500 AD. Over longer time scales, the relevance of natural proxies increases for understanding climate variations across Europe. In this regard, and in line with the previously stated limitations, successful long-term efforts utilizing TRW data include temperature reconstructions for Scandinavia (Grudd et al. 2002), the European Alps (Büntgen et al. 2005), and the Carpatian Arc (Büntgen et al. 2007). In contrast, long precipitation or drought reconstructions have been developed for southern Germany (Wilson et al. 2005) and Morocco (Esper et al. 2007) and in the Mediterranean basin (Griggs et al. 2007).

It would obviously be desirable to fill the large spatial gaps that exist between current local reconstructions, so that more meaningful assessments of spatial climate variability can be derived. This could either be achieved by determining suitable locations, which have not yet been targeted for sampling, and/or finding proxy-types or parameters, such as isotopic data (Treydte et al. 2006) or quantifiable wood anatomical features (Fonti et al. 2007) that most skillfully serve in all regions.

Herein we compile a network of TRW data and analyze the climatic response as a function of the climate itself. We attempt to characterize the importance of forcing factors on growth for

DOI:10.2312/GFZ.b103-08056

the European region in terms of geographic position and climatic state-space. Broad concepts analyzed herein are well known from dendrochronological principles, large network analysis (Neuwirth et al. 2007), and modeling studies (Nemani et al. 2003), however, implications for spatially-resolved climate reconstructions, especially in consideration of recent and rapid warming, may make such a compilation relevant.

Data and Methods

The compiled network consists of nearly all sites available from the International Tree Ring Databank within the European Region (10°W- 20°E, 30°N-70°N). Tree-ring data were detrended on a site-by-site basis in ARSTAN (Cook 1985) using both 32-year splines to emphasize decadal to interannual scale variation and Regional Curve Standardization (RCS; Esper et al. 2003) to preserve inter-annual to centennial-scale variability. It should be noted that the predominant nature of the network (low sample replication and sites with only living trees) adds uncertainties particularly to the RCS results.

A biweight robust mean (Cook 1985) was used to average the detrended series together for each site, and the variance was subsequently stabilized to prevent artifacts related to changes in sample replication (MEANr correction as in Frank et al. 2007). Initial screening and quality control resulted in the identification of 403 sites with data in the 20th century. Chronologies were truncated at a sample replication of >4 series and were additionally required to have at least 60 years of data (after truncation) within the 1901-2002 period. This second step resulted in 376 sites for the final analysis.

All detrended data were correlated with various monthly and seasonal gridded temperature and precipitation data from the nearest gridpoint of the CRUT2.1 0.5° x 0.5° dataset (Mitchell & Jones 2005). In addition to computations with the raw data, correlations were also calculated for high and low-pass filtered (30-year spline) TRW and instrumental series.

For analyses related to absolute climatic conditions, we calculated the elevational difference between tree-ring sites and the elevation corresponding to the CRUT2.1 grid-cell. A lapse rate of 6.5 °C/km was utilized to adjust the instrumental mean temperature. For the five cases where elevation data were not available, no adjustments were made. Precipitation data were not adjusted.

Results

Correlations, expressed as grey shades, between mean June-August (JJA) temperature and RCS TRW data (both high-pass filtered) were plotted as a function of the mean annual temperature (y-axis) and mean monthly precipitation (x-axis) for each site (Fig. 1, upper panel). It is evident that the highest correlations are obtained for sites with low mean annual temperatures, with relatively little dependence upon summer precipitation. Geographically, sites with highest correlations are found in Scandinavia and along the Alpine arc (Fig. 1, lower panel). The Northern UK and the Pyrenees mountains also contain sites with moderately high correlations to summer temperature. A similar but opposite pattern is observed for JJA precipitation with highest correlations obtained for sites with low mean annual precipitation and high mean annual temperatures (Fig. 2, upper panel). Compared to the temperature response patterns, sites with highest correlations to precipitation data are more widely distributed, and in fact, cover most areas of Europe except for the northern United Kingdom, northern Scandinavia, and surprisingly much of Italy (Fig. 2, lower panel). Similar results were obtained with the unfiltered and spline-detrended chronologies (not shown).

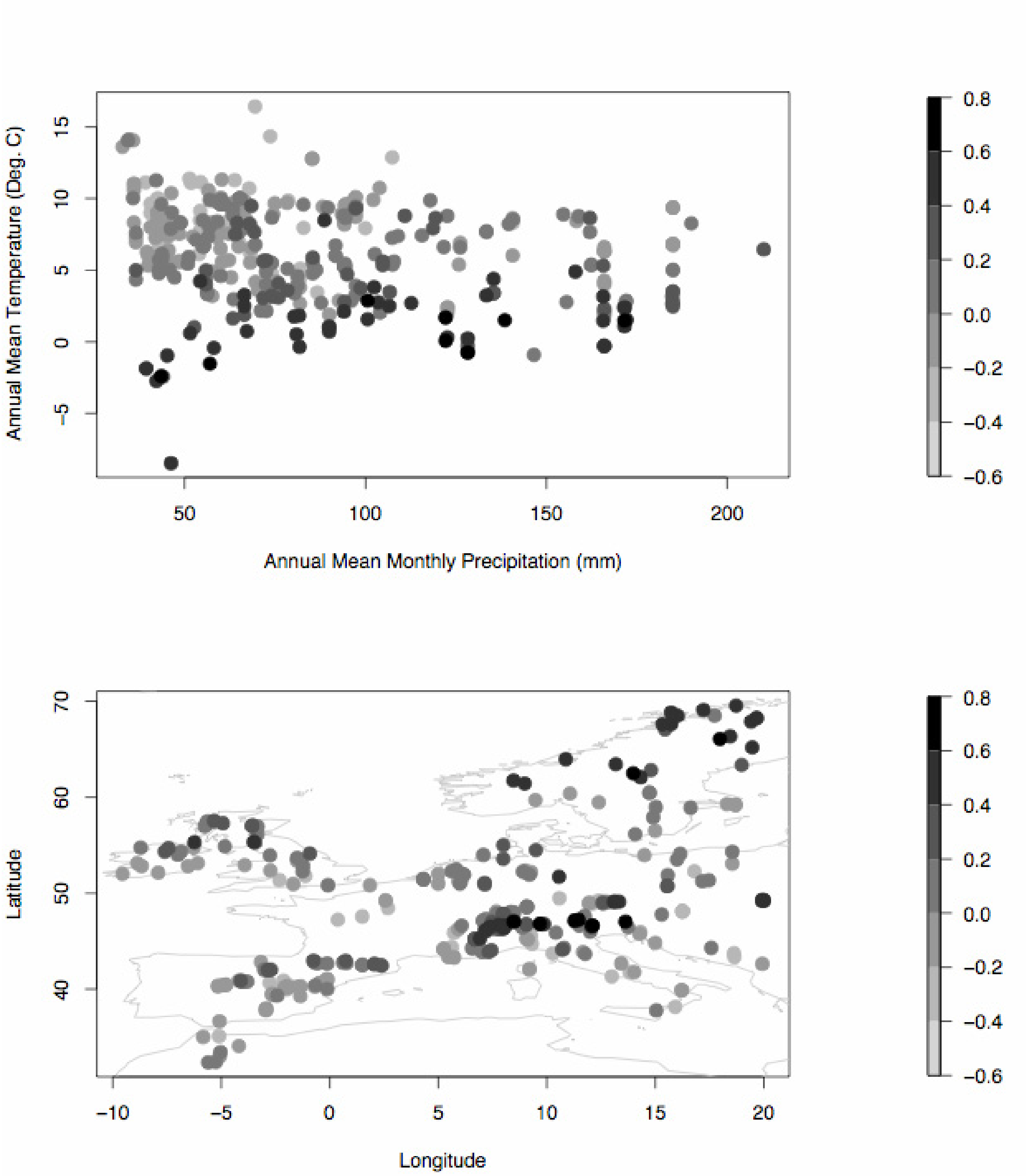

Figure 1: Correlations between TRW chronologies and JJA temperature data, plotted as a function of annual mean temperature and monthly mean precipitation at each site (upper) and according to geographic position (lower).

DOI:10.2312/GFZ.b103-08056

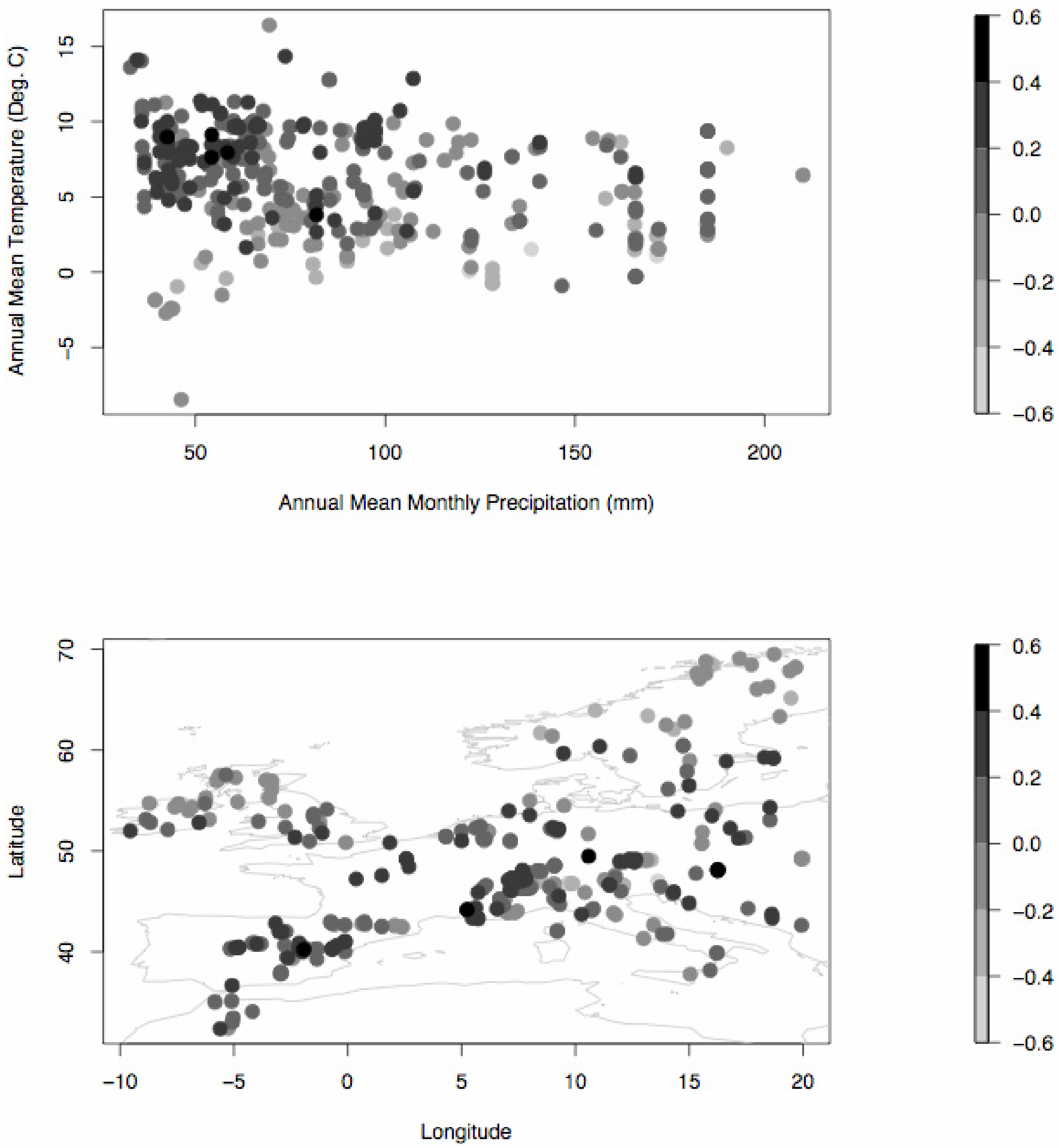

Figure 2: As figure 1, except for correlation between TRW chronologies and JJA precipitation data.

Given the apparent spatial constraints for temperature sensitive TRW data, it might be relevant to ask how spatially representative would the average of two reconstructions, one from Scandinavia and one from the Alps, be for the European landmass. To provide a simple assessment, we averaged JJA station temperature data from Haparanda (65.83N, 24.15E; Sweden) and Säntis (47.25N,9.35E; Switzerland) and correlated the mean series with all JJA CRUT2.1 gridpoints. As expected, this average has two correlation epicenters: northern Scandinavia and along and north of the Alpine arc (Fig. 3). However, what is perhaps surprising, especially when considering that this result is derived from instrumental series free of any proxy noise, is that the variance explained for most of Europe is rather low and is in fact only > 50% for only a small region in Scandinavia. This has to do with the broad independence -- at least in the frequency domains represented by the summer season instrumental data -- for temperatures between the Alpine and Scandinavian regions. The correlation between the JJA instrumental series from these regions is only 0.07. The development of two regional reconstructions or a more generalized point-by-point approach (Cook et al. 1994), possibly represent reasonable and simple solutions to increasing the explained variance for most European areas.

However, it should be noted, if we do not care about spatially resolved reconstructions, and seek to reconstruct European average temperatures, a simple average of the JJA temperatures from the 5637 gridpoints within the European region bounded by 30-70° N and -10-40°E correlates with the Säntis-Haparanda mean at .791 (> 60% variance explained) over the 1901-1991 common period. This result demonstrates increased skill of these two locations (and methodology) for assessing average European temperatures, although with the caveat that this mean is spatially biased in accordance with figure 3.

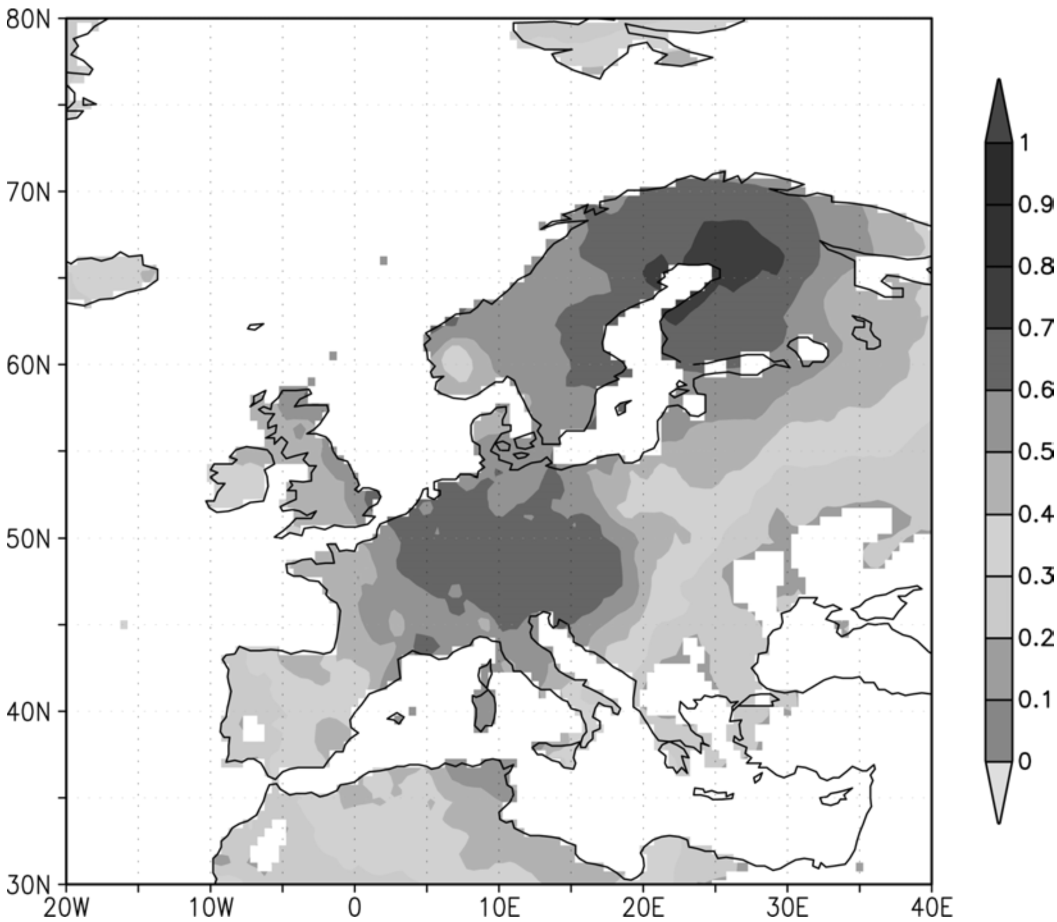

Figure 3: Correlation between the mean of Säntis and Haparanda JJA temperatures and JJA temperature from the CRUT2.1 dataset computed over the 1901-1991 period.

DOI:10.2312/GFZ.b103-08056

Discussion and Conclusions

Using a large European network, we have demonstrated how the climate response of TRW data is closely related to climate itself. This fact, although well-established in the dendrochronological literature, has implications for the spatial reconstruction and representation of climate variability. Additional assessment of other tree-ring parameters, including maximum-latewood density, earlywood/latewood width, isotopic composition, and vessel data will help determine the possibilities and limitations for dendroclimatic efforts within Europe and beyond. It has been shown, for example, that maximum latewood density generally has a stronger climatic response with a more “forgiving” climatic and ecological range than TRW data (Frank and Esper, 2005; Kienast et al. 1987).

Our results have quantified the well known dendrochronological principle -- the need to go to the elevational or latitudinal treeline for most skillful temperature reconstructions -- based on numerous sites across Europe. While maximum JJA correlations are lower for precipitation than for temperature, better quantification of the optimal target season is needed. It is likely that a dendroclimatic year spanning previous August to current July is a more appropriate season for precipitation reconstructions (not shown). The broader spatial area of tree-ring sites that correlate significantly with precipitation variations is promising for the development of spatially resolved precipitation or drought reconstructions. This is critical because of the much lower spatial autocorrelation for precipitation than for temperature. The length of most currently existing records will place limitations on the length of any such reconstructions, however.

If we assume that the response-gradients demonstrated, represent physiological limitations for trees to respond in the same way to a variable climate, the ability of TRW data to serve as a valid predictor across a wide range of climate conditions is perhaps limited. This might serve as a conceptual basis for concerns of reductions in temperature sensitivity (e.g., D’Arrigo et al. 2007) and demonstrate the utility of pointer-year analysis (Schweingruber 1986) and/or forward growth modeling studies (Anchukaitis et al. 2006) to understand the suite of climatic parameters that jointly act in forcing wide and narrow sequences in tree-ring data. Further studies along elevational transects (Wilson & Hopfmueller 2001) or using growth-climate response surfaces may also provide insight into the climate forcing of forest growth across a wide-range of climate conditions.

Acknowledgements

We thank Anne Verstege for help in compiling this dataset and Gerd Helle for comments on an earlier draft. This research is supported by the Swiss National Science Foundation (NCCR-Climate), the EU (Millennium #017008-2), and the MAIF foundation (project ECLID).

References

Anchukaitis, K.J., Evans, M.N., Kaplan, A., Vaganov, E.A., Hughes, M.K., Grissino-Mayer, H.D., Cane, M.A. (2006): Forward modelling of regional-scale tree-ring patterns in the southeastern United States and the recent influence of summer drought. Geophysical Research Letters 33: L04705. doi: 10.1029/2005/GL025050.

Auer, I., and 31 Co-authors (2007): HISTALP – Historical instrumental climatological surface time series of the Greater Alpine Region. International Journal of Climatology 27: 17-46. doi:10.1002/joc.1377.

Brázdil, R., Pfister, C., Wanner, H., von Storch, H., and Luterbacher, J. (2005): Historical climatology in Europe – The State of the Art, Climatic Change, 70, 363 - 430.

Büntgen, U., Esper, J., Frank, D.C., Nicolussi, K., Schmidhalter, M. (2005): A 1052-year tree-ring proxy for Alpine summer temperatures. Climate Dynamics 25, 141-153.

Büntgen, U., Frank, D.C., Kaczka, R.J., Verstege, A., Zwijacz-Kozica, T., Esper, J. (2007): Growth/climate response of a multi-species tree-ring network in the Western Carpathian Tatra Mountains, Poland and Slovakia. Tree Phyiology 27, 689-702.

Cook, E.R. (1985): A time series analysis approach to tree-ring standardization. PhD dissertation, University of Arizona, Tucson, AZ.

Cook, E.R., Briffa, K.R., Jones, P.D. (1994): Spatial regression methods in dendroclimatology: a review and comparison of two techniques. International Journal of Climatology 14: 379-402.

D'Arrigo, R., Wilson, R., Liepert, B and Cherubini, P. (2007): On the 'Divergence Problem' in Northern Forests: A Review of the Tree-Ring Evidence and Possible Causes. Global and Planetary Change. In press.

Esper, J., Cook, E.R., Krusic, P.J., Peters, K., Schweingruber, F.H. (2003): Tests of the RCS method for preserving low-frequency variability in long tree-ring chronologies. Tree-Ring Research 59, 81-98.

Esper, J., Frank, D., Büntgen, U., Verstege, A., Luterbacher, J., Xoplaki, E. (2007): Long-term drought severity variations in Morocco. Geophysical Research Letters 34, doi: 10.1029/2007GL030844.

Fonti, P., Solomonoff, N., García-González, I. (2007): Earlywood vessels size of Castanea sativa records temperature before their formation. New Phytologist 173, 562-570.

Frank, D., Esper, J. (2005): Characterization and climate response patterns of a high-elevation, multi-species tree-ring network for the European Alps. Dendrochronologia 22, 107-121.

Frank, D., Esper, J., Cook, E.R. (2007): Adjustment for proxy number and coherence in a large-scale temperature reconstruction. Geophysical Research Letters 34, doi: 10.1029/2007GL030571.

Fritts, H.C. (1976): Tree rings and climate. Academic Press, London, pp 567.

Griggs, C.B., Degaetano, A.T., Kuniholm, P.I., Newton, M.W., (2007): A regional reconstruction of May-June precipitation in the north Aegean from oak tree-rings, AD 1089-1989. International Journal of Climatology 27, 1075-1089.

Grudd, H., Briffa, K.R., Karlen, W., Bartholin, T.S., Jones, P.D. and Kromer, B. (2002): A 7400-year tree-ring chronology in northern Swedish Lapland: natural climatic variability expressed on annual to millennial timescales. The Holocene, 657-665.

Kienast, F., Schweingruber, F.H., Bräker, O.U., Schär, E., 1987: Tree-ring studies on conifers along ecological gradients and the potential of single-year analyses. Canadian Journal of Forest Research 17, 683 - 696.

Luterbacher, J., Dietrich, D., Xoplaki, E., Grosjean, M., Wanner, H. (2004): European seasonal and annual temperature variability, trends and extremes since 1500. Science 303:1499-1503.

Mitchell, T.D., Jones, P. (2005): An improved method of constructing a database of monthly climate observations and associated high-resolution grids. International Journal of Climatology 25, 693 – 712.

Nemani, R.R., Keeling, C.D., Hashimoto, H., Jolly, W.M., Piper, S.C., Tucker, C.J., Myneni, R.B., Running, S.W. (2003): Climate-driven increases in global terrestrial net primary production from 1982 to 1999. Science 300: 1560-1563.

Neuwirth, B., Schweingruber, F., Winiger, M. (2007): Spatial patterns of central European pointer years from 1901 to 1971. Dendrochronologia 24: 79-89.

Pfister C., (1999): Wetternachhersage: 500 Jahre Klimvariationen und Naturkatastrophen (1496-1995). Haupt: Bern

Schweingruber, F.H. (1996): Tree Rings and Environment: Dendroecology. Haupt: Bern.

Treydte, K., Schleser, G.H., Helle, G., Frank, D.C., Winiger, M., Haug, G.H., Esper, J. (2006): Millennium-long precipitation record from tree-ring oxygen isotopes in northern Pakistan. Nature 440, 1179-1182.

Wilson, R.J.S., Hopfmueller, M. (2001): Dendrochronological investigations of Norway spruce along an elevational transect in the Bavarian Forest, Germany. Dendrochronologia 19, 67-79.

Wilson, R.J.S., Luckman, B.H., Esper, J. (2005): A 500-year dendroclimatic reconstruction of spring-summer precipitation from the lower Bavarian forest region, Germany. International Journal of Climatology 25, 611-630.

Climatic drivers of beech growth in the Vosges and Jura Mountains

U. Büntgen[1], D. Frank[1], K. Bareiss Valle[2], O. Bouriaud[3] & J. Esper[1]
[1] Swiss Federal Research Institute WSL, 8903 Birmensdorf, Switzerland
[2] Department of Geography, University of Bonn, 53115 Bonn, Germany
[3] Forest Research and Management Institute, 725100 Câmpulung Moldovonesc, Romania
Email: buentgen@wsl.ch

Introduction

Common beech (*Fagus sylvatica* L.) is one of the key tree species of Central European mixed mountain forests between 600-1400 m asl. This dominant broadleaf species is known to reflect distinct inter-annual signal strength over larger scales (Neuwirth et al. 2007). To date, various dendroclimatological and -ecological studies have assessed the growth response of beech (Biondi 1993, Dittmar & Elling 2007, Piovesan et al. 2003, Rozas 2001), with some emphasis on productivity changes under warming and/or drying climates (Leuzinger et al. 2005). More methodological approaches analyzed long-term trends in ring width (Badeau et al. 1995), physiological controls on wood density (Bouriaud et al. 2004), and vessel lumen size (Sass & Eckstein 1995) of the diffuse-porous beech. Additional effects of soil conditions and water control on beech growth have recently been analyzed (Granier et al. 2007, Thimonier et al. 2000).

Due to the increased climate sensitivity of beech trees that grow near their distributional boundary (Z'Graggen 1992), we here compiled tree-ring width (TRW) data from nine sites in the Vosges, Jura and Swiss northern pre-Alps. This network was analyzed to understand inter-annual to decadal-scale growth variations over space and time, and to reveal its responses to regional temperature and precipitation fluctuations over the past ~200 years.

Data and Methods

TRW series from the Jura Mts. and northern pre-Alps collected in the 1980s (Z'Graggen 1992) are re-used and combined with an update from the Vosges Mts. that extends until 2003. Data include ~28,600 annual measurements, derive from elevations between 560-1390 m asl, and roughly cover the region 46-48° N and 6-8° E (Fig. 1). Relevant information on the TRW site chronologies is summarized in table 1.

DOI:10.2312/GFZ.b103-08056

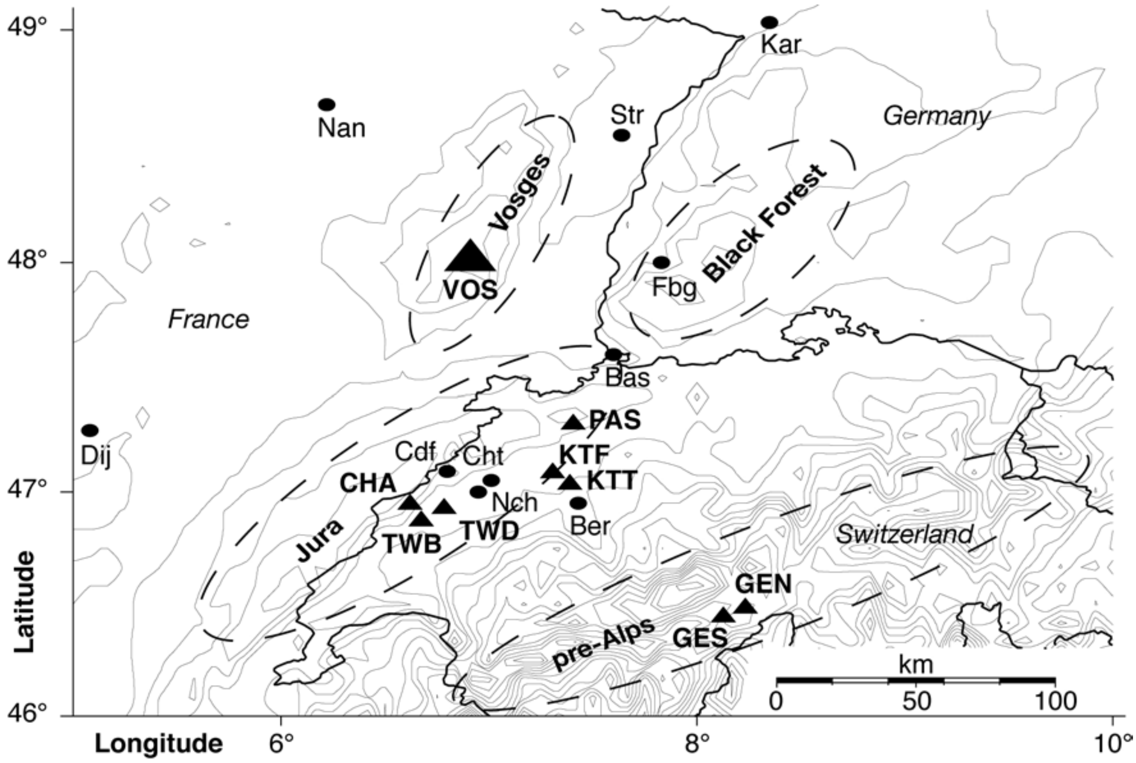

Figure 1: Location of the TRW sites (triangles) and instrumental stations (circles) used in this study. While each triangle represents one beech stand, the larger VOS triangle integrates samples from various stand locations along the Central Vosges Mountains.

Table 1: Characteristics of the site chronologies after spline detrending. Loc=Location (Lat/Lon), Ele=Elevation (m asl), Pep=Replication (Series), Per=Period, Per >5=Period >5 series, MSL=Mean Segment Length (Years), AGR=Average Growth Rate (mm/year), Lag-1=autocorrelation at year one. Bold chronologies were considered in the mean Swiss-French record.

Site	Loc	Ele	Rep	Per	Per >5	MSL	AGR	Lag-1
VOS	**48°00/6°90**	**1230**	**53**	**1781-2003**	**1781-2003**	**135**	**1.05**	**0.33**
TWD	47°05/6°90	560	24	1844-1987	1844-1987	121	1.59	0.45
TWB	47°05/6°80	630	26	1890-1987	1890-1987	78	2.24	0.28
PAS	**47°30/7°40**	**1080**	**24**	**1842-1987**	**1842-1987**	**130**	**1.11**	**0.28**
CHAS	**47°06/6°21**	**1370**	**24**	**1859-1987**	**1859-1987**	**93**	**1.59**	**0.42**
KTT	47°01/7°34	700	24	1825-1987	1825-1987	136	1.00	0.46
KTF	47°00/7°35	630	24	1879-1987	1879-1987	95	2.10	0.29
GENS	46°46/8°20	1390	23	1849-1987	1849-1987	95	1.34	0.43
GENN	**46°45/8°20**	**1320**	**24**	**1796-1987**	**1796-1987**	**144**	**1.10**	**0.25**

Raw measurements were first checked for dating errors on a site-by-site basis and individual spline detrending applied to remove non-climatic, tree-age related growth trends from the series (Fritts 1976). For the preservation of inter-annual to decadal scale variability, TRW series were individually detrended using cubic smoothing splines with 50% frequency-response cutoff equal $^{2}/_{3}$ the series length (Cook & Peters 1981). Indices were then calculated as residuals from the estimated growth curves after power transformation (details in Cook & Peters 1997). Mean chronologies were calculated using a bi-weight robust mean,

DOI:10.2312/GFZ.b103-08056

with their variance stabilized using methods described in Frank et al. (2007b). Based on inter-series correlations between the nine site chronologies and elevation criteria, data from four sites (VOS, PAS, CHAS, GENN) were subsequently selected to develop a mean Swiss-French beech chronology (Fig. 2).

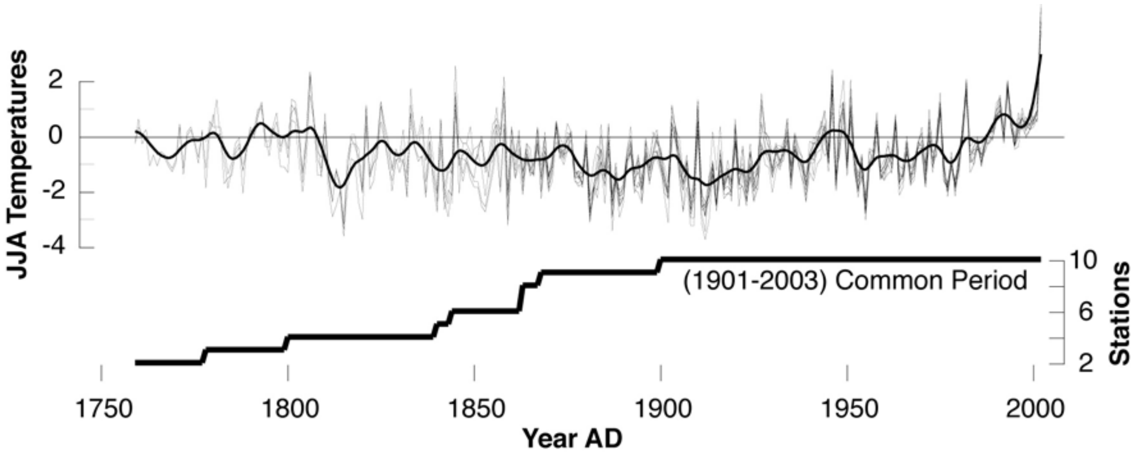

Figure 2: Summer (June-August) instrumental temperature data expressed as anomalies with respect to 1971-2000. Grand average correlation between the 10 stations for the annual, winter and summer data is 0.88, 0.93 and 0.94, respectively. Inter-station correlations range from 0.53 (Cht/Str) to 0.97 (Bas/Kar) for annual, from 0.81 (Chat/Str) to 0.99 (Kar/Str) for winter and from 0.88 (Nan/Nch) to 0.97 (Bas/Cht) for summer. Lag-1 autocorrelation of the mean summer (June-August) temperature record is 0.20. Smoothed mean curve is a 20yr low-pass filter.

Signal strength of this record (VOS-PAS-CHAS-GENN) was assessed using 'moving window' inter-series correlation (*RBAR*), and the Expressed Population Signal (*EPS*) computed along the time-series (Wigley et al. 1984).

For growth-climate response analysis, monthly temperature means and precipitation sums from 10 instrumental stations were employed (Fig. 1). Relevant information on these stations is summarized in table 2.

Table 2: Characteristics of the instrumental station data used in this study. Ele=Elevation (m asl), T-record=Period covered by temperature measurements (monthly), P-record=Period covered by precipitation measurements (monthly).

Site	Station	Country	Lon	Lat	Ele	T-record	P-record
Bas	Basel-Binningen	CH	7°60	47°60	316	1760-2003	1861-2003
Ber	Bern	CH	7°43	46°95	565	1760-2003	1856-2003
Cht	Chaumont	CH	6°99	47°05	1073	1864-2003	1864-2003
Dij	Dijon-Longvic	FR	5°08	47°27	227	1845-2003	1831-2003
Cdf	La Chaux de Fonds	CH	6°80	47°09	1018	1901-2003	1900-2003
Nan	Nancy-Essey	FR	6°22	48°68	217	1841-2003	1811-2003
Nch	Neuchatel	CH	6°95	47°00	485	1864-2003	1856-2003
Str	Strasbourg-Entzheim	FR	7°64	48°55	150	1801-2003	1803-2003
Fbg	Freiburg/Breisgau	DE	7°83	48°00	300	1869-2003	1869-2003
Kar	Karlsruhe	DE	8°35	49°03	112	1779-2003	1801-2003

DOI:10.2312/GFZ.b103-08056

For further details including the reliability of early data and homogenization procedures, see Auer et al. (2007). Correlations between the proxy and target data were computed for an 18-month window from previous-year April to current-year September over the full 1806-2003 period of overlap. Four split periods of equal length were additionally used to detect temporal changes in climate sensitivity.

Monthly temperature means averaged from 10 instrumental stations (Fig. 1, Tab. 2) indicate high inter-annual to multi-decadal scale variability. June-August temperatures describe a decline from the beginning of the observations until the early 20th century (with superimposed depressions centered ~1785, 1816, 44, 88 and 1913), followed by increasing values peaking in 2003 (with superimposed depressions centered ~1940, 56, 78, and 1996) (Fig. 2).

Even though the common period covered by all stations is restricted to 1901-2003, the herein considered station measurements most likely provide reliable high-frequency variability back to 1760 (Auer et al. 2007), conditions worldwide limited to Central Europe. For a detailed summary of potential lower frequency uncertainties in early (<1850) instrumental station measurements that can systematically bias inferred relationships with tree-growth, see Frank et al. (2007b).

Monthly precipitation sums averaged from the 10 instrumental stations (Fig. 1, Tab. 2) indicate slightly lower inter-annual to decadal scale variability compared to the temperature variations. June-August precipitation portrays no longer-term trend over the past 200 years, but prominent decadal fluctuations (Fig. 3). These include below-average summer precipitation sums centered ~1838, 59, 70, 85, 1906, 23, the 1940s, 1962, 84 and 2003.

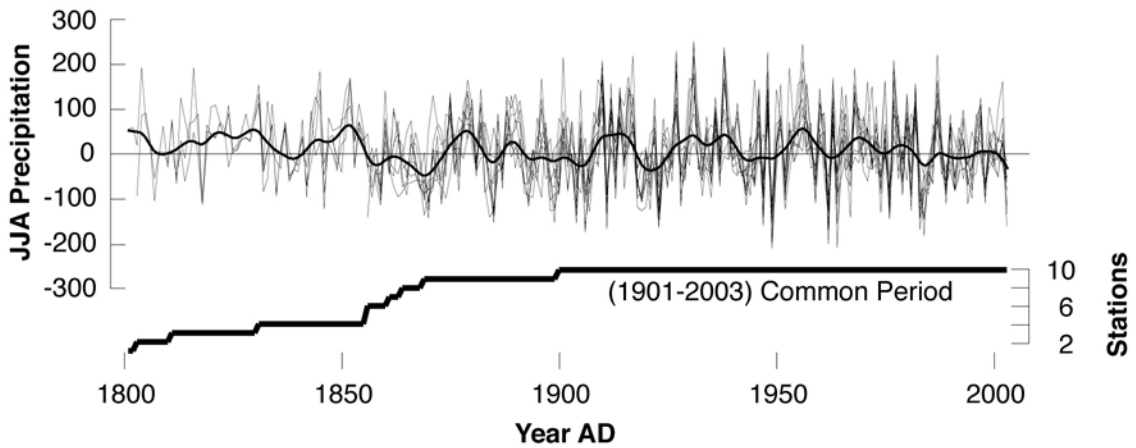

Figure 3: Summer (June-August) instrumental precipitation data expressed as anomalies with respect to 1971-2000. Average correlations between the 10 stations for the annual, winter and summer data are 0.77, 0.80 and 0.68, respectively (1901-2003). Inter-station correlations range from 0.57 (Kar/Nch) to 0.93 (Cht/Cdf) for annual, from 0.66 (Dij/Kar) to 0.95 (Cht/Cdf) for winter and from 0.45 (Dij/Kar) to 0.92 (Cht/Nch) for summer. Lag-1 autocorrelation of the mean summer (June-August) precipitation record is -0.10. Smoothed curve is a 20yr low-pass filter.

Results and Discussion

Mean correlation between the four TRW site chronologies (VOS, PAS, CHAS, GENN) is 0.47, and ranges from 0.27 between PAS and GENN to 0.61 between the VOS chronology and data from both PAS and CHAS. After combining measurements from these sites, a new mean chronology was developed that due to the sampling design (only living trees) and detrending method (individual series) only contains inter-annual to decadal-scale variability (Fig. 4a).

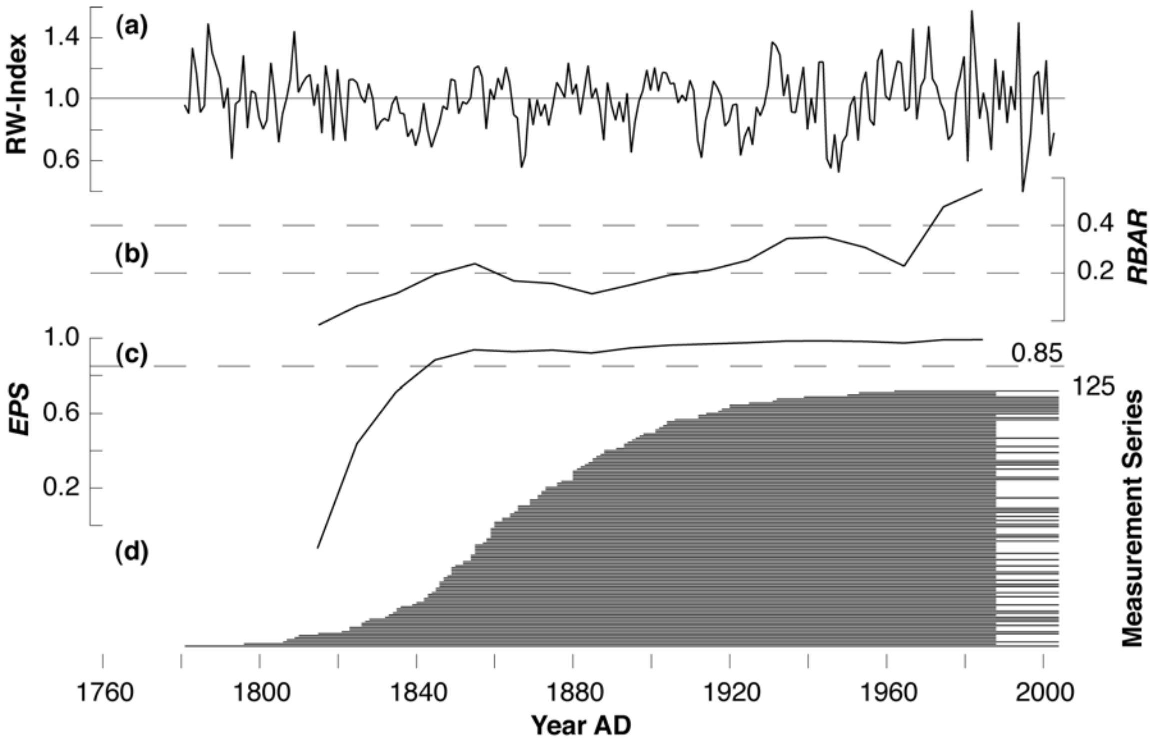

Figure 4: Characteristics of the (a) mean Swiss-French beech chronology and their (b) RBAR, (c) EPS and (d) replication. RBAR and EPS values were calculated over 30yr windows lagged by 20 years along the chronology. Lag-1 autocorrelation of the record is 0.24.

This novel Swiss-French mean record describes a slight upward trend from around the 1790s into the early 19th century, a well-known period of reduced solar activity and increased explosive volcanism (e.g., Büntgen et al. 2006a). Stronger decadal-scale fluctuations are revealed from around the 1840s to the 1920s, with episodes of high growth rates ~1860, 1880 and 1900. Distinct 20th century growth depressions occurred in the 1940s, 70s and 1990s. Abrupt growth reductions are found in 1793, 1867, 1895, 1913, 1923, 1948, 1981 and 1995; and positive anomalies in 1787, 1809, 1879, 1931, 1982, 1971 and 1994. In this regard, one must note that (artificial) variance changes i.e., increased variance before ~1830 and after ~1930, have not fully been removed. These are most likely related to the general decrease in sample size back in time, and the inclusion of juvenile and less correlating wood during the early 1830-1930 period (Fig. 4d), affecting the comparison of annual extremes over the past centuries. Interestingly, Biondi (1993) and Piovesan et al. (2003) both reported cross-dating difficulties related to the presence of very narrow, incomplete or even missing rings, especially near the pith. For a discussion and more methodological details on related variance stabilization techniques, see Frank et al. (2007a). Additional pruning at the end of each of the measurement series (i.e., some sort of age-

banding methodology, Briffa et al. 2001) would result in a more even distribution of similar tree-ages along the record, and potentially help such affects to be diminished.
Hence, caution is advised with any interpretation of the new Swiss-French beech chronology, as various quality changes through time must be considered. Reasonable signal-strength is found for the past 150-200 years, as demonstrated by the *EPS* values above the commonly applied quality threshold of 0.85 until 1840 (Fig. 4b-c). Interestingly, the *RBAR* values constantly decrease back in time. Uncertainty during the chronology's first portion is most likely caused by low sample replication and should be considered (together with the observed variance changes) when comparing the proxy record with the instrumental target data.
Significant correlations between beech TRW and temperatures (using monthly means from previous year April to September of the growing season) are not obtained when computing over the full 1806-2003 period of proxy/target overlap (Fig. 5a). Highest correlations of 0.43 and 0.38 are derived from previous year April and current year August temperatures over the 1806-1855 and 1855-1904 periods, respectively. The most significant negative correlation (*r* =-0.46) is obtained with March temperature. The overall response to temperature describes no or negative relationships to previous year spring, generally negative correlations with previous year July-August and positive correlations with the previous autumn, and again no pattern with winter prior to the growing season. Overall negative correlations are found between March-June, followed by positive relationships for July-August. While correlations based on the four split periods indicate some noise, the overall response behavior is confirmed by the (relatively diminished) correlation results obtained from the full 1806-2003 period of proxy/target overlap.

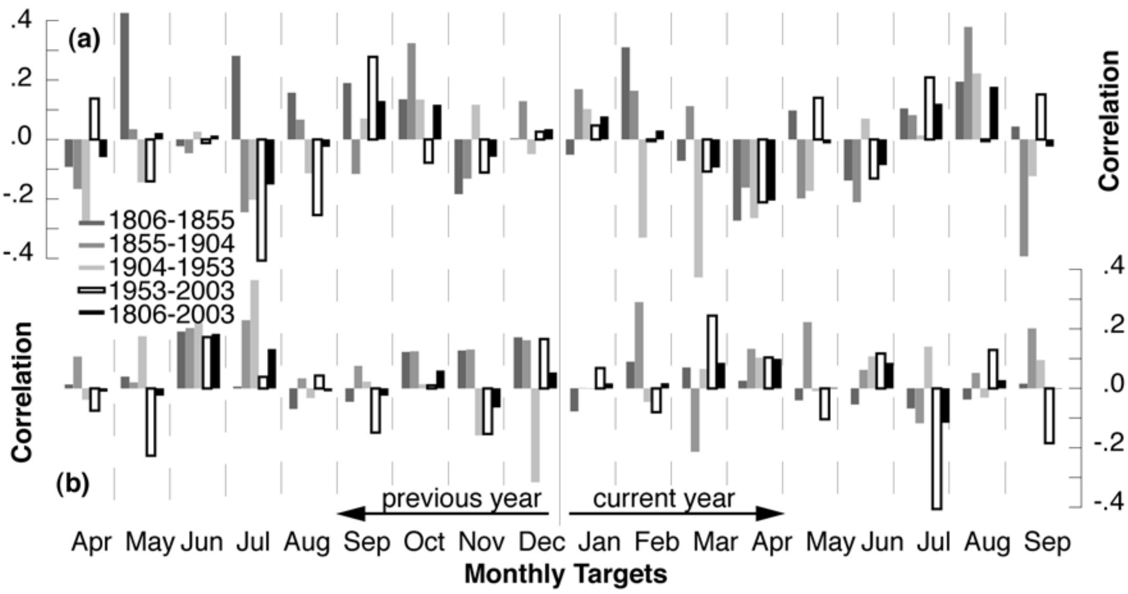

Figure 5: Comparison between the mean Swiss-French beech chronology and (a) monthly temperature means and (b) monthly precipitation sums from previous year April to current year September. Correlations were computed over the full 1806-2003 and four split periods of equal length. Significant levels are not provided as lag-1 autocorrelation varies between each monthly climate target and the different periods considered.

In contrast, correlation analysis using monthly precipitation sums revealed overall less pronounced patterns in seasonal response (Fig. 5b). Some positive relationship is though indicated for previous year June-July, while negative correlations are found with July of the growing season. Besides (abiotic) shifts in growth responses to climate, which most likely result from changing temperature and precipitation regimes, (biotic) tree age-related changes in growth-sensitivity and/or response seasonality may account for some of the herein observed temporal variance. An overall response shift from former temperature to current precipitation (drought) sensitivity as reported from a spruce network (Büntgen et al., 2006b) is, however, not observed. Despite such temporal weakening in the growth/climate response of the mean Swiss-French chronology, some individual sites may show a more stable response behavior over time.

Comparison of the herein obtained TRW extremes with those reported from a beech network across the Bavarian-Forest and -Alps, reveals a high degree of temporal coherency between both regions, including growth depressions in higher altitudinal beech forests in the 1970s, 80s and 1995). Increased frequency of negative pointer years during the past three decades is also reported from an Italian high-elevation beech chronology (Piovesan et al. 2003). In this regard, Dittmar & Elling (2007) suggested reduced ecological fitness and stability of all age-classes, as low-elevation beech growth mainly suffered from below-average precipitation, whereas high-elevation beech growth was generally limited by pronounced temperature depressions. Interestingly, none of the meteorological and hydrological parameters is reported to significantly correlate with beech TRW at elevations ~1000 m asl; results that are (partly) confirmed by this study (Fig. 5).

Causes and scales of abrupt beech growth depressions are not fully understood. See Gessler et al. (2007) for potential risks of the European beech related to a warmer and dryer climate as projected for the future (IPCC 2007). In a free atmosphere experiment, Leuzinger et al. (2005) found a two-year sequence of reduced basal stem area growth of beech (and four other deciduous species), most likely caused by the severe summer drought of 2003 (Schär et al. 2004). Similar climatic conditions, i.e., negative water budget due to the precipitation/evaporation ratio, forced late summer soil desiccation and drought-induced growth reductions in the 1940s and 70s (Fig. 2). In this regard, one must note that beech has relatively shallow roots in comparison to oak (Leuschner et al. 2001a, b). Due to the complexity of cell length, wood anatomy and hydraulic properties such as elasticity of storage tissue and stomata control over tree water status (Hacke & Sperry 2001, Gessler et al. 2007), species-specific cavitation risk – even though the large oak early wood vessels are much more exposed to cavitation than the small beech vessels – is only weakly understood (Gessler et al. 2007, Leuzinger et al. 2005). Any argumentation towards vessel-size dependent drought-sensitivity could thus be misleading.

Three beech stands distributed across Central Europe showed most significant growth reductions in the year following the severe 2003 summer drought (Granier et al. 2007). Since beech is further assumed to allow water storage to be directly utilized for basal area increases (Bouriaud et al. 2004), growing season length and character may additionally impact annual growth rates. Nevertheless, one should consider that water storage can only last for a limited period (in the range of one day), and thus most likely becomes irrelevant during longer drought periods (Breda et al. 2006). A close relationship between photosynthetic production and TRW potentially allows some of the negative feedbacks of beech growth under a warming climate to be compensated, as related increases in radiation (and higher rates of photosynthesis) possibly promote vessel lumen formation, independent of any soil water deficit (Bouriaud et al. 2004). In contrast, one could argue that warmer summer temperatures and increased radiation don't necessarily have to cause an increase in photosynthesis rates, as the amount of summer radiation often excides the total of radiation usable for plants, which becomes even more critical for deciduas trees.

Further modifications of the generally observed drought-sensitivity of beech TRW may arise from the soil storage capacity at a given site (Garnier et al. 2007, Saas & Eckstein 1995), as soil water deficit can significantly hamper vessel formation (Aranda et al. 2000, Rozas 2001). In addition, various degrees of species-specific drought-sensitivity may result from differences in the adaptation rate of physiological parameters (Gessler et al. 2007, Peuke et al. 2002, Steppe & Lemeur 2007).

Conclusions

We compiled a network of nine TRW beech chronologies and instrumental station measurements for the Central northern pre-Alps and the past ~200 years. Growth-climate response analysis demonstrated the ability of inter-annual to decadal-scale variations in beech growth to reflect common climatic signals over a wider region. However, a distinct climatic driver (temperature or precipitation) was not found to dominate average beech TRW (~1000 m asl) when combining measurements from four sites distributed across the Vosges and Jura Mts.

In an attempt to further detail the 'complex' growth response of beech under potential future warming and induced drought stress, more local studies and more tree-ring data from heterogeneous sites e.g., high-to-low-elevation, dry-to-wet sites, juvenile-to-mature trees and additional climate parameters, e.g., reliable drought metric, water vapor and cloud cover data are required. Besides the spatial aspect, composite chronologies of living and historic material that may allow age-related detrending methods to be successfully applied and lower frequency information accordingly to be preserved, could further help benchmarking the extreme late 20th century conditions into a longer-term context. Such studies would subsequently provide useful insight on the role of forest growth in relation to estimates of large-scale biomass productivity and carbon sequestration.

Acknowledgements

Supported by the SNSF NCCR-Climate and Euro-Trans (#200021-105663). We thank P. Fonti, A. Gallé, and one anonymous reviewer for critical comments and discussion.

References

Aranda, I., Gil, L., Pardos, J. (2000): Water relations and gas exchanges in *Fagus sylvatica* L. and *Quercus petraea* (Matuschka) Liebl. in a mixed stand at their southern limit of distribution in Europe. *Trees Structure and Function* 14: 344-352.

Auer, I., and 31 Co-authors (2007): HISTALP – Historical instrumental climatological surface time series of the Greater Alpine Region. *International Journal of Climatology* 27: 17-46.

Badeau, V. Dupouey, J., Becker, M., Picard J (1995): Long-term trends of Fagus sylvatica L. in northeastern France. A comparison between high and low density stands. *Acta Oecologica* 16: 571-583.

Biondi, F. (1993): Climatic signals in tree rings of *Fagus sylvatica* L. from the central Apennines, Italy. *Acta Oecologica* 14: 57-71.

Bouriaud, O., Bréda, N., Le Moguédec, G., Nepveu, G. (2004): Modelling variability of wood density in beech as affected by ring age, radial growth and climate. *Trees Structure and Function* 18: 264-276.

Breda, N., Huc, R., Granier, A., Dreyer, E. (2006): Temperate forest trees and stands under severe drought: a review of ecophysiological responses, adaptation processes and long-term consequences. *Annual Forest Sciences* 63: 625-644.

Briffa, K., Osborn, T., Schweingruber, F., Harris, I., Jones, P., Shiyatov, S., Vaganov. E. (2001): Low-frequency temperature variations from a northern tree ring density network. *Journal Geophysical Research* 106: 2929-2941.

Büntgen, U., Frank, D., Nievergelt, D., Esper, J. (2006a): Summer temperature variations in the European Alps, AD 755-2004. *Journal of Climate* 19: 5606-5623.

Büntgen, U., Frank., D., Schmidhalter., M., Neuwirth, B., Seifert., M., Esper., J. (2006b): Growth/climate response shift in a long subalpine spruce chronology. *Trees Structure and Function* 20: 99-110.

Cook, E., Peters, K. (1981): The smoothing spline: A new approach to standardizing forest interior tree-ring width series for dendroclimatic studies. *Tree-Ring Bulletin* 41:45-53.

Cook, E., Peters, K. (1997): Calculating unbiased tree-ring indices for the study of climatic and environmental change. *The Holocene* 7: 361-370.

Dittmar, C., Elling, W. (2007): Dendroecological investigation of the vitality of Common Beech (*Fagus sylvatica* L.) in mixed mountain forests of the Northern Alps (South Bavaria). *Dendrochronologia* 25: 37-56.

Frank, D., Büntgen, U., Böhm, R., Maugeri, M., Esper, J. (2007a): Warmer early instrumental measurements versus colder reconstructed temperatures: shooting at a moving target. *Quaternary Science Reviews* 26: 3298-3310.

Frank, D., Esper, J., Cook, E. (2007b): Adjustment for proxy number and coherence in a large-scale temperature reconstruction. *Geophysical Research Letters* 34: doi 0.1029/2007GL030571.

Fritts, H. (1976): *Tree rings and climate.* Academic Press, New York.

Gessler, A., Keitel, C., Kreuzwieser, J., Maatyssek, R., Seiler, W., Rennenberg, H. (2007): Potential risks for European beech (*Fagus sylvatica* L.) in a changing climate. *Trees Structure and Function* 21: 1-11.

Granier, A., and 37 co-authors (2007): Evidence for soil water control on carbon and water dynamics in European forests during the extremely dry year: 2003. *Agricultural and Forest Meteorology* 143: 123-145.

Hacke, U., Sperry, J. (2001): Functional and ecological xylem anatomy. *Perspectives in Plant Ecology, Evolution and Systems* 4: 97-115.

IPCC (2007) *Climate Change 2007: The Physical Science Basis. Contribution of Working Group I to the Fourth Assessment Report of the IPCC.* Cambridge University Press. Cambridge, United Kingdom and New York.

Leuschner, C., Backes, K., Hertel, D., Schipka, F., Schmitt, U., Terborg, O., Runge, M. (2001a): Drought responses at leaf, stem and fine root levels of competitive *Fagus sylvatica* L. and *Quercus petraea* (Matt.) Liebl. trees in dry and wt years. *Forest Ecology and Management* 149: 33-46.

Leuschner, C., Hertel, D., Coners, H., Buttner, V. (2001b): Root competition between beech and oak: a hypothesis. *Oecologia* 126: 276-284.

Leuzinger, S., Zotz, G., Asshoff, R., Körner, C. (2005): Responses of deciduous forest trees to severe drought in Central Europe. *Tree Physiology* 25: 641-650.

Neuwirth, B., Schweingruber, F., Winiger, M. (2007): Spatial patterns of central European pointer years from 1901 to 1971. *Dendrochronologia* 24: 79-89.

Peuke, A., Schraml, C., Hartung, W., Rennenberg H. (2002): Identification of drought-sensitive beech ecotypes by physiological parameters. *New Phytologist* 154: 373-387.

Piovesan, G., Bernabei, M., Di Filippo, A., Romagnoli, M., Schirone, B. (2003): A long-term tree ring beech chronology from a high-elevation old-growth forest of Central Italy. *Dendrochronologia* 21: 13-22.

Rozas, V. (2001): Detecting the impact of climate and disturbances on tree-rings of *Fagus sylvatica* L. and *Quercus robur* L. in a lowland forest in Cantabria, Northern Spain. *Annual Forest Sciences* 58: 237-251.

Sass, U., Eckstein, D. (1995): The variability of vessel size in beech (*Fagus sylvatica* L.) and its ecophysiological interpretation. *Trees Structure and Function* 9: 247-252.

Schär, C., Vidale, P., Lüthi, D., Frei, C., Häberli, C., Liniger, M., Appenzeller, C. (2004): The role of increasing temperature variability in European summer heatwaves. *Nature* 427: 332-336.

Steppe, K., Lemeur, R. (2007): Effects of ring-porous and diffuse-porous stem wood anatomy on the hydraulic parameters used in a water flow and storage model. *Tree Physiology* 27: 43-52.

Thimonier, A., Dupouey, J., Le Tacon, F. (2000): Recent losses of base cations from soils of *Fagus sylvatica* L. stands in northeastern France. *Ambio* 29: 314-321.

Wigley, T., Briffa, K., Jones, P. (1984): On the average of value of correlated time series, with applications in dendroclimatology and hydrometeorology. *Journal of Climatology and Applied Meteorology* 23:201-213.

Z'Graggen, S. (1992): *Dendrohistometrisch- klimatologische Untersuchung an Buchen (Fagus sylvatica L.)*. Dissertation, Universität Basel. 165.

DOI:10.2312/GFZ.b103-08056

Calibration trails using very long instrumental and proxy data

J. Esper[1], R. Niederer[1], J. Luterbacher[2,3], U. Büntgen[1] & D. Frank[1]
[1] *Swiss Federal Research Institute WSL, 8903 Birmensdorf, Switzerland*
[2] *National Centre of Competence in Research on Climate (NCCR) and Institute of Geography, University of Bern, 3012 Bern, Switzerland*
[3] *Oeschger Centre for Climate Change Research, University of Bern, 3012 Bern, Switzerland*
Email: esper@wsl.ch

Introduction

The European Alps are one of the few places that allow comparisons of natural climate proxies, such as tree-rings, with instrumental and documentary data over multiple centuries. Evidence from local and regional tree-ring analyses in the Alps clearly showed that tree-ring width (TRW) data from high elevation, near treeline environments contain substantial temperature signals (e.g., Büntgen et al. 2005, 2006, Carrer et al. 2007, Frank and Esper 2005a, 2005b, Frank et al. 2005). This sensitivity can be evaluated over longer timescales by comparison with instrumental temperature data recorded in higher elevation (>1,500 m asl) environments back to the early 19th century, and, due to the spatially homogenous temperature field, back to the mid 18th century using observational data from stations surrounding the Alps (Auer et al. 2007, Böhm et al. 2001, Casty et al. 2005, Frank et al. 2007a, Luterbacher et al. 2004). Further, the combination of such instrumental data with even older documentary evidence (Pfister 1999, Brázdil et al. 2005) allows an assessment of temporal coherence changes between tree-rings and combined instrumental and documentary data back to AD 1660. Such analyses are outlined here using TRW data from a set of *Pinus cembra* L. sampling sites from the Swiss Engadin, and calibrating these data against a gridded surface air temperature reconstruction integrating long-term instrumental and multi-proxy data (Luterbacher et al. 2004).

Material and methods

Tree-ring data and detrending

Core and disc samples from three high elevation (Tam, Muo, Sil) and one middle elevation (Cel) stone pine sites in the Swiss Engadin in the Central Alps were collected (Fig. 1). In total, 642 samples from 335 trees (Tab. 1) were processed, including TRW measurements, crossdating, and quality control (Esper and Gärtner 2001, Fritts 1976, Schweingruber 1983, Cook and Kairiukstis 1990). Mean segment and chronology lengths of the sites range from 125-206 years and AD 1564-1742, respectively. TRW data were detrended by taking residuals from 300-year cubic smoothing splines (Cook 1985) fitted to the power transformed (Cook and Peters 1997) measurement series. This procedure removes tree-age related trends (Bräker 1981), but emphasizes inter-annual to multi-decadal scale variance in the resulting index series (Cook et al. 1995, Esper et al. 2003).

DOI:10.2312/GFZ.b103-08056

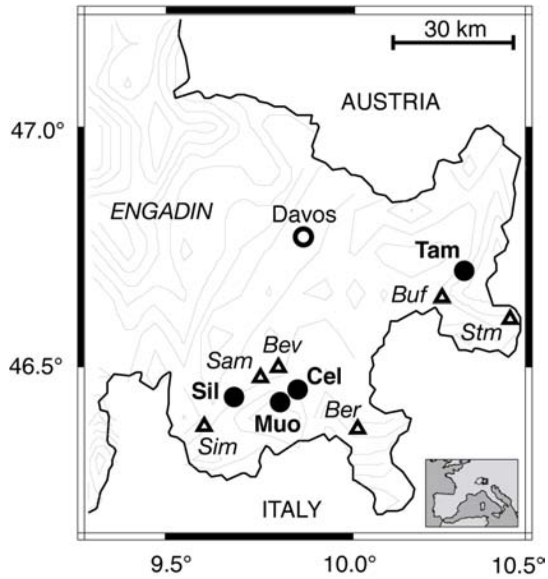

Figure 1: Tree-ring sampling sites (dots), and meteorological stations (triangles) in the Swiss Engadin south of Davos. Stations include Bernina Pass (Ber), Bever (Bev), Buffalora (Buf), Samedan (Sam), Sils Maria (Sil), Station Maria (Stm).

Table 1: Sampling site and tree-ring data characteristics.

Site	Elevation [m asl]	Core sample number	Mean series length [yrs.]	Chronology period (> 4 series)
Muo	2,180	141	125	1682-2002
Tam	2,180	177	206	1564-2002
Sil	2,140	170	140	1660-2002
Cel	1,840	154	191	1742-2002

Site chronologies were calculated using the bi-weight robust mean, and the variance of these mean timeseries stabilized considering changes in sample replication and interseries correlation (Frank et al. 2007b).

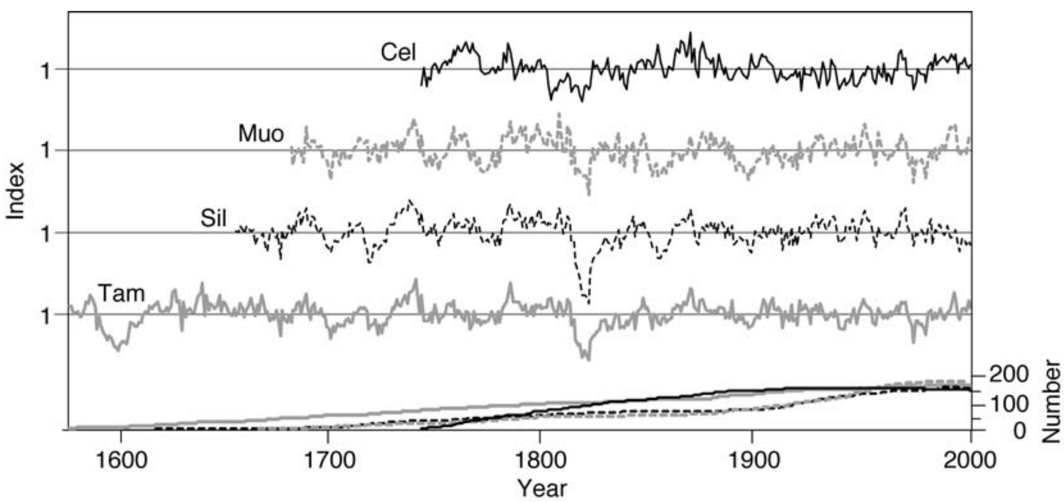

Figure 2: Spline detrended site chronologies from Cel, Muo, Sil, and Tam. Chronologies truncated at <5 series. Curves at the bottom show sample replication per site. Black curve is Cel, grey is Tam, dashed black is Sil, and dashed grey is Muo.

DOI:10.2312/GFZ.b103-08056

The site chronologies show common inter-annual to decadal scale (e.g., 1810s) variability (Fig. 2). Coherence between site chronologies ranges from r = 0.27 to 0.82 (mean = 0.55) calculated over the common 1741-2002 period (Tab. 2). Correlations of Cel (mean = 0.35) were lower than those of Muo (0.57), Sil (0.63), and Tam (0.65), indicating that this mid elevation site contains some different signals in comparison to the high elevation sites. Correlations do not decline back in time -- at least not back to 1701 as revealed in Table 2 -- indicating that inter-site coherence is fairly stable also during the less replicated early chronology periods (see replication curves at the bottom of Fig. 2). Interestingly, the chronology from Sil shows a negative trend over the most recent decade, a feature not revealed in any other site.

Table 2: Inter-site correlations over the 1741-2002, 1901-2002, 1801-1900, and 1701-1800 periods.

		1741-2002			
		Tam	Sil	Muo	Cel
1901-2002	Tam		0.82	0.72	0.41
	Sil	0.52		0.71	0.36
	Muo	0.73	0.60		0.27
	Cel	0.48	0.21	0.36	

		1801-1900			
		Tam	Sil	Muo	Cel
1701-1800	Tam		0.91	0.70	0.46
	Sil	0.84		0.73	0.38
	Muo	0.73	0.72		0.46
	Cel	——	——	——	

Instrumental and multi-proxy data

For comparison of tree-ring chronologies with instrumental and documentary data, we used the European scale gridded multi-proxy network from Luterbacher et al. (2004, hereafter abbreviated Lut04). For the grid points near the Swiss Engadin, this network contains information from regional long-term instrumental stations extending back to about 1760 (Auer et al. 2007), and temperature estimates derived from regional documentary evidence before that time back to 1500 (Luterbacher 2004, see Supporting Online Material).

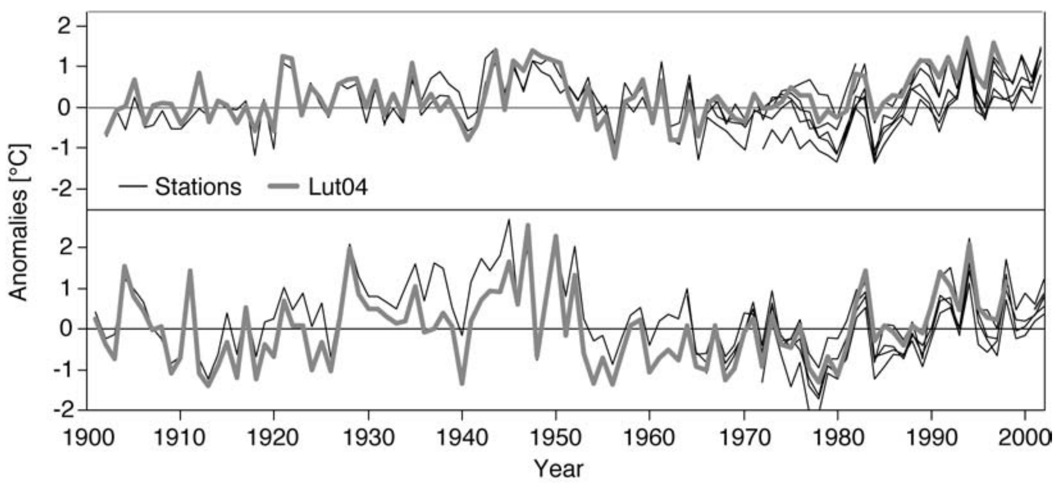

Figure 3: Temperature data from local observational stations and Lut04 since 1900. Top panel shows annual, bottom panel JJA temperatures. Thin black curves are the stations Ber, Bev, Buf, Sam, Sil, and Stm ranging from 1,390-2,256 m asl (see Fig. 1). Thick grey curve is Lut04. Series shown as anomalies with respect to the 1971-2000 period.

Correlations of Lut04 against local station data (see Fig. 1) range from 0.81-0.96 (mean = 0.90) for annual, and from 0.84-0.97 (mean = 0.93) for JJA temperatures, calculated over the 1970-2002 period. Visual comparison of the JJA and annual mean temperatures (Fig. 3) clearly demonstrates that Lut04 represents regional climate conditions as recorded in the six meteorological stations surrounding the tree sampling sites, and we used Lut04 for calibration trails over distinct periods and in a sliding window approach back to 1660.

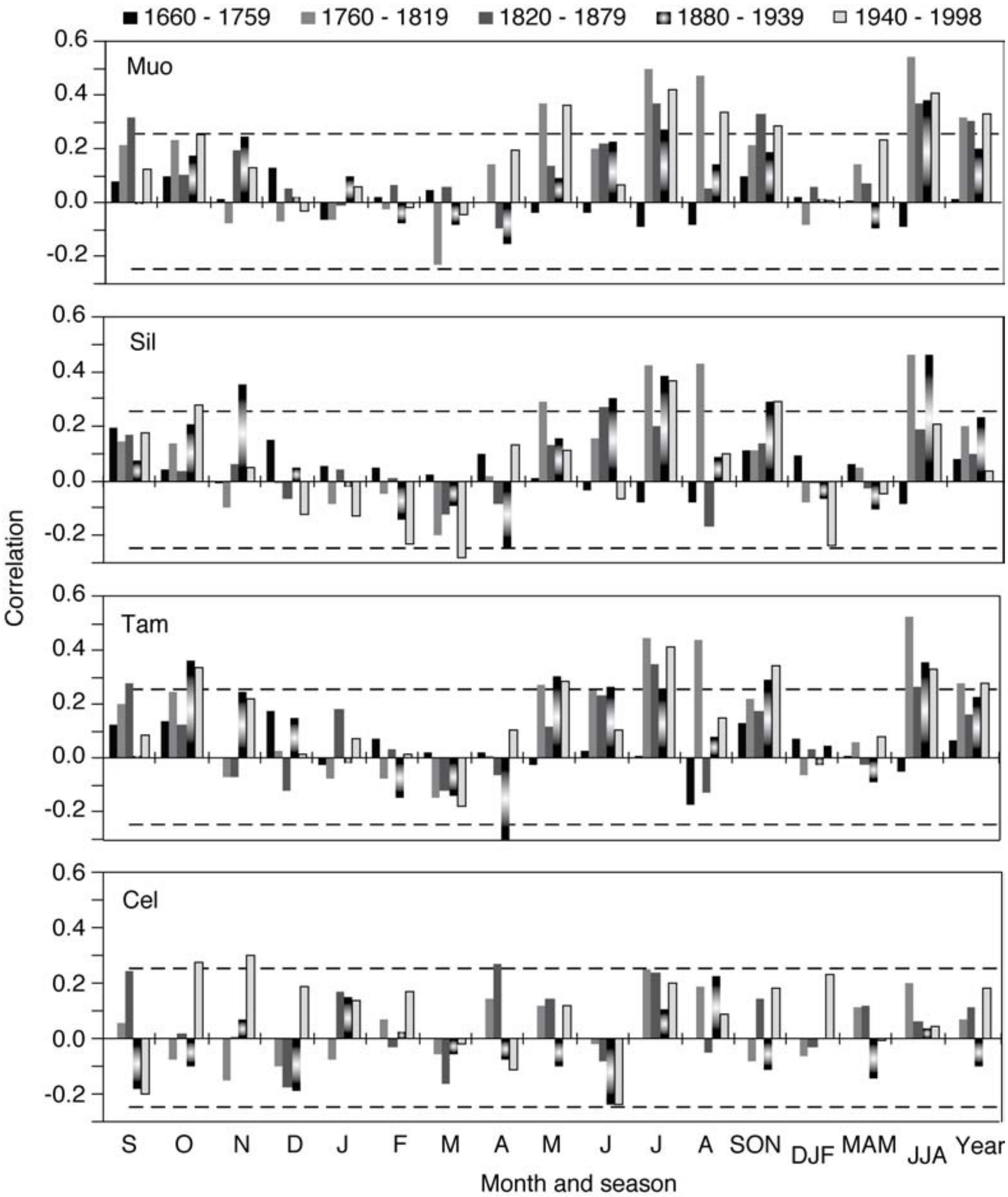

Figure 4: Monthly and seasonal correlations between four tree sites and Lut04 over the 1660-1759, 1760-1819, 1820-1879, 1880-1939, and 1940-1998 periods. Dashed curves approximate $p<0.05$.

Results

Climate response of the tree sites

The seasonal course and strength of climatic signals were quite similar between the three high elevation sites Muo, Sil, and Tam, but different in the mid elevation site Cel (Fig. 4). For the high elevation sites, significant correlations were found during some periods with

DOI:10.2312/GFZ.b103-08056

previous year fall temperatures, and fairly strong responses for most of the current year summer months. Highest values were typically obtained for July and JJA mean temperatures. In comparison, the Cel sampling site from only about 300 m below the high elevation collections showed effectively no temperature signal, but was dominated by mixed impacts of cold/warm and wet/dry conditions (not shown).

Temporal variations in climate calibration

Comparison of the monthly and seasonal TRW versus Lut04 correlations over five distinct periods since 1660 indicated that the maximum sensitivity to July and mean JJA temperatures is largely stable back to 1760 at the high elevation sites (Fig. 4). The signal, however, disappeared over the early 1660-1759 period, during which both sample replication of the high elevation tree sites (especially Muo and Sil) declined considerably, and a change from early observational measurements towards estimates from documentary evidence in Lut04 occurred.

Computation of correlations between the tree sites and Lut04 JJA temperatures in a running 30-year window allowed further assessment of this temporal change, highlighting a strong decline in coherence including negative values in the pre-1760 period (Fig. 5). The course of correlation values was rather similar for all tree sites over the past 300+ years, adding some confidence to this analysis. The analysis, however, also indicated a drop in correlation during recent times in Sil, a feature that is likely related to the negative growth trend recorded at this site since the late 1980s.

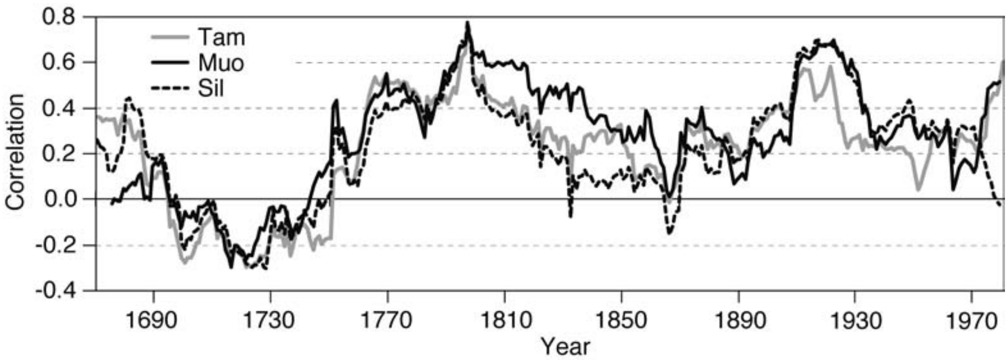

Figure 5: 30-year sliding window correlations of the Tam, Muo, and Sil site chronologies against mean JJA temperatures from Lut04.

Discussion

While our analyses revealed coherence between high elevation pine sites, between the Lut04 gridded and local station temperature data, and between the tree sites and regional temperatures as expressed by Lut04, calibration against early pre-1760 Lut04 data indicated no or even slightly negative correlations between tree growth and documentary evidence.

Our results are particularly robust over the past 2-3 centuries during which sample replication of the three treeline pine sites is rather high, but become less reliable before the 18th century when only the chronology from Tam is composed of a fairly high number of trees.

The loss of coherence between TRW and Lut04 data before 1760 either signifies that the climatic signal stored in the early, less replicated portions of the tree-ring chronologies diminished, and/or that the same signal weakened at the time the regional temperature measurements (e.g., Basel and Geneva temperature records started in the 1750s) were replaced with estimates derived from documentary evidence and measurements from more remote stations. Further research is needed to figure which of these alternatives is more important.

Acknowledgements

Supported by the EC project Millennium (Grant No. 017008), the SNSF through the National Centre for Competence in Climate Research (NCCR-Climate), and the Oeschger Centre for Climate Change Research.

References

Auer, I., and 31 Co-authors (2007): HISTALP – Historical instrumental climatological surface time series of the Greater Alpine Region. *International Journal of Climatology* 27: 17-46.

Böhm, R., Auer, I., Brunetti, M., Maugeri, M., Nanni, T., Schöner, W. (2001): Regional temperature variability in the European Alps: 1760-1998 from homogenized instrumental time series. *International Journal of Climatology* 21: 1779-1801.

Bräker, O.U. (1981): Der Alterstrend bei Jahrringdichten und Jahrringbreiten von Nadelhölzern und sein Ausgleich. *Mitteilungen der Forstlichen Bundesversuchsanstalt Wien* 142: 75-102.

Brázdil, R., Pfister, C., Wanner, H., von Storch, H., Luterbacher, J. (2005): Historical climatology in Europe – the state of the art. *Climatic Change* 70: 363-430.

Büntgen, U., Esper, J., Frank, D.C., Nicolussi, K., Schmidhalter, M. (2005): A 1052-year tree-ring proxy for Alpine summer temperatures. *Climate Dynamics* 25: 141-153.

Büntgen, U., Frank, D.C., Schmidhalter, M., Neuwirth, B., Seifert, M., Esper, J. (2006): Growth/climate response shift in a long subalpine spruce chronology. *Trees* 20: 99-110.

Carrer, M., Nola, P., Eduard, J.L., Motta, R., Urbinati, C. (2007): Regional variability of climate–growth relationships in *Pinus cembra* high elevation forests in the Alps. *Journal of Ecology* 95: 1072-1083.

Casty, C., Wanner, H., Luterbacher, J., Esper, J., Böhm, R. (2005): Temperature and precipitation variability in the European Alps since 1500. *International Journal of Climatology* 25: 1855-1880.

Cook, E.R. (1985): *A Time Series Analysis Approach to Tree-ring Standardization*. Lamont-Doherty Geological Observatory, New York.

Cook, E.R., Kairiukstis, L.A. (1990): *Methods of Dendrochronology – Applications in the Environmental Science*. Kluwer, Dordrecht.

Cook, E.R., Peters, K. (1997): Calculating unbiased tree-ring indices for the study of climatic and environmental change. *The Holocene* 7: 361-370.

Cook, E.R., Briffa, K.R., Meko, D.M., Graybill, D.A., Funkhouser, G. (1995): The `segment length curse´ in long tree-ring chronology development for palaeoclimatic studies. *The Holocene* 5: 229-237.

Esper, J., Gärtner, H. (2001): Interpretation of tree-ring chronologies. Erdkunde 55: 277-287.

Esper, J., Cook, E.R., Krusic, P.J., Peters, K., Schweingruber, F.H. (2003): Tests of the RCS method for preserving low-frequency variability in long tree-ring chronologies. *Tree-Ring Research* 59: 81-98.

Frank, D.C., Esper, J. (2005a): Characterization and climate response patterns of a high-elevation, multi-species tree-ring network for the European Alps. *Dendrochronologia* 22: 107-121.

Frank, D., Esper, J. (2005a): Temperature reconstructions and comparisons with instrumental data from a tree-ring network for the European Alps. *International Journal of Climatology* 25: 1437-1454.

Frank, D., Wilson, R.J.S., Esper, J. (2005): Synchronous variability changes in alpine temperature and tree-ring data over the last two centuries. *Boreas* 34: 498-505.

Frank, D.C., Büntgen, U., Böhm, R., Maugeri, M., Esper, J. (2007a): Warmer early instrumental measurements versus colder reconstructed temperatures: shooting at a moving target. *Quaternary Science Reviews*, in press.

Frank, D.C., Esper, J., Cook, E.R. (2007b): Adjustment for proxy number and coherence in a large-scale temperature reconstruction. *Geophysical Research Letters* 34, L16709.

Fritts, H.C. (1976): *Tree rings and climate.* Academic Press, New York.

Luterbacher, J., Dietrich, D., Xoplaki, E., Grosjean, M., Wanner, H. (2004): European seasonal and annual temperature variability, trends and extremes since 1500. *Science* 303: 1499-1503.

Pfister, C. (1999): Wetternachhersage: *500 Jahre Klimavariationen und Naturkatastrophen 1496-1995*. Haupt, Bern.

Schweingruber, F.H. (1983): *Der Jahrring: Standort, Methodik, Zeit und Klima in der Dendrochronologie*. Haupt, Bern.

DOI:10.2312/GFZ.b103-08056

Contrasting long-term drought signals in proxy records from northwestern Europe and the Mediterranean

V. Trouet[1] & J. Esper[1]

[1]*Swiss Federal Research Institute WSL, 8903 Birmensdorf, Switzerland*

Email: trouet@wsl.ch

Introduction

The Mediterranean region (including northern Africa) has in recent decades been subject to a distinctly decreasing precipitation trend, starting in the 1970s (Dünkeloh and Jacobeit 2003, Xoplaki et al. 2004, Luterbacher et al. 2006). A trend towards wetter winters occurred over the same time period in northwestern Europe (Jones and Conway 1997, Kiely 1999, Mills 2005). Winter precipitation in both regions is closely linked to hemispheric circulation patterns (e.g., Xoplaki et al. 2004, Pauling and Paeth 2007) and to the North Atlantic Oscillation (NAO) in particular (Hurrell 1995). Positive NAO winters are characterized by a deeper than normal trough over Iceland and a higher than normal ridge over the Azores (Fig. 1a), resulting in an anomalously strong westerly flow, wet conditions over northwestern Europe, and dry conditions in the Mediterranean. During negative NAO phases, precipitation patterns are effectively inverted, and the subtropical High, Icelandic Low, and westerly flow are weak (Fig. 1b). The NAO pattern shows a large amount of interannual variance, but is also variable on decennial time-scales (Van Loon and Rodgers 1978, Hurrell 1995).

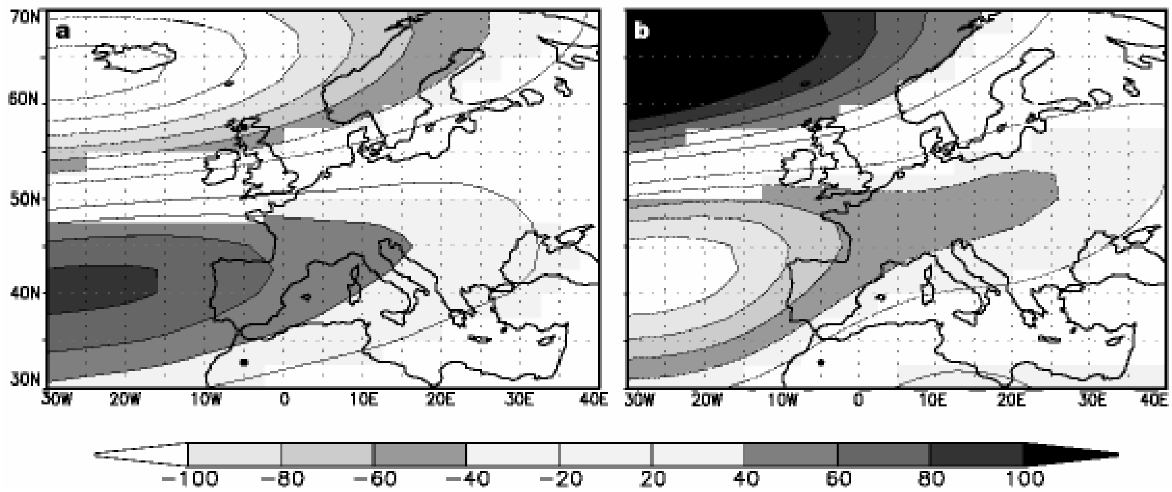

Figure 1: Anomaly (from the 1948-2000 average) composites of January-March 500 hPA patterns of the five highest (a) and the five lowest (b) NAOI years (1949-2000). Positive anomalies are indicated by full lines, negative anomalies by dashed lines. Shaded areas reflect significant (p<0.1) differences, calculated using a Student's t-test. The locations of the two proxy records from Scotland and Morocco are marked by black dots.

The co-occurrence of opposing trends in winter precipitation anomalies in northern versus southern Europe in recent decades has been ascribed to the concomitant dominance of positive winter NAO modes (Hurrell 1995, Hurrell and Van Loon 1997, Dünkeloh and

DOI:10.2312/GFZ.b103-08056

Jacobeit 2003). To put the recent multi-decadal precipitation trend in a historical context, long-term analysis of regional precipitation variability is needed. The use of proxy climatic data provides a mean to extend precipitation records back in time and thus to analyse past precipitation anomalies (e.g., Luterbacher et al. 2006).

In this paper, we combine a millennium-long speleothem-based precipitation proxy from Scotland (Proctor et al. 2000) with a tree-ring based drought reconstruction from Morocco (Esper et al. in press). The location of the two proxies in core regions of the European/NW-African precipitation dipole, and near the centers of action of the NAO (Fig. 1), allows for testing the temporal stability of spatial climate patterns and the prevailing hemispheric circulation patterns controlling them.

Data

The Morocco drought reconstruction

A 953-year long (1049-2002) tree-ring chronology was developed based on ring-width data from 178 *Cedrus Atlantica* trees from the Atlas Mountains in Morocco (Esper et al. in press). A combination of Regional Curve Standardization (Esper et al. 2003a), regular normalization (Esper et al. 2003b), and individual standardization (Fritts 1976) was applied to preserve multi-decadal and multi-centennial variability. This tree-ring chronology was used in a linear regression model to reconstruct February-June Palmer Drought Severity Index (PDSI; Palmer 1965) variability. PDSI is a standardized measure of surface moisture conditions with limited seasonality. The resulting reconstruction is therefore a good representation of winter drought conditions. The decreasing precipitation trend since the 1970s, as recorded in regional observational station data (Knippertz et al. 2004), is fully retained in the reconstruction (Fig. 2).

The Scotland precipitation reconstruction

An actively growing stalagmite from a cave in NW Scotland provided a 1100-year long (900-1993) precipitation proxy (Proctor et al. 2000). The continuous, annual luminescent bands formed by organic matter in the stalagmite, allowed for precise determination of growth rate variations. Growth rates were found to be controlled by precipitation variability, and annual band width data were used to reconstruct winter precipitation over the last millennium. The resulting reconstruction proved to be highly sensitive to multi-decadal variations in NAO over the instrumental period (1865-1990; Proctor et al. 2000).

Large-scale geopotential height patterns

For the instrumental period, we used an extended version of the traditional winter NAO index, which is defined as the normalized pressure difference between the Azores and Iceland (Hurrell 1995). This extended version of the index (back to 1824) was developed by including data from Gibraltar and Stykkisholmur (Jones et al. 1997).

To investigate long-term associations of the proxy records with atmospheric circulation patterns, we applied composite map analysis. This non-linear method captures the possible asymmetric character of the associations (Rimbu et al. 2006). We used reconstructed (1659-

DOI:10.2312/GFZ.b103-08056

2001) fields of monthly 500 hPA geopotential height, developed by Luterbacher et al. (2002). The years of most positive (95th percentile) and most negative (5th percentile) difference in precipitation between Scotland and Morocco were identified and the respective geopotential height data averaged for these sets of extreme years. The significance of the differences in composite climatic conditions between extreme years was determined using a Student's t-test (Brown and Hall 1999).

Results

The contrasting moisture conditions since the 1970s in northwestern Europe (wet) and northwestern Africa (dry) are reflected in the drought reconstructions from Scotland and Morocco (Fig. 2).

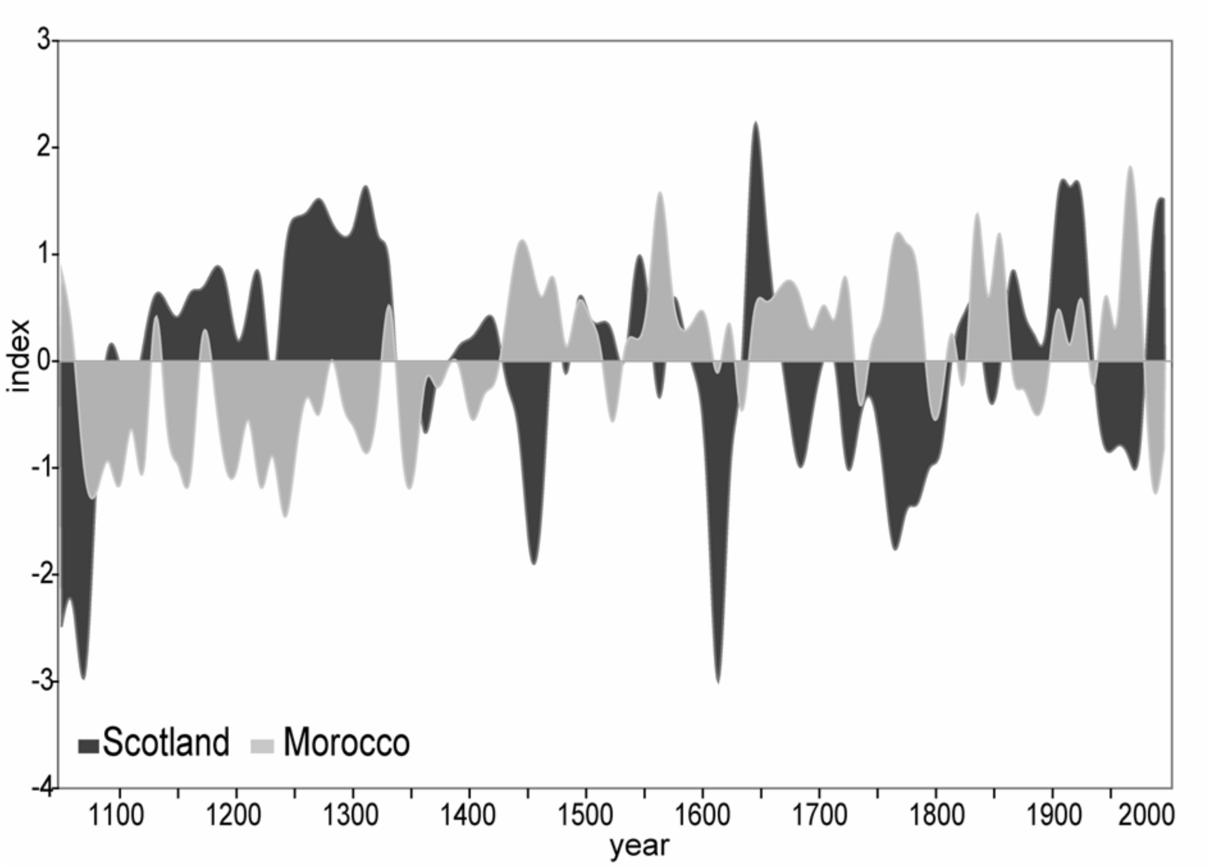

Figure 2: Decadal scale variance in Morocco PDSI and Scotland precipitation. Series were computed from 10-year, non-overlapping averages, and then smoothed using a cubic spline for presentation (unsmoothed values used in correlation analysis).

Multi-decadal variations of both reconstructions are characterized by quasi-regular occurrences of contrasting conditions over the last millennium. Contrasting moisture conditions were particularly strong during the Medieval Warm Period (MWP; 1000-1350), the 18th century, and since the 1940s (Fig.2). The reconstructions contain substantial multi-decadal scale variability that was shown to correlate negatively ($r=-0.26$; $p<0.05$) using sequential 10-year non-overlapping means.

The NAO influence on the contrasting precipitation regimes was investigated by calculating the difference between the standardized, decadally smoothed Scotland and Morocco time series. This residual series (MSres) was then correlated with the NAOI over the instrumental period (1824-1993), revealing rather strong and positive correlations (r=0.75, p<0.01; Fig. 3). Positive MSres values correspond to positive NAO phases, and vice versa. While MSres followed the NAOI closely from 1850 onwards, substantial differences were found over the 1824-1850 period during which the Gibraltar/Stykkisholmur series showed higher values.

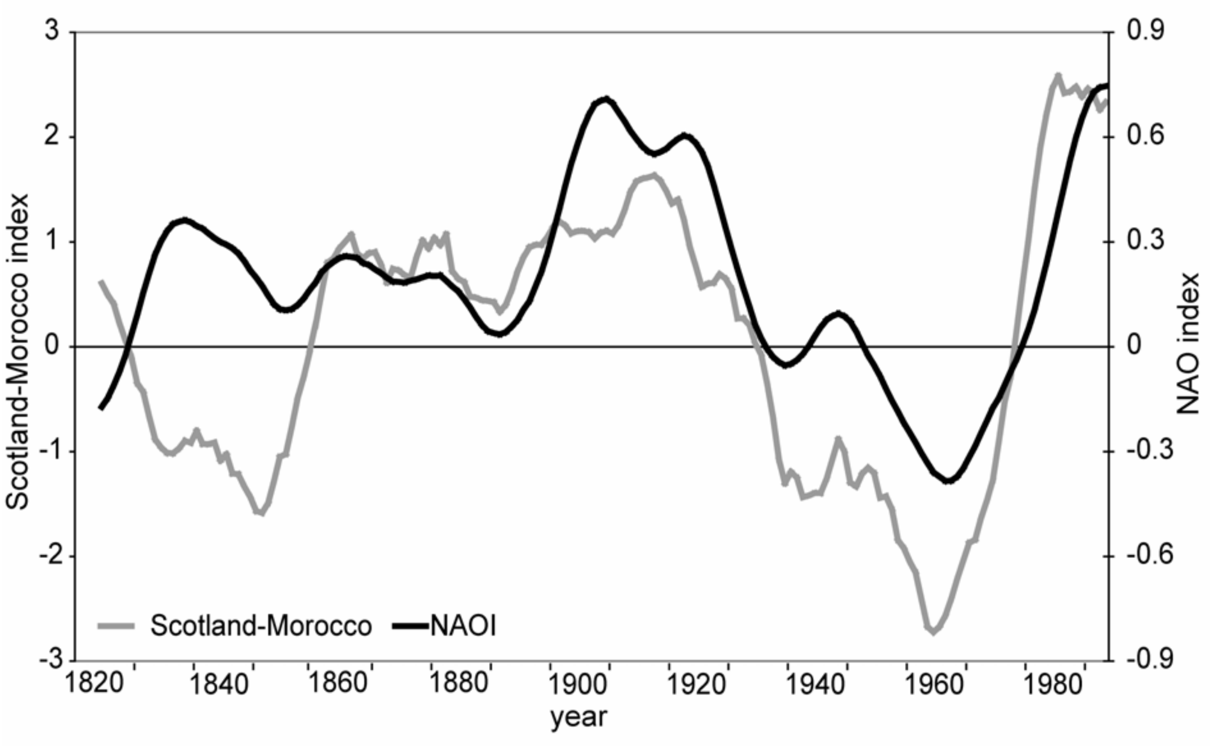

Figure 3: Interdecadal variation in MSres and NAOI. Series were standardized and smoothed using a 10-year moving average.

The reconstructed (1659-2001) geopotential height fields (Luterbacher et al. 2002) provide a test bed to study NAO influence on precipitation patterns over longer time-scales. Reconstructed geopotential height anomalies during the most positive MSres years (Fig. 4a) closely reproduce positive NAO geopotential height patterns over Europe, as derived from observational pressure data (1949-2000; Fig. 1a). The Icelandic Low is deeper than usual and a strong ridge prevails over the Azores and the whole Mediterranean. Reverse geopotential height conditions characterize strongly negative MSres years (Fig. 4b), as was the case in the late 18th century, when a consistent anomalously high Icelandic Low resulted in a reduced pressure gradient between the Icelandic Low and the Azores High (typical for a negative NAO phase; Fig. 1b) and weakened westerlies across the North Atlantic (Fig. 4b). During this period drier and cooler than normal winter conditions prevailed over northwestern Europe, while warmer and wetter winters occurred in the Mediterranean (Fig. 2).

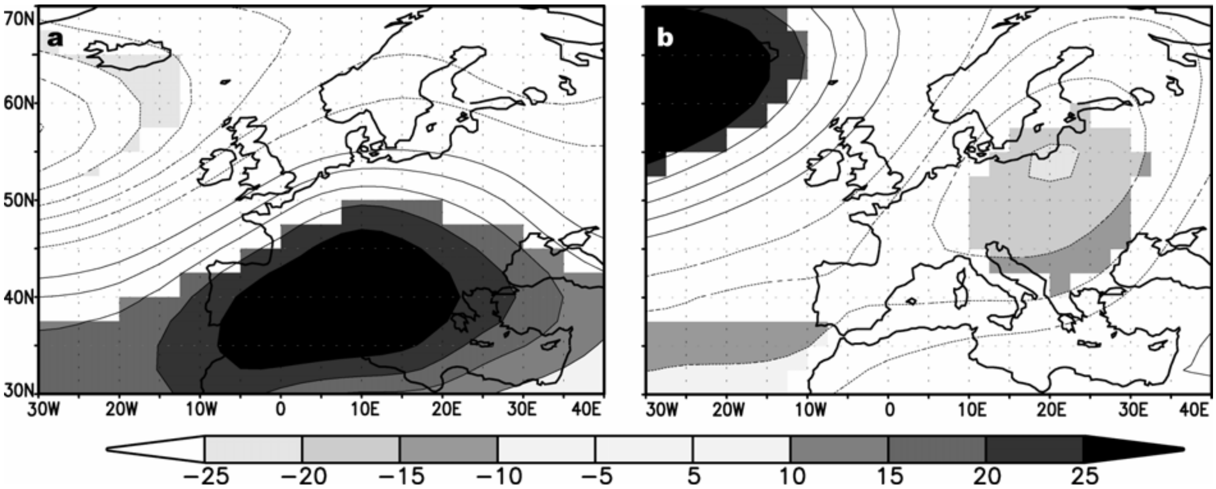

Figure 4: Anomaly (from the 1659-2000 average) composites of January-March 500 hPA patterns of the 5% highest (a) and the 5% lowest (b) values in MSres. Positive anomalies are indicated by full lines, negative anomalies by dashed lines. Shaded areas reflect significant ($p<0.1$) differences, calculated using a t-test.

Discussion

Combination of two drought-sensitive, millennium-long climate proxies from western Europe and northwestern Africa revealed potential to reconstruct extreme, decadal scale NAO phases over the past millennium.

The decadal resolution of the speleothem record from Scotland restricts our analysis to a multi-decadal time-scale, which corresponds to the dominant frequency domain of the NAO (6-10 years; Hurrell and Van Loon 1997). A combination of the two proxies, which are located near the prevailing centers of action of this dipole, closely reflects the decadal scale NAO variability over most of the instrumental period (Fig. 3). This association was weak, however, over the early observational data period (1824-1850).

The proxy combination shows a strong moisture contrast between Scotland and Morocco since the 1970s, corresponding to the concomitant highly positive NAO phase. Additionally, the high index phase from the turn of the 20th century until the 1930s (Hurrell 1996) and the minimum in the 1960s (Hurrell and Van Loon 1997) are well captured in the proxy record. Periods of contrasting moisture conditions over Europe were also associated with NAO-like geopotential height patterns over longer time-periods (Fig. 4).

Our results indicate that the strong moisture contrast between Scotland and Morocco since the 1970s is not exceptional within the millennium-long context provided by the reconstructions (Fig. 2) and multi-decadal and multi-centennial contrasting periods have occurred regularly over the last millennium. Reconstructed precipitation over Scotland was consistently high through much of the MWP, whereas several periods of low precipitation occurred during the subsequent Little Ice Age (LIA; ca. 1500-1850). The Morocco proxy record, in contrast, is characterized by persistent medieval drought and LIA moistening. The MWP-LIA fluctuations in the isotopic signature of a speleothem in the central Alps (Mangini et al. 2005), suggest changes in the strength of winter westerlies across northern Europe, associated with a NAO phase shift (Graham et al. 2007). The centennial-scale moisture fluctuations resulting from this shift, as well as the contrasting moisture conditions in recent decades, co-occurred with moisture anomalies around the globe (Hoerling and Kumar 2003, Cook et al. 2007, Seager et al. 2007). The global character of this centennial-scale hydroclimatic variability implies forcing by fluctuating global ocean-atmosphere states (Seager et al. 2007). A persistently positive NAO in the Medieval period could be teleconnected with prevailing La Niña-like conditions in the tropical Pacific (Graham et al. 2007), which in turn could arise as a result of positive radiative forcing and reduced volcanic activity (Cook et al. 2007). Model simulations further suggest that a switch in radiative forcing could be a contributing factor in the long-term shift in NAO phase between the MWP and the LIA (Shindell et al. 2003).

Our combined millennium-long proxy record reflects extreme NAO phases accurately on a multi-decadal to multi-centennial time-scale. By combining two drought proxies with opposite long-term trends, we link long-term fluctuations in European winter precipitation patterns to variations in large-scale circulation, which may help to improve our understanding of the climate system, its natural variability, and its forcing factors.

Acknowledgements

We thank A. Baker for providing data and helpful suggestions. Supported by the EC project Millennium (Grant No. 017008), and the SNSF through the National Centre for Competence in Climate Research (NCCR-Climate).

References

Brown, T. J., Hall, B. L. (1999): The use of t-values in climatological composite analyses. *Journal of Climate*: 2941-2944.

Cook, E. R., Seager, R., Cane, M.A., Stahle, D.W. (2007): North American droughts: reconstructions, causes and consequences. *Earth Science Reviews*: 93-134.

Dünkeloh, A., Jacobeit, J. (2003): Circulation dynamics of Mediterranean precipitation variability 1948-1998. *International Journal of Climatology*: 1843-1866.

Esper, J., Cook, E. R., Krusic, P. J., Peters, K., Schweingruber, F. H. (2003a): Tests of the RCS method for preserving low-frequency variability in long tree-ring chronologies. *Tree-Ring Research*: 81-98.

Esper J., Shiyatov, S. G., Mazepa, V. S., Wilson, R. J. S., Graybill, D. A., Funkhouser, G. (2003b): Temperature-sensitive Tien Shan tree ring chronologies show multi-centennial growth trends. *Climate Dynamics*: 699-706.

Esper, J., Frank, D., Büntgen, U., Verstege, A., Luterbacher, J., Xoplaki, E. (in press): Long-term drought severity variations in Morocco. *Geophysical Research Letters* .

Graham, N., Hughes, M.K., Ammann, C.M., Cobb. K.M., Hoerling, M.P., Kennett, J.P., Rein, B., Stott, L., Wigand, P.E., Xu, T. (2007): Tropical Pacific-Mid latitude teleconnections in Medieval times. *Climatic Change*: 241-285.

Hoerling, M. P., Kumar, A. (2003): The perfect ocean for drought. *Science*: 691-694.

Hurrell, J. W. (1995): Decadal trends in the North Atlantic Oscillation: regional temperatures and precipitation. *Science*: 676-679.

Hurrell, J. W. (1996): Influence of variations in extratropical wintertime teleconnections on Northern Hemisphere temperature. *Geophysical Research Letters*: 665-668.

Hurrell, J. W., Van Loon, H. (1997): Decadal variations in climate associated with the North Atlantic Oscillation. *Climatic Change*: 301-326.

Jones, P. D., Conway, D. (1997): Precipitation in the British Isles: an analysis of area average data updated to 1995. *International Journal of Climatology*: 427-438.

Jones, P. D., Jónsson, T., Wheeler, D. (1997): Extension to the North Atlantic Oscillation using early instrumental pressure observations from Gibraltar and South-West Iceland. *International Journal of Climatology*: 1433-1450.

Knippertz, P., M. Christoph, and P. Speth (2004): Long-term precipitation variability in Morocco and the link to the large-scale circulation in recent and future climates. *Meteorological and Atmospheric Physics*: 67–88.

Kiely, G. (1999): Climate change in Ireland from precipitation and streamflow observations. *Advances in water resources*: 141-151.

Luterbacher, J., and 48 coauthors (2006): Mediterranean climate variability over the last centuries: A review, in *The Mediterranean Climate*, edited by P. Lionello et al., pp. 27-148, Elsevier, Amsterdam.

Mangini, A., Spötl, C., Verdes, P. (2005): Reconstruction of temperature in the Central Alps during the past 2000 yr from a d18O stalagmite record. *Earth and Planetary Science Letters*: 741-751.

Mills, T. C. (2005): Modelling precipitation trends in England and wales *Meteorological applications*: 169-176.

Palmer, W. C. (1965): Meteorological drought. *Research Paper 45*, 58 pp., U.S. Dept. of Commerce, Washington.

Pauling, A., Paeth, H. (2007): On the variability of return periods of European winter precipitation extremes over the last three centuries. *Climate of the Past*: 65-76.

Proctor, C. J., Baker, A., Barnes, W.L., Gilmour, M.A. (2000): A thousand year speleothem proxy record of North Atlantic climate from Scotland. *Climate Dynamics*: 815-820.

Rimbu, N., Felis, T., Lohmann, G., Patzold, J. (2006): Winter and summer climate patterns in the European-Middle East during recent centureis as documented in a morthern Red Sea coral record. *The Holocene*: 321-330.

Seager, R., Graham, N., Herweijer, C., Gordon, A.L., Kushnir, Y., Cook, E. (2007): Blueprints for Medieval hydroclimate. *Quaternary Science Reviews*.

Shindell, D. T., Schmidt, G.A., Miller, R.L., Mann, M.E. (2003): Volcanic and solar forcing of climate change during the pre-Industrial period. *Journal of Climate*: 4094-4107.

Van Loon, H., Rodgers, J.C. (1978): The seesaw in winter temperatures between Greenland and northern Europe. Part I: general description. *Monthly Weather Review*: 296-310.

Xoplaki, E., J.F. González-Rouco, J. Luterbacher, and H. Wanner (2004): Wet season Mediterranean precipitation variability: influence of large-scale dynamics and predictability. *Climate Dynamics*: 63-78.

DOI:10.2312/GFZ.b103-08056

Tree-ring based drought reconstruction in the central Hengduan Mountains region (China) since A.D. 1655

Z. Fan & A. Bräuning

Institute of Geography, University of Erlangen-Nuremberg, Kochstr. 4/4, D-91054 Erlangen, Germany

Email: fanzexin@yahoo.com.cn; abraeuning@geographie.uni-erlangen.de

Introduction

The Tibetan plateau has a mean elevation of more than 4,000 m asl. and covers an area of more than 2 million km^2. Thus, it acts as a heating surface during spring and summer and plays a key role in driving the Asian summer monsoon circulation (Murakami 1987, Webster *et al.* 1998). However, climate stations were not installed on the Tibetan plateau before 1950. This limits the analysis of long-term climate trends from meteorological records and requires the study of climate history from high-resolution proxy data like tree rings. In recent years, considerable progress was achieved to construct century to millennial-long tree-ring chronologies from north-eastern Tibet (e. g. Zhang *et al.* 2003, Shao *et al.* 2004) and from the southern parts of the Tibetan Plateau (Wu *et al.* 1991, Bräuning 2004, Bräuning and Grießinger 2006). However, only few dendroclimatological studies were conducted in the north-south oriented Hengduan Mountains. Here we present four new tree-ring width chronologies from the central Hengduan Mountains at the southern rim of the Tibetan plateau. We analyze the relationships between tree growth and climatic variables to examine the regional climate variability during the past 350 years.

Material and Methods

Chronology development

The four chronologies presented in this study come from three coniferous tree species, i.e. *Picea likiangensis* Pritz, *Tsuga dumosa* (D. Don) Eichler, and *Abies ernestii* Rehd. Increment cores from 93 trees (136 cores) were extracted with an increment borer at four sites on the west facing slopes of the Baima Snow Mountains, NW Yunnan (Fig. 1). The forests at the sampling sites are hardly disturbed by human activity. At each site, a minimum of sixteen trees were cored at breast height. Ring widths were registered with a LINTAB measuring system with a resolution of 0.01 mm, and all cores were cross-dated by visual growth pattern matching, skeleton plotting and statistical tests (sign-test and t-test) in the software package TSAP (Stokes and Smiley 1968, Rinn 1996). The variance of each series was stabilized using a data-adaptive power transformation, then standardization was carried out in two steps in ARSTAN (Cook 1985). After fitting a negative exponential or a linear regression curve of negative slope, the tree-ring sequences were detrended with a cubic smoothing spline with a 50% frequency-response cutoff equal to 67% of the series length. The final tree-ring index chronologies were obtained by calculating differences between the transformed ring width measurements and the fitted splines. All detrended series were averaged to chronologies by computing the biweight robust mean in order to reduce the influence of

DOI:10.2312/GFZ.b103-08056

outliers (Cook and Kairiukstis 1990). To reduce the potential influence of decreasing sample depth with increasing age, the variance of the chronology was stabilized (Osborn *et al.* 1997).

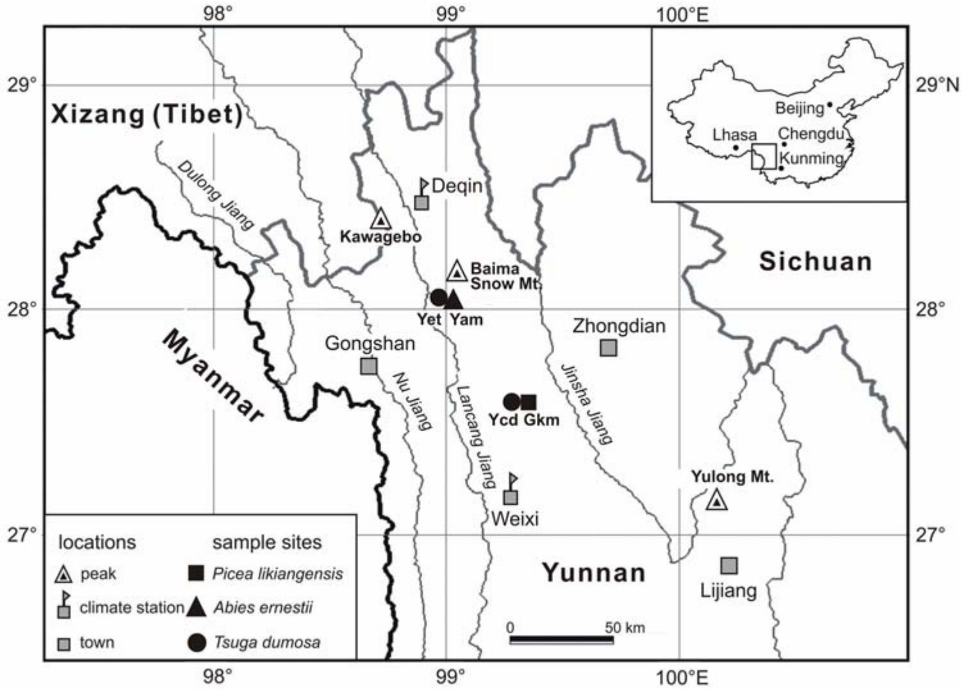

Figure 1: Map of the sampling sites in the Baima snow mountains, northwestern Yunnan.

Climate data

The region's climate is temperate and is characterized by a rainfall maximum during the summer months. Summer rains originate from monsoonal air masses flowing over the Bay of Bengal, whereas winters are generally dry (Xu *et al.* 2003). There are two meteorological observation stations relatively close to the sampling sites (Figure 1), located in Deqin (28.48^{o}N, 98.92^{o}E, 3320 m a.s.l., record length 1957-2000) and Weixi (27.17^{o}N, 99.28^{o}E, 2325 m a.s.l., record length 1961-2000). A dataset for the Palmer drought severity index (PDSI) on a 2.5^o×2.5^o grid was developed by Dai *et al.* (2004). The two grid points (26.25^{o}N, 98.75^{o}E and 28.75^{o}N, 98.75^{o}E) next to our sampling sites were used for detecting the growth response to moisture conditions. A regional series of climate data was created from the two meteorological stations for their common period of 1961-2000, and from the two PDSI grid points for 1951-2000 (Jones and Hulme 1996).

Growth-climate response

The climate-growth relationships were examined by computing correlation functions between climate data and tree-ring index chronologies and the score of PC#1, respectively. Pearson correlation coefficients were calculated between the ring width chronologies and the monthly regional series of temperature and precipitation for a 15 month period ranging from July of the summer prior to growth until September of the growth year (Deqin *v.s* Yam and Yet; Weixi *v.s* Gkm and Ycd). PC#1 was compared with the regional climate series of relative humidity and PDSI for a 15-month period from July of the summer prior growth to September of the growth year.

DOI:10.2312/GFZ.b103-08056

Results

The Rbar and EPS statistics of the site chronologies signal strength range from 0.28 to 0.37 and from 0.77 to 0.87, respectively. Three site chronologies meet the 0.85 EPS criterion after AD 1655, except for site Yet whose EPS is above 0.75 at 1655 and reaches the 0.85 limit only after 1730. Nevertheless, we regarded the period 1655-2005 (351 years) as common period of acceptable chronology quality for further analyses. Despite of the different species analyzed, the four chronologies correlate with each other significantly over the common period 1655-2005, with correlation coefficients ranging from 0.40 to 0.55 ($p<0.01$). Ring-width patterns are very similar among the four chronologies, especially concerning high and middle frequency growth variations. The principle component analysis of the four chronologies shows that only the eigenvalue of PC#1 was greater than one and that PC#1 accounts for 60.5% of the total variance. The four chronologies show common positive loadings on PC#1: 0.78 for Gkm, 0.79 for Ycd, 0.75 for Yam and 0.79 for Yet, respectively. Therefore, PC#1 reflects the common growth response to regional climatic variations, and the score of PC#1 can be used to evaluate the regional climate-growth relationships and to indicate regional climate variability. Correlation analyses indicate that tree growth is mainly affected by early spring precipitation, especially during January, March and May (Fig. 2). The correlation coefficients between seasonal precipitation (March to May) and the residual ring-width index chronologies are significant ($p<0.05$) except for site Yet ($r=0.56$ for Gkm, 0.57 for Ycd, 0.33 for Yam, 0.25 for Yet).

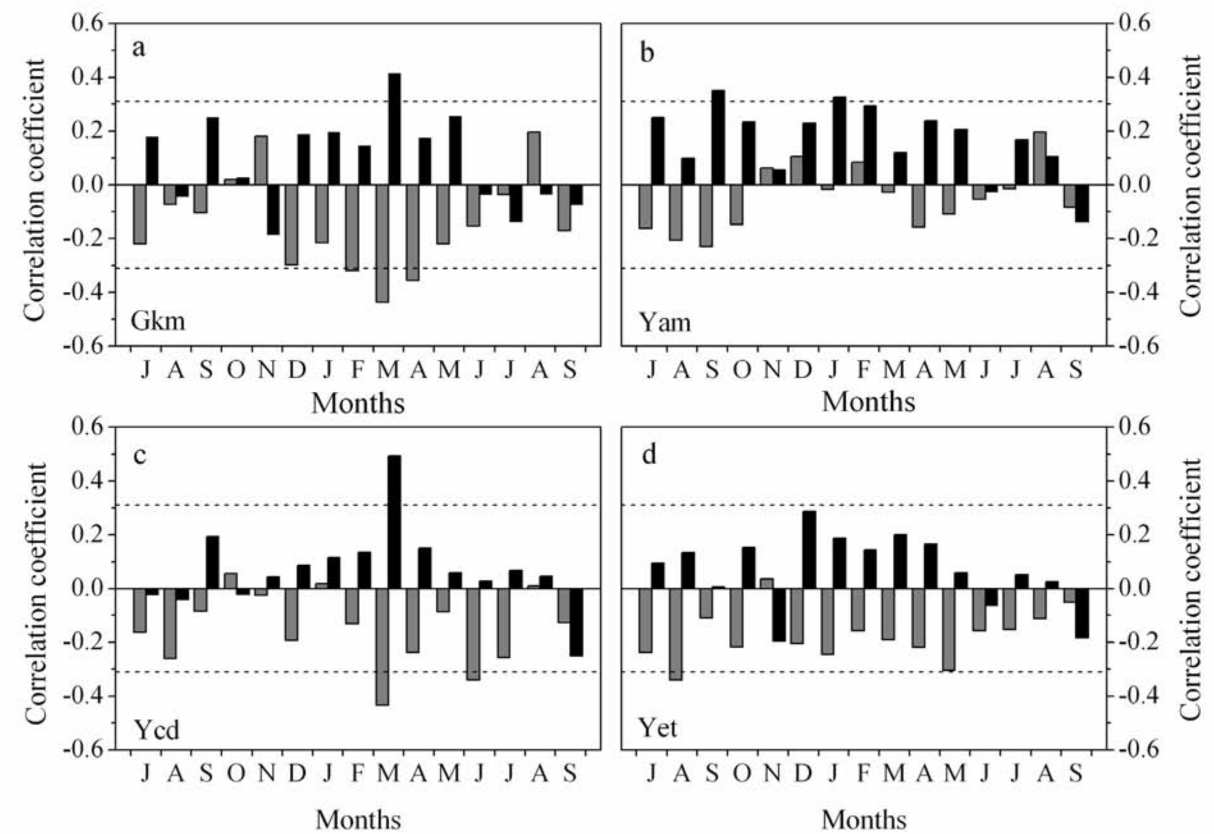

Figure 2 Correlation coefficients between radial growth and monthly mean temperature (gray) and total monthly precipitation (dark) at nearby meteorological stations. Correlations are computed from previous year July to current year September over 1957-2000 for Deqin and 1961-2000 for Weixi. Horizontal dashed lines denote the 95% levels of significance.

DOI:10.2312/GFZ.b103-08056

When standard chronologies instead of residual chronologies are compared with climate parameters, we find the same general patterns but lower correlations (not shown). PC#1 of the four residual chronologies correlates positively with the PDSI (Fig. 3a) and with relative humidity (Fig. 3b) in the spring of the growth year. The highest correlation between PC#1 and PDSI occurs for the season March to May (r=0.65, p<0.01) which was therefore reconstructed by using PC#1 of the four residual chronologies as predictor variable.

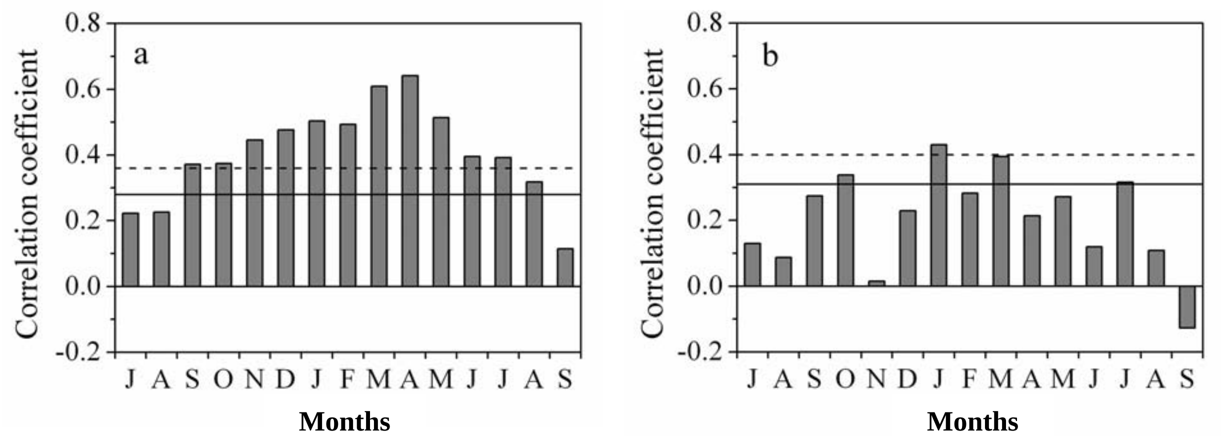

Figure 3 Correlation of thePC#1 with (a) PDSI data (1951-2000) and (b) the regional monthly relative humidity (1961-2000) from previous year July to current year September. Horizontal bold and dashed lines denote the 95% and 99% significance levels, respectively.

A linear regression model was developed to reconstruct the drought history for the central Hengduan Mountain region. During the common period of tree rings and PDSI data (1951-2000), the reconstruction accounted for 42% of the actual PDSI variance (Tab. 1).

Table 1: Statistics of calibration-verification test results for the common period 1951-2000.

Split-sample calibration-verification								
	Calibration				*Verification*			
Period	*R*	*R^2*	*F*	*Period*	*Sign test*	*Pmt*	*RE*	*CE*
1951-1980	*0.65*	*0.42*	*20.4***	*1981-2000*	*14/6***	*2.50***	*0.318*	*0.298*
1981-2000	*0.68*	*0.47*	*15.9***	*1951-1980*	*22/8**	*2.51***	*0.374*	*0.359*
1951-2000	*0.65*	*0.42*	*34.5***					
Leave-one-out verification								
1951-2000	*0.61*				*38/12***	*2.75***	*0.372*	

The spring PDSI estimates derived from this model show high agreement with the yearly departures from the long-term mean in the observed data (Fig. 4a). Split-sample calibration-verification and leave-one-out cross verification methods (Michaelsen 1987) were employed to evaluate the statistical fidelity of this model. The reduction error (RE) and the coefficient of efficiency (CE) are positive, which indicate significant skill in the tree-ring estimates (Fritts 1976). The results of the sign test and product mean test demonstrate the validity of our regression model (Tab. 1).

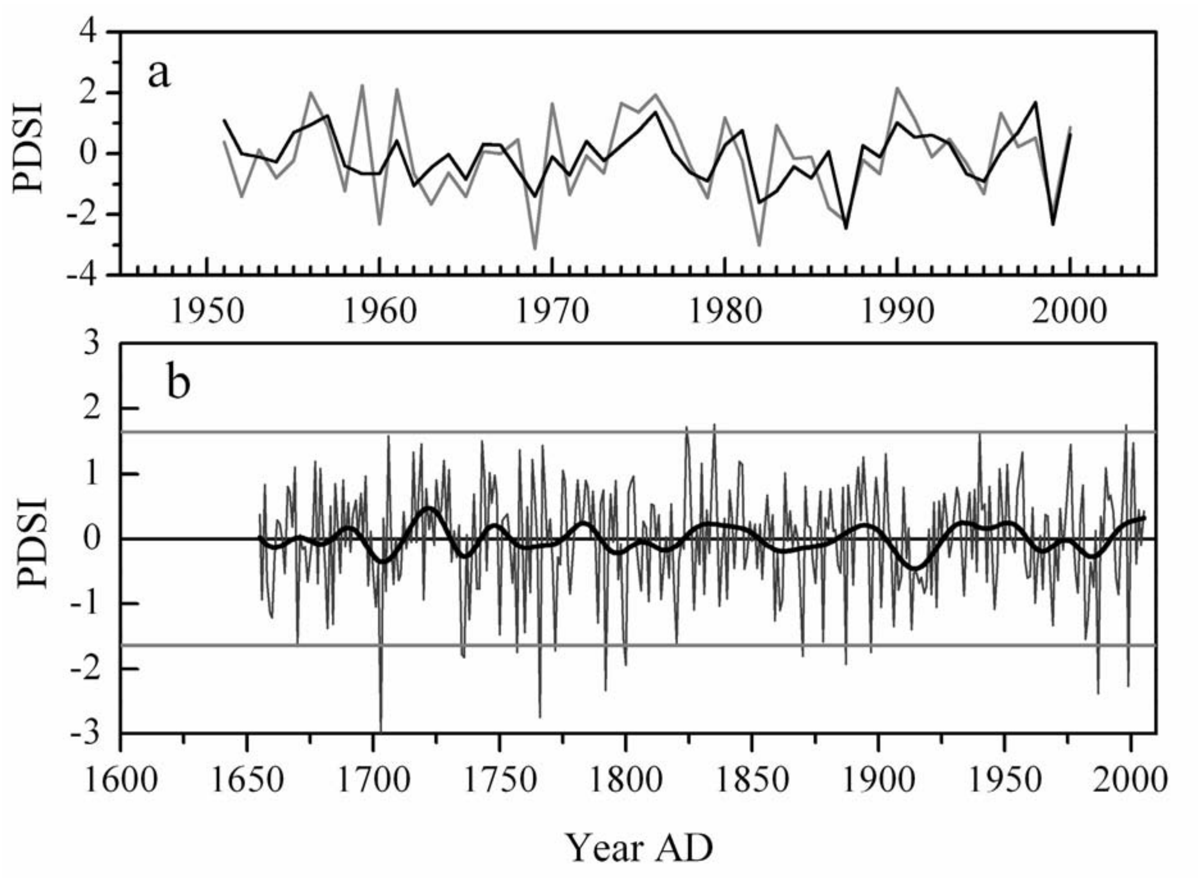

Figure 4: a) Actual (gray) and reconstructed (dark) March to May PDSI during their common period 1951-2000. b) The reconstruction of March-May PDSI in the central Hengduan Mountain region over the past 350 years. The thin line represents the annual value and the thick line was smoothed with an 11-year FFT-filter (Fast Fourier Transform) to emphasize long-term fluctuations. The gray line indicates the ±2 SD values.

The spring (March-May) PDSI reconstruction (Fig. 4b) shows that wet periods prevailed in the 1690s, 1715-1730, 1750s, 1780s, 1825-1850,1900s, 1930-1960, and 1990-present. Extremely wet years (≥2SD) occurred in AD 1703, 1824, 1835, 1940, and 1998. In contrast, the intervals AD 1700-1715, 1733-1745, 1790-1820, 1860-1890, 1910-1925, and 1960-1990 were relatively dry. Extremely dry years (≤2SD) were more frequent than extremely wet years and are concentrated during AD 1730-1800 and 1870-1900, and after 1980, respectively. From the higher mean correlation between the four individual chronologies, it can be concluded that these were time periods of strong climatic forcing of regional tree growth patterns. Particularly dry years occurred in AD 1670, 1706, 1735-1736, 1757, 1766, 1772, 1792, 1800, 1820, 1870, 1887, 1897, 1987, and 1999.

Discussion

We found significant positive correlations between tree growth and precipitation in January, March and May (Fig. 2). The correlation between PC#1 and relative humidity and the PDSI also indicates that the spring moisture availability is a major limiting factor for tree-ring growth (Fig. 3). In southern Tibet, dry and warm conditions before the onset of the summer monsoon cause drought stress to the trees and are thus limiting growth (Bräuning and Grießinger

2006). Thus, tree growth benefits from former winters' and current spring precipitation, which increase the soil moisture content during the early part of the growing season. This growth response is not surprising for trees growing on steep slopes in a subtropical climate. Our study sites are located at middle elevations, far away from the upper tree line which lays around 4200 meters a.s.l. in the Baima Mountain region.

Although our PDSI reconstruction is based on the residual tree-ring chronologies, considerable decadal scale moisture variability is retained in our reconstruction. The dry springs in the 1700s, 1730s and 1790s-1820s (Figure 4b) were also detected as dry periods in the same area by Wu *et al.* (1988). The dry periods in the 1800s are synchronous with dry conditions in Mongolia and in the western Himalaya (Pederson *et al.* 2001, Singh *et al.* 2006). Other intervals in the 18^{th} century were relative wet, especially the period 1715-1730. The period 1825-1850 was a relatively prolonged wet period, which has also been reported as a prolonged phase with wet springs (AD.1820s to 1840s) in the western Himalayan region of India (Singh *et al.* 2006).

The most severe drought period in the past 350 years occurred during 1910-1925. This severe drought has also been recorded in tree-rings from North China (Liang *et al.* 2006) and southern Tibet (Bräuning and Grießinger 2006). Liang *et al.* (2006) combined tree-ring records and historical records (meteorological, hydrological and documentary evidence) and reported that the 1920s drought was severe and sustained across northwest China. Spring climate was relatively wet from 1930 to 1960, which was also reported by Wu *et al.* (1988). The period 1960-1990 was relatively dry, especially in 1983-1988. The last ca. 15 years were comparatively wet, but were still within the range of fluctuations over the last 350 years.

Acknowledgements

The authors thank Mrs. Iris Burchardt for her aid on ring-width measurements. The work was financially supported by the Max-Planck-Gesellschaft.

References

Bräuning, A., Mantwill, B. (2004): Summer temperature and summer monsoon history on the Tibetan plateau during the last 400 years recorded by tree rings. *Geophysical Research Letters* **31**: L24205, Doi: 10.1029/2004GL020793.

Bräuning, A., Grießinger, J. (2006): Late Holocene variations in monsoon intensity in the Tibetan-Himalayan region-evidence from tree rings. *Journal Geological Society of India* **69** (3): 485-494.

Cook, E.R. (1985): *A time-series analysis approach to tree-ring standardization*. PhD dissertation, the University of Arizona Press: Tucson.

Cook, E.R., Kairiukstis, L.A. (1990): *Methods of Dendrochronology*. Kluwer Academic Press: Netherlands.

Dai, A.G., Trenberth, K.E., Qian, T. (2004): A global dataset of Palmer Drought Severity Index for 1870-2002: relationship with soil moisture and effects of surface warming. *Journal of Hydrometeorology* **5**: 1117-1130.

Fritts, H.C. (1976): *Tree rings and climate*. Academic Press: London.

Jones, P.D., Hulme, M. (1996): Calculating regional climatic time series for temperature and precipitation: methods and illustrations. *International Journal of Climatology* **16**: 361-377.

Liang, E.Y., Liu, X.H., Yuan, Y.J., Qin, N.S., Fang, X.Q., Huang, L., Zhu, H.F., Wang, L.L., Shao, X.M. (2006): The 1920s drought recorded by tree rings and historical documents in the semi-arid and arid area of Northern China. *Climatic Change* **79**: 403-432.

Michaelsen, J. (1987): Cross-validation in statistical climate forecast models. *Journal of Climate and Applied Meteorology*. **26**: 1589-1600.

Murakami, T. (1987): *Effects of the Tibetan Plateau*. In: Chang, C-P, Krishnamurti, T N (eds.): *Monsoon Meteorology*. Oxford Monographs on Geology and Geophysics **7**: 235-270.

Osborn, T.J., Briffa, K.R., Jones, P.D. (1997): Adjusting variance for sample size in tree-ring chronologies and other regional mean timeseries. *Dendrochronologia* **15**: 89-99.

Pederson, N., Jacoby, G.C., D'Arrigo, R.D., Cook, E.R., Buckley, B.M. (2001): Hydrometeorological reconstructions for Northeastern Mongolia derived from tree rings: 1651-1995. *Journal of Climate* **14**: 872-881.

Rinn, F. (2003): *TSAPWin: Time series analysis and presentation for dendrochronology and related applications.* Version 0.55 User reference, Heidelberg, 76p.

Singh, J., Park, W.-K., Radav, R.R. (2006): Tree-ring-based hydrological records for western Himalaya, India, since A.D. 1560. *Climate Dynamics* **26**: 295-303.

Shao, X.M., Huang, L., Liu, H.B., Liang, E.L., Feng, X.Q., Wang, L.L. (2004): Reconstruction of precipitation variation from tree rings in recent 1000 years in Delingha, Qinghai. *Science in China (D)* **34(2)**: 145-153. (in Chinese with English Abstract)

Stokes, M.A., Smiley, T.L. (1968): *An Introduction to Tree-Ring Dating*. The University of Chicago Press, Chicago and London, pp.73.

Webster, P.J., Magana, V.O., Palmer, T. N., Shukla, J., Tomas, R.A., Yanai, M., Yasunari, T. (1998): Monsoons: Processes, predictability, and the prospects for prediction. *Journal of Geophysical Research* **103** (C7): 14,451-14,510.

Wu, X.D., Li, Z.Y., Sun, L. (1988): A preliminary study on the climatic change of the Hengduan Mountains area since 1600 A.D. *Advances in Atmospheric Sciences* **5**(4): 437-443.

Wu, X.D., Zhan, X.Z. (1991): Tree-ring width and climatic change in China. *Quaternary Science Reviews* **10**: 545-549.

Xu, X.D., Miao, Q.J., Wang, J., Zhang, X.J. (2003): The water vapor transport model at the regional boundary during the Meiyu Period. *Advances in Atmospheric Science* **20**: 333-342.

Zhang, Q.B., Cheng, G.D., Yao, T.D., Kang, X.C., Huang, J.G. (2003): A 2,326-year tree-ring record of climate variability on the northeastern Qinghai-Tibetan Plateau. *Geophysical Research Letters* **30(14)**: 1739, Doi:10.1029/2003GL017425.

SECTION 2

DENDROECOLOGY

Differential effect of drought on *Pinus nigra* Arn. radial growth in mesic and xeric sites from southeastern Spain

D.Martín-Benito[1], P. Cherubini[2], M. del Río[1] & I. Cañellas[1]

[1] Departamento Sistemas y Recursos Forestales. CIFOR-INIA. Crta. La Coruña km 7.5 28040 Madrid, Spain

[2] Swiss Federal Institute for Forest, Snow and Landscape Research WSL, CH-8903 Birmensdorf, Switzerland

Email: dmartin@inia.es

Introduction

Different water regimes are of great importance in ecosystems under Mediterranean climate, where drought is the most important factor limiting tree growth and productivity (Specht 1981). Climate change models for south-eastern Mediterranean Spain predict a decrease of annual mean precipitation between 6% and 14% (Sumner et al. 2003). Therefore, the frequency of extreme droughts may increase in the future, which could lead to a reduction of forest productivity and changes in species composition. A necessary pre-requisite for the appropriate management of forest is to understand their growth dynamics, including their response to drought.

Pinus nigra Arn. (black pine) is very widely distributed and is one of the most commonly used pines in large plantations all over the Mediterranean region and other parts of Europe. This makes it very susceptible to the increase in temperature and decrease in precipitation already observed in western Mediterranean (Rodrigo et al. 1999) and predicted by climate change models (Sumner et al. 2003).

Our study, thus, explores the response to drought of black pine trees growing in sites differing in water availability, slope and location. In xeric sites, water is supposed to be less abundant and more dependent on current year rainfall than in mesic sites. In the later, water accumulation from runoff as well as possible water table likely assures a more constant water supply for trees.

Material and Methods

Study sites

The study sites are located in the Cazorla Mountain Range in southeastern Spain (Fig. 1). Forests made up of Mediterranean pines (*P. nigra, P. halepensis* Mill., and *P. pinaster* Ait.) cover most of the area. Altitude ranges from 600 m to 2107 m a.s.l. The main soil types in the region are based on a dolomite and calcareous bedrock (Sanchez-Palomares et al. 1990). Soils are leptosols (rendzinas) on higher slopes, and luvisols on flat terrain with alluvial and colluvial deposits (Sanchez-Palomares et al. 1990; FAO 2006).

Tree stands were selected from the network of permanent research plots (PRP) that was established by INIA (Spanish National Institute of Agricultural Research) in 1964, and inventoried 8 times afterwards (1964-2006). In order to represent different conditions of water availability, we selected two sites of high slope near the top of ridges and distant from any

DOI:10.2312/GFZ.b103-08056

water current ('xeric') and two in flat terrain in valleys ('mesic'). All plots were even aged and located in well stocked stands where trees originated from natural regeneration.

Figure 1: Distrubution of Pinus nigra in the Iberian Peninsula and location of study sites in southeastern Spain (circle).

Sampling and standard dendrochronological methods.

In June 2006, 15 -16 dominant trees were sampled from each plot. Dominant trees were defined as those within each plot that had had the largest DBH during the eight inventories (1964-2006). For each tree, two cores were taken from the upper slope side at a 120º angle from each other, to avoid reaction wood.

Applying a standard procedure, cores were mounted to grooved boards and sanded with three different grits (80-400). Widths of three tree-ring sections (i.e. total ring (TR), earlywood (EW) and latewood (LW)) were measured to the nearest 0.01 mm with a measuring table and registered using TSAP (Rinn 1996). Qualitative visual aspects (darkening and tracheid size) were used to define transition from EW to LW.

Raw ring-width series were visually and statistically cross-dated in TSAP. Then, ring-width index were developed in ARSTAN using the Huggershoff equation (Cook and Holmes 1994). This equation is a combination of a polynomial and a negative exponential. Since it only has one turning point with increasing age, it allows for increasing growth during the juvenile phase of the tree and a curvilinear decline as the tree ages (Warren 1980, Bräker 1996).

Climate data, correlation analysis and response function

Mean monthly temperatures (ºC) and precipitation (mm) were collected from the meteorological station at Santiago de la Espada (Jaén) (38º06' N, 02º33' W, 1340 m a.s.l.), approximately 25 km from sampling sites. For the period considered (1940-2005) mean annual temperature was 12.9º C. Absolute maximum and minimum temperatures were 40 ºC and -22 ºC, and frost was possible from November to April. Precipitation (annual mean of 730 mm) showed a winter maximum and summer drought in the area lasted three-four months (June-September). Mean monthly temperature and total monthly precipitation (predictor variables) were regressed against ring-width indexes to assess climate-growth relationships (Fritts 1976). Correlation and response function were calculated with DENDROCLIM2002 (Biondi and Waikul 2004).

Superposed epoch analysis (SEA)

The nonparametric technique of superposed epoch analysis (SEA) was used to assess the relationship between extreme climatic events (drought) and the strength of the response in the corresponding year (tree growth indices) (Haurwitz and Brier 1981). Centered in the year of the drought, five years before and five years after were taken as background years for comparison. For this study, drought was defined as an extraordinary departure from mean cool season (October to May) precipitation, lower than the mean by one standard deviation for the period 1940-2005. The ten selected drought years were 1942, 1943, 1945, 1950, 1953, 1967, 1968, 1981, 1995, and 1999. Although the year 2005 was the driest for the period, it was not considered for the SEA because there were not five post-drought years to compare it with. The differences between the ring-width index (RWI) of the three tree-ring sections of each core and their means were calculated and later averaged for event years and background years (Orwig and Abrams 1997). The *T* statistic as described by Haurwitz and Brier (1981) and modified by Prager and Hoenig (1989) was used to test whether the RWI of the drought years differed significantly from pre- and post-drought years. These departures from the mean did not meet the general assumptions for normality so Monte Carlo randomizations were run in SAS (SAS Institute Inc. 2004) to select 10 000 sets of 11 years to compute confidence intervals for *T*.

Raw ring width values during drought years were compared to the years before and after the drought to quantitatively analyze growth decreases and recoveries (Fekedulegn et al. 2003). Percent growth changes were calculated as follows:

- drought vs prior year: $[(D_0-D_{-1})/ D_{-1}]\cdot 100$
- post-drought year vs pre-drought year: $[(D_{+1}- D_{-1})/ D_{-1}]\cdot 100$
- drought year vs five years pre-drought : $[(D_0- D_{-5})/ D_{-5}]\cdot 100$
- five years post-drought vs drought year: $[(D_{+5}- D_0)/ D_0]\cdot 100$
- five years post-drought vs five years pre-drought: [(D+5- D-5)/ D-5]·100

where D_0 is the raw ring width (RW) for any of the tree-ring sections the year of drought, D_{-1} is RW for the year prior to drought, D_{+1} is RW for the year after drought, D_{-5} is the average of RW for the five years prior to drought, and D_{+5} is the average of RW for the five years after drought. Analysis of variance for multiple comparisons was carried out using proc GLM in SAS (SAS Institute Inc 2004).

DOI:10.2312/GFZ.b103-08056

Table 1: Chronology statistics in dominant trees of xeric and mesic sites for each ring section calculated in raw ring-width data before detrending.

Plot	Altitude (m)	No. of trees	Chronology time-span (years)	TRW			EW			LW		
				Rbar	MS	AC	Rbar	MS	AC	Rbar	MS	AC
Xeric sites												
J03	1440	15	1806-2005 (200)	0.64	0.28	0.76	0.66	0.28	0.77	0.44	0.42	0.54
J04	1475	16	1910-2005 (96)	0.60	0.31	0.70	0.59	0.33	0.68	0.47	0.46	0.49
Mesic sites												
J02	1100	15	1830-2005 (176)	0.47	0.27	0.80	0.50	0.28	0.79	0.33	0.38	0.63
J18	1295	15	1910-2005 (96)	0.41	0.24	0.71	0.54	0.27	0.69	0.24	0.32	0.59

TRW, total ring; EW, earlywood; LW, latewood
Rbar, mean interseries autocorrelation; MS, mean sensitivity; AC, first-order serial autocorrelation coefficient.

Results and Discussion

As expected, xeric sites showed higher mean sensitivities (MS) than in mesic sites, particularly in the latewood (LW) (Tab. 1). Lower water availability caused LW widths to be less correlated with previous year growth as shown by autocorrelation coefficients (AC). This is further supported by results shown in figure 2. In xeric sites there is a higher abundance of years with narrow LW (curve is more left-skewed) and earlywood (EW) tends to be wider (less left-skewed) than mesic sites. In these later sites, EW and LW curves are more balanced and more similar to each other.

These results seem to indicate that mesic sites are growing more evenly every year and for a longer period (wider LW), whereas in xeric sites growth differs more from year to year, especially at the end of the season (narrower LW). However, the fact that there is a higher proportion of wide EW in xeric than in mesic sites (Fig. 2) shows that trees in xeric sites might have similar or wider diameter growth than trees in more mesic sites. Irrigation has been shown to increase LW production in *Pinus sylvestris* L. (Rigling et al. 2003) in a similar way that trees in mesic sites produced wider LW.

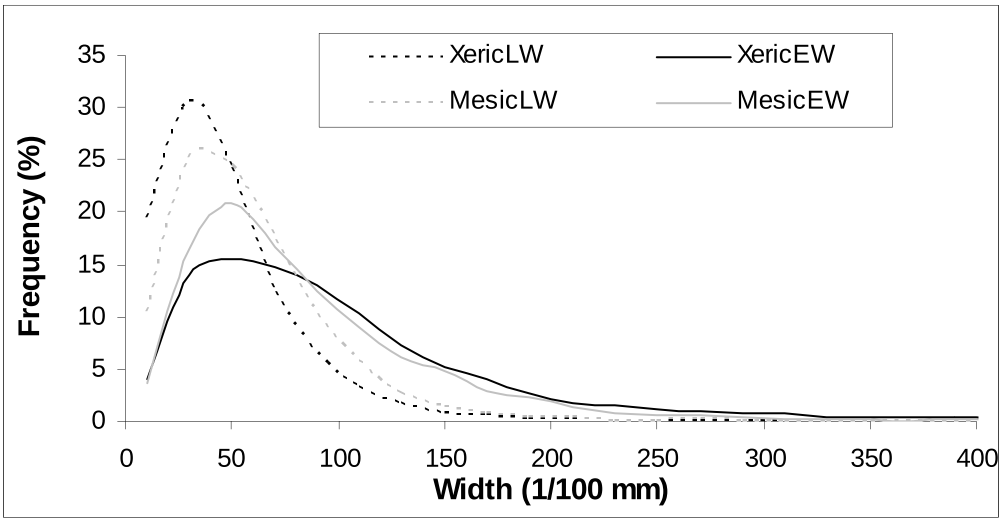

Figure 2: Relative frequency (%) of early- (EW) and latewood (LW) widths in mesic and xeric sites.

DOI:10.2312/GFZ.b103-08056

Radial growth of trees was positively influenced by moist and warm previous-year autumn, and cool and wet current-year spring (Tab. 2). Current-year late summer temperature positively affected trees in mesic sites, most likely showing that a higher water content in the soil allows these trees to grow after summer temperature decreases. However, the significance of September temperature on EW could also be a statistical artifact.

Table 2: Tree growth response to temperature and precipitation (response functions). O*, significant coefficients at 95%. Shaded areas show negative coefficients.*

		TEMPERATURE													
		Previous year				Current year									
		SEP	OCT	NOV	DEC	Jan	Feb	Mar	Apr	May	Jun	Jul	Aug	Sep	Oct
TRW	mesic				O			O						O	
	Xeric	O			O						O				
EW	mesic				O						O			O	
	Xeric	O			O						O				
LW	mesic										O				
	Xeric										O	O			

		PRECIPITATION													
		Previous year				Current year									
		SEP	OCT	NOV	DEC	Jan	Feb	Mar	Apr	May	Jun	Jul	Aug	Sep	Oct
TRW	mesic				O										
	Xeric				O					O					
EW	mesic														
	Xeric									O					
LW	mesic				O										
	Xeric				O					O					

Spring precipitation was only significantly correlated with growth in xeric sites, suggesting that in these sites water is more a limiting factor, than in mesic sites. Thus, the higher relative abundance of wider latewood in tree-rings from mesic sites (Fig. 2). This is also supported by the negative influence of temperatures in previous-year summers and current-year springs in xeric sites (Tab. 2) that might decrease the availability of water in the soil through evapotranspiration. High temperatures in July reduced growth of LW in xeric sites only, probably showing a longer period of water stress.

During drought periods, all tree-ring sections showed reduced growth as compared with five years previous and after the drought (Fig. 3). LW was the most affected ring section (Fig. 3; Tab. 3), and EW the least. This suggests that water stress at the beginning of the growing season might not greatly differ from dry to normal years since soil water reservoir is charged during the wet-cool season (October-May). These differences increase later in the spring or summer.

Trees growing in xeric sites experienced greater tree-ring reductions during droughts than those in mesic sites (Fig. 3, Tab. 3), which is in accordance with findings on *Pinus ponderosa* Dougl. Ex. Laws (Adams & Kolb 2005) but contrasts with those on *Pinus virginiana* Mill.

(Orwig & Abrams 1997.) All these results point toward a species specific site-drought response for the mentioned pines species. In xeric sites, LW formed during dry years was on average 25% narrower than those of five years pre- and post-drought. This difference was 14% in mesic sites (Tab. 3). One year after drought, trees in mesic stands recovered or exceeded normal growth by 14%. On the second year, trees achieved a growth greater than that before the drought and trees in xeric sites grew faster compared to mesic sites (Fig. 3). Prolonged post-drought reductions in black pine were not observed, in accordance with similar results in *P. virginiana* (Orwig & Abrams 1997.)

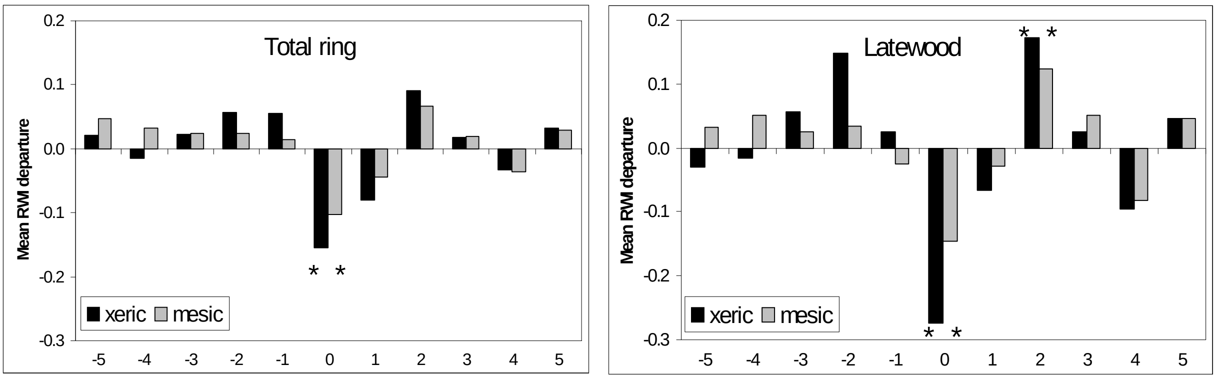

Figure 3: Mean RWI departures of TRW and LW in the SEA for the drought years and five years before and after drought. (*) denotes a departure greater than expected to occur by chance from 10,000 random simulations (P<0.005).

Table 3: Means±SE and relative changes (%±SE) in raw ring width in xeric (X) and mesic (M) sites for each ring compartment. Departures are pooled from the ten drought episodes considered. Means in a column with the same letter are not significantly different at P <0.005.

Ring compart.		Drought vs prior year (%)	Post- vs pre-drought (%)	Drought vs 5 year pre-drought (%)	5- year post-drought vs drought (%)	5 year post- vs 5 year pre-drought (%)
TRW	X	-7.0±2.7 a	-2.8±3.1 a	-17.0±1.4 b	21.0±1.9 b	6.4±1.5 a
	M	-7.1±2.1 a	-0.1±2.4 a	-11.5±1.3 ab	23.5±2.3 b	-0.9±1.5 bc
EW	X	-2.1±3.0 a	-0.8±3.8 a	-11.9±1.5 ab	15.1±1.9 b	6.2±1.5 a
	M	-5.9±2.0 a	-4.3±2.2 a	-9.1±1.3 a	16.0±2.2 b	1.8±1.4 ab
LW	X	-9.0±3.2 a	6.3±3.6 ab	-25.1±1.6 c	55.4±3.9 a	4.2±1.8 ab
	M	-2.9±3.17 a	14.1±4.0 b	-13.9±1.9 ab	55.1±4.8 a	-5.7±1.8 c

TRW, total-ring width; EW, earlywood; LW, latewood.

Conclusions

It was clearly shown that drought periods impose a higher than regular water stress for black pine growth regardless of the site type (mesic or xeric). Mesic sites have better developed soils with higher soil water capacity and higher amount of run-off water. Black pine trees in these sites seem to withstand drought better than trees in xeric sites and recover faster from growth-decrease after drought. However, when soil water is not such a limiting factor, trees in xeric sites could have ring growth similar or wider than trees in more mesic sites.

DOI:10.2312/GFZ.b103-08056

References

Adams, H.D., Kolb, T.E. (2004): Drought responses of conifers in ecotone forests of northern Arizona: tree ring growth and leaf d13C. *Ecologia*, 140, 217–225.

Biondi, F., Waikul, K. (2004): DENDROCLIM2002: A C++ program for statistical calibration of climate signals in tree-ring chronologies. *Comput Geosci* 30:303-311.

Bräker O. U. (1996): Growth Trends of Swiss Forests: Tree-Ring Data. Case Study Toppwald. - In: Spiecker, H.; Mielikäinen, K.; Köhl, M.; Skovsgaard, J.P. (eds) Growth Trends in European Forests. European Forest Institute Research Report No.5. Berlin, Heidelberg, Springer. 199-217.

Cook E.R., Holmes, R.L. (1984): Users manual for Program ARSTAN. Laboratory of Tree-Ring Research. Tucson, Arizona, USA.

FAO (2006) World reference base for soil resources (2006): Food and Agriculture Organization of the United Nations, Rome.

Fekedulegn, D., Hicks, R.R. Jr., Colbert, J.J. (2003): Influence of topographic aspect, precipitation and drought on radial growth of four major tree species in an Appalachian watershed. *For Ecol Manag* 177:409-425.

Fritts, H.C. (1976): Tree rings and climate. Academic Press, London, UK.

Haurwitz, M.W., Brier, G.W. (1981): A critique of the superposed epoch analysis method: its application to solar-weather relations. *Mon Weather Rev* 109:2074-2079.

Orwig, D.A., Abrams, M.D. (1997): Variation in radial growth responses to drought among species, site, and canopy strata. *Trees* 11:474-484.

Prager, M.H., Hoenig, J.M. (1989): Superposed epoch analysis: a randomization test of environmental effects on recruitment with application to chub mackerel. *T Am Fish Soc* 118: 608-618.

Rigling, A., Brühlhart, H., Bräker, O., Forster, T., Schweingruber, F.H. (2003): Effects of irrigation on diameter growth and vertical resin duct production in *Pinus sylvestris* L. on dry sites in the central Alps, Switzerland. *For Ecol Manag* 175: 285-296.

Rinn, F. (1996): TSAP-reference manual. Frank Rinn, Heidelberg, Germany.

Rodrigo, F.S., Esteban-Parram M.J., Pozo-Vázquez, D., Castro-Díez, Y. (1999): A 500-year precipitation record in Southern Spain. *Int J Climatol* 19:1233-1253.

Sánchez-Palomares, O., Elena-Roselló, R., Carretero-Carrero, M.P. (1990): Caracterización de edáfica de los pinares autóctonos españoles de *Pinus nigra* Arn. Comunicaciones INIA. Serie: Recursos Naturales Nº 55. INIA, Madrid, Spain.

SAS Institute Inc (2004): SAS/STAT 9.1 user's guide. SAS Institute Inc. Cary, USA.

Specht, R.L. (1981): Primary production in Mediterranean climate ecosystems regenerating after fire. In: Di Castri F, Goodall DW, Specht RL (eds), Mediterranean-type shrublands. Elsevier, Amsterdam, pp 257-267.

Sumner, G,N., Romero, R., Homar, V., Ramis, C., Alonso, S., Zoritam E. (2003): An estimate of the effects of climate change on the rainfall of Mediterranean Spain by the late twenty first century. *Clim Dynam* 20:789-805.

Warren, W.G. (1980): On removing the growth trend from dendrochronological data. *Tree-Ring Bull*. 40: 35–44.

DOI:10.2312/GFZ.b103-08056

Dendroecological studies on subfossil pine and oak from "Totes Moor" near Hannover (Lower Saxony, Germany)

J. Eckstein[1], H.H. Leuschner[1] & A. Bauerochse[2]

[1] *University of Göttingen, Albrecht-von-Haller-Institute, Department of Palynology and Climate Dynamics, Untere Karspüle 2, 37073 Göttingen, Germany*

[2] *Lower Saxony State Service for Cultural Heritage, Hannover, Scharnhorststraße 1, 30175 Hannover, Germany*

Email: jan.eckstein@biologie.uni-goettingen.de

Introduction

The “Totes Moor” is a 33 km² large wetland, located in the Weser-Aller lowlands, about 25 km north-west of Hannover on the southern margin of the North German lowlands (Lower Saxony, Germany; Schneekloth & Schneider 1970, Tüxen 1979). It is situated at the northern margin of a shallow depression northwest of lake “Steinhuder Meer”. The depression, which has been formed by thermokarst, is filled with fluvioglacial sediments and covered by peatlands. Surface inequalities containing small basins, channels and walls characterize the relief of the mineral ground at the end of the last glaciation (Merkt 1979). In the first half of the Holocene, this caused a heterogeneous vegetation mosaic with different tree stands, reeds and ponds to develop. In most parts of this area, raised bog growth started in the Atlantic period.

At present the area is used for industrial peat cutting. Thereafter the peat harvest fields are rewetted and classified as nature conservation areas.

The climate in the area is slightly of Atlantic character. Mean annual precipitation (based on the period 1961-1991) is 630 mm, more than half of which (c. 360 mm) precipitates from April through September (DWD 2007).

During peat harvesting, large amounts of subfossil wood, primarily pine (*Pinus*) and oak (*Quercus*), but also alder (*Alnus*), are excavated and provide evidence of former environments. This wood is most important for dendroecological investigations. They form the main focus of a supra-regional research project funded by the German Research Foundation (DFG; LE 1805/2-1) that investigates the usefulness of bog pines as indicators for climate change

The aims of the study are:

- Cross dating of the pine samples to establish dated or, floating chronologies. Although there exists no master pine chronology for northern Germany, it can be expected that well replicated and extended pine data series can be crossdated with the bog oak master chronology for Lower Saxony (LSBOC; Leuschner et al. 2006, Leuschner et al. 1987) which spans the period from 6,069 BC to AD 931.
- Reconstruction of the spatial and temporal distribution of former pine woodlands.
- Reconstruction of the ecological context of former mire pine woodlands, their establishment, population dynamics and decline.

DOI:10.2312/GFZ.b103-08056

- Documentation of stress as an indicator of changes of ecological conditions. It can be assumed that hydrology is a main factor for tree growth in mire woodlands, and therefore, common growth depression phases may indicate wetter conditions (Leuschner et al. 2002; Sass-Klaassen 2006).
- Determination of whether recorded stress, changes in growth pattern, and population dynamics of pines results from local environmental changes in the "Totes Moor" area or from regional phenomena which can be linked to supra-regional environmental shifts also documented from other Lower Saxony peatland sites like “Oytener Moor” and “Heseper Moor”.

Below first results of these investigations are discussed.

Materials and Methods

Sampling

Samples were taken from the central part of the bog (52.51°N 9.39°E), where industrial peat harvesting proceeds. The sampling sites are distributed over an area of about 1 km². Most of the samples were recovered from four sub-sites with laboratory codes M723, M724, M725 and M726 (Fig. 1).

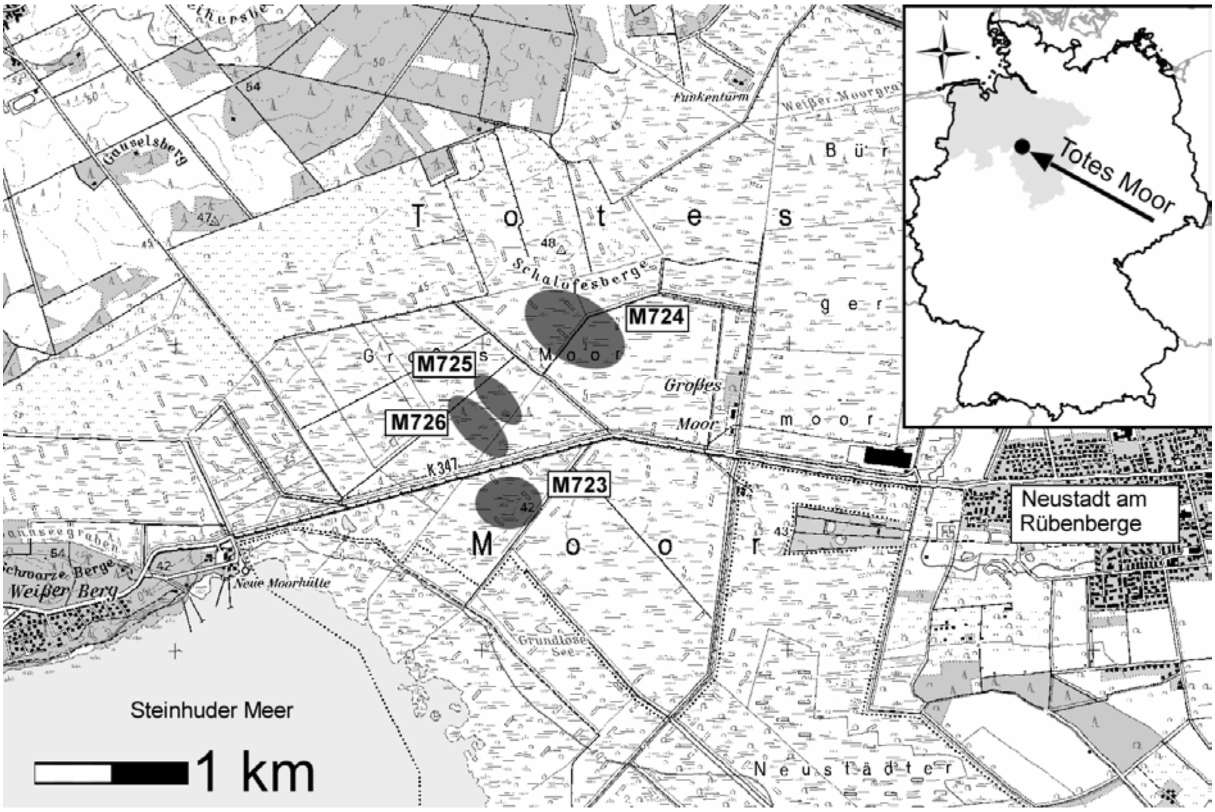

Figure 1: Outline map of the "Totes Moor" northwest of lake “Steinhuder Meer”. Location of the four sample sites are indicated in dark grey.

The subfossil wood which has bee recovered during peat harvesting was removed from the fields and dropped at their edges. Most of the investigated samples were taken from these

DOI:10.2312/GFZ.b103-08056

wood cops around the harvesting sites. In addition in situ samples had been taken from ditches and from the surface of the harvesting fields.
Most of the wood is pine, whereas oak is relatively sparse and mainly preserved as lying tree trunks without any trace of trunk-bases or roots. Compared to oak, pine is mostly found as very short stumps with a more or less complete root system or, less frequently, as lying trunks, often with remains of roots. Our sampling strategy aimed at covering the entire spectrum of tree sizes, root system morphologies, and different states of preservation represented in the wood remains. 89 oak and 309 pine samples were collected in total.

Sample preparation, measurement of tree-ring width and dating

The dendrochronological investigation followed standard procedures, described for example by Leuschner (1994). Radial sections of the discs were cut and smoothed with surgical blades and razor blades (Iseli & Schweingruber 1989, Leuschner & Schweingruber 1996). Chalk was rubbed on the surface to enhance contrast and tree-ring boundary visibility. Tree-ring widths were measured with a precision of 1/100 mm by using a semi-automatic measuring stage (type Aniol) and the program CATRAS (Aniol 1983). Cross-dating between the tree-ring series was performed and matches were detected and statistically evaluated by calculating the coefficient of parallel variation (GL) and the t-value (Baillie & Pilcher 1973). The statistical approach was backed and finally proved by visual comparisons of the tree-ring series. Measuring mistakes and missing rings detected by statistical and visual cross-dating of the tree-ring series were manually corrected.

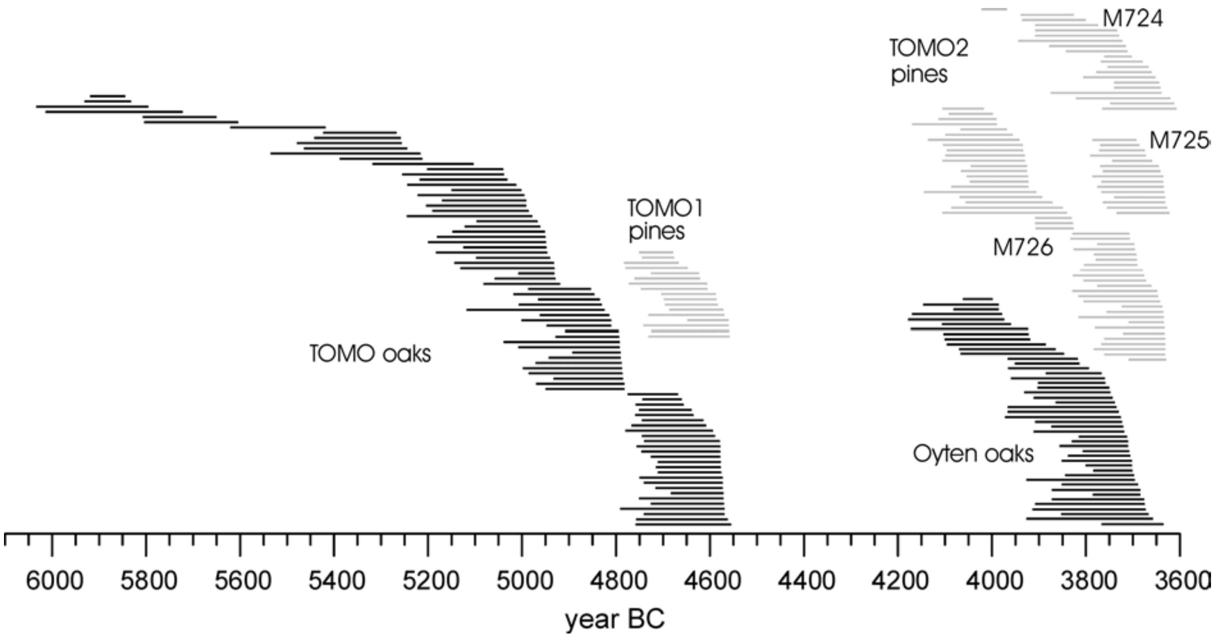

Figure 2: Temporal distribution of subfossil oaks (black) and pines (grey) from "Totes Moor" (TOMO) and oaks from “Oytener Moor” (Oyten), 80 km west of “Totes Moor”, sorted by dying-off dates and grouped by site. TOMO1 and TOMO2 refer to two absolutely dated pine chronologies from “Totes Moor”. If not preserved estimated missing rings to germination and dying-off are added.

Results

Crossdating

83 out of 89 oak samples could be crossdated with reference to the LSBOC. These samples cover the period 6,014 to 4,570 BC. The resulting TOMO oak chronology matches well with the LSBOC (t=19.6; GL=68 %). Pines were first crossdated among themselves by using inter series correlation t-values higher than 5.5. Then some series were corrected for missing rings but no false ring was detected. From 309 recovered pine samples 175 could be crossdated yielding 13 independent chronologies. Two chronologies, TOMO1 (224 years, 17 samples) and TOMO2 (563 years, 84 samples) yielded a significant match with the oak master LSBOC (t=6.9 GL=67 % and t=6.1 GL=61 % respectively). Eventually the positions for TOMO1 and TOMO2 were backed by visual comparison with the LSBOC. TOMO1 covers the period 4,782 4,559 BC and TOMO2 ranges from 4,170 – 3,608 BC.

Peat stratigraphy

A systematic study of peat profiles associated with wood remains in "Totes Moor" has yet to be carried out but preliminary investigations reveal that most of the pine samples occur at the fen/bog transition where pine did form dense stands. Pines were also present at various positions within the raised-bog peat, but in more open stands of only small trees. Several TOMO2 samples were found in situ along a drainage ditch at site M726 (Fig. 1). A peat profile taken adjacent to a sampled tree stump indicates their position at the fen/bog transition (Tab. 1) which is also confirmed by the pollen diagram (F. Schlütz unpubl.).

Table 1: Peat stratigraphy at site M726 with the TOMO2 pine wood layer.

Depth in cm	Description
-	due to peat extraction the upper part of the peat layer is missing,
0 - 40	weakly decomposed *Sphagnu*m peat (white peat), mostly Acutifolia peat containing *Oxycoccus*, *Calluna*, *Eriophorum vaginatum*
41 - 102	strongly humified *Sphagnum* peat (black peat) containing several layers of *Eriophorum vaginatum* and especially on its base *Pinus* wood remains (**TOMO2 wood layer**)
103 - 191	strongly humified fen peat containing *Betula*, *Carex*, *Menyanthes*
191 - 206	fine to medium organic silt containing *Betula*, *Alnus*
207 - 216	*Alnus* wood
217 - 224	*Carex* fen peat
225 - 251	moss fen peat containing *Scorpidium, Carex*, *Menyanthes*, *Alnus*
252 - 255	organic silt with fine sand
256 - 266	glacial fluviatile medium sand with some silt and gravel (< 7 mm)

Most of the youngest oaks from site M724 (Fig. 1) were found in situ in the fen/raised bog transition zone. They are pale in colour, indicating preservation in raised bog peat (without

DOI:10.2312/GFZ.b103-08056

iron).They probably died due to increased raised bog growth at about 4,550 BC and were covered by *Sphagnum* peat.

Temporal distribution

The temporal distribution of both, pine and oak samples, shows that germination and dying-off (GDO) events are not randomly distributed over time (Fig. 2). Germination and dying-off phases sometimes overlap. This is not un-expected, since intensive regeneration has been only possible in open stands after the dying-off of old trees. TOMO1 pine samples parallel those of the youngest oak generation from "Totes Moor". Almost all sample trees germinated between 4,780 and 4,700 BC, and the last pine died off 4,559 BC (the last oak died off 4,555 BC). There must have been stress events affecting both pines and oaks over the same period in similar ways to create such equal patterns of temporal distribution. The results indicate a simultaneous occurrence of pines and oaks between 4,782 and 4,559 BC in the area. However, both species did not grow together at the same site. Locations of pine (M723) and oak (M724) samples from that period are about 1.2 km apart from each other. The TOMO2 pine samples are younger than the oak samples. Yet, in their temporal distribution they show a similar grouping in subsequent woodland generations (Fig. 2). Two generations can be recognised, one from 4,170 to 3,920 BC and another from 3,830 to 3,610 BC with only a few overlapping samples. These two woodland generations are most obvious for sampling site M726. At site M725, only trees from the younger generation are present. Oak samples from “Oytener Moor”, about 80 km west of "Totes Moor", show a very similar temporal distribution as the TOMO2 pines, with similar germination and dying-off phases (Fig. 2). This indicates that some of the stress factors triggering these population dynamics had a supra-regional dimension. However, more research is needed to get a better understanding of these relationships.

Stress signs

In order to identify the rules behind the germination and dying-off phases in former mire woodlands, we looked for stress indicators in the TOMO2 samples. Therefore we recorded scars, the start of reaction wood, burnt outer surface as a reference to fire, and common long term growth depression phases as stress indicators. About 23 % of the TOMO2 samples have a burnt outer surface, hinting at frequent fires. Yet, wounds which may also caused by fire are scattered over time and we do not observe common growth release phases which would point at large scale fire events. So, fires were frequent in the pine woodland but they had not the destructive power to explain the observed dying-off phases.

Reaction wood may point at storm events if many trees were put in an inclined position in the same year. But the starting of reaction wood is also scattered over time and does not coincide with germination or dying-off phases among the TOMO2 samples. Therefore storm events can not explain the population dynamics.

Common growth depression phases are observed especially at the end of the TOMO2 layer. Periods during which many samples indicate growth depressions include around 3,720 BC and from 3,660 to 3,620 BC, when most of the younger sample trees died-off.

DOI:10.2312/GFZ.b103-08056

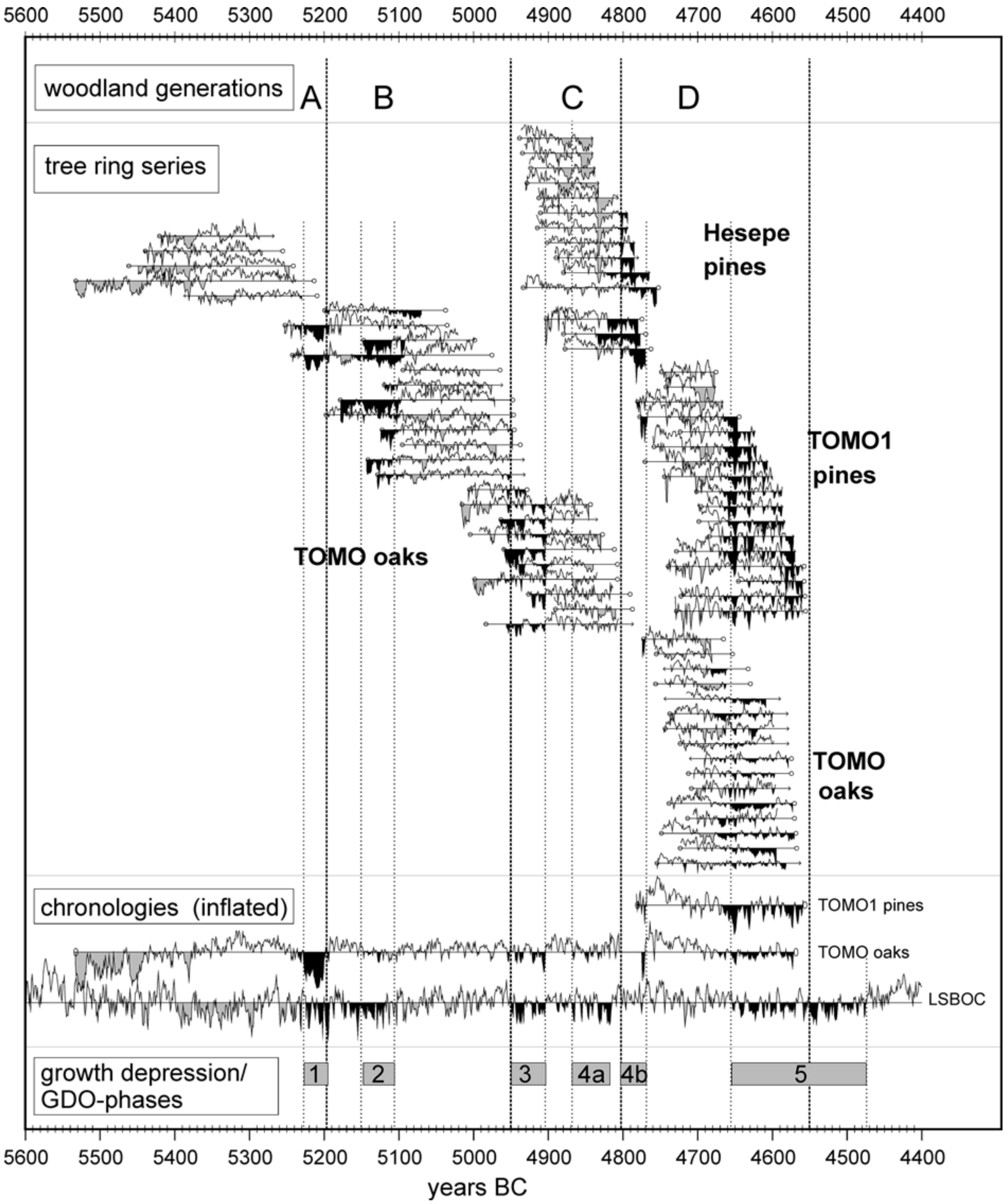

Figure 3: Tree ring series of oaks and pines from "Totes Moor" (TOMO) and "Heseper Moor" (Hesepe), 140 km north-west of "Totes Moor". Periods with growth depression are coloured grey, or black if they coincide with germination and dying-off (GDO) phases (modified after Bauerochse et al. 2006).

A comparison of the tree ring series of the simultaneously occurring pines (TOMO1) and oaks shows that GDO phases are associated with growth depressions in both taxa (Fig. 3). These stress phases with very narrow rings do not only occur in tree-ring series of oaks and pines from "Totes Moor", they are also present in the oak master LSBOC. In the period 4,800 to 4,770 BC (GDO phase 4b in Fig. 3) a GDO phase in the TOMO samples can be linked to

DOI:10.2312/GFZ.b103-08056

growth depressions in pine samples from “Heseper Moor”, 140 km west of "Totes Moor". This relationship is further discussed by Bauerochse et al. (2006).

Discussion

Dendro-dated subfossil oak and pine remains from "Totes Moor" demonstrate the existence of extended pine and oak woods in the area of this wetland from about 6,100 to 3,600 BC. Yet, oaks and pines did not occur together at the same time in the same site. The start of raised-bog formation occurred at different times in different parts of "Totes Moor". At site M724, conditions changed to ombrotrophy around 4,550 BC and at site M726 around 3,600 BC, as indicated by *in situ* findings of oaks (site M724) and pines (M726). At that time, we have to imagine the "Totes Moor" area as a mosaic of different habitats where alder and birch carrs, oak stands, pine forests and raised bogs where riddled with patches of sandy hills and small lakes. This patchy landscape was a result of a varied relief shaped by the last ice age. Later, with increasing raised-bog formation the area was covered more and more by open *Sphagnum* bogs and the huge, more or less uniform, raised bog landscape – today´s “Totes Moor” – was created.

Both the pine and the oak samples show distinct woodland generations separated by GDO phases (Fig. 2 and Fig. 3). Burnt outer surfaces and scars at some samples demonstrate frequent fires in one of these pine stands (TOMO2). These fires must have been natural fires, lit by lightning, for there are no traces of human activities in the area during this time. The fires did not coincide with germination or dying-off phases and the patchy distribution of pine stands probably prevented fires from spreading over extended areas.

In many instances GDO phases are associated with long term growth depressions. In spite of the varied relief moulded during the last ice age and the patchy distribution of oak and pine woods, GDO and depression phases occurred simultaneously both in pine and oak samples from "Totes Moor" and can even be linked to other wetland sites in Lower Saxony. Since the depression phases persisted several decades, they cannot be explained by single catastrophes such as extended fires or heavy storm events, but must have caused by slow responding environmental factors. In wetlands a raising water table is an important stress factor for tree growth. Therefore long-term growth depressions are probably induced by increased wetness as proposed by Leuschner et al. (2002) for oak samples from mire sites. At least some of the GDO phases have a supra-regional dimension and therefore are probably triggered by climatic changes affecting the hydrology of wetland sites over a extended areas in the same way.

Future efforts will focus on extent and character of ecological changes during the fen/bog transition inferred by tree-ring width, shape of pine root systems, peat stratigraphy, intra-annual anatomical features and comparisons between many different sites in Lower Saxony.

Acknowledgements

The dendroecological analysis is part of an ongoing research project, funded by the German Research Foundation (LE 1805/2-1), aiming at extended investigations on subfossil bog pines in Lower Saxony. The field work at site “Totes Moor” had been greatly supported by the Torfwerk ASB-Grünland, Neustadt am Rübenberge. We would like to thank Dr. G. Caspers (LBEG, Hannover) for aid with the peat stratigraphy and Dr M. Wagner (Sheffield) for linguistic corrections.

References

Aniol, R. W. (1983): Tree-ring analysis using CATRAS. *Dendrochronologia* 1: 45-53.

Baillie, D. M., Pilcher, J. R. (1973): A simple cross-dating program for tree-ring research. *Tree-Ring Bulletin* 33: 7-14.

Bauerochse, A., Leuschner, B., Leuschner, H. (2006): Moorhölzer und Archäologie - umweltgeschichtliche und siedlungsarchäologische Befunde. *Berichte zur Denkmalpflege in Niedersachsen* 2/2006: 40-45.

Deutscher Wetterdienst (DWD; 2007): *www.dwd.de/de/FundE/Klima/KLIS/daten/online/nat/index_mittelwerte.htm* (31.08.2007)

Iseli, M., Schweingruber, F. H. (1989): Sichtbarmachen von Jahrringen für dendrochronologische Untersuchungen. *Dendrochronologia* 3: 8-13.

Leuschner H. H. (1994): Jahrringanalysen. In: Herrmann B. (ed.), Archäometrie. Naturwissenschaftliche Analyse von Sachüberresten. Springer: 121-135.

Leuschner, H. H., Bauerochse, A., Metzlar, A. (2006): Environmental change, bog history and human impact around 2900 B.C. in NW Germany - preliminary results from a dendroecological study of a sub-fossil pine woodland at Campemoor, Dümmer Basin. *Vegetation History and Archaeobotany* 16: 183-195.

Leuschner, H. H., Delorme, A., Hoefle, H. C. (1987): Dendrochronological study of oak trunks found in bogs of northwest Germany. In Jacoby, G. C. J.,Hornbeck, J. W. (eds.): *Proceedings of the International Symposium on Ecological Aspects of Tree-Ring Analysis, Tarrytown, New York*. U.S. Department of Energy, Publication CONF-8608 144: 298-318.

Leuschner, H. H., Sass-Klaassen, U., Jansma, E., Baillie, D. M., Spurk, M. (2002): Subfossil European bog oaks: population dynamics and long-term growth depressions as indicators of changes in the Holocene hydro-regime and climate. *The Holocene* 12: 695-706.

Leuschner, H. H., Schweingruber, F. H. (1996): Dendroökologische Klassifizierung und Auswertung häufig auftretender intraannueller holzanatomischer Merkmale bei Eichen und Kiefern. *Dendrochronologia* 14: 273-285.

Merkt, J. (1979): Seeablagerungen. In: Voss, H.-H.: Geologische Karte von Niedersachsen. Erläuterungen zu Blatt Nr. 3522 Wunstorf. 43-48, Hannover.

Sass-Klaassen, U., Hanraets, E. (2006): Woodlands of the past - The excavations of wetland woods at le-Stadshagen (the Netherlands): Growth pattern and population dynamics of oak and ash. *Netherlands Journal of Geosciences* 85: 61-71.

Schneekloth, H., Schneider, S. (1970): Die Moore in Niedersachsen 1.Teil: Bereich des Blattes Hannover der Geologischen Karte der Bundesrepublik Deutschland (1:200000). Gebr. Wurm KG, 70 S., 1 Karte.

Tüxen, J. (1979): Moorbildungen. In: Voss, H.-H.: Geologische Karte von Niedersachsen. Erläuterungen zu Blatt Nr. 3522 Wunstorf. 48-52, Hannover.

Various factors influencing the pointer year analysis

Sz. Bijak
Department of Dendrometry and Forest Productivity, Faculty of Forestry, Warsaw Agricultural University
Email: Szymon.Bijak@wl.sggw.pl

Introduction

Cross-dating is considered as a key target and one of the most important procedures in dendrochronological studies (Fritts 1976). In general, it is based on matching a certain calendar year with an individual tree-ring or linking a ring from one series with a corresponding ring from the other. However, constantly changing environmental conditions affect the formation of a ring by favouring or limiting tree growth. This results in the variety of the tree-ring widths, which hinders the process of cross-dating. Especially wider or narrower tree-rings are the witnesses of extreme growth conditions (Schweingruber 1996). Such events do not occur very often and thus can be easily placed in time. Therefore tree-rings of significantly bigger or smaller dimension become particularly important as potential linkages in the cross-dating process. Analysis of the tree-ring width series that leads to ferreting out those extraordinary increments enables also to determine the most or the least favourable conditions for tree growth. This information, in turn, may play an important role in silviculture and other utilisation of trees.

The concept of pointer year as an individual calendar year when tree growth was significantly different than in other years has its roots in the pioneer dendrochronological studies. However the term itself was defined much later (Schweingruber et al. 1990). At the beginning, the identification of pointer years was based on the 'skeleton plot' method (Douglass 1939) and applied visual assessment of individual tree-rings in comparison with neighbouring increments. Scientific and statistic foundations of the pointer year analysis were introduced by Huber (1943, 1951) as well as Eckstein and Bauch (1969). Since then several methods of pointer year assignment were developed and the analyses were carried out for various regions and species. However, this variety of methods as well as different, very often mutually exclusive, approaches of individual scientists make any attempts to compare the results of pointer year analyses very difficult and complicated (Meyer 1998/1999).

The present paper aims to investigate how the number of pointer years changes when different criteria or methods are applied as well as whether and when the results obtained from dendrochronological analysis correspond to those from the climatological analysis.

In the following an 'event year' is defined as, adopting the definition presented by Schweingruber et al. (1990) and Kaennel and Schweingruber (1995), a specific year when a single tree has formed a conspicuously wider or narrower ring. And thus, following the same basis, the term 'pointer year' describes a certain year when the majority of the investigated tree-ring series shows the same kind of extreme growth reaction. Using the terms 'threshold' or 'threshold value' we understand the certain values applied in utilised methods that allow determining either the 'event' (tree threshold) or 'pointer' (stand threshold) years.

DOI:10.2312/GFZ.b103-08056

Data

The study utilises a set of raw tree-ring measurements taken from lowland Norway spruce (*Picea abies* (L.) Karst.) stands located in the Borecka Primeval Forest in north-eastern Poland. We sampled 43 trees growing on three different site types of different moisture content. Since the distance among these sampling plots was relatively small (ca 1-1,5 km), all sites were assumed to represent the same mezo-climate conditions and therefore considered as a whole. The dendroclimatological description of that data can be found in Bijak (2007).

In order to provide the maximum synchronisation of the samples included in the set, the most similar tree-ring series were chosen based upon the *Gleichläufigkeit* (GLK) criterion. The index was calculated according to the concept presented in Kaennel and Schweingruber (1995). Only series that showed the GLK coefficient with the master chronology higher than 65% were accepted. After this selection, in total 24 series remained for the further analysis.

We used data on mean monthly and annual temperature and precipitation from meteorological station in Suwałki (approximately 60 km eastwards from the Borecka Primeval Forest) to present the climate characteristics for the investigated area.

Methods

Two methods, statistical and visual, were applied to assign the pointer years. Low-pass filtering based on running means and standard deviations of ring-width measurements, the so-called ‘normalisation in a moving window’ method, proposed originally by Cropper (1979) was used to determine pointer years statistically. The procedure consists of three steps, that is: (i) normalisation of the measurements, (ii) calculation of the event years series and (iii) establishment of the pointer year series. The standardisation was carried out within windows of 5, 7 and 9- years’ length according to the following formula:

$$Z_i = (x_i - M_w)/SD_w$$

where:

Z_i is standardised tree-ring width for i-th year, x_i is raw measurement for i-th year, M_w is mean ring width within a window (i-t ,..., i+t, where f=2t+1 is a window length) and SD_w is standard deviation of ring widths within a window

A given year was considered an event year when its z-transformed ring width exceeded a certain tree threshold value. Threshold values for event year determination were applied in 0,05 intervals starting from 0,05. When the ratio of trees showing an event year in a certain calendar year was higher than the stand threshold value, this year was assigned as pointer year. Applied stand threshold values changed from 0,50 to 1,00 (majority criterion) with 0,02 interval.

The visual method of the pointer year determination was carried out with the intention to be possibly similar to the statistical method in the procedure mechanism. It included two stages, that is: (i) assessment of the outstanding increments in the ring-width series which allowed to

establish event years series and then (ii) application of the stand threshold in order to receive the set of pointer years. An individual year increment was compared with its neighbours within ca 3 years distance both back- and forward in time. Again, in order to meet the majority criterion the stand threshold values ranged from 0,50 to 1,00 and the analysis was carried out in 0,02 intervals. An individual year was considered a pointer year when the share of trees revealing an event year exceeded the given threshold value.
In both cases pointer years were determined for the period 1951-2000. This provided that the investigation considered only mature trees that are not affected by juvenile growth and intensive silviculture treatment. The character of the individual pointer years (negative or positive) was not considered and they were counted in total.

Meteorological pointer years were determined in a two-staged procedure. Firstly we calculated pointer years separately for mean annual temperature and annual sum of precipitation. These calculations were based on the comparison of the mean annual temperature and precipitation for individual years with the average values for the period 1931-2003. This allowed dividing both features into five classes. The thermal classification included division into normal, warm/cold and very warm/very cold years. An individual year was classified as a normal when its mean annual temperature was within the range of +/- 0,5 SD (standard deviation) from the mean (M) calculated for the period 1931-2003. Years characterised by the mean annual temperature in the range M+0,5 SD to M+1,25 SD and M-1,25 SD to M-0,5 SD were classified as warm and cold respectively. When mean annual temperature exceeded the value of M+1,25 SD or M-1,25 SD, then the year was classified as very warm or very cold respectively. The pluvial classification assumed division into normal, wet/dry as well as very wet or very dry years and was based on the calculation of the ratio between individual year annual sum of precipitation and the mean calculated for the 1931-2003 period (later referred to as M). When annual precipitation was within the range 0,9 M to 1,1 M the respective year was considered normal. Values between 0,75 M and 0,9 M and between 1,1 M and 1,25 M were classified as dry and wet year respectively. The annual sum of precipitation higher than 1,25 M or lower than 0,75 M meant that the year was classified as very wet or very dry. In the next step, each class was given a rank, which for normal years equalled 0, for warm, cold, wet or dry – 1, and for very warm, very cold, very wet or very dry – 2. Then summing up the ranks combined these results. A year with total rank higher than 3 was considered meteorological pointer year e.g. a year with extreme climate conditions.

Results and Discussion

Influence of window length

Authors that used the ‘normalisation in a moving window’ method in pointer year analyses, applied different lengths of the window within which tree-ring widths are standardised i.e.: 5 years – e.g. Cropper (1979), Neuwirth et al. (2007a), 7 years – e.g. Koprowski and Zielski (2002), or 13 years – e.g. Neuwirth et al. (2007b). However, they give no explanation of the reasons for such choice of this parameter. Application of the various window lengths in the statistical determination method resulted in slightly different numbers of received pointer years. In general, none of the applied window lengths gave constantly higher or lower number of pointer years for the same tree or stand threshold values. For example, application of the 9-year window resulted in the highest number of received pointer years when the stand threshold values were low (0,5-0,6) or high (0,9-1). However, for stand threshold values between 0,6 and 0,7, the number of determined pointer years was the lowest among all applied window lengths (Fig. 1a). Similar relationships can be observed for other window lengths and tree threshold values (Fig. 1b).

a)

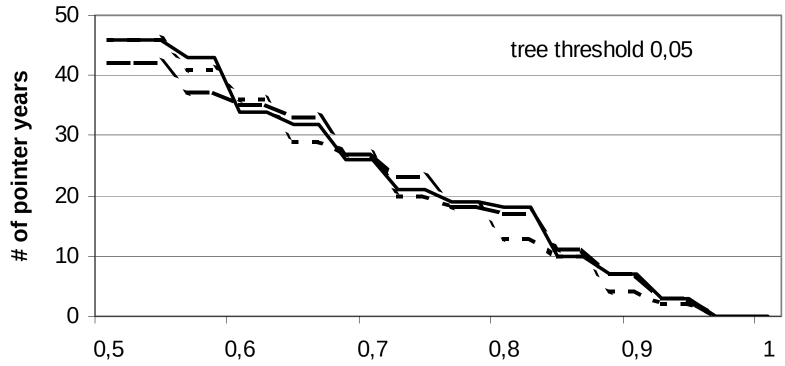

b)

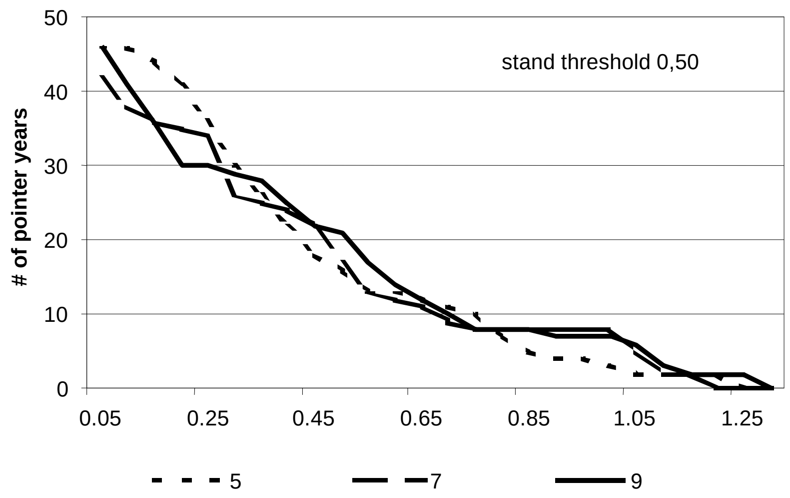

Figure 1: Number of pointer years in period 1951-2000 in the dependence on, the presented at x- axis, a) stand threshold and b) tree threshold value for various lengths of normalisation window (line type).

No obvious pattern in combination of the threshold values was observed during the investigation of the occurrence of a certain number of pointer year either. By analysing the threshold values required for the occurrence of a single pointer year one can see that the application of a certain window length may result in both strict and soft conditions (Fig. 2). Received results do not suggest which window length to choose as the number of obtained pointer years does not differ obviously with respect to that parameter.

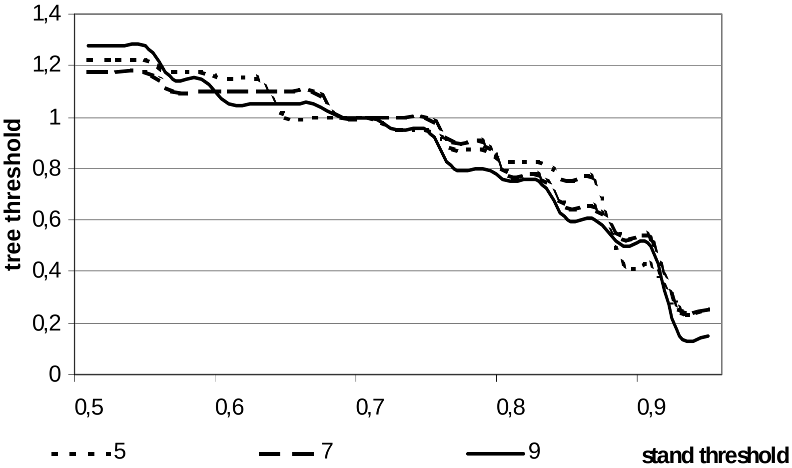

Figure 2: Combinations of tree and stand threshold values required for the occurrence of a single pointer year for various lengths of normalisation window (line type)

Influence of threshold values

Expected results were received when analysing the relationships between number of pointer years and tree or stand values. Application of the more strict conditions in pointer year determination (i.e. higher values of the threshold) resulted in smaller numbers of received pointer years (Fig. 3).

a)

b)

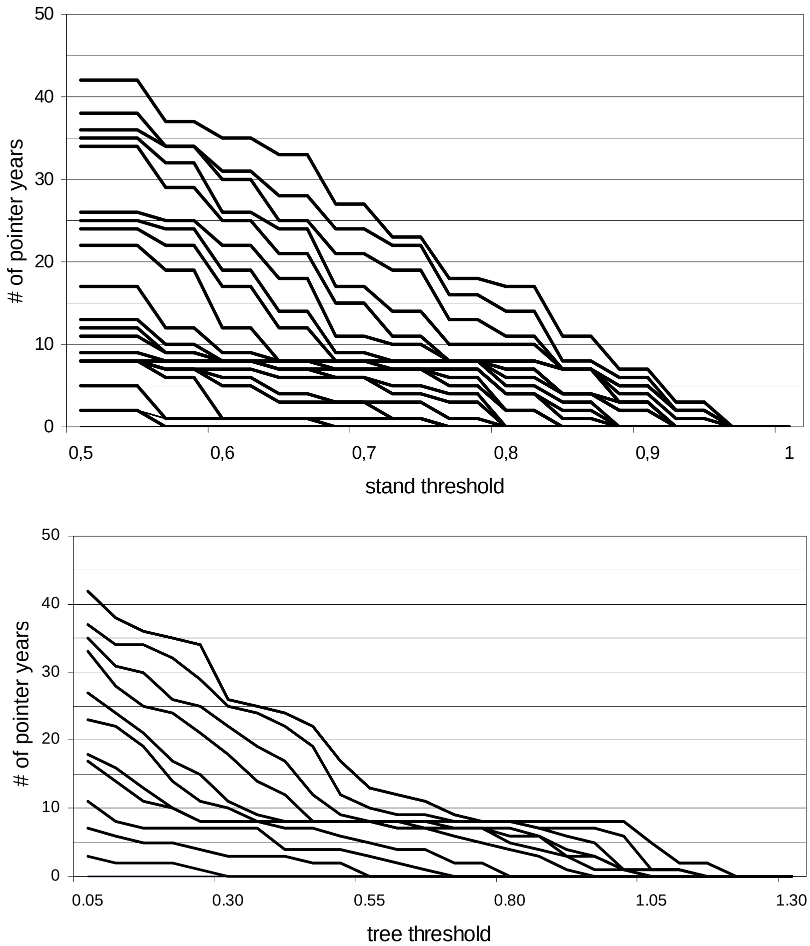

Figure 3: Number of pointer years in the dependence on a) stand threshold and b) tree threshold values for normalisation in 7-year windows.

DOI:10.2312/GFZ.b103-08056

The most crucial question that arises from this analysis is what the “right” values of the thresholds are. Neuwirth et al. (2007a, b) proposed application of the criteria based on normal distribution for assignment of what here is called tree threshold. However in the ‘normalisation in a moving window’ method mean and standard deviation are calculated within a window of the predefined length and that is why an extremely wide or narrow ring may not stand out so clearly as if these parameters were calculated for the whole series. On the other hand this latter calculation method requires prior indexing of the measurement series. Despite this fact, this proposal is the only attempt to apply objective criteria in determination of pointer years.
Literature review gives also wide range of stand threshold values applied. They varied from 0,4 (Neuwirth et al. 2007b) to 0,9 (Cedro 2007). Again, the reasons for the choice of the certain value were not explained. Of course, the objectives and the conditions of the study as well as individual author’s preferences were behind these subjective choices.

Statistical vs. visual method

Results of the statistical method of the pointer year determination were compared to those from the visual method. Residuals between number of pointer years received for particular tree thresholds in the statistical method and amount of pointer years from visual assignment were calculated for each of the applied stand threshold values. Correlation analysis pointed out that the results of the application of 0,95 (for 5-year window) and 1,05 (for 7- and 9-years windows) tree thresholds are the most similar to those achieved with the visual method. Pearson’s correlation coefficients equalled 0,974; 0,844 and 0,892 respectively. For the same stand threshold (0,5) not only the number of pointer years, but also individual years were similar. The visual method revealed positive pointer years in 1967 and 1974, and negative ones in 1964, 1979,1992 and 1998. Exactly the same results were received when the 9-year window was applied. Application of 5-year window missed the negative pointer years 1964 and 1979. When the 7-year long window was used, analysis did not reveal a positive year in 1974, nor a negative one in 1964, but an additional negative pointer year was detected in 1980. However, despite these small differences, the results of the two compared methods are very similar, which confirms observations of Weber (1995). Even though the described visual method of pointer years determination is time consuming, its great advantage is the fact that it requires application of only stand threshold, which decreases the subjectiveness of the procedure.

Comparison to meteorological data

The applied procedure resulted in total amount of 11 meteorological pointer years in the period 1951-2000. Only two of them (1970 and 1976) are pointer years with respect to both, extreme temperature and precipitation. The remaining ones were characterised only with either unusual precipitation (3 cases) or temperature (6 cases). The received pattern of pointer years does not resemble the results of the dendrochronological analyses. Even the years that are distinctively recognised in tree-ring width series e.g. 1967 or 1992 (Vitas 2002, Koprowski and Zielski 2002, Bijak 2007) were not present in the investigation of the meteorological data. Although climate influences the formation of tree-rings to a large extent, event and pointer years may have very different causes and are not only the result of extraordinary weather conditions (Schweingruber et al. 1990). Moreover, if climate impact is considered, these are conditions in particular periods (e.g. months) that cause formation of the conspicuously wider or narrower rings. This great difference in pointer years obtained from dendrochronological and meteorological method disables the utilisation of the latter one as a supporting tool in pointer year determination.

Conclusions

Although the term ‘pointer year’ is quite clear as far as its definition is concerned, the different aspects of the determination process seem to require more detailed specification. The phenomenon of extraordinary wider or narrower tree-rings is very complex. The causes include not only extreme climate conditions, but also insect outbreaks, fires or physiological conditions (e.g. defoliation). As extreme conditions occur from time to time it is very difficult to state or assume the “right” number of such events. That is why there is, and probably will be, no answer to the question about the proper number of pointer years. However the issue of subjective application of various criteria in the determination methods that results in great differences in number and character of obtained pointer years and hence in difficulty in comparison of pointer years detected for different areas should be discussed widely. Agreement on the same method and applied criteria based rather on statistical bases than on subjective preferences of researcher will make pointer years analyses more objective as well as comparable and therefore available for more comprehensive utilisation.

References

Bijak, Sz. (2007): Tree growth-climate response in relation to habitat type in spruce stands of the Borecka Primeval Forest. In: Haneca K., Verheyden A., Beeckman H., Gärtner H., Helle G., Schleser G. (eds.) TRACE- Tree rings in archeology, climatology and ecology Volume 5: 54-59.

Cedro, A. (2007): Tree-ring chronologies of downy oak (Quercus pubescens), pedunculate oak (Quercus robur) and sessile oak (Quercus petraea) in the Bielinek nature reserve: comparison of the climatic determinants of tree-ring width. *Geochronometria 26*: 39-45.

Cropper, J.P. (1979): Tree-ring skeleton plotting by computer. *Tree-ring Bulletin 39*: 47-59.

Douglass, A.E. (1939): Crossdating in dendrochronology. *Journal of Forestry 39*: 825-831.

Eckstein, D., Bauch, J. (1969): Beitrag zur Rationalisierung eines dendrochronologischen Verfahrens und zur Analyse seiner Aussagesicherheit. *Forstwissenschaftliches Centralbl. 88*: 230-250.

Fritts, H.C. (1976): Tree rings and climate. Academic Press, London. pp 567.

Huber, B. (1943): Über die Sicherheit jahrringchronologischer Datierung. *Holz 6*: 263-268.

Huber, B. (1951): Datierung von Holzproblem aufgrund der Jahrringfolge. In: Freund H. Handbuch der Mikroskopie V/I: 172-192.

Kaennel M., Schweingruber F.H. (1995): Multilingual Glossary of Dendrochronology. Terms and Definitions in English, German, French, Spanish, Italian, Portuguese and Russian.

Birmensdorf, Swiss Federal Institute for Forest, Snow and Landscape Research, Berne, Stuttgart, Viena, Haupt. pp 467.

Koprowski, M., Zielski, A. (2002): Lata wskaźnikowe u świerka pospolitego [Picea abies (L.) Karsten] na Pojezierzu Olsztyńskim. *Sylwan* 2002/11: 29-39.

Meyer, F.D. (1998/1999): Pointer years analysis in dendroecology: a comparison of methods. *Dendrochronologia 16-17*: 193-204.

Neuwirth, B., Friedrichs, D., Hennen, M., (2007): 2003- where is the negative pointer year? A case study for the NW-German low mountain ranges. In: Haneca K., Verheyden A., Beeckman H., Gärtner H., Helle G., Schleser G. (eds.) Tree rings in archeology, climatology and ecology TRACE 5: 113-120

Neuwirth, B., Schweingruber, F.H., Winiger, M., (2007): Spatial patterns of Central European pointer years. *Dendrochronologia 24*: 79-89.

Schweingruber, F.H. (1996): Tree rings and environment- dendrochronology. Haupt, Bern: pp 609

Schweingruber, F.H., Eckstein D., Serre-Bachet F., Bräker O.U. (1990): Identification, presentation and interpretation of event years and pointer years in dendrochronology. *Dendrochronologia 8*: 9-38.

Vitas, A. (2002): Impact of climate factors on the radial increment of Norway spruce [Picea abies (L.) Karsten]. PhD thesis

Weber, U. (1995): Ring width measurements versus skeleton plot. *Dendrochronologia 13*: 147-148.

Tree-ring analysis of *Juniperus excelsa* from the northern Oman mountains

U. Sass-Klaassen[1], H.H. Leuschner[2], A. Buerkert[3] & G. Helle[4]

[1] *Forest Ecology and Forest Management (FEM), Wageningen University and Research Centre, P.O. Box 47, 6700 AA Wageningen, The Netherlands*

[2] *Laboratory for Dendroecology, Department of Palynology and Climate Dynamics, Albrecht-von-Haller Institute of Plant Science, University of Goettingen, Wilhelm-Weber-Str. 2a, 37073 Goettingen, Germany*

[3] *Organic Plant Production and Agroecosystems Research in the Tropics and Subtropics, University of Kassel, 37213 Witzenhausen, Germany*

[4] *Forschungszentrum Jülich GmbH, ICG-5, 52425 Jülich, Germany*

Email: Ute.SassKlaassen@wur.nl

Introduction

Background

Oman has a rich history of irrigation agriculture which was largely shaped by changes in climate conditions throughout the last millennia. The historical development of oasis agriculture in the mountainous north of the country reflects changes in settlement patterns that are thought to be strongly related to recurrent droughts (Siebert et al. 2004). To study (i) the driving role of climate, i.e. rainfall for the oasis agriculture in the past and (ii) the effects of possible changes in climate on the still existing oases long climate records are needed. However, for the whole Arabian Peninsula such records are scarce and – if available - only date back until the last century, when the British established the first weather stations in the region.

The only published climate archive which fulfils the requirements of longevity and high resolution originates from a varved sediment core of the NE Arabian Sea (von Rad et al. 1999). This 5,000-yr record was dated at an extraordinary precision (about one order of magnitude smaller than typical AMS ^{14}C data) and allowed to reconstruct the strength of both the winter and the late summer monsoon affecting the area. Nevertheless this record may be of only limited value for Oman with its more arid climate largely influenced by the Indian Summer Monsoon. The recent stalagmite records of Fleitmann et al. (2007) in contrast are from northern Oman and cover a timespan of 10,000 years but their resolution is limited.

Potential of Dendrochronology

Dendrochronological studies on long-live tree species have the potential to provide long time series that reflect changes in climate conditions. In the high altitude Al Jabal al Akhdar mountains of Oman extended *Juniperus excelsa* stands exist growing under suitable site conditions. Tree-ring analysis of comparable material has been successfully conducted in both tropical and dry (mountainous) forests in Africa (Fichtler et al. 2004; Couralet et al. 2005; Schöngart et al. 2006, Trouet et al. 2006). Based on initial observations we assumed that these juniper trees form annual rings as they grow under harsh climatic conditions in the dry mountainous forests with a single pronounced dry season. Also a preliminary study by

DOI:10.2312/GFZ.b103-08056

Fisher et al. (1994) on *J. excelsa* from Oman suggested that *Juniperus excelsor* has potential for dendrochronology.
However, uncertainty remained about the periodicity of ring formation in trees growing under extremely dry conditions (Wils & Eshetu 2007) Theoretically both false or double rings and missing rings may occur in juniper (Couralet et al. 2005). False rings may be caused by a bimodal rainfall distribution in certain years due to winter rains and a strong monsoon event in any one year. Missing or partly missing rings (=wedging rings), in contrast, are frequently formed during years with little rainfall.

Objectives
In this study we therefore addressed the following research questions: (1) Does *Juniperus excelsa* from Oman form clearly distinguishable growth layers? (2) What is the mean annual growth level and estimated age of juniper in the study area? (3) Is cross-dating of tree-ring series between different trees possible? And ultimately (4) what is the potential of *Juniperus excelsa* for the reconstruction of climate records?

Materials and methods

Study site and sample material
The sampling area is located in the Jabal al Akhdar mountain range in the northern part of Oman (Fig. 1a). Unfortunately, the only climate records from Oman are available from the coast at Muscat (Fig. 1b). The climate diagram from Muscat indicates a dry seasonal climate with a prolonged dry season from April to mid November during which drought conditions can be expected.

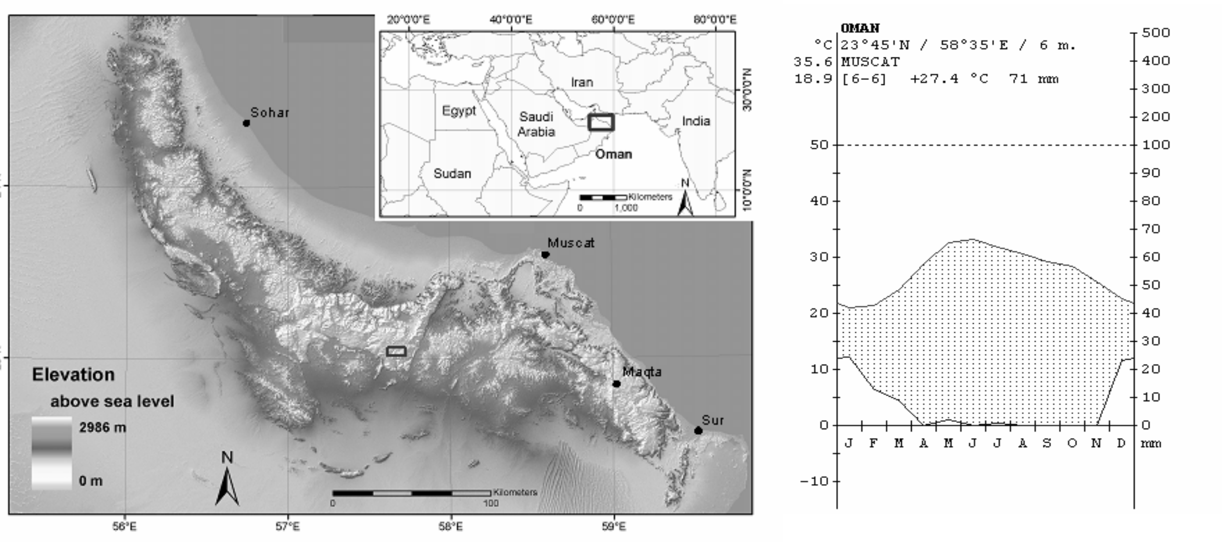

Figure 1: Location with the old Juniperus excelsa stands (see marked square on the insert) on Al-Jabal-al-Akhdar mountain range of northern Oman (left). Climate diagram from Muscat (Seeb Airport, right).

The climate at the high mountain study location is considerably cooler with a long term annual average air temperature of 18.1°C, a minimum of -3.6°C and a maximum of 36.3°C, the coolest and hottest month being January and June, respectively (Department of Civil

DOI:10.2312/GFZ.b103-08056

Aviation and Meteorology, Muscat, Oman). The juniper trees (*Juniperus excelsa* ubsp. *Polycarpos)* are growing at about 2,300 m a.s.l. in an open dry mountainous forest. The trees are strongly protected which makes cutting of trees for sample collection impossible. However, in addition to 12 cored trees, from which two cores were taken at breast height in January 2004, four stem disks were available from trees cut due to recent road construction.

Cross-dating of tree-ring series

According to the above mentioned tree ring uncertainties (double rings, missing rings), the measured tree-ring series were visually crossdated in a stepwise hierarchical order: Starting with comparisons of series from the cores of the same tree we identified disagreements and went back to the wood surface to check the wood structure in the problematic area. In order to adjust the series, the single tree-ring series were edited in TSAP by adding missing rings and merging false or double rings. The corrected tree-ring series were then averaged into *tree chronologies,* which were visually checked and corrected as in the previous tree-level-check. After successful cross-dating the corrected tree-ring series were combined into a *site chronology*. The final result of the visual cross-dating were statistically verified by running correlation analysis performed with the software program COFECHA (Holmes 1983).

^{14}C dating

As tree-ring formation in juniper from Oman is expected to be very spurious we decided to use ^{14}C dating to check whether dendrochronological detection of tree rings coincides with the age suggested by ^{14}C dating. For that purpose ^{14}C dating was done on the 10 innermost tree rings of the three samples with most tree rings (111, 105, disk 27 in table 1) and compared to the result of the dendro-dating after measuring and cross dating of two radii.

Age determination and statistical description of tree-ring series

The number of measured (and corrected) tree rings indicates the minimum tree age. An exact age determination is, however, only possible if cores include the pith (=centre of the tree) and if reliable corrections for the missing rings according to the sampling heights can be made. The mean tree-ring width (and the standard deviation) describes the general growth level and the variability in tree-ring width and gives an indication about the chance of missing rings in the tree-ring record. Mean sensitivity and autocorrelation of first order are standard parameters in dendrochronology to describe the changes in tree-ring width from year to year and the persistence of the tree-ring pattern (Cook & Kairiukstis 1990).

$\delta^{18}O$ analyses

Many tree-ring series show alternating phases of high-frequency dominated or low-frequency dominated variation with the enhanced high–frequency signal being caused by the regular occurrence of very narrow rings. It is, however, well possible that these narrow rings resemble density variations, that is second growth phases that occur in periods with a strong bimodal rainfall distribution (Fig. 1b). This growth behaviour has been proved for many species growing under dry condition, such as in the Mediterranean's where temporary dry spells cause a bimodal growth pattern with a recovery of growth after a summer drought (Cherubini et al. 2003). If so, changes in spectral behaviour of the tree-ring series can be used to point out shifts in large-scale climate-driving factors such as monsoon activity that trigger the amount and the distribution of rainfall throughout the year. $\delta^{18}O$ is known to be a sensitive indicator of changes in water availability and hence rainfall patterns. To study whether or not changes in the spectral behaviour of a tree-ring series are corresponding with the isotopic ($\delta^{18}O$) composition, $\delta^{18}O$ was measured in altogether 50 ring layers of sample 27. 25 consecutive tree rings bridging 1905 to 1930 the change from a high–frequency signal period to a period with moderate variability and b) 25 layers from the more recent (moderate as well) period 1975 to 2000.

Results and Discussion

Does Juniperus excelsa from Oman form clearly distinguishable growth layers?

Wood anatomical characteristics of Juniperus excelsa

As in case of conifers from regions with non-ambiguous annual tree rings, the growth rings in juniper are mostly defined by the sharply edged contrast between the last few rows of flattened and thick-walled late-wood tracheids and the larger and thin-walled early-wood tracheids of the next growth ring. These rings could be clearly identified and measured. However, some small rings consisted of only a few cell rows of early and late-wood with a less typically contrast in cell size but clear and sharp edges to the previous or next ring. These layers could not be clearly identified as density fluctuations, false rings or real “annual” rings (Fig. 2).

Figure 2: Cross section of Juniperus excelsa *from with distinct tree rings. The dark part (late wood) and light part (early wood) constitute a single annual growth layer (left). Partly missing rings and density variations in* Juniperus excelsa *(right).*

What is the mean annual growth level and estimated age of juniper in the study area?

The growth of the juniper trees from Al Jabal al Akhdar was very slow with an average of 0.52 mm (Tab. 1). However, it varied considerably between trees. The high variability indicates that growth conditions of the juniper trees are affected by different micro-site conditions such as surface slope-dependent water supply, matching the observations by Fisher & Gardner (1995).

Table 1. *(Statistical) description of tree-ring series. No. rings = number of measured tree rings, Mean TRW = mean tree-ring width [mm], Stdv = Standard deviation, AC(1)= 1st order autocorrelation, MS = mean sensitivity.*

Tree no.	Sampling date	No. rings	Mean TRW	Stdv	AC(1)	MS(%)
101	2004	214	1.37	1.154	0.02	91
102	2004	207	0.57	0.387	0.35	64
103	2004	172	0.58	0.357	0.43	51
104	2004	364	0.52	0.334	0.10	69
105	2004	604	0.27	0.144	0.21	55
106	2004	306	0.57	0.405	0.10	72
107	2004	392	0.34	0.173	0.20	53
108	2004	213	0.27	0.163	0.40	51
109	2004	482	0.24	0.141	0.52	45
110	2004	387	0.67	0.508	0.13	82
111	2004	783	0.21	0.154	0.34	59
112	2004	267	0.38	0.229	0.20	65
Disk 1	2005	306	0.46	0.415	0.34	64
Disk 2	2005	100	1.10	1.132	0.49	56
Disk 3	2005	146	0.48	0.303	0.27	59
Disk 27	2003	622	0.39	0.301	0.23	71

The number of measured tree rings provided an indication of minimum tree (pith-) age and varied considerably between the sample trees with tree 111 being the oldest tree (783 rings) with the lowest growth level and tree 'disk 2' being the youngest tree with 100 measured rings. However, as most samples did not include the pith, an unknown number of inner rings might have been omitted. The number of measured tree rings shows that junipers in this area can get very old which makes them highly valuable for climate reconstruction. Nevertheless, it has to be noticed that radial growth – especially in old individuals - under these extremely harsh climate and edaphic conditions can be extremely slow and might even stop for several (consecutive) years.

Comparison between ^{14}C dating and tree ring measurements

The ^{14}C dating of the juniper sample showed that there was at least – according to the youngest border of the 95.4 % probability level, Oxcal Calibration - a difference between the ^{14}C date and the dendro date of 30, 25 and 20 tree rings, respectively, for the three samples covering 783, 622 and 604 years. This indicates that some more missing rings have to be expected in the measured tree-ring series.

Is cross-dating of tree-ring series between different trees possible?

Tree-ring characteristics and tree-ring patterns

Tree-ring formation in the juniper trees from Al Jabal al Akhdar was very irregular with abrupt changes between wider rings and extremely small rings (Fig. 2). Wedging, that is partly missing rings, was frequently visible on the cores which suggests that a considerable number of missing rings can be expected (Fig. 2). Double rings, that is density variations, only occured on wide tree rings (>1.5 mm). This leads to a generally high sensitivity and low autocorrelation in tree-ring series (Tab. 1).

Unfortunately the tree-ring patterns from two cores of the same tree differed considerably. This was likely due to the eccentric growth pattern of the trees whereby wood formation around the circumference was very variable and made tree-ring analysis based on two cores difficult (Fig. 2). Cross-dating between two (or three) cores of the same tree showed that sometimes up to 30 rings were missing in one tree-ring record. Missing rings mainly occur during phases of depressed growth. However, we also observed that tree rings disappeared during phases of apparently normal growth. Given the fact that double rings most often occurred in wide tree rings, it was assumed that shifts in tree-ring series are mainly due to missing rings. The tree-ring series were corrected by tracing well-matching parts in two tree-ring series and fitting tree rings in until both series matched well. This extremely time-consuming process was applied to all 12 samples and the samples of the stem disks separately. Eventually all samples were matched and combined into a site chronology.

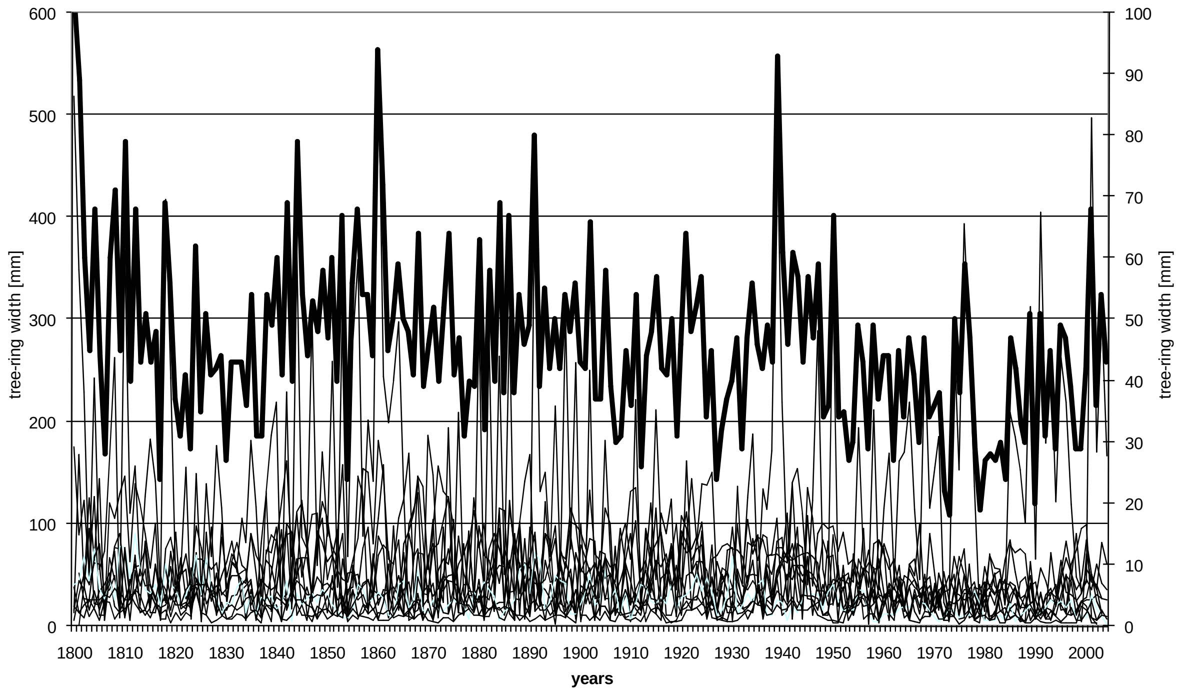

Figure 3: Cross-dated tree-ring series of 12 juniper trees from Al-Jabal-al-Akhdar together with the chronology (shifted, on top).

Calculation of a (preliminary) site chronology and description of tree-ring series

Figure 3 shows the cross-dated and corrected tree-ring series of 12 juniper trees (trees101-112) with the site chronology on top. The fact that such a site chronology could be developed

demonstrates that the tree-ring series of single trees show periods of striking similarity. Figures 3 illustrates the tree-ring patterns in the period from 1800 to 2003 only. Cross-dating was possible throughout the whole period where at least two tree-ring series overlapped (1400-2004).
The single tree-ring series exhibited no clear age trend. Instead all trees showed a very sensitive growth pattern whereby phases of wider tree rings alternated with depressed tree growth. Obvious growth depressions occured in the 1860ies, around 1915 and around 1980. However, the trees were apparently able to recover from these depressions and there also was no indication of a prolonged decline in growth activity in recent decades.

Changes in spectral behaviour – δ^{18}O *isotope composition*

In single tree ring series striking changes in spectral behaviour of tree-ring widths could be detected. Phases of high sensitivity alternate with phases of dominant low frequency. In can be seen in sample 27 (Fig. 4), where a slight tendency towards more decadal variations was observed after the major depression in c. 1910. However, also in the chronology it was possible to distinguish phases that either contained more high frequency (annual) variation or more decadal variation (Fig. 3). In view of this, the δ^{18}O analyses on two 25-year periods in sample 27 yielded interesting results. The major switch in spectral behaviour of the tree-ring width, recorded around 1913, was related to a shift in the δ^{18}O-isotope composition towards significantly higher values known to reflect more humid conditions. The isotope composition of the second sample taken in the more recent period from 1975 to 2000 shows the same high values of δ^{18}O. Although these results need much more support by additional studies they indicate that frequency changes in tree-ring width are related to changes in the hydrological regime, which in turn could be related to changes in the amount or distribution of precipitation throughout the year.

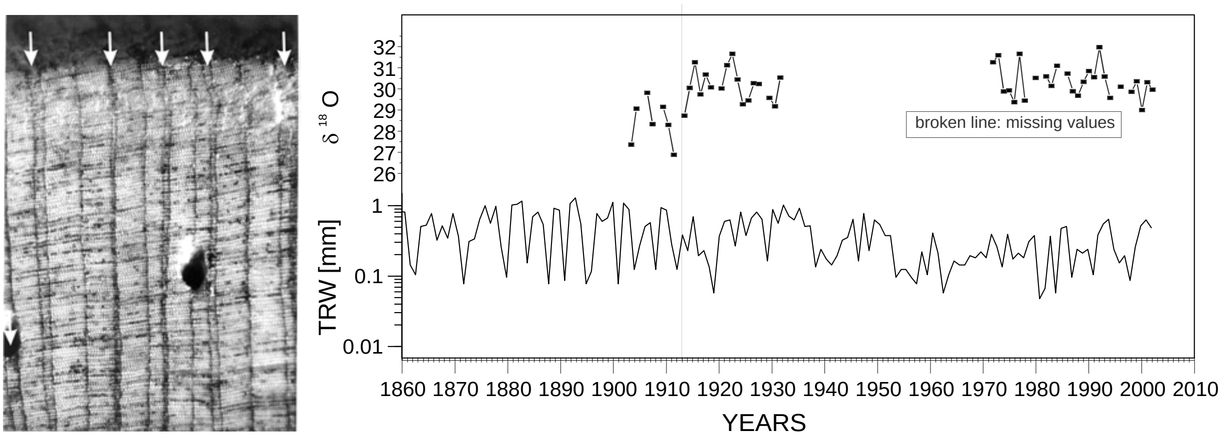

Figure 4. Typical growth pattern with small rings in 2-3 layers distance during a high frequency growth period. The interpretation of the small layers as annual rings, double rings or extreme density fluctuations is unclear (left). Tree-ring series of sample 27 with a shift between a phase with high frequency variation due to occurrence of small rings and more low- frequency variation. The δ^{18}*O composition data (above curves) of two 25-year segments indicate a strong and persistent increase in humidity from c. 1915 onwards (right).*

DOI:10.2312/GFZ.b103-08056

What is the potential to use Juniperus excelsa for climate reconstruction?
The calculated site chronology has to be regarded as preliminary. It certainly needs further support by integrating more material from – preferably - stem disks. However, as the juniper trees are strongly protected in Oman it is not likely that it will be possible to collect enough such material to considerably complement our samples. But even if stem-disk collection would not be such a major problem, it is still questionable if this material is appropriate to build up long tree-ring chronologies with the classical dendrochronological techniques that have been used in these and other studies. Juniper from Oman has proved to be very difficult material for several reasons: (1) the trees are generally slow growing; (2) show a very irregular growth pattern with alternating phases of sensitive (mainly annual variation) and very complacent (mainly decadal variation) growth; real tree-ring boundaries are often difficult to distinguish from density variations, that is double rings frequently occur; (4) (partly) missing rings are a very common phenomenon. The last point causes major trouble and the ^{14}C analyses suggested that even after thorough crossdating, that already resulted in tracing many (partly) missing rings, there still were rings that could not be detected.

Taking into account these aspects the following recommendations can be made:
Tree-ring analysis with juniper from Oman needs support by additional techniques. ^{14}C Wiggle matching (Kuzmin et al. 2004) is essential in order to check whether all missing trees can be traced via cross dating of tree-ring series. A carefully selection of samples, preferably stem disks, that undergo extensive wiggle matching could provide the exact time frame for verifying dendrochronological dating.

Once the preliminary chronology is supported by using these techniques the study material will provide a unique record to study (changes in) rainfall dynamics of up to 900 years in this region strongly susceptible for climate change. Integration with already existing networks of juniper chronologies in Pakistan (Esper 2000, Treydte et al. 2006) and Tibet (Bräuning 1999, 2001) and other (paleo)records, such as speleothems (Fleitmann et al. 2002, 2003, 2007) and varves and turbidites (Berger & Rad 2002) will contribute to a better understanding of large scale climate circulation patterns and their changes on the Arabian Peninsula throughout the last millennium. For Oman a reconstruction of rainfall will be of paramount importance to further elucidate the historic development of oasis agriculture.

Acknowledgements
The authors are indebted to Maher Nagieb for collecting many of the tree cores and to the Deutsche Forschungsgemeinschaft for funding (BU 1308).

References
Berger, W.H., Rad, U., von (2002): Decadal to millenial cyclicity in varves and turbidites from the Arabian sea: hypothesis of tidal origin. *Global and Planetary Change* 34: 313-325.
Bräuning, A. (1999): Dendroclimatological potential of drought-sensitive tree stands in Southern Tibet for the reconstruction of monsoonal activity. *IAWA Journal 20*(3): 325-338.

Bräuning, A. (2001): Climate history of the Tibetan Plateau during the last 1000 years derived from a network of juniper chronologies. *Dendrochronologia* 19:127-37.

Cherubini, P., Gartner, B.L., Tognetti, R., Bräker, O.U., Schoch, W., Innes, J.L. (2003): Identification, measurement and interpretation of tree rings in woody species from mediterranean climates. *Biol. Rev*. 78: 119-148.

Cook, E.R., Kairiukstis, L.A. (1990): Methods of Dendrochronology: Applications in the Environmental Sciences. International Institute for Applied Systems Analysis*, Kluwer Academic Publishers*, Boston, MA, USA.

Couralet, C., Sass-Klaassen, U., Sterck, F., Bekele, T., Zuidema, P.A. (2005): Combining dendrochronology and matrix modelling in demographic studies: An evaluation for Juniperus procera in Ethiopia. *Forest Ecology and Management* 216: 317-330.

Esper, J. (2000): Long-term tree-ring variations in Juniperus at the upper timber-line in Karakorum (Pakistan). *The Holocene* 10: 253-60.

Fisher, M. (1994): Is it possible to construct a tree-ring chronology for *Juniperus excelsa* (Bieb.) subsp. *polycarpos* (K. Koch), Takhtajan from the northern mountains of Oman? *Dendrochronologia* 12: 119-127.

Fisher, M., Gardner, A.S. (1995): The status and ecology of a *Juniperus excelsa* subsp. polycarpos woodland in the northern mountains of Oman. *Vegetation* 119: 33-51.

Fichtler, E., Trouet, V., Beeckman, H., Coppin, P., Worbes, M. (2004): Climatic signals in tree rings of *Burkea africana* and *Pterocarpus angolensis* from semiarid forests in Namibia. *Trees* 18, 442–51.

Fleitmann, D., Burns, S.J., Neff, U., Al-Subbary, A.A., Al-Aowah, M.A., Matter, A., Mangini, A. (2002): Climate change in Southern Arabia: Speleothems from Yemen and Oman as archives for monsoon rainfall over the last 330,000 years. *Yemeni Journal of Science* 4: 15-23.

Fleitmann, D., Burns, S.J., Mudelsee, M., Neff, U., Kramers, J., Mangini, A., Matter, A. (2003): Holocene forcing of the Indian monsoon recorded in a stalagmite from Southern Oman. *Science* 300: 1737-1739.

Fleitmann, D., Burns, S.J., Mangini, A., Mudelsee, M., Kramers, J., Villa, I., Neff, U., Al-Subbary, A.A., Buettner, A., Hippler, D., Matter, A., 2007. Holocene ITCZ and Indian monsoon dynamics recorded in stalagmites from Oman and Yemen (Socotra). Quaternary Science Reviews 26, 170–188.

Kuzmin, Y.V., Slusarenko, I.Y., Hajdas, I. Bonani, G. Christen, A. (2004): The Comparison of 14C Wiggle-Matching Results for the 'Floating' Tree-*Ring Chronology of the Ulandryk-4 Burial Ground (Altai Mountains, Siberia).* Radiocarbon 46: 943-948.

von Rad, U., Schaaf, M., Michels, K.H., Schulz, H., Berger, W.H., Sirocko, F. (1999): A 5000-yr Record of Climate Change in Varved Sediments from the Oxygen Minimum Zone off Pakistan, Northeastern Arabian Sea. *Quaternary Research* 51 (1): 39-53.

Schöngart, J.B., Orthmann, K.J., Hennenberg, S., Porembski, Worbes, S. (2006): Climate-growth relationships of tropical tree species in West Africa and their potential for climate reconstruction. *Global Change Biology* 12: 1139-50.

Siebert, S., Häser, J., Nagieb, M., Korn, L., Buerkert, A. (2005): Agricultural, architectural and archaeological evidence for the role and ecological adaptation of a scattered mountain oasis in Oman. *Journal of Arid Environments* 62: 177-197.

Trouet, V., Coppin, P., Beeckman, H. (2006): Annual growth ring patterns in *Brachystegia spiciformis* reveal influence of precipitation on tree growth. *Biotropica* 38, 375-82.

Treydte, K.S., Schleser, G.H., Helle, G., Frank, D.C., Winiger, M., Haug, G.H., Esper, J. (2006): The twentieth century was the wettest period in northern Pakistan over the past millennium. *Nature* 440 (27), 1179-1182.

Wils, T.H.G., Eshetu, Z. (2007): Reconstructing the flow of the River Nile from *Juniperus procera* and *Prunus africana* tree rings (Ethiopia) – an explorative study on cross-dating and climate signal. *TRACE, Vol.* 5, 277-284.

Worbes, M. (1995): How to measure growth dynamics in tropical trees, a review. *IAWA Journal* 16 (4): 337-351.

SECTION 3

ISOTOPES

DOI:10.2312/GFZ.b103-08056

Stable oxygen isotopes in juniper trees from the Tibetan plateau as a proxy for monsoonal activity

J. Grießinger[1,2], A. Bräuning[1], A. Thomas[3] & G.H. Schleser[2]

[1] *Institute of Geography, Friedrich-Alexander-University of Erlangen-Nürnberg, Germany*

[2] *Research Centre Jülich GmbH, Department of Chemistry and Dynamics of the Geosphere, ICG-V: Sedimentary Systems, Germany*

[3] *Institute of Geography, Justus-Liebig-University of Giessen, Germany*

Email: jgriess@geographie.uni-erlangen.de

Introduction

Extracting climatic and environmental information from stable isotopes in tree rings is of growing importance for reconstructing past environments. In recent publications, several authors (Helle & Schleser 2003, Treydte 2003, Treydte et al. 2006, McCarroll & Loader 2004, Schleser et al. 1999) confirmed the high potential inherent to stable isotopes for dendroclimatological investigations. In this study we present annually resolved stable oxygen ($\delta^{18}O$) isotope series of tree ring cellulose from three upper tree-line sites on the Tibetan plateau. Our sampling sites are situated along a hydrological gradient in the south-eastern part of Tibet with increasing moisture towards the East (Fig. 1).

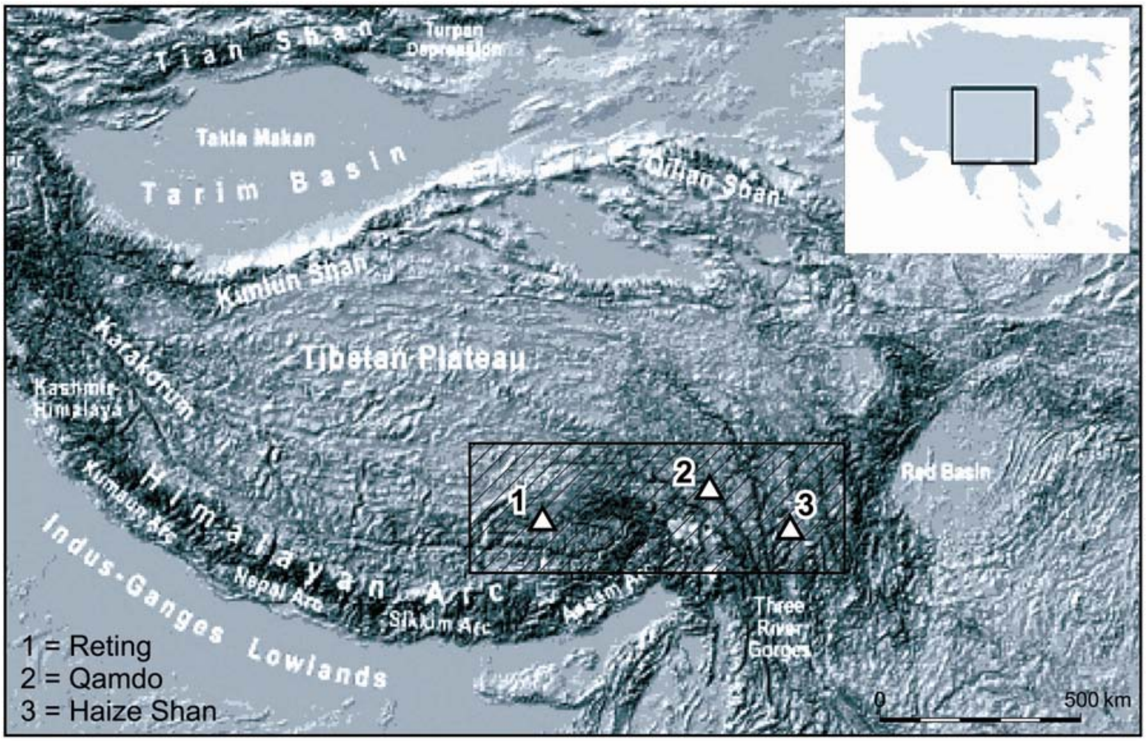

Figure 1: Main geographic units of High-Asia and location of the sample sites in Southeast-Tibet. Map: Böhner (2006).

We selected three stands of juniper trees (*Juniperus tibetica*) from southern exposed slopes. All sites are characterized by slope angles between 30 and 35°, well-drained soil conditions and are situated in the sub-alpine belt at 4300 to 4400 m.a.s.l. Former analysis of ring width

DOI:10.2312/GFZ.b103-08056

showed that the trees at the study sites are very sensitive to climate variations and therefore suited for a detailed proxy-climate investigation (Bräuning 1999). The study area is influenced by a seasonal change of two major atmospheric circulation systems: during summer, humid air masses of the Indian summer monsoon and the East Asian monsoon are the prevailing factors of regional climate. In winter, cold westerly winds with small amounts of precipitation are predominant (Webster et al. 1998).

Material and Methods

For the annual isotope analysis, 4 to 6 dominant trees per sampling site were selected. For the exact dating of ring widths, each core was measured and synchronized with existing site-chronologies by Bräuning (1999, 2001). After dating, tree rings were accurately separated on an annual base using a razorblade. For each site, tree-rings of the same calendar age were pooled prior to analysis, following a method suggested by Leavitt & Long (1984) as well as Borella et al. (1998). Thereafter, cellulose was extracted adapting a standard procedure described by Kürschner & Popik (1962). For the analysis of $\delta^{18}O$, samples are transferred into sample gas by pyrolizing them to CO at a temperature of 1080 °C. Measurement of the isotope ratios was done by using an elemental analyser interfaced to a continuous flow isotope ratio mass spectrometer (Micromass Optima) (for further details see McCarroll & Loader 2004, 2006). The resulting $\delta^{18}O$-values are expressed as deviations from the international VSMOW-standard. Overall, we were able to establish three annually resolved $\delta^{18}O$-isotope series with different time spans reaching from 820 (site of Haize Shan), 840 (Reting) up to 1520 years (Qamdo).

To obtain information about climate-proxy relationship concerning the $\delta^{18}O$-series we compared different climate parameters such as temperature, precipitation and potential evapotranspiration (PET), to incorporate a more complex climate parameter. The associated climate data originate from adjacent meteorological stations, extended by calculated PET datasets by Chen et al. (2006). At the site Qamdo, we used the nearby station for our calibration studies. For the sites of Reting and Haize Shan we had to build regional means from two adjacent stations following the methods of Jones & Hulme (1996) to ensure spatial representativeness.

Results and discussion

In a first step, all $\delta^{18}O$ series were calibrated with the common climate parameters, temperature and precipitation. With the exception of the easternmost site, which is strongly influenced by the summer monsoon, all tree stands indicate highly significant negative relationships between $\delta^{18}O$ and precipitation during the summer months. In contrast, correlations for all sites with temperature are predominantly positive, although not always highly significant (for $p<0.1$). Due to the site conditions with steep slopes and well-drained soils, influence of groundwater during water uptake can be excluded. This leads to the assumption of a distinct summer precipitation signal, recorded in the tree-ring $\delta^{18}O$-variations. The apparent $\delta^{18}O$-precipitation relationship is modified by site ecological differences (Fig. 2).

Reting junipers	Qamdo junipers	Haize Shan junipers
semi-arid	*temperate*	*cold-humid*

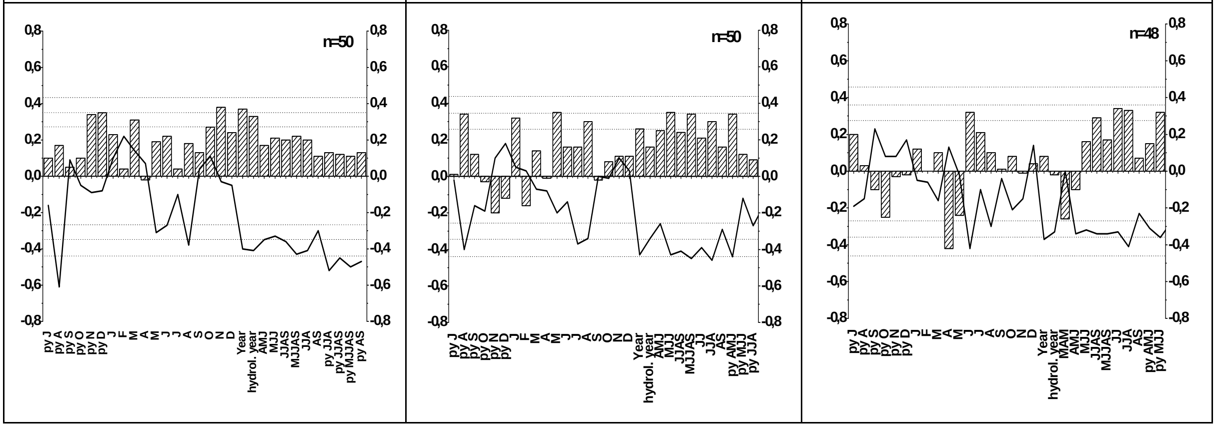

Figure 2: Site-specific climate-proxy-relationships between δ18O, temperature (columns) and precipitation (lines) for monthly means of the actual and the previous year (py). Dotted lines represent levels of significance with p<0.5; p<0.1 and p< 0.01.

Oxygen isotopes show highest negative correlations for monthly and seasonal means of rainfall of the previous and the actual year. For the dry and warm site Reting in the western part of the investigation area, correlation is highest with previous year precipitation in August (r=-0.61). With increasing influence and intensity of the summer monsoon to the East, correlations to previous year conditions disappear. In contrast, the other juniper sites indicate highest correlations with precipitation during the actual vegetation period.

For this reason, we assume that the dry and warm site is characterized by a storage effect during δ^{18}O-fixation which leads to a re-mobilization of previous years´ storage into the tree ring. Caused by the strong site-specific dependency on precipitation, this could be interpreted as a local plant physiological adaptation towards water stress during the vegetation period. This may cause site-specific water use and storage strategies during monsoonal rainfalls from May to September. Additionally, it has to be taken into account that some unexpected relationships at Reting within the calibration period could also be caused by the calculation with the regional mean climate series.

To investigate the relationship between site specific transpiration rates and δ^{18}O-fixation in tree rings, we analyzed PET-values of Chen et al. (2006). The results are illustrated in Figure 3. Again, highest similarities are found for the semi-arid site Reting, where highly significant positive correlations with the previous years´ August are apparent (r=0.65).

DOI:10.2312/GFZ.b103-08056

Reting junipers	Qamdo junipers	Haize Shan junipers
semi-arid	*temperate*	*cold-humid*
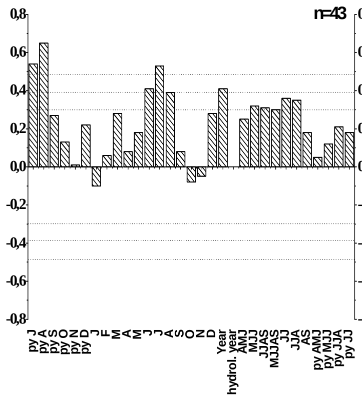	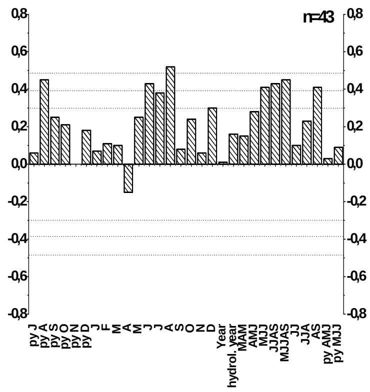	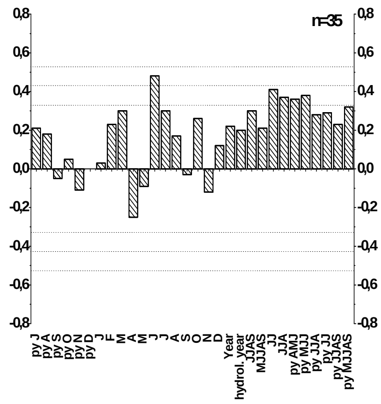

Figure 3: Site-specific climate-proxy relationships between $\delta^{18}O$ and potential evapotranspiration (PET) for monthly means of the actual and the previous year (py). Dotted lines represent levels of significance with p<0.5; p<0.1 and p< 0.01.

The other sample sites Qamdo (r=0.52 in August) and Haize Shan (r=0.48 in June) also indicate significantly higher results compared to precipitation datasets (Fig. 2). Similar as for calculations with precipitation, signal strength decreases with increasing influence of monsoonal activity. These results confirm the general assumptions, that increases in precipitation (in this case the summer monsoon) will lower local air temperature whereby transpiration rate is decreasing (Bendix 2004). During the summer monsoon season, water supply by precipitation combined with high temperatures leads to higher transpiration rates.

Conclusions

The results of this study of three ecological contrasting sites in Southeast-Tibet reveal a strong influence of summer precipitation for $\delta^{18}O$ isotope variations in juniper tree-rings. At all sites, oxygen isotope signatures show highly significant negative correlations with summer rainfall and highly significant positive correlation with PET-datasets. Signal strength of precipitation and PET decreases with the increasing influence of monsoonal activity from west to east. Both, $\delta^{18}O$-relationship with precipitation as well as with PET trace obviously monsoonal signals within the tree-rings. In summary, $\delta^{18}O$ is a well-suited proxy for reconstructions of monsoonal activity and intensity for Southeast-Tibet. In contrast, ring width of Tibetan juniper shows a different behaviour: at the more humid sites Haize Shan and Qamdo, ring width is related to temperature (Bräuning 2001), whereas at the dry site Reting ring width is correlated to spring precipitation (Bräuning & Grießinger 2006).

Acknowledgements

The authors wish to thank the laboratory staff of the Research Centre Jülich ICG-V and of the Institute of Geography, Erlangen for their active assistance during the PhD-project. This work was supported by the German Research Foundation (DFG), BR 1895/13-1.

References

Bendix, J. (2004): Geländeklimatologie. 282 S., Gebrüder Borntraeger Verlag, Stuttgart.

Böhner, J. (2006): General climatic controls and topoclimatic variations in Central and High Asia. *Boreas* 35(2): 279-295.

Borella, S., Leuenberger, M., (1998): Reducing uncertainties in ^{13}C analysis of tree rings: pooling, milling and cellulose extraction. *Journal of Geophysical Research* 103: 19519–19526.

Bräuning, A. (1999): Dendroclimatological potential of drought-sensitive tree stands in Southern Tibet for the reconstruction of the monsoonal activity. *IAWA Journal* 20 (3): 325-338.

Bräuning, A. (2001): Climate history of the Tibetan Plateau during the last 1000 years derived from a network of Juniper chronologies. *Dendrochronologia* 19 (1): 127-137

Bräuning, A., Grießinger, J. (2006): Late Holocene variations in monsoon intensity in the Tibetan-Himalayan region - evidence from tree-rings. *Journal of the Geological Society of India* 68 (3): 485-493

Chen, S., Lin, Y., Thomas, A. (2006): Climatic Change on the Tibetan Plateau: Potential evapotranspiration trends from 1961-2000. *Climatic Change* 76 (3-4): 291-319.

Helle, G., Schleser, G.H. (2003): Beyond CO_2 fixation of Rubisco-an interpretation of $^{13}C/^{12}C$ variations in tree rings from novel intra-seasonal studies on broad-leaf trees. *Plant, Cell and Environment* 27: 367-380.

Jones, P.D., Hulme, M. (1996): Calculating regional climatic series for temperature and precipitation: methods and illustrations. *International Journal of Climatology* 16:361-377.

Kürschner, K., Popik, M.G. (1962): Zur Analyse von Hölzern. *Mitteilungen zur Chemie, Biologie und Technologie des Holzes* 16(1): 1-11.

McCarroll, D., Loader, N.J. (2004): Stable isotopes in tree rings. *Quaternary Science Reviews* 23: 771-801.

McCarroll, D., Loader, N.J. (2006): Isotopes in tree rings. *Isotopes in Palaeoenvironmental Research* 10: 67-116.

Schleser, G.H., G. Helle, Lücke, A., Vos, H. (1999): Isotope signals as climate proxies: the role of transfer functions in the study of terrestrial archives. *Quaternary Science Reviews* 18: 927-943.

Treydte, K. (2003): Dendro-Isotope und Jahrringbreiten als Klimaproxies der letzten 1200 Jahre im Karakorumgebirge/Pakistan. Diss., Schriften des Forschungszentrums Jülich, Reihe Umwelt/Environment, Bd. 38.

Treydte K., Schleser, G.H., Helle, G., Winiger, M., Frank, D., Haug, G., Esper, J. (2006): The twentieth century was the wettest period in northern Pakistan over the past millennium. *Nature* 440: 1179-1182.

Webster, P.J., V.O. Magana, T.N. Palmer, J. Shukla, R.A. Thomas, M. Yanai & T. Yasunari (1998): Monsoons: Processes, predictability and the prospects for prediction. *Journal of Geophysical Research* 103 (C7): 14,451-14,510.

DOI:10.2312/GFZ.b103-08056

Detecting annual growth rhythms from high-frequency densitometry and carbon isotopes in tropical mountain rain forest trees in southern Ecuador

P. von Schnakenburg[1], A. Bräuning[1] & Gerd Helle[2]

[1] *Institute of Geography, University of Erlangen-Nuremberg, Kochstr. 4/4, D-91054 Erlangen, Germany*

[2] *Forschungszentrum Jülich*

Email: pvons@web.de

Introduction

Dendroclimatological investigations in temperate and northern climate zones are commonly based on the tree-ring parameters ring width and maximum latewood density. While dendroclimatology contributed significantly to our knowledge of past climate variability in higher latitudes, only sparse information has been gained by dendroecological studies in tropical regions so far. Due to the lack of pronounced climatic seasonality, trees in the inner tropics usually do not form distinct annual growth boundaries and this often hampers tree-ring analyses using ring width. To derive information about past climate variability in the humid tropics, we applied a combination of different methodological approaches, namely isotope analysis and high-frequency densitometry. This study is part of a comprehensive ecosystem research project about a tropical mountain rain forest in southern Ecuador (Beck & Müller-Hohenstein 2001).

Study area

The location of the study site “El Bosque” is near the equator at 4°S latitude in the province of Loja (southern Ecuador). It is a protected area near the Podocarpus National Park at the western slope of the eastern Andean Range (Cordillera Real) in an altitude of 2200 m a.s.l. The nearby crest line reaches up to more than 3500 m a.s.l., whereas some kilometres to the west the basin of Vilcabamba descends to 1530 m a.s.l. The climatic situation is characterized by a strong horizontal and altitudinal gradient of humidity. In austral winter “El Bosque” is in a leeward position of the Andes and a period of reduced rainfall occurs from July to September. After Richter (2003), the calculated number of humid months per year is 8–10 months at the study site. Precipitation has to be estimated, as the only nearby weather station is just running for a short period of time. Annual precipitation varies from 7000-8000 mm at the crest line to 1200 mm in an altitude of 1970 m a.s.l. near Vilcabamba (Emck 2007). For ”El Bosque”, we estimate the annual amount of rainfall between 1200-2000 mm. Annual mean temperature is ca. 15°C with a daily temperature amplitude from 10-25 °C. The samples where taken with an increment borer in September 2006 and March 2007.

DOI:10.2312/GFZ.b103-08056

Methods

Approach

Earlier investigations in this project showed that some tree species react on seasonal climate variability by forming visible density variations and growth boundaries (Bräuning & Burchardt 2006; Volland-Voigt 2006). For this study we used the conifer *Prumnopitys montana* (Podocarpaceae) that shows visible density variations. The tree diameters of up to 1m and the slow growth rates (Bräuning et al. 2008) point to potentially high living ages of several centuries. High-frequency densitometry and the analyses of stable carbon and oxygen isotopes are used to gain information about growth rhythms and past climate variability.

High frequency densitometry

The relatively new method "High-frequency-densitometry" is used to identify density variations in the wood by utilizing its dielectric properties. A micro-electrode-probe emitting electromagnetic waves passes over a smoothed wood-sample. The receiver electrode quantifies the dispersed radiation, representing the density of wood. Wood density is determined by the growth-conditioned relationship of cellulose and other cell components, of which the cell walls are composed, to air in the cell lumens (Schinker et al. 2003, Hansen 2004). With this method it is possible to identify maximum latewood density as well as even small wood density variations, which help to identify indistinct growth boundaries.

A major advantage of this method is that it is non destructive, so that the sample can be used after measuring density for further analysis, e.g. for the analysis of stable isotopes. To achieve this, a well primed and even sample surface is essential. A synchronisation of the density curves with the isotope signals shall finally enable a detection of annual growth boundaries which is the basis for the derivation of long-term climate reconstructions.

Oxygen and carbon isotope analyses

The periodicity of the density variations in *Prumnopitys montana* is not known. Because of this and the fact, that studies on intra-annual variations on stable isotopes in wood showed "significant seasonal changes in the carbon and oxygen isotope composition" (Helle & Schleser 2004), the ^{13}C analyses were carried out on thin-sections of 70 µm thickness. Doing so, stable isotope values and density variations could be assigned to corresponding topological parts of the studied increment core. For a first test, the youngest 12 mm from each core were prepared.

The seasonal change in the prevailing wind direction (Bendix et al. 2005, Richter 2003) causes a change of the dominant moisture source, which should be reflected by intra-annual variations of the $\delta^{18}O$-signal in the wood. Crossing the Amazon catchment area, the moisture of the Atlantic is depleted in $\delta^{18}O$ on its way to the Andes. Because of this continental effect, it is possible to distinguish the origin of the precipitation water. On the other hand, the $\delta^{18}O$ -signal is influenced by the amount of rainfall (the higher the rainfall the more $\delta^{18}O$ -signal is diluted). In contrast, the intra-annual variations of $\delta^{13}C$ reflect the seasonality of water availability. By using the $\delta^{13}C$-signal it ought to be possible to verify, if changes in $\delta^{18}O$ depend on drought stress or on alterations of the atmospheric circulation. Since the slopes in

DOI:10.2312/GFZ.b103-08056

the study area are very steep, no groundwater contact of the root systems is expected, so that the $\delta^{18}O$ signal of the cellulose should reflect the isotopic composition of the precipitation water taken up by the roots.

In contrast, the $\delta^{13}C$ signal should enable the detection of dry phases (which are represented by high $\delta^{13}C$ values) since the $\delta^{13}C$ discrimination mainly depends on the relative humidity of the air and the resulting opening of the stomata apertures. Analysing the $\delta^{13}C$- and the $\delta^{18}O$ –signal, it should be kept in mind, that these signals are also influenced by physiological and biochemical processes, e.g. storage effects (Helle & Schleser 2004; Kagawa et al. 2006).

Results

High-frequency-Densitometry

Prumnopitys montana wood shows visible density variations, especially in the brighter sapwood. As expected, these visible structures are reflected by the density curve (Fig.1); each peak in the density curve represents a darker density band. Further analyses have to reveal the temporal periodicity and the physiological causes of these density variations

.

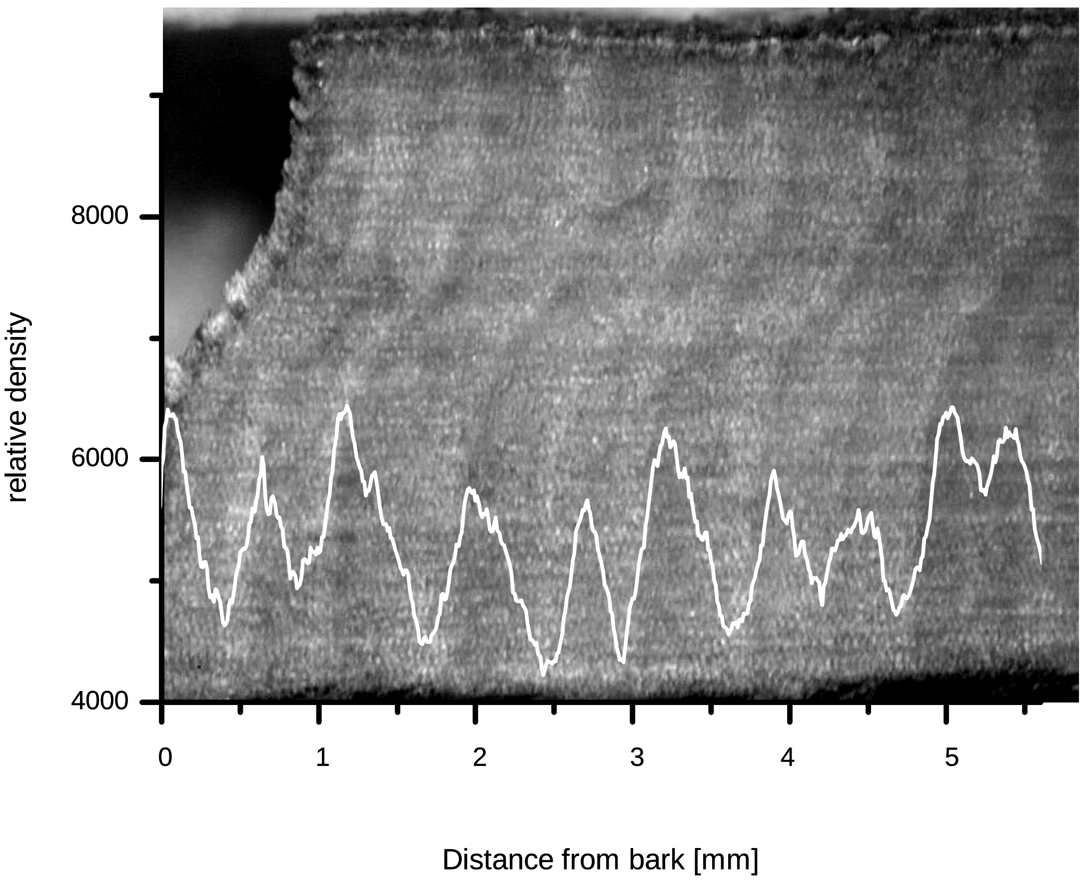

Figure 1: Relative density variations of Prumnopitys montana. The white line shows the measured density variations, whereas the background shows the corresponding part of the sample with the visible wood structures.

DOI:10.2312/GFZ.b103-08056

^{13}C Analyses

Fig. 2 shows the stable carbon isotope variations of the outermost 12 mm of the examined stems. We assume that the distinctive minima and maxima in the isotope curve (as marked by the arrows) represent wood that was formed synchronously under certain climate conditions. However, these parts of probably same formation time are situated at different distances from the bark in the various trees. This is the result of different growth rates of the studied individuals.

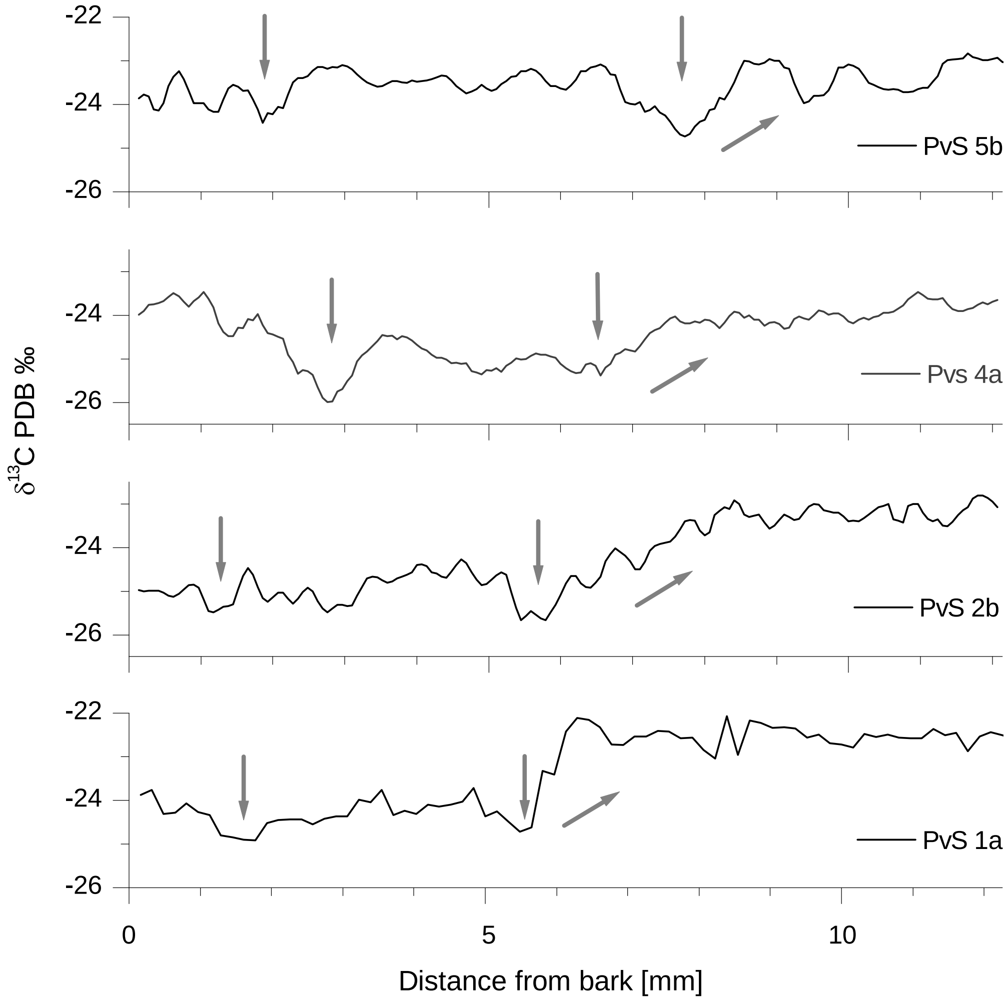

Figure 2: $\delta^{13}C$-values from four individuals of Prumnopitys montana. The curves are smoothed by a 5 point moving average. Grey arrows indicate the occurrence of certain minima and trends in the isotopic composition which are probably caused by climatic events affecting all trees synchronously.

Conclusions and outlook

It could be seen that HF-density as well as $\delta^{13}C$ measurements show pronounced variations along the examined increment cores. In a next step we will examine if these variations can be synchronised within the same parameter and if wood density and $\delta^{13}C$ variations reflect the same seasonal patterns. At the moment, however, the available results suffer from two restrictions: First, the $\delta^{13}C$-curves are yet too short and have to be enlarged to proof accordance of isotope variations between different individuals over a longer period of time. Second, the number of studied individuals should be increased from 4 up to a minimum of 6. Calibration studies of wood density and stable isotope composition with climate data shall be carried out separately for the two wood parameters to evaluate if there exists a causal link between density and stable carbon isotope variations. Although the applied combination of techniques is very time consuming, it seems very promising to better understand the linkage between tree growth and climate variability in tropical mountain reagions.

Acknowledgements

The study was financed by the Deutsche Forschungsgemeinschaft (DFG) within the research group FOR 402 (BR 1895/8-1). Thorsten Peters (Erlangen) has contributed climate data.

References

Beck, E., Müller-Hohenstein, K. (2001): Analysis of undisturbed and disturbed tropical mountain forest ecosystems in Southern Ecuador. *DIE ERDE* 132: 1-8.

Bendix, J., Rollenbeck, R., Reudenbach, C. (2005): Diurnal patterns of rainfall in a tropical Andean valley of southern Ecuador as seen by a vertically pointing K-band Doppler radar. *International Journal of Climatology*: DOI: 10.1002/joc.127.

Bräuning, A., Burchardt, I. (2006): Detection of growth dynamics in tree species of a tropical mountain rain forest in southern Ecuador. *TRACE - Tree Rings in Archaeology, Climatology and Ecology*, Vol. 4: Proceedings of the DENDROSYMPOSIUM 2005, April 21 23 2005, Fribourg: 127-131.

Bräuning A., Homeier, J., Cueva, E. Beck, E., Günter, S. (2008): Growth dynamics of trees in tropical mountain ecosystems. Ecological Studies 198, *in press.*

Emck, Paul (2007): A climatology of south Ecuador. *[PhD Thesis, University of Erlangen-Nürnberg]* 197 p.

Helle, G., Schleser, G. H. (2004): Beyond CO_2-fixation by Rubisco - an interpretation of 13C/12C variations in tree rings from novel intra-seasonal studies on broad-leaf trees. Plant, Cell and Environment 27: 367-380

Hansen, N. (2004): Zur retrospektiven Lokalisation von Zuwachszonen in subtropischen Laubhölzern mittels der Methode der Hochfrequenz-Densitometrie. *Freiburger forstl. Forsch. 27 [PhD Thesis, University of Freiburg]* 172 p.

Kagawa, A., Sugimoto, A., Maximow, T. C. (2006): $^{13}CO_2$ pulse-labelling of photoassimilates reveals carbon allocation within and between tree rings. *Plant, Cell and Environment*, doi: 10.1111/j.1365-3040.2006.01533.x

Richter, M. (2003): Using epiphytes and soil temperatures for eco-climatic interpretation in southern Ecuador. *Erdkunde* 57 (3): 161-181.

Schinker, M.; Hansen, N.; Spiecker, H. (2003): High-frequency densitometry - a new method for the rapid evaluation of wood density variations. *IAWA Journal*, Vol. 24 (3): 231-239.

Volland-Voigt, F. (2006): Jahrringökologische Untersuchungen zum Zusammenhang zwischen Baumwachstum und Witterungsverlauf an ausgewählten Baumarten in einem Bergregenwald in Süd-Ecuador (Provinz Loja). *[Master Thesis, unpublished]*. 109 p.

Helle, G., Schleser, G. H. (2004): Beyond CO_2-fixation by Rubisco - an interpretation of ^{13}C /^{12}C variations in tree rings from novel intra-seasonal studies on broad-leaf trees. *Plant, Cell & Environment* 27: 367 – 380.

Reaction of siberian subarctic larch trees to abrupt climatic changes derived from tree-ring and isotope data

O. Sidorova[1], T. Boettger[2], R. Siegwolf[3], M. Saurer[3], M. Naurzbaev[1] & E. Vaganov[1,4]

[1] *V.N. Sukachev Institute of Forest SB RAS, 660036 Krasnoyarsk, Akademgorodok, Russia*

[2] *Helmholtz Center for Environmental Research – UFZ, Theodor-Lieser Str. 4, 06120 Halle/Saale, Germany*

[3] *Paul Scherrer Institute, 5232 Villigen, Switzerland*

[4] *Siberian Federal University, 660041 Svobodniy av, 79, Russia*

Email: ovsidorova@forest.akadem.ru

Introduction

The Siberian Subarctic region is highly interesting for the investigation of climatic and environmental changes because of its sensitivity to climate change [Vaganov and Shiyatov 1999; Körner 2000; IPCC 2007]. The application of long-term tree-ring chronologies (a natural archive for studies of climatic changes) can help us to evaluate climatic and environmental changes in the past and to understand the mechanisms of these changes. Stable isotopes in tree rings provide an additional proxy for paleoclimate with a defined annual resolution [Leng 2006].

It is well known that volcanic eruptions play an important role in climatic changes. Major volcanic eruptions eject particles and aerosols into the stratosphere leading to global cooling for up to several years due to a decrease in incoming solar radiation [Robock 2000; Zielinski 2000]. Recently, many reports about the influence of volcanic eruptions on tree ring width have been published [Baillie 1994; Briffa et al. 1998; Zielinski 2000; D'Arrigo 2001; Krakauer and Randerson 2003]. Only few studies were carried out to analyze the isotopic composition in trees in response to volcanic eruptions [Battipaglia et al. 2007] but none for the high latitudes of Eurasia.

A prominent example is the "dust-veil" event (AD 536) [Baillie, 1994], which had a catastrophic effect on the environment and civilization. Many scientists tried to explain this event [Baillie 1994; Zielinski et al. 1994; Briffa et al. 1998; Stothers 1999]. One hypothesis is that dry fogs spawned by large volcanic eruptions cooled the climate during that time by partially blocking incident sunlight and perturbed the atmospheric circulation patterns. The climatic and epidemiological consequences of seven intense volcanic dry fogs of the past 21 centuries, detected in Europe and the Middle East, were investigated using historical reports, supplemented by tree-ring data and polar-ice acidity measurements. An alternative hypothesis suggests that cosmic phenomena (asteroid or comet) could have caused the strong climatic changes during this time [Rigby et al. 2004]. European chronologies showed a decreasing radial growth during 10 years after the AD 536 event [Baillie 1994; Stothers, 1999].

The goal of this paper is to reveal the reaction of larch trees from the Siberian Subarctic (Eastern Taimyr) after the abrupt climatic change in AD 536, an event, which was characterized by cooling throughout the vast territory of Subarctic Eurasia. Tree rings and

DOI:10.2312/GFZ.b103-08056

isotopic data ($\delta^{13}C$, $\delta^{18}O$) were examined for a better understanding of physiological responses of trees to climatic and environmental changes.

Material and Methods

The investigation was carried out in the Siberian Subarctic - in Eastern Taimyr (72N-102E). This region is characterized by an extra continental climate, short vegetation periods (32-65 days), a growth limiting temperature regime, low amount of precipitation (300 mm) and permafrost. A well-replicated chronology based on ring-width measurements is available for the period BC 431 - AD 2006 [Naurzbaev et al., 2002, Sidorova et al., 2003, 2007 in preparation]. The June-July air temperature reconstruction was available from AD 1-1996 [Naurzbaev et al., 2002; Sidorova, 2003].

For the isotope analyses we chose four stem discs from dead larch trees (*Larix gmelinii* Rupr.) for the period AD 516-560 (20 years before and 24 years after the event of AD 536). Resins were extracted from wood samples in ethanol for 36 hours in a Soxhlet apparatus and then the samples were washed in distilled water and dried [Cook et al., 1990]. All samples were first measured and cross-dated according to standard dendrochronological procedures [Cook et al. 1990]. The age of these trees was 350 years excluding the influence of the “juvenile effect” [Cook et al. 1990; McCarrol and Loader 2004]. The samples were split into individual years for all analyzed trees. Sample preparations for the isotope analysis and cellulose extraction were carried out according to standard procedures described by Loader et al. [1997].

The measurement of the stable isotope ratios of $\delta^{13}C$ and $\delta^{18}O$ of cellulose was carried out by a mass-spectrometer Delta Plus XL (Thermo Quest Finnigan, Germany) at the Helmholz Centre for Environmental Research - UFZ, laboratory of Isotope Hydrology and at the Paul Scherrer Institute (PSI), Laboratory of Atmospheric Chemistry, Stable Isotope and Ecosystem Fluxes.

The $\delta^{13}C$ and $\delta^{18}O$ of wood and cellulose were expressed in the delta notation:

$$\delta_{sample} = (R_{sample}/R_{standard}-1) \times 1000$$

where R is the $^{13}C/^{12}C$, or the $^{18}O/^{16}O$ ratio of the sample and standard (VPDB for carbon, VSMOW for oxygen), respectively.

Results and Discussion

The dendrochronological analyses revealed decreased tree radial growth (Fig. 1) and decreased June-July air temperature of up to 3.2°C for 23 years after AD 536, which testifies to exceptional conditions. Continuous cooling over a 23 year period could result in very negative or even catastrophic effects on the environment and civilization).

As mentioned before, this signal in European chronologies was observed for a shorter period emphasizing the climatic sensitivity of the study area.

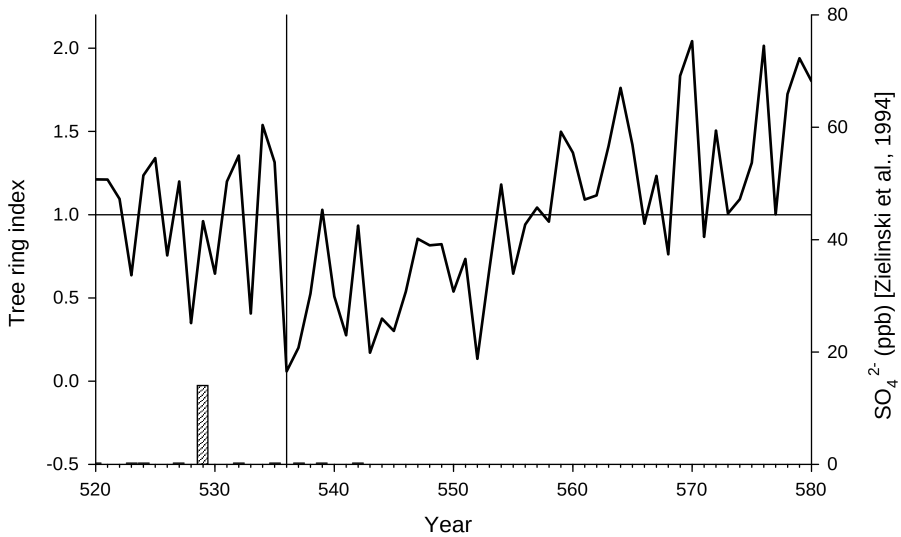

Figure 1: Reaction of larch trees from eastern Taimyr to the event AD 536 reflected in tree ring growth.

We established an isotope chronology for $\delta^{13}C$ and $\delta^{18}O$ in cellulose of four individual trees for the period AD 516-560. The correlation coefficients between the four different trees were very high for carbon ($r=0.8$; $p<0.05$) and somewhat lower for oxygen ($r=0.6$; $p<0.05$).

The $\delta^{13}C$ and $\delta^{18}O$-data of cellulose confirmed the occurrence of a stress factor during the period from AD 535-560, similar to tree-ring width, showing decreasing isotope values (Fig. 2 a b).

We observed the highest correlation coefficient ($r=0.62$; $p<0.05$) for the relationship between $\delta^{13}C$ of cellulose and the reconstructed June-July air temperature. This relationship was not as strong for $\delta^{18}O$ of cellulose ($r=0.42$; $p<0.05$). The isotope values reflect not only temperature changes like tree ring width, but also reflect the influence of relative humidity during this time.

Regression analysis between carbon and oxygen isotope ratios for the Eastern Taimyr shows a significant relationship ($r=0.70$; $p<0.05$) that indicates a combined effect of temperature and relative humidity after such a strong event.

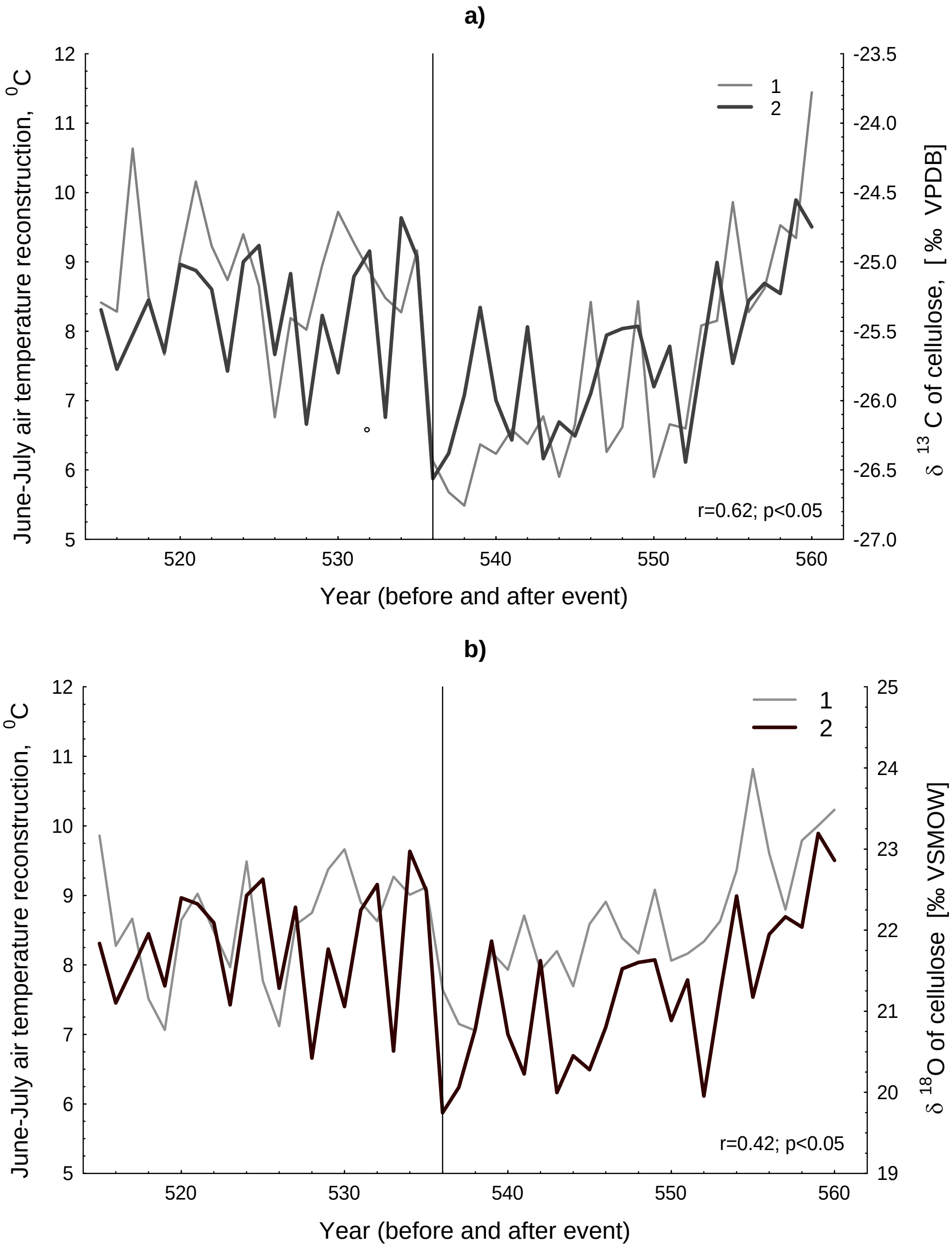

Figure 2: The δ^{13}C (a), δ^{18}O (b) of cellulose (1) and June-July air temperature reconstruction (2) *in comparison.*

Conclusions

The isotope values δ^{13}C, δ^{18}O of cellulose confirm the information stored in tree-ring width and show decreasing isotope values during the same period when growth was reduced after the major event of AD 536 (we assume major volcanic eruption). These results indicate an increase of relative humidity, which could have led to higher stomatal conductance and lower photosynthetic capacity due to a reduction of solar radiation and subsequent temperature decrease. The combination of isotope and ring-width data provide strong data base from which we can learn more about the effect of the drastic AD 536 event on the Boreal forest ecosystems.

DOI:10.2312/GFZ.b103-08056

Acknowledgements:

This work was supported by UFZ- research grant, European Science Foundation -SIBAE- № 1389 (exchange visits), by RFBR 07-04-96819-Yenisey-a, 06-05-64095a grants. A thank goes to Ute Helmstedt, Wolfgang Stadter for the laboratory assistance and Gomez-Holmes Katherine Emma for her help. A special thank a goes to Marika Haupt for her help and support.

References:

Baillie, M.G.L. (1994): Dendrochronology Raises Questions about the Nature of the AD 536 Dust-Veil Event, *The Holocene*, 1, 4: 212-217.

Battipaglia, G., Cherubini, P., Saurer, M., Siegwolf, R., Strumia, S., Cotrufo, F. (2007): Volcanic explosive eruptions of the Vesuvio decrease tree-ring growth but not photosynthetic rates in the surrounding forests. *Global Change Biology* 13: 1-16.

Briffa, K.R., Jones, P.D., Schweingruber, F.H., Osborn, T.G. (1998): Influence of volcanic eruptions on Northern Hemisphere summer temperatures over the past 600 years. Nature 393: 450-455.

Cook, E.R., Kairiukstis, L.A. (Eds.) (1990): Methods of Dendrochronology. Applications in the environmental sciences, Dordrecht; Boston; London: Kluwer Acad. Publ., 394 p.

D'Arrigo, R, Frank, D, Jacoby, D, Pederson, N. (2001): Spatial response to major volcanic events on AD 536, 934 and 1258: Frost rings and other dendrochronological evidence from Mongolia, Climatic Change, 49: 239-246.

IPCC (2007): 4th Assessment report Intergovernmental panel on climate change, chap. 6: 434-497.

Körner, C. (2000): Biosphere responses to CO_2 enrichment, *Ecological Applications*, 10 (6): 1590-1619.

Krakauer, N.Y., Randerson, J.T. (2003): Do volcanic eruptions enhance or diminish net primary production? Evidence from tree rings, *Global Biogeochemical Cycles*, 17, 4: 1118, doi: 10.1029/2003GB002076

Leng, M.J. (Ed.) (2006): Isotopes in Palaeoenvironmental Research, Springer, Netherlands, 307 pp.

Loader, N.J., Robertson, I., Barker, A.C., Switsur, V.R., Waterhouse, J.S. (1997): Improved technique for the batch processing of small whole wood samples to alpha-cellulose, Chemical Geology 136: 313-317.

McCaroll, D., Loader, N.J. (2004): Stable isotopes in tree rings, Quaternary Science Reviews, 23: 771-801.

Rigby, E., Symonds, M., Ward-Thompson, D. (2004): A comet impact in AD 536. *Astronomy and Geophysics*, 45 (1): 1.23-1.26.

Robock, A. (2000): Volcanic eruptions and climate. *Review of Geophysics*, 38, 2: 191-219.

Stothers, R. (1999): Volcanic dry fogs, climate cooling and Plague pandemics in Europe and the Middle east. *Climate Change* 42: 713-723.

Vaganov, E.A., Shiyatov, S.G. (1999): The role of dendroclimatical and dendrohydrological study in development of global and regional ecological problems, Siberian Ecological Journal, VI, 2: 111-115.

Zielinski G.A. (2000): Use of paleo-records in determining variability within the volcanism-climate system. *Quaternary Science Reviews,* 19: 417-438.

Zielinski, G.A., Mayewski, P.A., Meeker, L. D., Whitlow, S., et al. (1994): Record of volcanism since 7000 B.C from the GISP 2 Greenland ice core and implications for the volcano-climatic system, *Science,* 264: 948 -952.

DOI:10.2312/GFZ.b103-08056

SECTION 4

GEOMORPHOLOGY

DOI:10.2312/GFZ.b103-08056

Tree-ring study of the island formation and riparian forest along a gravel-bed river in the Polish Carpathians

R.J. Kaczka[1], B. Wyżga[2] & J. Zawiejska[3]
[1] *Faculty of Earth Sciences, University of Silesia, Sosnowiec, Poland*
[2] *Institute of Nature Conservation, Polish Academy of Sciences, Kraków, Poland*
[3] *Institute of Geography, Pedagogical University, Kraków, Poland*

Introduction

The Białka River is one of the last relatively undisturbed, gravel-bed rivers in Central Europe (Baumgart-Kotarba 1980, 1985). Although its riparian zone and floodplain are partly subject to human activities, the character of both island vegetation and the river channel remain typical of the formerly widespread, semi-natural, braided rivers in the Carpathians (Fig. 1). Such conditions give an opportunity to investigate islands remaining in an almost undisturbed form as well as their development. The study aims at reconstructing spatial and temporal dynamics of the island evolution in a gravel-bed river.

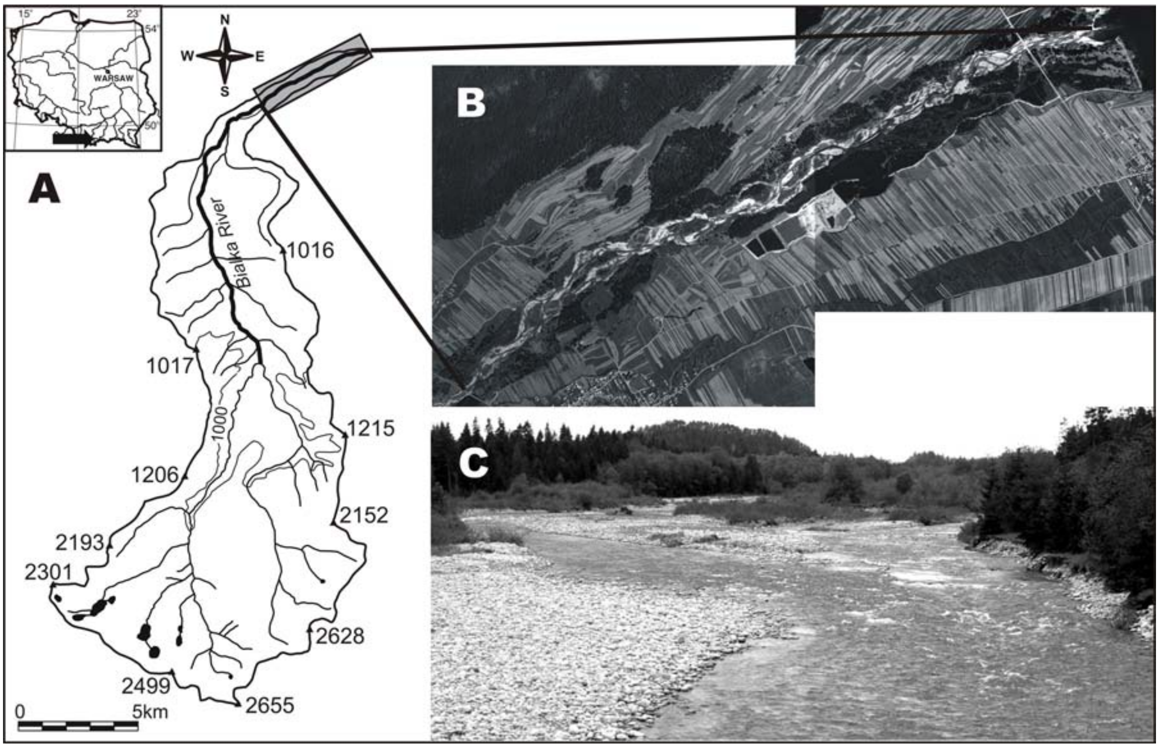

Figure 1: Catchment of the Białka River with location of the studied section (shaded) (A). Island-braided channel of the Białka River as shown on an orthophoto (B) and a ground photo (C).

Geographical setting, data and methods

The Białka River drains an area of 230 km^2 in the Western Carpathians, including a part of the high-mountain Tatras. With high flow variability and a steep channel slope, the river is characterised by the occurrence of a cobble bed and a highly dynamic pattern of braids, bars and islands within its active zone. The research was conducted in a 5 km long section of the

DOI:10.2312/GFZ.b103-08056

lowest river course, where the river is widest (up to 420 m) and islands and bars are most common. Willow and alder predominate on most of the islands, whereas spruce and pine grow on older islands and in the riparian forest. Twenty-six established islands, their entire population in the section, and the associated pioneer islands were analysed. Initial investigations revealed the existence of two types of islands: (i) islands developing by vegetation growth on mid-channel bars; and (ii) those originating as a result of dissection of riparian forest or already existing islands by braids. Here, we present the results of a study focused on the first type, represented by the population of 12 islands located in the lower course of the investigated river section. Standard dendrochronological techniques were employed to determine the age structure of trees growing on the islands and in the riparian forest. The age of the oldest specimens was considered to represent a minimal age of the island. Age structure of the vegetation in five different zones of the islands was employed as a proxy of their spatial development (Fig. 2).

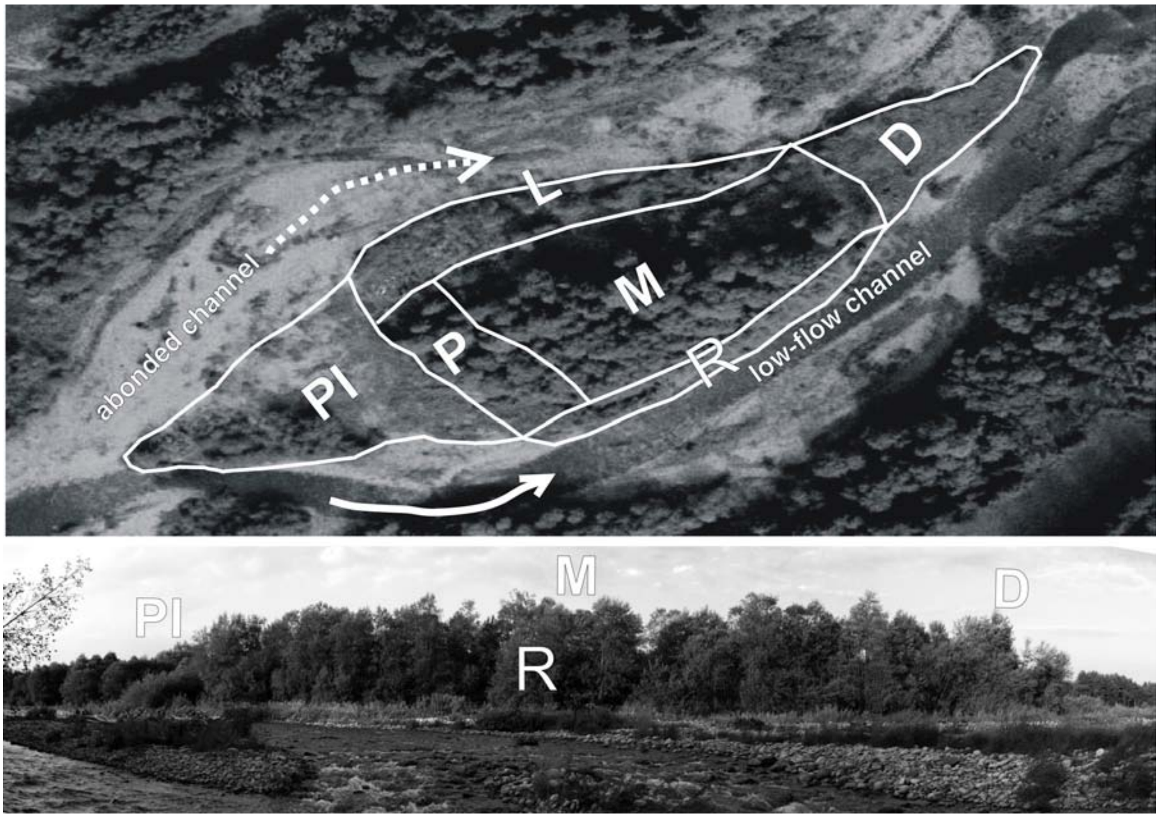

Figure 2: Sampled zones of islands: PI - initial proximal side of island, upstream zone, P - proximal zone with well-established trees/shrubs, M - middle part of island, R - right marginal zone, L - left marginal zone, D - distal, downstream part of island.

Results and discussion

So-defined minimal age of islands is related to the occurrence of major floods that effectively change the pattern of a braided channel. On the Białka River, such floods last occurred in 1997 and 2001. Although a signal of previous floods is less apparent in tree-ring dating, a comparison of the age of the islands (average age of sampled trees amounts to 7 years, n=216) and the riparian forest (34 years, n=60) reveals significant differences in the factors controlling development of both elements of the riverine landscape. The age of islands is related to the occurrence of floods, whereas that of the riparian forest is more independent of a natural dynamics and largely determined by human activity. While the river has an ability to form braids within its active zone freely, lateral migration of the entire channel is limited in many locations by channelization structures.

In most of the cases, the youngest trees grow on the head of island (PI) and age of trees gradually increases through the proximal zone (P) to the middle zone (M) (Fig 3). The downstream zone of island (D), less protected from the action of flood waters than the middle one (M), is overgrown by younger trees than both M and P zones. No significant difference between the age of trees on both sides of island (R and L) was found. The island head is the place where gravel and woody debris are trapped during floods. That process, observed on all studied islands, implies their growth in the upstream direction, by which new space for vegetation succession is created.

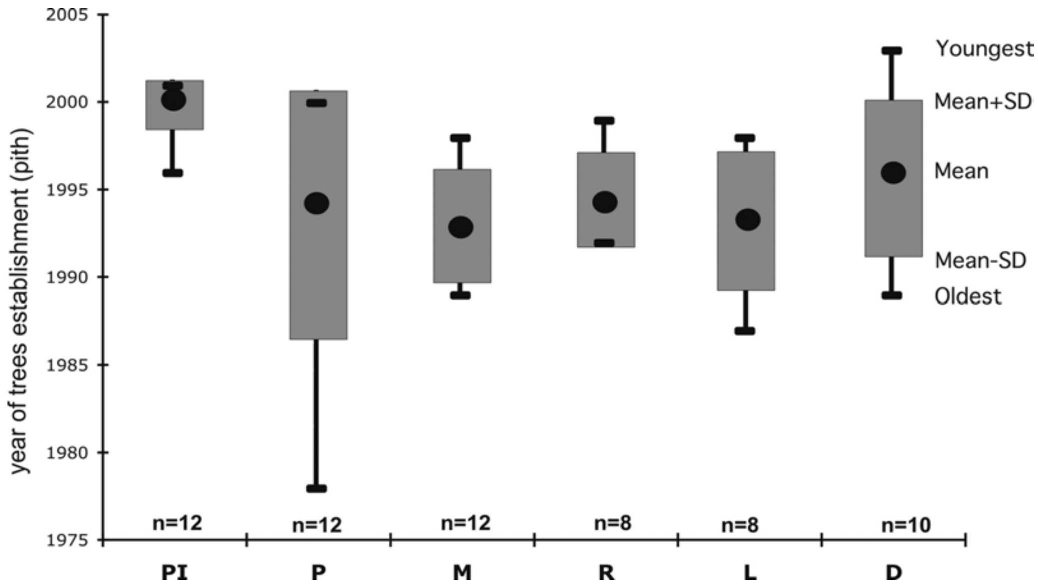

Figure 3: Age structure of trees in particular island zones as a proxy of spatial island development. The age of oldest specimens represents a minimal age of the island. Island head (PI), where gravel and woody debris are trapped, is the youngest, whereas the well-protected, middle zone (M) is the oldest one.

One of the factors responsible for island initiation is the presence of large woody debris (LWD) in the river channel (Abbe & Montgomery 1996, Edwards et al. 1999, Gurnell et al. 2001). The size and amount of LWD is crucial for this process (Millar 2000). In the rivers of the western part of North America, draining pristine and old-growth forests, large fallen trees are stable in-channel features, which promote sediment deposition and vegetation establishment (Fetherstone et al. 1995). The relatively small size of LWD delivered to the Białka River is a consequence of young age of the managed, riparian forest. Moreover, removal of larger wood pieces from this, and also other European rivers, for firewood (cf. Piégay 1997, Kollmann et al. 1999, Gurnell et al. 2001) reduces wood quantity and increases its mobility. Small pieces of trees and bushes remaining in the rivers are unable to play a key role in island development. Under such conditions, vegetation is a major factor controlling island development. The age structure of vegetation on the investigated islands indicates island development in the upstream direction (Fig. 4A), rather than in a downstream one as is typically observed when large trees protect the head of island (Fig. 4B). This pattern of island formation seems to be representative of European braided rivers, in which the amount and size of LWD are strongly controlled by human activity (Edwards et al. 1999, Ward et al. 1999, Gurnell & Petts 2002).

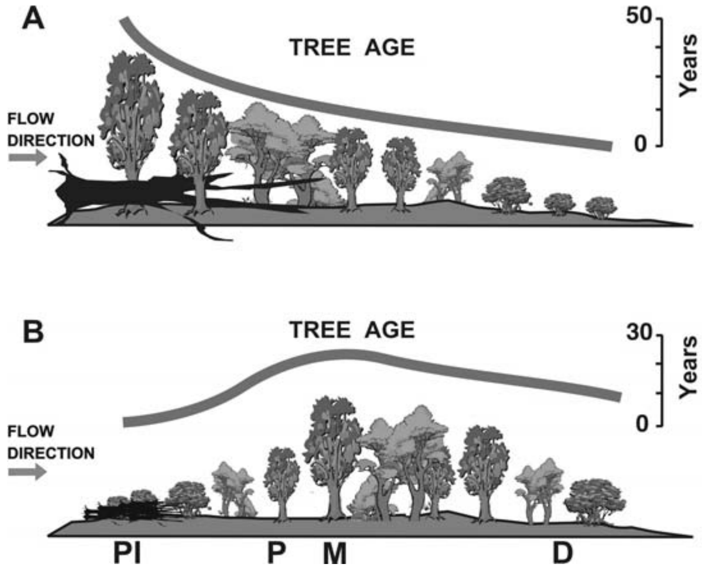

Figure 4: Models of island growth for: (A) rivers of the Pacific Northwest (bigger trees, important role of LWD in island development), (adapted from Fetherstone et al. 1995); and (B) European braided rivers (smaller trees and bushes, important role of vegetation in island growth).

Conclusions

1. Though preliminary results indicate different scenarios of the island initiation and development, registered in the tree-ring proxy, a common pattern exists - the oldest trees grow in the central, best protected part of the islands.
2. The decrease in tree age from the island centre is more pronounced in the upstream than in the downstream direction. Centrally growing trees play an important role in the island development as they trap wood and mineral sediment on the upstream island margin, hence stimulating growth of islands in the upstream direction.
3. That pattern of island formation seems typical of mountain European rivers, from which large wood pieces are typically removed and where the resultant lack of key-member fallen trees prevents initiation of bar and island formation in their hydraulic shadow.

Acknowledgements

This research was financed by Research Grant 2 P04G 092 29 of the Polish Ministry of Science and Higher Education.

References

Abbe T.B., Montgomery D.R. (1996): Large woody debris jams, channel hydraulics and habitat formation in large rivers. Regulated Rivers 12: 201-221.

Baumgart-Kotarba M. (1980): Braided channel changes at chosen reaches of the Białka River, the Podhale, Western Carpathians. Stud. Geomorph. Carp.-Balcan. 14: 113-134.

Baumgart-Kotarba M. (1985): Different timescales of examining the river bed and valley floor evolution (braided river Białka Tatrzańska as example). Stud. Geomorph. Carp.-Balcan. 19: 61-76.

Edwards P.J., Kollmann J., Gurnell A.M., Petts G.E., Tockner K., Ward J.V. (1999): A conceptual model of vegetation dynamics on gravel bars of a large Alpine river. Wetlands Ecology and Management 7: 141-153.

Fetherstone K.L., Naiman R.J., Bilby R.E. (1995): Large woody debris, physical process, and riparian forest development in montane river network of the Pacific Northwest. Geomorphology 13: 133-144.

Gurnell A.M., Petts G.E. (2002): Island-dominated landscapes of large floodplain rivers, a European perspective. Freshwater Biology 47: 581-600.

Gurnell A.M., Petts G.E., Hannah D.M., Smith B.P.G., Edwards P.J., Kollmann J., Ward J.V., Tockner K. (2001): Riparian vegetation and island formation along the gravel-bed Fiume Tagliamento, Italy. Earth Surf. Proc. Landforms 26: 31-62.

Kollmann J., Vieli M., Edwards P.J., Tockner K., Ward J.V. (1999): Interactions between vegetation development and island formation in the Alpine river Tagliamento. Applied Vegetation Science 2: 25-36.

Millar R.G. (2000): Influence of bank vegetation on alluvial channel patterns. Water Res. Research 36: 1109-1118.

Piegay H. (1997): Interactions between floodplain forests and overbank flows: data from three piedmont rivers of southeastern France. Global Ecology and Biogeography Letters 6: 187-196.

Ward J.V., Tockner K., Edwards P.J., Kollmann J., Bretschko G., Gurnell A.M., Petts G.E., Rossaro B. (1999): A reference river system for the Alps: the Fiume Tagliamento. Regulated Rivers: Res. Management 15: 63-75.

DOI:10.2312/GFZ.b103-08056

Meandering river bank erosion and channel lateral migration recorded in black alder *(Alnus glutinosa)* tree rings

I. Malik[1] & D. Ciszewski[2]

[1] *University of Silesia, Department of Quaternary Paleogeography and Paleoecology, Sosnowiec 41–200, ul. Bedzinska 60, Poland; Email:irekgeo@wp.pl*

[2] *Institute Polish Academy of Science, Institute of Nature Conservation, Cracow 31-200, al. A. Mickiewicza 33, Poland; Email: ciszewski@iop.krakow.pl*

Introduction

Black alder belongs to pioneer woody species. It prefers area without plants for growing, for example new surfaces occurring after floods (Iversen 1973). Additionally black alder roots are adapted to growing under the water level (van Dijk 1978, Dilly et al. 2000). Therefore black alders often occupance meandering river banks and valley floors in European temperate climates (Grime 1981).

Due to bank erosion and lateral channel migration alders are under mechanical stress. Banks upon which they grow are systematically eroded and trees forming different growth forms to survive. Black alders growing on undercutting banks are mostly tilted and their stems are bended, usually they have exposed root systems (Fig. 1A). Clumps of alders growing on the concave banks numbered several stems (Fig.1B), the stems are 1/3 less in diameter than alders growing on straight or convex banks.

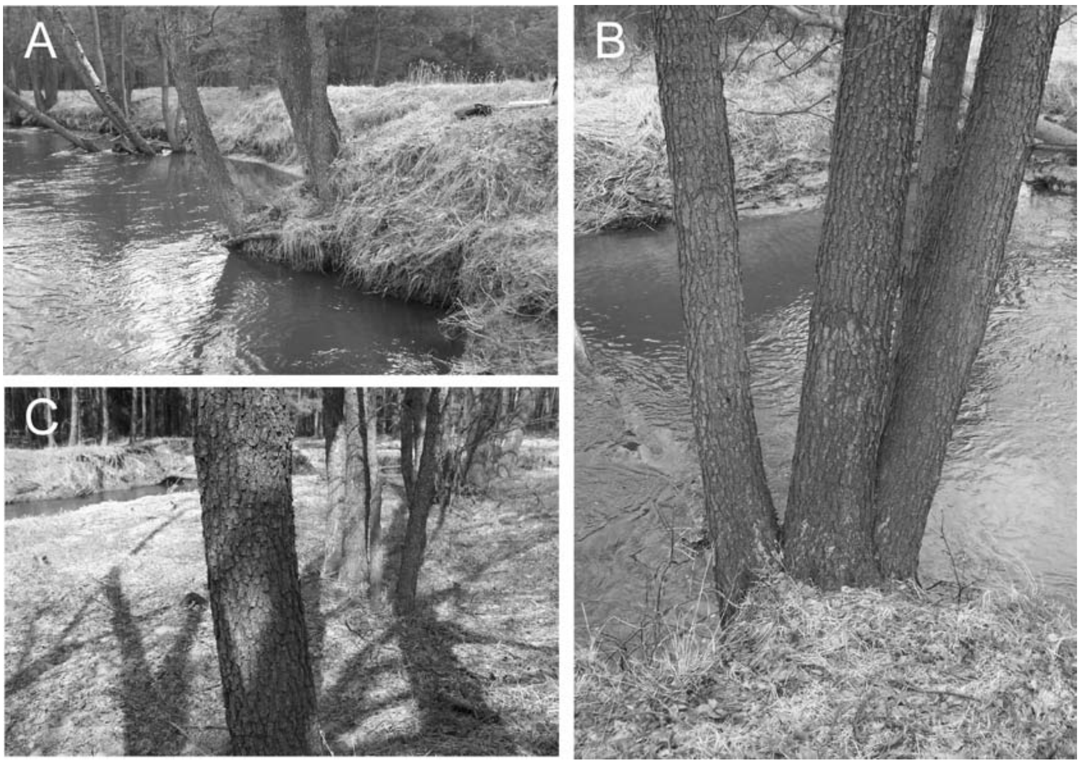

Figure 1: Examples of grow forms of riparian alder. A – alders tilted and advanced due to erosion in respect of river bank; B – clump growing on the river bank; C – alders growing due to lateral channel migration on the old bank line (palaeobank).

DOI:10.2312/GFZ.b103-08056

Alders are producing clumps with expended root systems because it predisposes the plant to obtain stability in contrast to individual stems. The clumps growing on banks forced by erosion are protruding in the middle of the river channel. The alders growing at some distance from convex banks often have similar shapes to trees observed on the straight and concave bank (Fig.1C). The similarity is caused by progressive lateral erosion and line of trees withdrawn from recent bank.
The aim of this study is to find bank erosion and channel migration records in riparian alder tree rings.

Study area
Study area was selected in the valley of the Mała Panew River runs along an east-west axis through the Opole Plain which forms part of the Silesian Lowland, southern Poland (Fig. 2a). The meandering Mała Panew flows through over 20 kilometres of compact forest complex. Therefore it is one of the few areas in Central Europe Lowlands where the impact of vegetation on river channel formation can be studied. The river is 131 km in length, and drains an area of about 2000 km². The bottom of the valley is covered by poorly sorted sands. Terraces of the Mała Panew River are covered with pine plantations, black alders mostly grow in the floodplain. The monthly precipitation in the study area is between 500 and 700 mm. The mean annual discharge at the Krupski Młyn gauge, 20 km downstream of the study area reaches, is 10 m³/s.

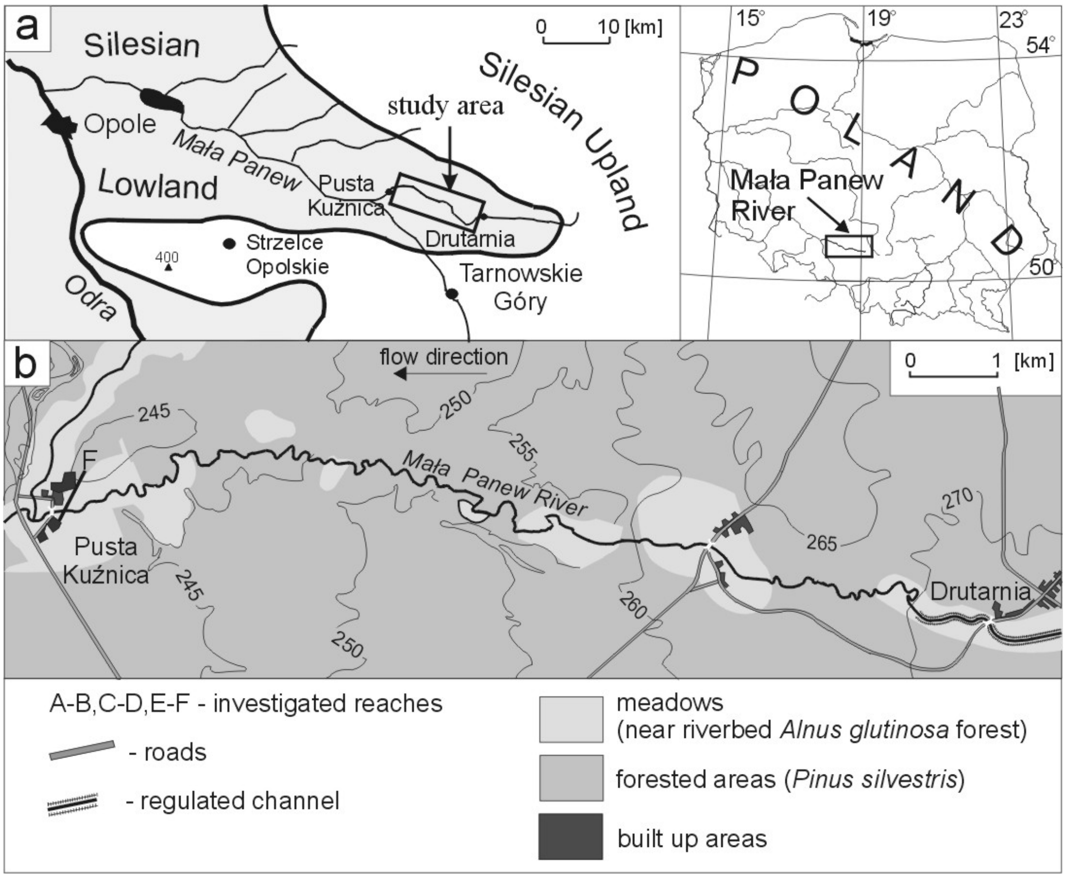

Figure 2: Location of study area.

During the last few decades several peak discharges have been 10-20 times higher, apart from an extraordinary flood event of 3 days in July 1997, when the water rose in same places 6 to 8 m above the flood plain (Malik 2006).
The study sites are located in the 12 kilometres between Drutarnia and Pusta Kuźnica (Fig. 2b). The Mała Panew forming in the study area numerous bends with varying diameters in the river—such features are typical for areas with forested banks. The channel cuts around 0.5–1.5 m deep into the floodplain. The gradient of the Mała Panew valley within the reach examined amounts to 1.2 ‰. The width of the river in forested areas does not exceed 15 m while its depth at average water stage reaches up to 1.5 m. Lateral migration rate of the Mała Panew channel at the studied sites is about 0.2 – 1.5 m/year (Malik 2005, 2006).

Methods

Firstly, 20 stems of alders growing on today undercutted bank with well visible formed growth transformation (bending, tilting, clumps forming) were selected for sampling. Twenty alder stems growing on the old bank line and 10 alder stems representing carr formation were selected to compare alder tree-ring series transformed by bank erosion and ring series not transformed. Two cores were sampled from individual 50 alders. The sampling level on each tree was about 0.5 metres above ground. Trees growing on undercutted banks and palaeobanks were sampled on the maximum tilt axis of the alders in a plane perpendicular to the riverbed. The first core was sampled from a location facing the riverbed, while the second faced the flood plain. Finally tree ring series from every tree and site chronology ware constructed and cross-dated to find bank erosion and lateral channel migration records. Additionally stem circumference and mean ring width from every stem were calculated.

Results and Discussion

Erosion records in the tree rings of tilted and bend alders

Tree rings formed by alders growing on undercutted banks are considerably thinner than rings formed by alders growing in the some distance form banks (Tab. 1).

Table 1: Ring width and eccentric growth in different types of alders form growth

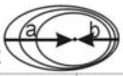

	mean ring width (mm)	degree of eccentric (%) river bank / riverbed: a	b
tilted alders growing on the river banks	2.56	145.7	100.0
alders growing on the river banks in clumps	2.90	124.6	100.0
alders growing on the palaeobanks	2.45	100.2	100.0
alders growing in carr formation	3.80	-	-

Alder stems undercutted by erosion produce eccentric tree rings. In individual tilted stems, rings facing the flood plain are 50% wider than rings facing the riverbed. After titling during the period without great erosion events alders gradually straighten stems, finally alders become hook shaped (Fig. 1A and 3).

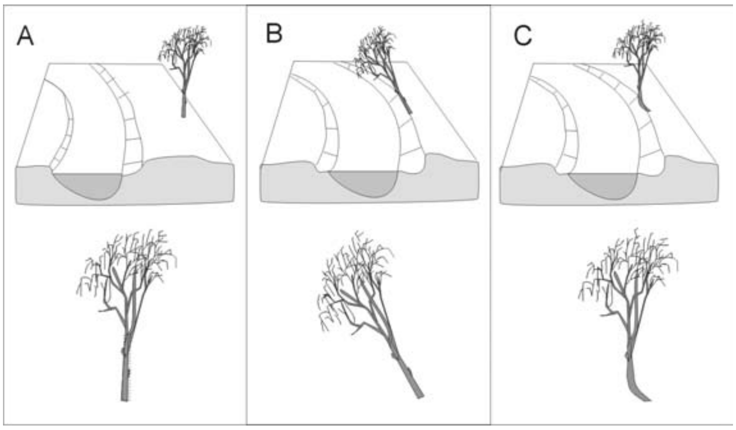

Figure 3: Riparian alders tilted and bend as a result of bank erosion. A – straight alder stem not transformed by erosion, B – tilted alder stem transformed by erosion, C – bend alder stem as a result of periods without erosive episodes.

Similar effects were observed for trees growing on continually creeping slopes by Patrizek and Woodruff (1957). The authors suggest the trees had been bowed because only the apical part of stem is able to grow vertically. Trees changing stem shape after soil creeping were also described by Schmid and Schweingruber (1994). Trees incline towards the slope after the event, while next years without soil creeping events overcompensation occurs and trees start to grow vertically again. Finally trees are S-shaped. Tilting and bending of alder stems are well recorded in tree rings. Alder tilting makes the width of the first ring facing the floodplain decrease and simultaneously the same ring facing the riverbed increases (Fig. 4, years 1987 and 1997).

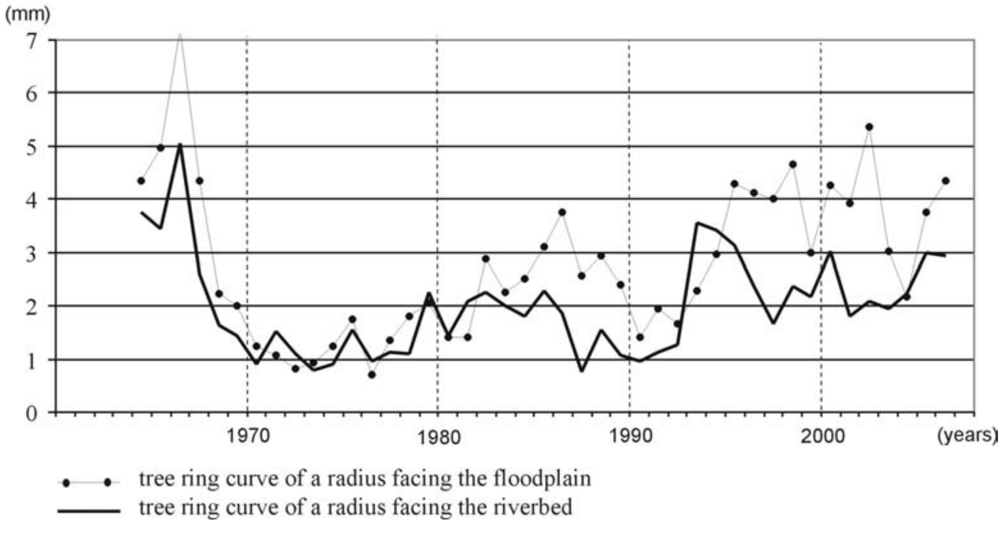

Figure 4: Example of tilted and bend alder tree ring series.

The riverbank on which the trees grew was undercut in 1987 and 1997 (Fig. 4). In these two years, water stages recorded at the nearby gauge were extremely high in June and July respectively. About 5 to 10 years after the tilting episode floodplain and riverbed facing tree rings reach gradually even widths. It means, the stem grows upright again after several years but the straightening period depends on the erosion episode frequency.

Lateral migration records in the tree rings of alder growing on palaeobanks

River channel may shift it's course during one flood. As a consequence, lines of alders are documenting old river channels after such a big flood (Fig. 5). Trees growing on palaeobanks gradually loose their bendiness and tiltness and start growing upward. When a channel has been shifted alders produce about 50% thinner tree rings than before shifting.

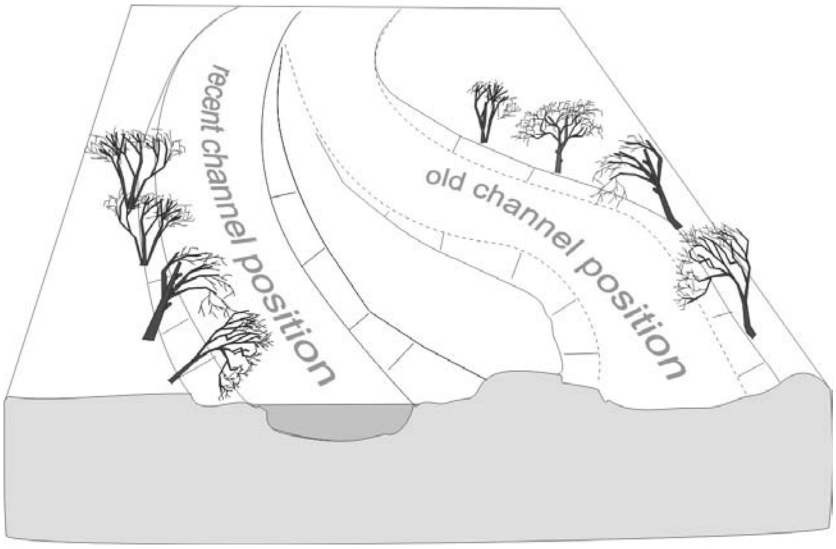

Figure 5. Alders growing along recent and old channels within a floodplain

Figure 6 reveals clearly visible growth reduction in alder stems when the river channel changed it's course in 1966 at this site. Probably the growth reduction results from a decreasing of water level after river channel shifting.

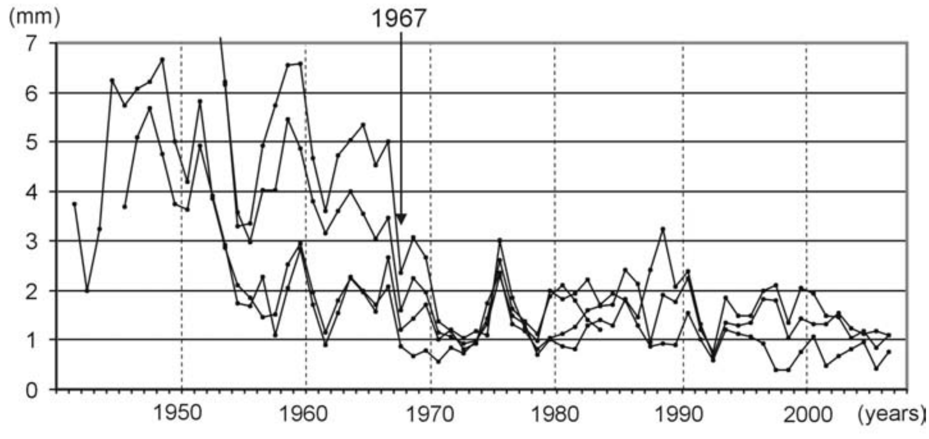

Figure 6. Example of ring curves of alders growing along palaeochannel at one site (ring reduction in 1967 showing year when the channel was shifted)

DOI:10.2312/GFZ.b103-08056

Conclusions

1. It is possible to reconstruct bank erosion and river channel migration by using riparian alders. Bank erosion and channel shifting are clearly reflect in riparian alder ring series.
2. After erosion episodes alders growing directly on the udercut bank are often tilted. The trees produce eccentric tree rings. Rings facing the floodplain are strongly wider than rings produced on the other side. After several years without any erosion episode alders begin grow straight again. A stem results hook shaped.
3. As soon as a channel has shifted it's course, alders established on an abandoned bank reduce growth ubruptly.

References

van Dijk, C. (1978): Spore formation and andophyte diversity in root nodules of *Alnus glutinosa* (L.) Vill. *New Phytologist* 81: 601–615.

Dilly, O., Bach, H.J., Buscot, F., Eschenbach, C., Kutsch, W.L., Middelhoff, U., Pritsch, K., Munch, J.C. (2000): Characteristics and energetic strategies of the rhizosphere in ecosystems of the Bornhöved Lake district. *Applied Soil Ecology* 15: 201–210.

Grime, J.P. (1981): Plant Strategies and Vegetation Processes. John Wiley & Sons, 223 pp.

Iversen, J. (1973): The development of Denmark`s nature since the Last Glacial. *Geology Survey of Denmark* 7: 7–126.

Malik, I. (2005): Rates of lateral channel migration along the Mała Panew River (southern Poland) based on dating riparian trees and Coarse Woody Debris. *Dendrochronologia* 23: 29–38.

Malik, I. (2006): Contribution to understanding the historical evolution of meandering rivers using dendrochronological methods: example of the Mała Panew River in southern Poland. *Earth Surface Processes and Landforms* 31: 1227–1245.

McVean, D.N. (1953): *Alnus glutinosa* (L.) Gaertn. (*A. rotundifolia* Stokes). *Journal of Ecology* 41: 447–465.

Parizek, E.J., Woodruff, J.F. (1957): Mass wasting and the deformation of trees. *American Journal of Science* 255: 63–70.

Schmid, H. Schweingruber, F.H. (1994): Datierung und Nachweis von Rutschungen mit Hilfe von Jahrringen. *Schweiz. Z. Forstwes.* 146: 641–659.

DOI:10.2312/GFZ.b103-08056

SECTION 5

WOOD ANATOMY

DOI:10.2312/GFZ.b103-08056

Tree ring width and basic density of wood in different forest types

E. Přemyslovská, J. Šlezingerová & L. Gandelová
Department Wood Science, Mendel University of Agriculture and Forestry in Brno, Czech Republic
Email: premyslo@mendelu.cz

Introduction

Wood is important renewable raw material for energy generation, building, veneering, furniture making. Its mechanical and physical properties make the wood one of the most important structural materials, because of its big stiffness and strength and relatively low density. We can't omit its desirable acoustical properties. All physical and mechanical properties are defined by structure and density of wood, i.e. by amount and distribution of structural elements.

Wood structure and thus its properties are determined during tree ontogeny. Anatomical structure reflects all environmental (abiotic and biotic) and genetic factors operated on a tree during its life. The influence of the stand (growing conditions) on wood properties is to be examined for a long period.

The one year increment of spruce wood compounds from the layer of earlywood, created during the initial period of growing season and typical by the wide cells with thin cell wall, and latewood, that is created during and at the end of growing season and is characterized by substantially thicker cell wall but narrower radial dimensions than earlywood (Vavrčík 2002). The radial dimensions of a cell and dimension of cell wall is influenced by temperature and water availability. Increasing temperature during earlywood formation period causes shortage of phase of radial expansion of young wood cells and therefore the radial dimensions of cells are smaller than normal. If the tree experiences higher temperatures during latewood formation period, the phase of radial expansion is prolonged. The maturing period extends if the temperature of environment is high for both earlywood and latewood. That leads to the significantly thicker cell wall.

Precipitation affects positively the radial growth period and maturing period and causes prolongation of these (Vavrčík 2002). The thickness of cell walls in newly formed wood depends on the carbohydrates stock, and is therefore indicator of metabolic proceeds of a given year (Larcher 1988).

The wood density is one of the most basic parameters of wood quality. It affects substantially mechanical properties of wood. Due to different density of early- and latewood the treering width is very important factor of wood quality, because the portion of earlywood increases with increasing tree ring width (Kollmann 1951). The earlywood have lower density, lower strength and stiffness and have smaller shrinkage during moisture change (Horáček 1998).

The aim of this work is to determinate an average tree ring width and basic density of Norway spruce (*Picea abies* [L.] Karst.) growing in different vegetation forest zones. Norway spruce is the most important commercial specie in Czech Republic and its portion of forest stands is 53 %.

DOI:10.2312/GFZ.b103-08056

Material and Methods

Trial areas were selected and assessed by the typological classification of forest zones of Forest Management Institute (Plíva 1971). The typological system consists of horizontal and vertical division of zones. There are 9 forest vertical vegetation zones: (1) the oak zone, (2) the beech with oak zone, (3) the oak with beech zone, (4) the beech zone, (5) the silver fir with beech zone, (6) the Norway spruce with beech zone, (7) the beech with spruce zone, (8) the Norway spruce zone and (9) the mountain pine zone (Tab. 1). The horizontal zonation applies to each one vertical vegetation zone. The zoning is based on general characteristics of soil environment, soil nutrients content and sometimes on the topography of the region.

Table 1: Forest vegetation zones and its share on the Czech forests (Forest management Institute, Report on forestry of the Czech Republic, 2007.)

Forest vegetation zone			Elevation above sea level	Average annual temperature	Annual precipitation	Growing season
code	prevailing species	%	m	°C	mm	days
0	pine	3.73	non-zonal			
1	oak	8.31	<350	>8.0	<600	>165
2	oak with beech	14.89	350-400	7.5-8.0	600-650	160-165
3	beech with oak	18.41	400-550	6.5-7.5	650-700	150-160
4	beech	5.69	550-600	6.0-6.5	700-800	140-150
5	beech with fir	30.04	600-700	5.5-6.0	800-900	130-140
6	beech with spruce	11.95	700-900	4.5-5.5	900-1050	115-130
7	spruce with beech	5.0	900-1050	4.0-4.5	1050-1200	100-115
8	spruce	1.69	1050-1350	2.5-4.0	1200-1500	60-100
9	dwarf pine	0.29	>1350	<2.5	>1500	<60

Primarily recognized are series, next on the basis of more detailed soil characteristics each series is subdivided into edaphic categories (Tab. 3). 124 stands located in Czech Republic were chosen for this research (Fig. 1). The age of stands in chosen areas was 70-100 years. On each trial area 20 trees were randomly selected, the wood cores have been taken using increment borer from each tree.

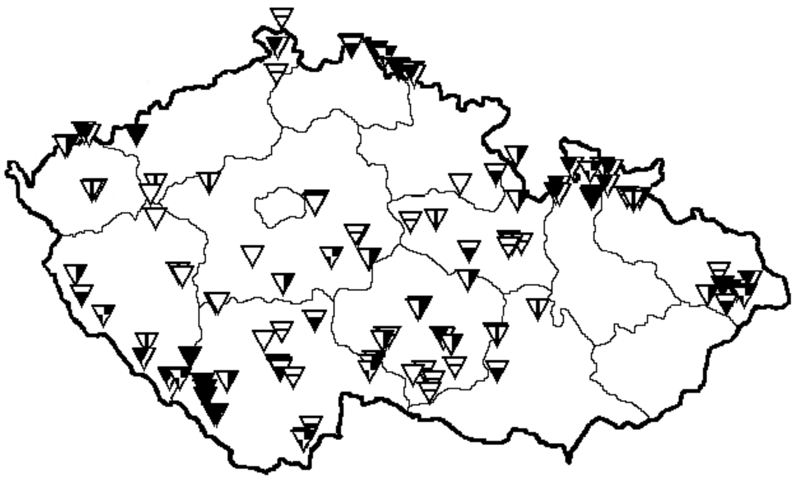

Figure 1: Map of Czech Republic with trial areas of this research marked by triangles

DOI:10.2312/GFZ.b103-08056

The Ericson's procedure (Ericson 1959) was applied to calculate basic density for the whole stem radius. Basic density of wood was determined by the method of Olesen (1971).

Basic density is defined as

$$_{k} = \frac{m_0}{V_w}$$

where ρ_k is basic density of wood, m_0 is mass of wood at moisture content 0 % and V_w is volume of wood above saturation point.
Finely, the average tree ring width for each sample was determined as length of core/number of tree rings.

Results and discussion
Relation between tree ring width and basic density was found for set of all tested samples. The assumption of decrease of wood density with increasing tree ring width has been validated as you can see in figure 2. This is caused by increasing portion of thin walled early wood in wide tree rings of gymnosperms.

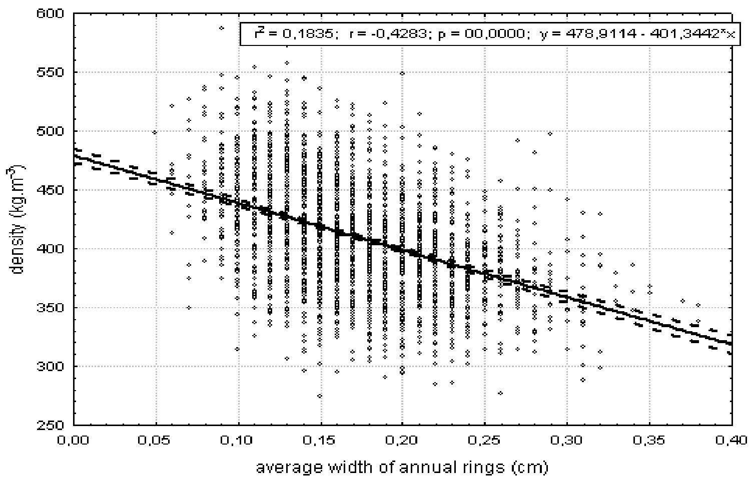

Figure 2: Relation between tree ring width and basic density.

The statistically significant differences between basic density values of samples from different vegetation zones and edaphic factors have been found. Resulting values of basic density and tree ring width are listed in the table 2 (according to vegetation zones) and table 3 (according to edaphic factors).
The highest value of basic density has been found for fourth (beech) vegetation zone – 445 kg·m^{-3} Together with that, the smallest average tree ring width 1.57 mm has been found for this group. After Tukey test of multivariate comparison there are statistically significant differences between sub-categories of edaphic series gleyic and between and between sub-categories P and B. Interesting is basic density of wood in sub-category P (462 kg·m^{-3}) and generally higher values of basic density on stands with lower pH.
Similarly high values of basic density and small average tree ring widths are typical for

second (beech with oak) vegetation zone (444 kg·m^{-3}, 1.65 mm) and third (oak with beech) vegetation zone (438 kg·m^{-3}, 1.69 mm), whereas the difference between values of basic density and average tree ring width in vegetation zones 2 – 4 are not statistically significant.
High values of basic density can be caused by effect of high temperatures and by longer vegetation period. If the tree experiences high temperature, the phase of radial growth of earlywood tracheids is shorten and of latewood tracheids is prolonged, simultaneously the phase of maturing is prolonged. The production of latewood is therefore boosted up and the earlywood tracheids have thicker cell wall and smaller radial dimension the those growing in colder environment.

Tab. 2 Results according vegetation zones (main value in cell is mean, first value in brackets is number of samples, second value is stand. deviation)

Prevailing species	oak with beech	beech with oak	beech	beech with fir	beech with spruce	spruce with beech	spruce	Mean
Vegetation zone code	**2**	**3**	**4**	**5**	**6**	**7**	**8**	
Basic density (kg.m^{-3})	443.98 *(200; 37.29)*	437.57 *(340; 41.87)*	445.00 *(282; 35.96)*	413.98 *(589; 43.96)*	392.34 *(465; 37.33)*	377.66 *(219; 34.37)*	374.14 *(400; 36.13)*	409.61 *(2495; 47.17)*
Tree ring width (mm)	1.65 *(200; 0.46)*	1.69 *(340; 0.51)*	1.57 *(282; 0.41)*	1.81 *(589; 0.58)*	1.99 *(465; 0.48)*	1.76 *(219; 0.44)*	1.59 *(400; 0.68)*	1.75 (2495; 0.55)

On the other hand, the smallest values of basic density can bee observed in eighth (spruce) vegetation zone (374 kg·m^{-3}), where is, however, narrow tree ring width (1.59 mm). It can be caused by production of latewood tracheids with thin cell wall, or perhaps by decreased production of latewood caused by lower average temperature during vegetation period in higher elevation. In the seventh vegetation zone (beech-spruce), on the contrary, the low value of basic density (378 kg·m^{-3}) seems to be caused by raised portion of earlywood, because the average tree ring width is big (1.76 mm).

There is significant difference between basic density in N and T edaphic category and others. Economically the most important is fifth (beech with fir) vegetation zone, that takes 30 % of the total forest area. The average value of the basic density is 414 kg·m^{-3}, and the average tree ring width is 1.81 mm. Statistically significant differences between edaphic categories can be found for M-I categories of acid series, where the values of the basic density higher, one exception is category gleyic – nutrient-poor with average value of basic density 460 kg·m^{-3}. Similar to the pattern of results of 5th vegetation zone are results of sixth (spruce with beech), where the average value of basic density is 392 kg·m^{-3} and simultaneously the highest value of the average tree ring width 1.99 mm.

DOI:10.2312/GFZ.b103-08056

Table 3: Results according edapfic categories (main value in cell is mean , first value in brackets is number of samples and second value is stand. deviation)

edaphic factor			basic density (kg.m^{-3})	tree ring width (mm)
extreme	xerothermal *(xerothermica)*	**X**		
	scrub *(humilis)*	**Z**	378.57 *(40; 35.30)*	1.49 *(40; 0.36)*
	skeletal *(saxatilis)*	**Y**		
acid	nutrient-poor *(oligotrophica)*	**M**	454.89 *(181; 36.36)*	1.22 *(181; 0.36)*
	acidic *(acidophila)*	**K**	403.19 *(429; 49.6)*	1.54 *(429; 0.64)*
	stony-acidic *lapidosa acidophila)*	**N**	427.34 *(121; 37.0)*	1.56 *(121; 0.37)*
	compacted-acid *(illimerosa acidophila)*	**I**	440.34 *(120; 41.22)*	1.65 *(120; 0.36)*
rich in nutrients	fresh, nutrient-medium *(mesotrophica)*	**S**	393.97 *(281; 41.98)*	1.87 *(281; 0.46)*
	slope (stony) nutrient-medium *(lapidosa mesotrophica)*	**F**	383.78 *(40; 43.23)*	2.29 *(40; 0.30)*
	water-deficient *(subxerothermica)*	**C**		
	nutrient-rich *(eutrophica)*	**B**	403.69 *(141; 44.29)*	2.14 *(141; 0.47)*
	limestone *(calcaria)*	**W**		
	loamy (compacted, nutrient-rich) *(illimerosa trophica)*	**H**	421.39 *(80;39.3)*	2.06 *(80; 0.38)*
enriched with humus	enriched-collurial *(deluvia)*	**D**	407.38 *(40; 45.76)*	2.08 *(40; 0.40)*
	stony-colluvial *(lapidosa acerosa)*	**A**	400.60 *(40; 26.23)*	2.15 *(40; 0.36)*
	talus *(saxatilis acerosa)*	**J**	449.97 *(20; 36.21)*	1.57 *(20; 0.45)*
enriched with water	floodplain *(alluvialis)*	**L**		
	valley *(vallidosa)*	**U**		
	mast to wet *(humida hygrophila)*	**V**	399.86 *(101; 37.40)*	2.05 *(101; 0.37)*
gleyic	nutrient-medium *(variohumida trophica)*	**O**	407.94 *(241; 40.7)*	1.95 *(241; 0.49)*
	acidic *(variohumida acidophila)*	**P**	427.07 *(162; 46.42)*	1.78 *(162; 0.47)*
	nutrient-poor (varihumida oligotrophica)	**Q**	417.21 *(180; 49.4)*	1.45 *(180; 0.44)*
water-logged	nutrient-poor, wet *(paludosa oligotrophica)*	**T**	400.31 *(60; 42.46)*	1.46 *(60; 0.36)*
	nutrient-medium, wet *(paludosa mesotrophica)*	**G**	373.34 *(120; 35.39)*	2.04 *(120; 0.51)*
peaty	nutrient-medium *(turfosa)*	**R**	379.35 *(98; 35.26)*	1.92 *(98; 0.46)*
	nutrient-poor *(turfosa)*			
mean			409.61 *(2495; 47.17)*	1.75 *(2495; 0.55)*

Conclusions

Significant influences of environment on wood formation (basic density, tree-ring width) have been proved. The highest value of basic density has been found for fourth (beech) vegetation zone and generally we can say that higher values of basic density are on stands with lower pH. Relation between tree ring width and basic density was found. To conclude, the research results of environment impact to properties of wood can improve forestry and wood industry management.

Acknowledgements

The project was financially supported by the research project of the Forest Faculty of the Mendel University in Brno, MSM 6215648902 and MZP CR VaV SP/2d1/93/07.

References

Vavrčík, H. (2002): Analýza xylému na buněčné úrovni s využitím fluorescenční mikroskopie, Disertation thesis, 145 p.

Larcher, W. (1988): Fyziologická ekologie rostlin, Academia Praha, 359 p.

Horáček, P.(1998): Fyzikální a mechanické vlastnosti dřeva I., MZLU Brno, 124 p.

Plíva, K. (1971): Typologický systém ÚHÚL, Cyklostylovaná příručka pro služební potřebu pracovníků ÚHÚL Brandýs n.L., 29 p.

Ericson, B. (1959): Mercury Immersion method for Determining the Wood Density of increment Cora Sections, *For. Res. Inst. o Sweden*, 1, p. 1-31.

Olesen, P.O. (1971): The Water Displacement Method, The Royal Veterinary and Agricultural University of Copenhagen, 18 p.

Kollmann, F. (1951) Technologie des Holzes und Holzwerkstoffe, Berlin – Gottingen – Heidelberg, 1050 p.

Forest Management Institute, (2007): Report on forestry of the Czech Republic by December 31, 2006, FMI, 128 p.

SECTION 6

ARCHAEOLOGY

DOI:10.2312/GFZ.b103-08056

Dendrochronological investigation on historical English oak (*Quercus robur* L.) in Lithuania and Latvia: problems and potential

A. Vitas[1] & M. Zunde[2]

[1] *Vytautas Magnus University, Faculty of Nature Sciences, Centre of Environmental Research, Group of Dendroclimatology and Radiometrics, Ž.E. Žilibero 2, LT-46324 Kaunas, Lithuania*

Email: a.vitas@gmf.vdu.lt

[2] *Institute of Latvian History, University of Latvia, Akadēmijas laukums 1, Rīga LV-1050, Latvia,*

Email: zunde@lanet.lv

Introduction

Investigations on historical oak wood in the West Europe enabled to construct ultra-long chronologies for different site conditions and regions and to reconstruct large-scale climate changes during the Holocene (Jansma 1995, Leuschner et al. 2000, Leuschner & Delorme 1988, Pilcher et al. 1984, Schmidt 1973, Spurk et al. 1998).

However, studies of oak tree rings in the Baltic States have so far produced very limited results. The main reason for this is the fairly rare occurrence of historical oak wood in the territory of the Baltic States. During the past two millennia, the extent of oak forest has been considerably reduced, not only because of climatic deterioration (e.g., the Little Ice Age from the 13th/14th to the 19th century), but mainly because of the rapid destruction of oak forests (clearance for agriculture of the most fertile forest lands, and the very frequent fires that followed; cutting of oak timber for shipbuilding, wood for barrels and other kinds of wood products, and for export in large quantities). Thus, the historical oak wood from the Baltic has in many cases been used for buildings, ships, furniture and works of art produced in Western European countries. Apart from this, part of the historical oak timber has been destroyed or has remained undated after being discovered in the course of archaeological excavations undertaken at the time when dendrochronological dating had not yet begun in the Baltic States.

However, in recent years it has proved possible to find historical oak wood in relatively small amounts in both Lithuania and Latvia. The aim of this work is to introduce with current results on tree rings dating of historical oak wood in the both Baltic States and to discuss the main factors limiting current achievements together with the potencies for the future investigations.

State of investigations

Dendrochronological investigations on tree rings of subfossil oaks in Lithuania began in 1968. One of the most important is collection of about 100 subfossil oak samples from Smurgainiai gravel pit – Neris riverine sediments (at present belongs to Byelorussia close to Lithuanian border) collected during the Soviet period, mainly in 1968-1972 (Vitas 2004, Битвинскас et al. 1978) (Fig. 1).

DOI:10.2312/GFZ.b103-08056

Figure 1: Sampling locations on historical oak timber in Baltic region: 1 – Smurgainiai, 2 – Vilnius, 3 – Klaipėda, 4 – Telšiai, 5 – Biržai, 6 – Riga, 7 – Seda river.

The first radiocarbon dating in the Soviet period was performed in Ural Pedagogical Institute and Tbilisi University (Битвинскас et al. 1978). Part of the samples (cross-sections) was re-dated at the group of Radiocarbon in the Botanical Institute of Lithuania and later by the Laboratory of Dendroclimatochronology by using counter LSC - 1220 "Quantulus”. Dendrochronological dating enabled to construct 10 floating chronologies comprising of approximately 100 samples (Fig. 2). Oaks from the oldest chronology grew approximately 5300-5500 BC. The longest gap between chronologies is around 2800-1380 BC. Bigger number of trees in chronologies is directly connected to wider tree rings, e.g. in 4700-3800 BC and 700BC-300 AD. The chronology from the youngest period is absolute dated to 778-1325 AD against oak chronology from Eastern Pomerania (Tomasz Wazny).

Bog oaks are also found in northern Lithuania in the past, but the number of wood samples obtained is small compared to material from Smurgainiai (Fig. 1). Six oak wood samples were found in peatbog near Biržai (Pukienė 2003a, 2003b, 2004). Dendrochronological dating enabled to construct two floating chronologies dated by radiocarbon to: 4400-4600 BC and 5000-5100 BC. Chronology of 4400-4600 BC approximately match the dates of the second oldest floating chronologies from Smurgainiai. Oak sample found in bog near Telšiai is much younger (radiocarbon dated to 3300-3500 BC) (Fig. 2).

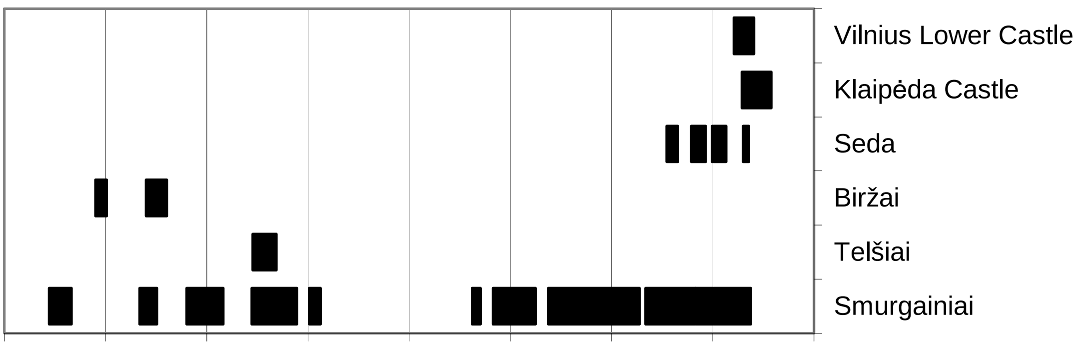

Figure 2: Historical chronologies of oak tree-rings derived from findspots in Lithuania and Latvia.

DOI:10.2312/GFZ.b103-08056

In Latvia, in contrast to Lithuania, most such finds are ancient oaks that had died naturally. The findspots of historical oak wood in the area of present-day Latvia are very widely dispersed. At several locations in Latvia, trunks of various-sized oaks that had died naturally have been found in peat deposits in bogs and at the sites of former river meanders. Geological and radiocarbon dating has shown that some of the oldest oaks grew at 6000–7000 BP. These have not been dendro-dated so far, mainly because there has not been sufficient interest or funding.

Exceptional in this regard are: (i) oak trunks from river Seda (northern Latvia) dated by radiocarbon to 500-1300 AD (Fig. 1, 2). This age is almost covered by the youngest oak chronology from Smurgainiai (778-1325 AD) and (ii) oak piles discovered in the second half of the 20th century in the 13th–14th century revetments along the Rivers Daugava and Rīdzene in Riga (Fig. 1). Unfortunately, archaeologists have so far not taken an interest in dating the trunks of oaks that had died naturally, and they are too young to shed light on topical issues in geology. Thus, the dating of these historical oak trunks has so far not been financially supported, and they have remained undated. It must be admitted that, along with the loss of these oak trunks, we have unfortunately lost information that would be useful for reconstructing past climatic conditions and answering questions relating to dendroprovenancing.

Discussion and Conclusions

Due to anatomical features, comparatively long age of trees and prevalence in bogs, and river sandy deposits wood of English oak is perfect source for long-term chronologies in West Europe. Because of sparse number of findings with oak wood in Lithuania the radiocarbon dating have gained greater importance in dendrochronological investigations compared to Western Europe. The absolute dating of oak samples from older periods is impeded by available small number of dated oak chronologies. One of the most important is chronology compiled by Tomasz Wazny from Eastern Pomerania (725-1985 AD). This chronology was successfully used for dating the youngest chronology from Smurgainiai sandy river deposits. In the Soviet period for a long existed incorrect opinion (probably because of the lack of contacts with western scientists) that pine wood is much more suitable in dendrochronological research, while oak wood is of lower importance. Therefore, oak wood from bog excavations sometimes was left at the findspots.

Oak chronologies from Smurgainiai might be used for absolute dating of historical oak trunks found in the Baltic area in the future. There is high chance that oak material from Seda River (northern Latvia) may be successfully dated against Smurgainiai chronologies. Therefore, dendro-dating of oak samples from Seda River seems to be promising for the future.

Dating of oak tree rings from buildings is more promising because of available reference chronologies compared to older material from bogs. Unfortunately, there is also very little oak wood preserved in standing structures from the Historical Era. In large measure, this can be explained in terms of the rapid reduction of oak forest during the 2nd millennium AD. In the past, a considerable quantity of oak timber was also exported to Western Europe. A proportion of the structural timbers of oak recovered in the course of earlier archaeological

DOI:10.2312/GFZ.b103-08056

excavation were not dendro-dated. The chances are promising that the study of oak wood from buildings will permit us to compile chronologies by extending the series based on living oaks. Since the stocks of historical oak wood are gradually being lost, there is a pressing need for dendrochronological study of this material.

References

Jansma, E. (1995): RemmembeRINGs. The development and application of local and regional tree-ring chronologies of oak for the purposes of archaeological and historical research in the Netherlands. PhD dissertation. University of Amsterdam. *Nederlanse Archeologische Rapporten (NAR)*, 19, 149 p.

Leuschner, H.H., Delorme, A. (1988): Tree-ring work in Goettingen – Absolute oak chronologies back to 6266 BC. *Pact*. 22: 123-131.

Leuschner, H.H., Spurk, M., Baillie, M., Jansma, E. (2000): Stand dynamics of prehistoric oak forests derived from dendrochronologically dated subfossil trunks from bogs and riverine sediments in Europe. *Geolines*, 11: 118-121.

Pilcher, J.R., Baillie, M.G.L., Schmidt, B., Becker, B. (1984): A 7272-year tree-ring chronology for western Europe. *Nature*, 312: 150-152.

Pukienė, R. (2003a): Analysis of subfossil bog oaks found in the North Lithuania. *Abstracts of the International Conference Eurodendro 2003*. Obergurgl. University of Innsbruck. P. 74.

Pukienė, R. (2003b): Sub-fossil oak timbers from the Mid Holocene as an evidence for Lithuanian forest history. *Baltic Forestry*, 9 (2): 71-75.

Pukienė, R. (2004): Iš Lietuvos ąžuolynų istorijos: prieš 6,5 tūkstantmečio augusių ąžuolų medienos tyrimas. *Dendrologia Lithuaniae*, 7: 99-107.

Pukienė, R., Ožalas, E. (2007): Medieval oak chronology from the Vilnius Lower Castle. *Dendrochronologia*, 24: 137-143.

Schmidt, B. (1973): Dendrochronologische untersuchungen an Eichen aus der Kölner Bucht und dem Were-Weser-Gebiet. *Archäologischs korrespondenzblatt*. 3: 155-158.

Spurk, M., Friedrich, M., Hofman, J., Remmele, S., Frenzel, S., Leuschner, H.H., Kromer, B. (1998): Revisions and extensions of the Hohenheim oak and pine chronologies of the younger Drias / Preboreal transition. *Radiocarbon*, 40(3): 1-10.

Vitas, A. (2004): Dendrochronological investigation on oak timber from gravel pit of Smurgainiai, Western Byellorussia. *Abstracts of the International Conference Eurodendro 2004*. Rendsburg: 50.

Битвинскас, Т., Дергачев, В., Даукантас, А., Лийва, А., Суурман, С., Шулия, К. (1978): Использование радиоуглеродного метода датирования в целях создания сверхдолгосрочных дендрошкал [Application of radiocarbon dating method for construction of supra-long chronologies]. Условия среды и радиальный прирост деревъев (ed. T. Bitvinskas). Kaunas: Lithuanian Institute of Botany: 51-55.

Building of the oak standard chronology for the Czech Republic

M. Rybníček[1], T. Kyncl[2], V. Gryc[1], E. Přemyslovská[1] & H. Vavrčík[1]
[1] Mendel University of Agriculture and Forestry Brno, Faculty of Forestry and Wood Technology, Department of Wood Science, Zemědělská 3, 613 00 Brno, Czech Republic
[2] DendroLab Brno, Eliášova 37, 616 00 Brno, Czech Republic
Email: michalryb@email.cz

Introduction

The correct dating of a sample depends on the used standard chronologies. These are created for each tree species individually by continuous overlapping of tree ring sequences towards the past. Individual standard chronologies differ by the area and by the time interval for which they are usable. The created standard chronology reflects the climate of the certain period at maximum and the local growth conditions of individual included trees at minimum (Rybníček 2007).

The overwhelming majority of historical wooden constructions in the Czech Republic are made of soft wood; hard wood (almost exclusively oak wood) appears only rarely. However, there are some types of constructions (e.g. bell stools, bridge piers and harbour equipment, well timbering and waste traps) in which oak wood dominates. Oak wood is more often found in archaeological findings. The availability of the standard chronology for oak wood dating is as important as the already created standard chronologies for coniferous tree species (Rybníček et al. 2004).

Material and methods

The taking, processing and dating of samples have been carried out in accordance with the standard dendrochronological methods (Cook & Kairiukstis 1990). The data used to create the Czech oak standard chronology were obtained from subfossil trunks, archaeological findings, historical constructions and living trees from the entire area of the Czech Republic (Fig. 1).

Figure 1: The map of locations of samples used to create the standard chronology.

We can divide them into three groups. The base of the oak standard chronology for the CR was created in 1998–2001 by Jitka Vrbová-Dvorská in the Institute of Archaeology of the Academy of Sciences of the CR. The standard chronology was named CZGES 2001 and it includes the data from archaeological excavations – especially the data obtained through the archaeological research in Mikulcice, at Prague Castle and during the research of the Breclav castle tower (Dvorská 2001). The second group consists of the data provided by the Institute of Botany of the Academy of Sciences of CR (Tomáš Kyncl, Josef Kyncl). These data come from the material from historical constructions and ruins of significant castles (e.g. Karlstejn, Ryzmburk, Buchlov, Bezdez, Valdek). The last part of the data used to create the standard chronology comes from the Dendrochronological Laboratory of the Department of Wood Science of Mendel University of Agriculture and Forestry Brno (Michal Rybníček). The data were mainly obtained in archaeological findings in the area of Brno and its surroundings (e.g. houses in Mecova street, Namesti svoboty, Cacovice weir and Modrice).

Tree-ring curves of individual trees are influenced by the growth trend. The trend is to a certain extent individual for each tree and that is why it weakens the demanded common signal (Schweingruber 1996). Therefore, the individual tree-ring curves have been detrended. To create the standard chronology, they were exported from PAST 32 to ARSTAN application (Grissino–Mayer et al. 1992), where they were detrended.

To remove the age trend, the detrending was carried out in two steps (Holmes et al. 1986). First, the negative exponential function or linear regression curve, which best express the change of growth trend with age, were used in dependence on the value of the determination index (Fritts et al. 1969; Fritts 1963). Other possible deviations of thickness increment values conditioned not by the climate but brought about by the competition or interventions of foresters were balanced using the cubic spline function (Cook & Peters 1981). The chosen length of the spline function was 32 years. Thanks to the use of the spline function, the accidental variability in tree-ring sequences was removed (Cook & Kairiusktis 1990). The resulting index tree-ring series shows relatively high values of autocorrelation (the dependence of a tree-ring width on the widths of the previous tree-rings).

Then, the data were exported from Arstan to PAST 32 and the oak standard chronology for the CR was created out of well-synchronizable curves.

Four locations were chosen to evaluate the necessity of detrending or non-detrending of tree-ring series and the creation of standard chronologies out of detrended tree-ring series. The tree-ring sequences of samples taken in these locations were measured. Then the tree-ring curves, both detrended and non-detrended, were created and compared with the detrended and non-detrended standard chronology in PAST 32. As the next step, the regression analysis of the data sets was carried out in the Statistica 7.1 application and the results were compared, especially the correlation coefficient, the confidence and prediction intervals. For the comparison normed values were used. The norm was defined by the highest value of the selected file.

Results

191 average tree-ring series were used to create the oak standard chronology, which was named CZGES 2005. It covers the period from 462 A.D. to 2004 A.D. (Fig. 2).

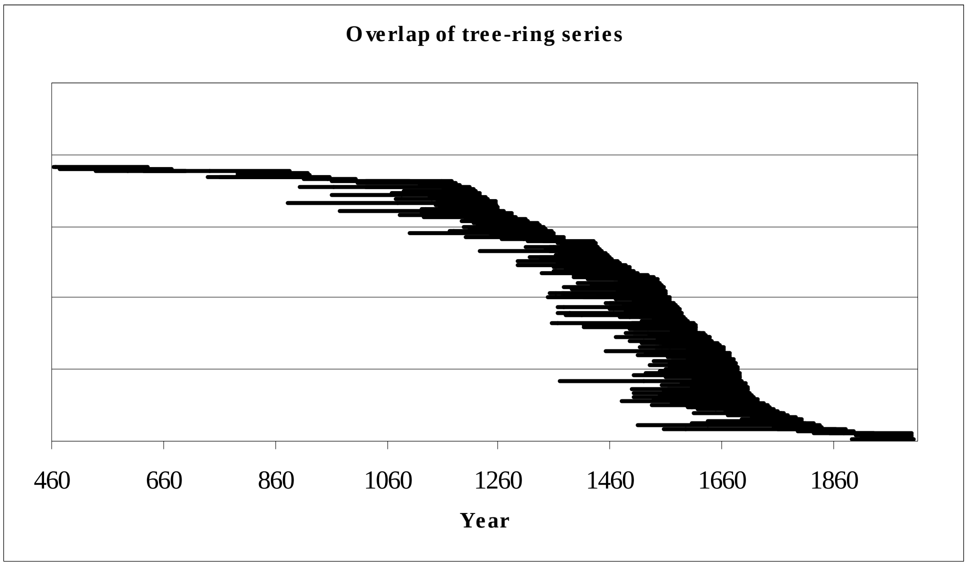

Figure 2: The range of individual average tree-ring series used to create the standard chronology of oak CZGES 2005

Two versions of the oak standard chronology CZGES 2005 were created – the standard chronology created out of detrended tree-ring series and the standard chronology created out of non-detrended tree-ring series (Fig. 3).

When these two versions of standard chronology were compared, the t-test values proved to be higher than ninety; however, there are some differences, especially in the areas where the standard chronology consists of a lower number of average tree-ring series. This is also confirmed by the value of Gleichläufigkeit being 91 %.

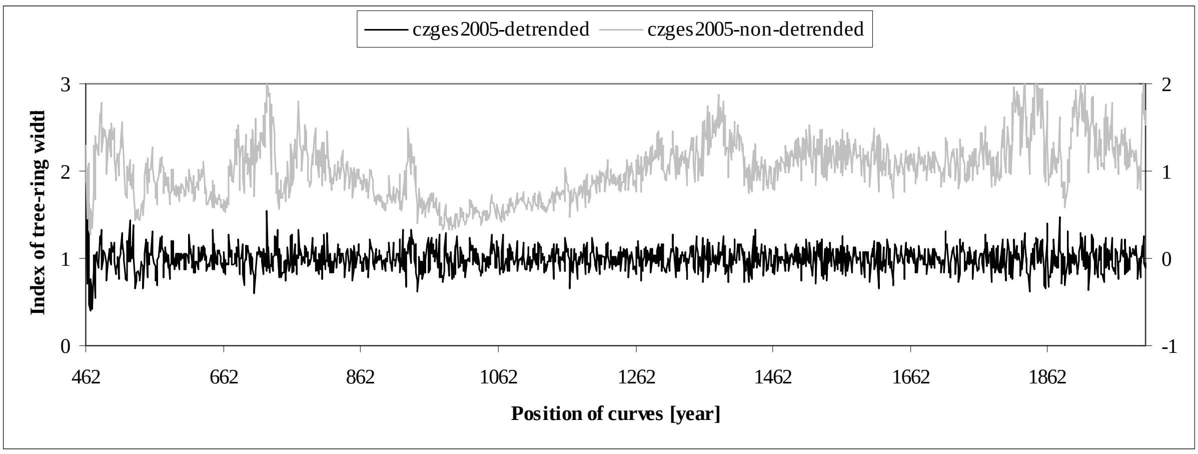

Figure 3: The synchronization of the detrended standard chronology CZGES2005 (black) with the non-detrended standard chronology CZGES 2005 (grey) for the period from 462 A.D. – 2004 A.D.

There were used oak standard chronology for Brandenburg (Heußner & Westphal 1998), oak standard chronology for South Germany (Becker 1981), oak standard chronology for Eastern Austria (Wimmer & Grabner 1998) and oak standard chronology for Silesia (Krapiec 1998) for comparison with the newly created standard chronology CZGES 2005. The statistical data show very high values. The highest values of statistical indicators appear when the standard chronology CZGES 2005 is compared with the East-Austrian standard chronology OstOestQP, the t-values being 24 and 25 and the Gleichläufigkeit 75 % with the overlap of 807 years for the detrended standard chronology and the t-values being 23 and 24 and the Gleichläufigkeit 73 % for the non-detrended standard chronology. The lowest values of statistical indicators appear when the standard chronology CZGES 2005 is compared with the Brandenburg standard chronology Branges, the t-values being 14 and the Gleichläufigkeit 65 % with the overlap of 1529 years for the detrended standard chronology and the t-values being 13 and the Gleichläufigkeit 64 % for the non-detrended standard chronology (Tab. 1).

Table 1: The statistical comparison of CZGES 2005 with the surrounding European standard chronologies of oak (black values for the detrended standard chronology and grey values for the non-detrended standard chronology)

	Standard chronology							
	Brandenburg (Branges)		South Germany (Sued2ges)		Eastern Austria (OstOesQP)		Silesia (DSL1)	
t-value according to Hollstein	14	13	17	16	24	23	20	18
t-value according to Baillie & Pilcher	14	13	18	17	25	24	19	18
Gleichläufigkeit [%]	65	64	66	65	75	73	68	67
Overlap [years]	1529		1489		807		1215	

To verify the validity of the newly created standard chronology CZGES 2005 and to compare the detrended and the non-detrended standard chronologies, samples from four locations were chosen – two archaeological locations in Namesti svobody in Brno (A30/05 a A93/05), research at 16 Orlí street and the construction of the Olsovec pond outlet in Jedovnice. Only the results from the first archaeological location in Namesti svobody (A30/05) are presented as an example; however, the results from the other locations were very similar.

When the dated curve overlaps the standard chronology by at least sixty tree-rings, the Student's critical value of t-division with 0.1 % significance level is 3.46 (Šmelko – Wolf 1977). Values of t–tests are much higher than 3.46, which proves the high reliability of the dating. The highest t-test values are achieved when the detrended and non-detrended average tree-ring curves are compared with the detrended standard chronology. When the average tree-ring curve is compared with the non-detrended standard chronology, the values of t-tests are lower. The highest curve Gleichläufigkeit is achieved when the non-detrended average tree-ring curve is compared with the detrended standard chronology (Tab. 2). The correctness of dating is also confirmed by the agreement of the standard chronology with the average tree-ring curve at most extreme values (Fig. 4).

Table 2: The results of the correlation of the detrended and the non-detrended average tree-ring curves with the detrended and the non-detrended Czech oak standard chronology CZGES 2005.

Standard chronology	*t*-value according to Baillie & Pilcher	*t*-value according to Hollstein	Gleichläufigkeit [%]	Overlap [years]	Year
Náměstí svobody A30/05 – 400 non-det.					
CZGES 2005 non-det.	6.37	7.6	72	94	1241
CZGES 2005 det.	6.93	8.53	75	94	1241
Náměstí svobody A30/05 – 400 det.					
CZGES 2005 non-det.	6.39	7.71	65	94	1241
CZGES 2005 det.	6.92	8.62	69	94	1241

Figure 4: The synchronization of the average detrended and non-detrended tree-ring curves with the detrended Czech oak standard chronology CZGES 2005

The confidence and mainly the prediction intervals of detrended tree-ring curves are considerable narrower than those of the non-detrended ones. The regression curve of detrended normed values of tree-ring curves is of a very similar character as the calibration curve. On the other hand, the regression curve of non-detrended normed values of tree-ring curves is of a very different character in comparison with the calibration curve. There is a significant, ever-increasing deviation from the calibration curve at the regression curve of non-detrended normed values. The increase of the deviation of the regression curve of detrended normed values of tree-ring curves is gradual and the maximum value of the deviation is negligible in comparison with non-detrended data (Fig. 5, fig. 6). The significance level of the regression model of detrended tree-ring curves is considerably higher than of non-detrended tree-ring curves (Tab. 3).

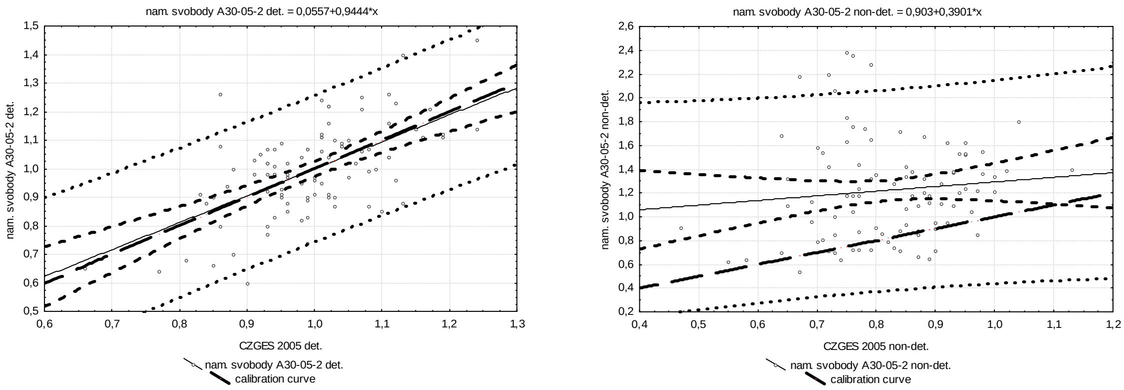

Figure 5: The comparison of the dependence of the progress of detrended and non-detrended tree-ring curves regression function on the detrended and non-detrended standard chronologies with the calibration curve (the prediction and confidence intervals of the function are marked in the graph).

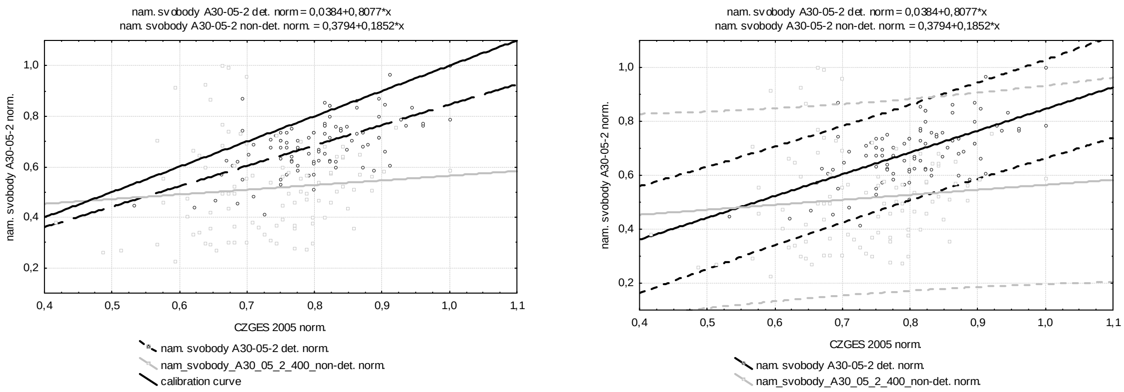

Figure 6: The comparison of the regression functions of the dependence of the detrended tree-ring curve on the detrended standard chronology with the dependence of the non-detrended tree-ring curve on the non-detrended standard chronology. The prediction intervals of the regression function (right) and the calibration curve (left) are marked in the graph.

Table 3: The results of the regression analysis of the values of detrended and non-detrended average tree-ring curves with the detrended and non-detrended Czech oak standard chronology CZGES 2005 (R – correlation coefficient, p – model – regression model significance level, β – regression model linear dependence slope).

		R	p – model	β
CZGES 2005 non-det.	A30/05 – 400 non-det.	0.10617385	0.308439	0.106
CZGES 2005 det.	A30/05 – 400 det.	0.60490529	0	0.605

Discussion and Conclusions

The main aim of this work was to create a national oak standard chronology. The CZGES 2005 standard chronology, which functions as a oak standard chronology for the Czech Republic, has been made up on the basis of 191 average tree-ring series and covers the periods from 462 AD – 2004 AD. This standard chronology correlates perfectly with the standard chronologies developed in the surrounding countries. So far there has been no

DOI:10.2312/GFZ.b103-08056

single national oak standard chronology that would encompass the oak data gathered all over the Czech Republic, and so it has been very difficult to process any oak sample files. Now that the oak standard chronology is available, dating of the oak samples collected on the territory of the Czech Republic can be done with a much greater precision. The standard chronology enables us to reflect - with the highest possible precision - the effects of the environment in which a particular tree has grown and which are typical of its particular location. Moreover, it will be possible to date those samples that due to the missing standard chronology have not been dated so far. Currently, the standard chronology enables dating of a vast majority of the oak wood found during the archaeological excavation and exploration works carried out in the historic buildings in the Czech Republic.

The CZGES 2005 oak standard chronology has filled a gap in the European network of oak standard chronologies. The standard chronologies should be used not only in the countries of their origin but also in the adjacent regions where the historic works of art were frequently exported (Krapiec 1998).

In addition to the aim stated above, the study was focused on the comparison between the detrended and non-detrended standard chronologies. The differences established between the detrended and non-detrended standard chronology have shown only too clearly how important it is to develop the detrended standard chronologies. The highest values of the t-test were achieved when comparing the detrended or non-detrended average ring curves only and exclusively with the detrended standard chronology. Similarly, the highest percentage of the curve Gleichläufigkeit was always established in comparison with the detrended standard chronology. The confidence and, more importantly, the prediction intervals of the detrended ring curves are considerably shorter than those of the non-detrended ones. The regression curves of the detrended standardised values of the ring curves are more similar to the calibration curve. The significance level of the regression models in the detrended ring curves is notably higher than in the case of the non-detrended ring curves.

All data used for the creation of the oak standard chronology are available in the database of dated objects, which is regularly updated and accessible on the web site www.dendrochronologie.cz.

There is only one way to prolong the existed standard chronology and that is dendrochronological dating of subfossil wood.

Acknowledgements

The project was prepared within a research plan of LDF MZLU in Brno, MSM 6215648902 and the CR Grant Agency 404/08/P367.

References

Becker, B. (1981): Fällungsdaten römischer Bauhölzer anhand einer 2350 jährigen süddeutschen Eichen Jahrringchronologie. Fundberichte aus Baden-Württ. 6: 369-386.

Cook, E.R., Kairiukstis, L.A. (1990): Methods of Dendrochronology – Applications in the Environmental Sciences. Kluwer Academic Publisher and International Institute for Applied Systems Analysis, Dordrecht, Boston, London: 394.

Cook, E.R., Peters, K. (1981): The smoothing spline: a new approach to standardizing forest interior tree–ring width series for dendroclimatic studies. *Tree Ring Bulletin 41*: 45–53.

Dvorská, J. (2001): 1462 Years Long Oak Chronology for the Czech Republic Area, *Book of abstracts, EuroDendro 2001*, Gozd Martuljek, Slovenia: 41.

Fritts, H.C., Mosimann, J.E., Bottorff, C.P. (1969): A Revised Computer Program for Standardizing Tree – Ring Series. *Tree Ring Bulletin 29*: 15 – 20.

Fritts, H.C. (1963): Computer programs for tree–ring research. *Tree–ring Bulletin 25 (3/4)*: 2-7.

Grissino-Mayer, H.D., Holmes, R., Fritts, H.C. (1992): International tree–ring data bank program library. Version 1.1. Laboratory of Tree–Ring Research, University of Arizona, Tucson.

Heußner, K.U., Westphal, T. (1998): Dendrochronologische Untersuchungen an Holzfunden aus frühmittelalterlichen Burgwällen zwischen Elbe und Oder: In: J. Henning and A. T. Ruttkay (Eds.), Frühmittelalterlicher Burgenbau in Mittel- und Osteuropa, Bonn: 223-235.

Holmes, R.L., Adams, R.K., Fritts, H.C. (1986): Tree–Ring Chronologies of Western North America: California, Eastern Oregon and Northern Great Basin with Procedures Used in the Chronology Development Work Including Users Manuals for Computer programs Cofecha and Arstan. – Chronology Series VI. Laboratory of Tree – Ring Research, University of Arizona, Tuscon, AZ, USA: 50-56.

Krapiec, M. (1998): Oak dendrochronology of the neoholocene in Poland, *Folia quaternaria 69*, Kraków: 5–133.

Rybníček, M. (2007): Dendrochronologické datování dřevěných částí historických staveb, archeologických vzorků a výrobků ze dřeva – sestavení národní dubové standardní chronologie. Disertační práce, MZLU v Brně: 111.

Rybníček, M., Kyncl, T., Vrbová, J. (2004): Oak standard chronology in the Czech Republic, *Abstracts EuroDendro 2004*, Rendsburg: 42–43.

Schweingruber, F.H. (1996): Tree Rings and Environment Dendroecology. Birmensdorf, Swiss Federal Institute for Forest, Snow and Landscape Research, Bern, Stuttgart, Vinna: 609.

Šmelko, Š., Wolf, J. (1977): Štatistické metódy v lesníctve. Príroda: 330.

Wimmer, R., Grabner, M. (1998): Dendrochronologie – heute, Standardchronologien in Österreich als Basis für die dendrochronologische Datierung, Archäologie Österreichs 9, 79-85.

DOI:10.2312/GFZ.b103-08056

Dating of wooden shelters in Polish High Tatras - tree rings records of the shepherding history in Carpathians

M. Opała & R.J. Kaczka
Faculty of Earth Science, University of Silesia, Będzińska 60, Sosnowiec 41-200, Poland
Email: magdaopala@hotmail.com

Introduction

Tatras is one of the main regions in Carpathian arc where seasonal pasturing on meadows located above timberline has been developed since 16th century. Over a period of centuries, Wallachian shepherds moved across mountains permanently transforming the natural environment, economy and culture of the Carpathians (Hołub-Pacewiczowa 1931, Dobrowolski 1970). In many locations, new openings for pastures were established and the treeline was driven back as a consequence. In this paper, the results of the systematic dating of shelters, the first project of this kind in the Tatras, are presented. Although shelters are located in many parts of the Carpathian Arc (Western Tatra Mts., Gorce Mts., Beskid Żywiecki Mts., Beskid Mały Mts.), those from High Tatras region are the most numerous and well-known for the historical and cultural value.

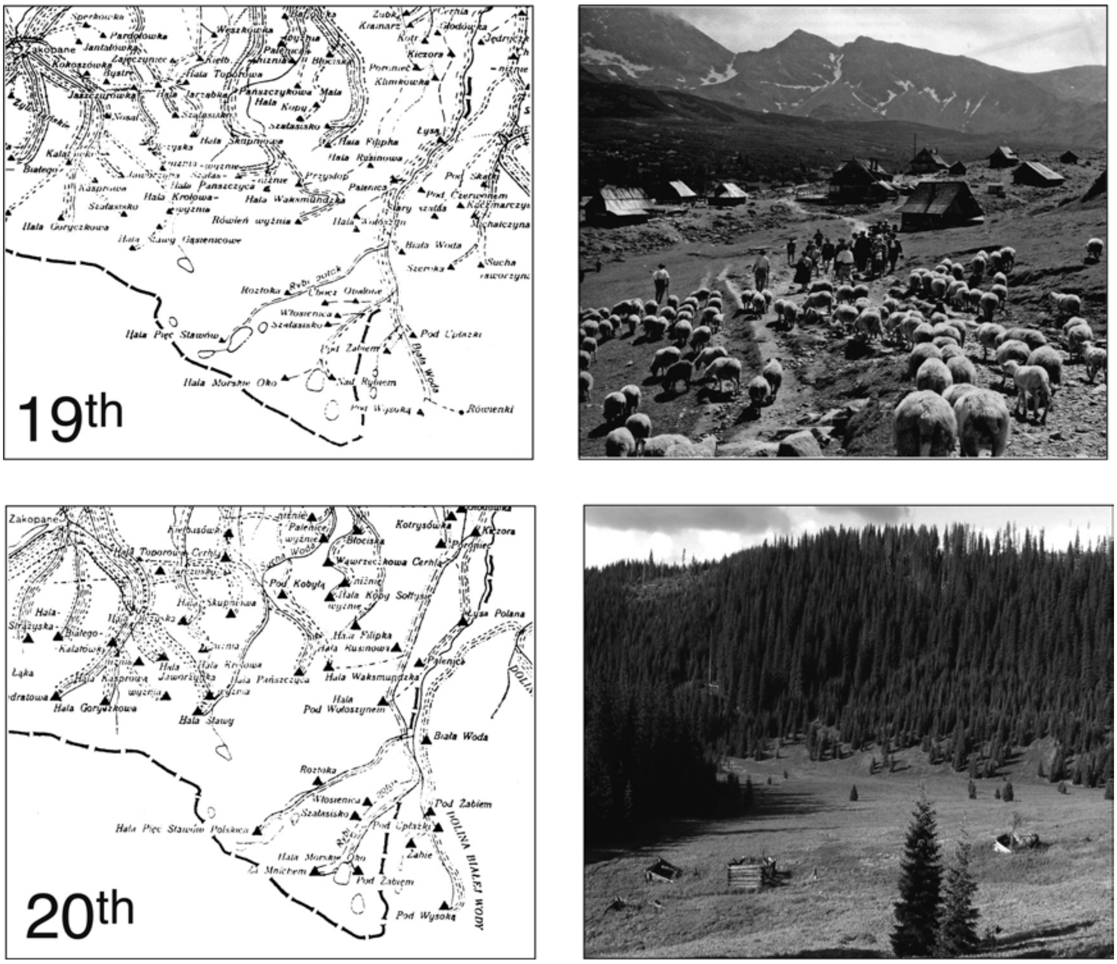

Figure 1: Changes of shelters distribution in High Tatras during 19th and 20th centuries.

DOI:10.2312/GFZ.b103-08056

Lately studies on the highest preserved remote shepherds' architecture have a special importance. Despite the fact that in 1978 High Tatra's wooden shelters were accepted as monuments of cultural heritage, the number of them has decreased four times in the last century (Fig. 1), mainly as a result of lack of proper maintenance. Shepherds' buildings are no more used since pasturage in the Tatra National Park became restricted

Material and methods

In total, 26 shelters from 10 glades (from elevations 1000 - 1900m a.s.l.) were investigated (Tab. 1). Standard techniques for sampling and dating of historical buildings were used (Ważny 2001). Approximately 10 samples were extracted from each shelter, though the number of core samples varied from 3 to 17, due to differing range of timber preservation. Cores were taken from both walls and roofs. Beams with bark and high number of rings were predominantly chosen for sampling. The wood species identification revealed that only norway spruce (*Picea abies* K.) has been used for construction of studied buildings. Hence the existing 400 years long spruce chronology (Kaczka & Büntgen 2006, Büntgen et al. 2007) was employed for cross-dating. Dating was carried out by visual cross-dating and statistically verified using COFECHA program. The criteria of dating depended on series length and value of correlation coefficient. Two conditions were recognized as necessary for confident dating (Cofecha output file):

1) >75 rings, cc=0,3281, max. 1 possible problem
2) 50-75 rings, cc=0.5, 0 possible problem

Cross-sections with less then 50 rings could not be dated with confidence.

Table 1: Geographical settings and amount of analysed samples.

Glade name	Number of shelters	Number of samples	Altitude [m a.s.l.]	Type of the forest
Olczyska	2	37	1035 - 1110	Lower montane forest
Jaworzynka	4	60	1065 - 1195	Lower and upper montane forest
Rusinowa	2	24	1180 - 1300	upper montane forest
Kopieniec	7	66	1210 - 1250	upper montane forest
Królowa	2	25	1230 - 1270	upper montane forest
Roztoka	1	4	1300	upper montane forest
Pańszczyca	1	14	1360 - 1440	upper montane forest
Waksmundzka	2	23	1364 - 1400	upper montane forest
Gąsienicowa	4	52	1480 - 1540	upper montane forest
Dol. Pięciu Stawów	1	5	1625 - 1900	Dwarf pine belt

Results and discussion

From all 310 samples, 57% have been successfully dated. The relatively low number of rings per sample and the condition of wood were the main problems of accurate cross-dating. The oldest wood belongs to one of the shelters located in Polana Kopieniec and dated back to 1756. Three more objects from the 18th century were dated. The variety of dates for individual shelters suggests that repairs and renovations occurred often during their lifetime. Differences in buildings age have been found in spite of their similar appearance (Fig. 2), the architectural form being inherited from a tradition that lasted at least two centuries

Figure 2: Differences of the age of the oldest beams dated within one glade (Kopaniec Glade 1230m a.s.l.)

Dendrochronological results correspond with historical documents about the evolution of the shepherding in Tatras. First mention about that activity occurred in 14th-15th centuries, but the oldest wood samples have been dated back to the 18th century. Tree ring records of shelters foundation and repairing can be linked with some important historical events (Fig. 3):

1. Period of industrial revolution can be noticed as decline of sheep farming (the emigrations from Tatra and Podhale region, decrease of wool prices as a result of competition with wool imported from Australia),
2. During First and Second World War, economical crises and restriction in emigration stimulated pasturing as a source of basic supplements (wool, milk, meat),
3. The establishment of the Tatra National Park and restriction of pasturing due to protection of natural remains of high-mountain environment in 50s and 60s of 20th century,
4. Extensive pasturing and renovations of shelters as a preservation of cultural heritage organised by Tatra National Park and The Department of Monuments Conservation of Tatra Museum.

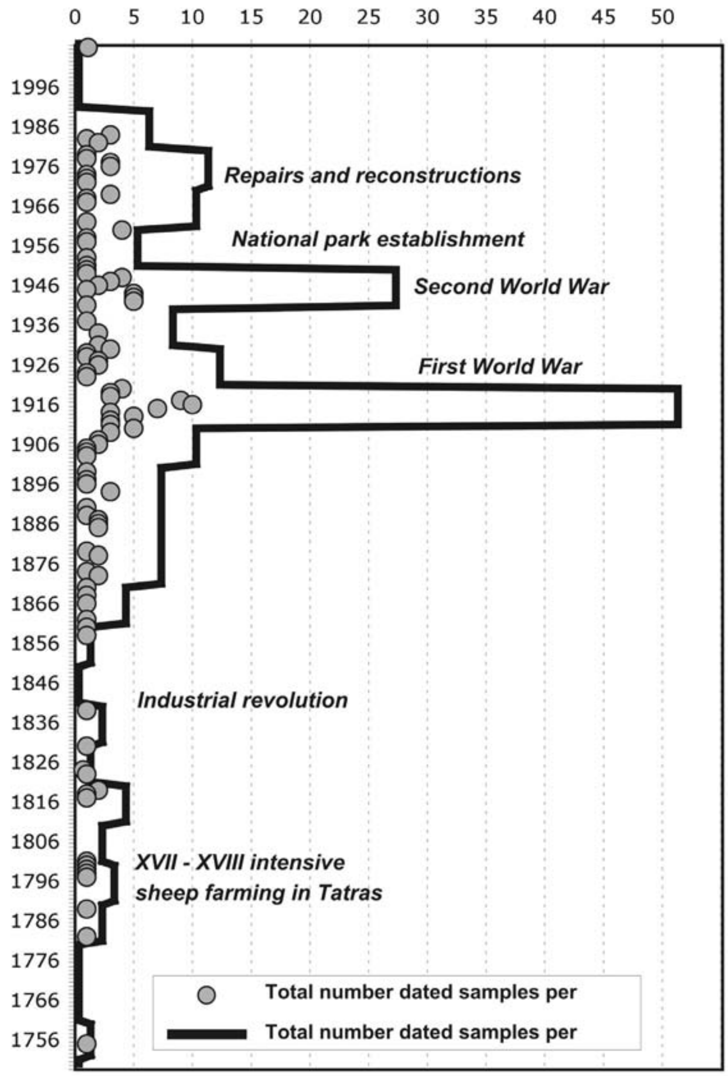

Figure 3: Tree-ring records of shelters foundations and renovations as proxy of human activity in high-mountain environment during last 250 years.

Eight local chronologies from historical wood was constructed and compared with master chronology (Fig. 4). The longest chronology was constructed for Kopieniec Glade spanning 1681-1968 period (1716 -1968 after truncation < 5 series). To assess the origin of timbers used for shelters construction, the relationship between elevation of glades and correlation between site chronologies and master chronology was studied. The master chronology was constructed based on 477 individual series from several timberline sites within entire Tatras (Kaczka & Büntgen 2006, Büntgen et al. 2007). The correlation coefficient varied from 0.413 for Rusinowa Glade up to 0.780 for Waksmundzka Glade. A significant relationship between sites elevation and correlation against master chronology is found (r^2=0.63, p=0.034) after excluding Rusinowa Glade, the shortest chronology. The very complex situation of land possession in this region suggested that for some sites, wood could arrive from other, including lower, locations. The comparison between dated beams and master, high-elevation chronology, confirm use of local timbers. The samples from historical wood of known provenancy can be included to regional chronology and improve its statistical parameters as was reported from high-elevation sites of Loetschental, Alps (Büntgen et al. 2006).

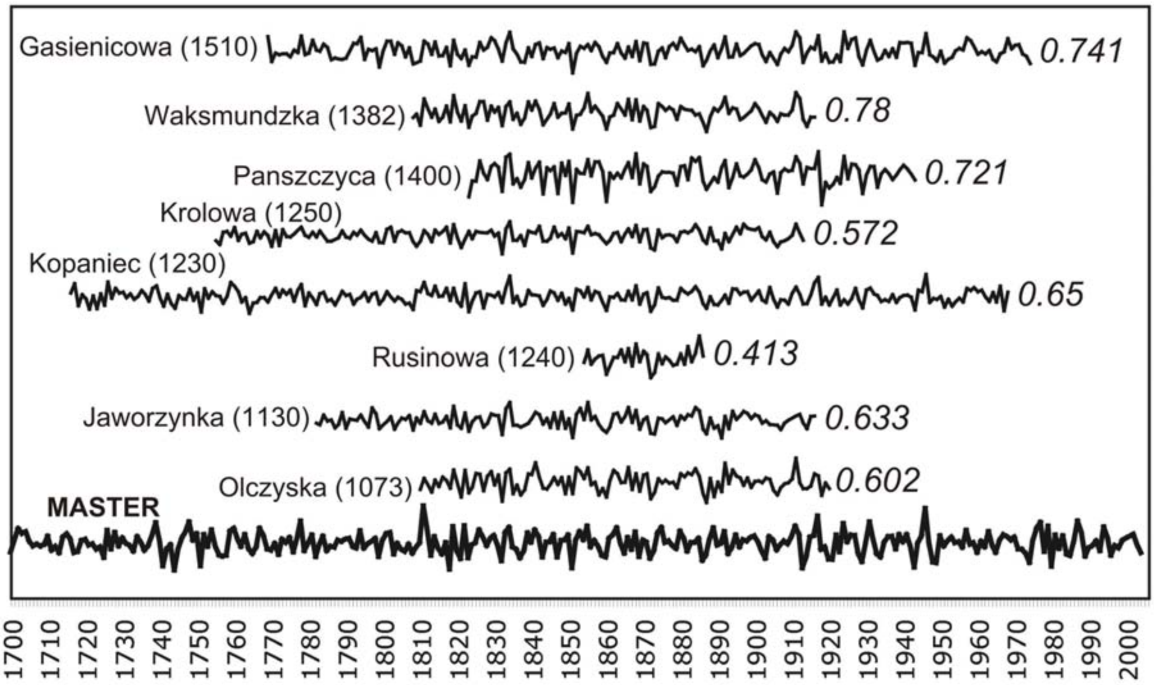

Figure 4: Local chronologies constructed using historical wood from 8 locations. The significant relationship between site elevation (m. a.s.l., in brackets) and correlation coefficient (italic) with high-elevation master chronology proves local origin of the wood.

Conclusions

1. Results obtained from dendrochronological dating have shown that preserved shelters are older (18th century) than previously evaluated by ethnological investigations (19th - 20th century) (Szafer 1966).
2. Though tree-ring dates are limited to the period of last 250 years and vary within each building, the general age structure reveals a significant relation to particular stages of expansion and restraint of human activity in the High Tatras.
3. Tree-rings proxies of past events are, in some cases, more pronounced than other historical documents.
4. Further analyses of relationships with climate dynamics and historical events can be provided for better understanding of natural and anthropogenic changes of alpine environment in the Carpathians.

References

Büntgen U, Esper J, Bellwald I, Kalbermatten H, Frank DC, Freund H, Schmidhalter M. Bellwald W, Neuwirth B (2006): 700 years of settlement and building history in the Lötschental/Valais. Erdkunde 60: 96-112.

Büntgen, U., David, F.C., Kaczka, R.J. Verstege, A., Zwijacz-Kozica, T. & Esper, J. (2007): Growth/climate response of a multi-species tree-ring network in the Western Carpathian Tatra Mountains, Poland and Slovakia. Tree Physiology 27: 689-702.

Kaczka, K.J., Büntgen U. (2006) Spatial autocorrelation and growth/climate response of a high elevation spruce network along the Carpathian arc. *TRACE* 5: 103-112

Dobrowolski, K. (1970): Studia nad kulturą pasterską w Karpatach Północnych, Typologia wędrówek pasterskich od XIV do XX wieku. In: Antoniewicz., W. Studia Podhalańskie oraz bibliografia Tatr i Podhala, Pasterstwo Tatr Polskich i Podhala Tom VIII. Polska Akademia Nauk: 98-122

Hołub-Pacewiczowa, Z. (1931): Osadnictwo pasterskie i wędrówki w Tatrach i na Podtatrzu. Polska Akademia Umiejętności: 418.

Szafer, T.P. (1966): Tatrzańskie bacówki pasterskie. In: Antoniewicz., W. Architektura i zabudowa pasterska Tatr Polskich i Podhala oraz góralska sztuka plastyczna, Pasterstwo Tatr Polskich i Podhala Tom VI. Polska Akademia Nauk: 91-117.

Ważny, T. (2001): Dendrochronologia obiektów zabytkowych w Polsce. Muzeum Archeologiczne w Gdańsku: 137.

DOI:10.2312/GFZ.b103-08056

SECTION 7

NEW APPLICATIONS

DOI:10.2312/GFZ.b103-08056

Application of multivariate cross-dating to historical timbers with less than 50 tree-rings from the Albrechtsburg Castle and the Meißen Cathedral, Saxony

J. König, B. Günther & C.T. Bues

Institute for Forest Utilization and Forest Technology, Chair for Forest Utilization, Technische Universität Dresden

Email: koenig@forst.tu-dresden.de

Introduction

An important branch of dendrochronology is the dating of historical wood samples coming from the restuction of buildings and archaeological activities. In many cases only few tree-rings can be used for dating due to the limited sample size. Samples with less than 50 tree-rings can often not be dated with required statistic accuracy by the conventional univariate cross-correlation of tree-ring width time series (Cramer and Eissing 1996, König et al. 2004, 2005 a, b, c).

The problem of dating small wood samples arose in recently accomplished investigations of timber constructions in the Albrechtsburg Castle (Donath 2006) and in the Cathedral (Donath 2007, König and Günther 2007) in Meißen. One possibility to solve the problem of dating small wood samples is to increase the number of tree-ring specific wood density features to be examined. So the numbers of degrees of freedom of the investigations as well as the security of dendrochronological dating can be increased by the x-ray densitometrical multivariate tree-ring analysis (König et al. 2005a).

Material

The roof truss construction of the western wing of the Albrechtsburg Castle in Meißen exhibits a heterogeneous structure. Dendrochronological investigations of certain elements of the roof truss were necessary in the background of reconstruction measures and their optimal calculation of costs. It had to be clarified whether the west wing of the roof structure was destroyed by the major fire in 1773 and rebuilt later or came from the original construction time of the Albrechtsburg Castle (approx. 1489). Among others, the investigation of small-sized construction elements of the roof structure with less than 50 tree-rings was necessary (Fig.1, left). In a second example the multivariate method was also applied to samples from boards of the terracotta figures "Mauritius" (M) and "Viktor" (V) standing in the Prince’s Chapel of the Cathedral in Meißen (Fig.1, right). Both figures are the biggest monolithic terracotta figures from the Middle Ages (Donath 2007).

DOI:10.2312/GFZ.b103-08056

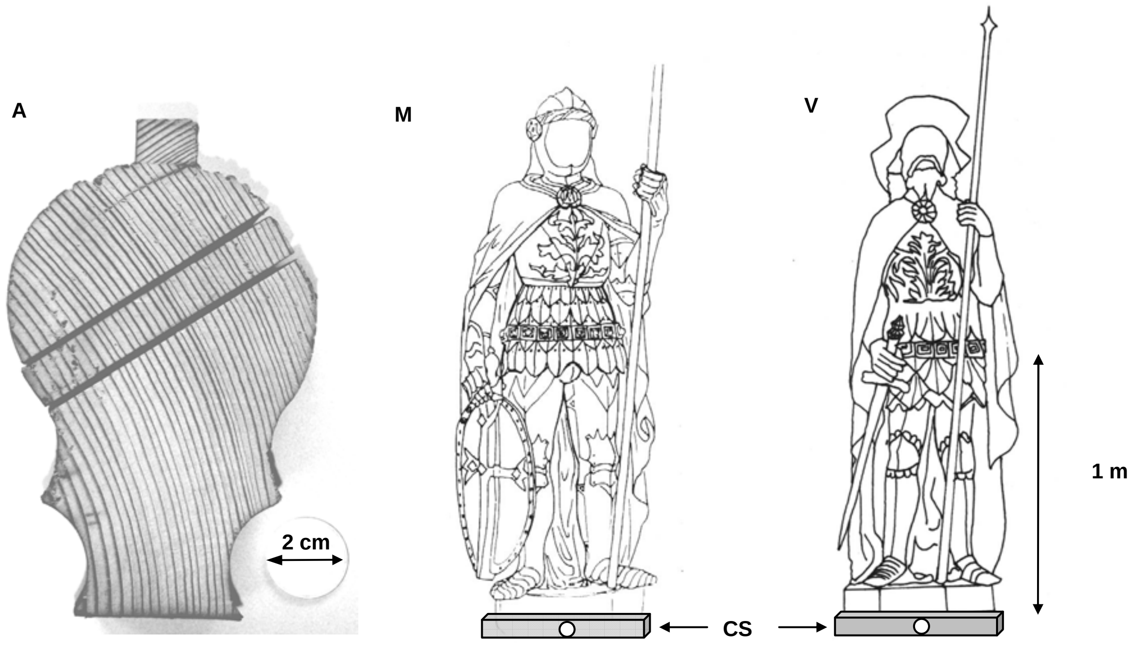

Figure 1: left: ornament of the roof structure in the west part of the Albrechtsburg Castle in Meißen with 36 tree-rings (A). right: drill core samples (CS) from the wood base plates of the terracotta figures (Mauritius: M; Viktor: V); pictures from Vohland (2007).

The firm adhesive binding between both terracotta figures and their wooden plates using albuminous glue directs not only to a simultaneous, but also to a very early installation of the figures in the Prince's Chapel of the cathedral. Dendrochronological investigations were based on the evaluation of drill cores taken from the two base plates (Prince's Chapel) and timber discs from the roof truss (Albrechtsburg Castle). All samples were spruce wood (*Picea abies* [L.] Karst.).

The multivariate cross-correlation analyses were made by using absolute x-ray densitometrical multivariate standard-chronologies for spruce (*Picea abies* [L.] Karst.) from regions in Saxony (123 stem disks of 20 sample sites at different elevations; in addition 75 samples - usually drill cores - of dated buildings).

Methods

The wood samples were formed out with a circular saw (sample thickness of 1.2 mm ± 0.01 mm). The extracted wood laths were air-conditioned under normal climate (20°C, 65% relatively air humidity). Afterwards the samples were arranged and x-rayed over radiographic films (*Agfa Microvision Ci*) with the x-ray unit *Baltographe* under controlled conditions (normal climate, voltage: 12.0 kV; amperage: 12.0 mA, duration time: 50 min.). The year-specific wood density structures of the images on the radiographic films were quantified by using the optometrical unit *Dendro 2003* (Walesch-Electronics). X-ray microdensitometric analysis was performed following the procedure described by Polge (1970) and Schweingruber (1980). The time series of the densitometrical tree-ring features derived from the drill cores were transformed by a computer programme called *TreeRingAnalyser* (König et al. 2004) into time series complexes to be summarized and analyzed. In a next step, the multivariate cross-correlation analysis between the sample complexes and the standard complex was performed by the *TreeRingAnalyser - TRA* (Fig.2).

DOI:10.2312/GFZ.b103-08056

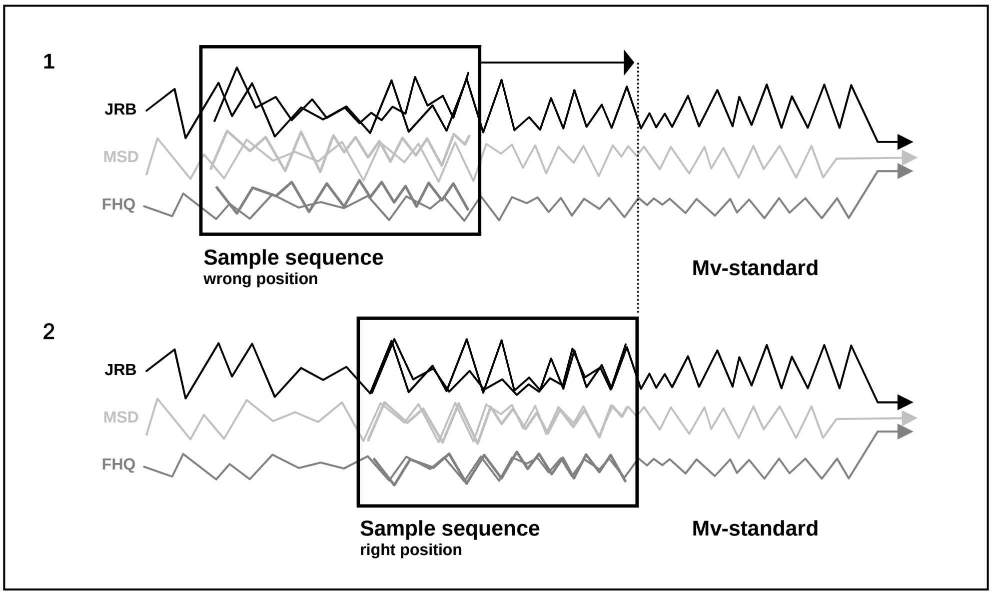

Fig.2: Model of the multivariate dating of time series complexes. Time series of different tree-ring features of the sample sequence with e.g. ring width (JRB), mean late wood density (MSD) and early wood mass (FHQ) are analyzed by cross-correlation analysis over a multivariate standard (Mv-standard); wrong solution (1); right solution (2): high similarity between sample and standard (König et al. 2005a).

Results and Interpretation

Univariate dating in comparison to the ring-width standard chronology:

On the basis of ring-width measurements of the drill core samples from the boards under the terracotta figures, two time series could be formed and dated using the spruce ring width chronology of Saxony. Fig.3 clarifies that the series of measurements of the sample "Viktor" with 50 tree-rings could be dated significantly to the calendar year 1406. The demarcation to the wrong solution amounted to approx. 37%. The right dating result in the beginning of the 15th century was verified by additional investigations of the statue, using thermo luminescence technique.

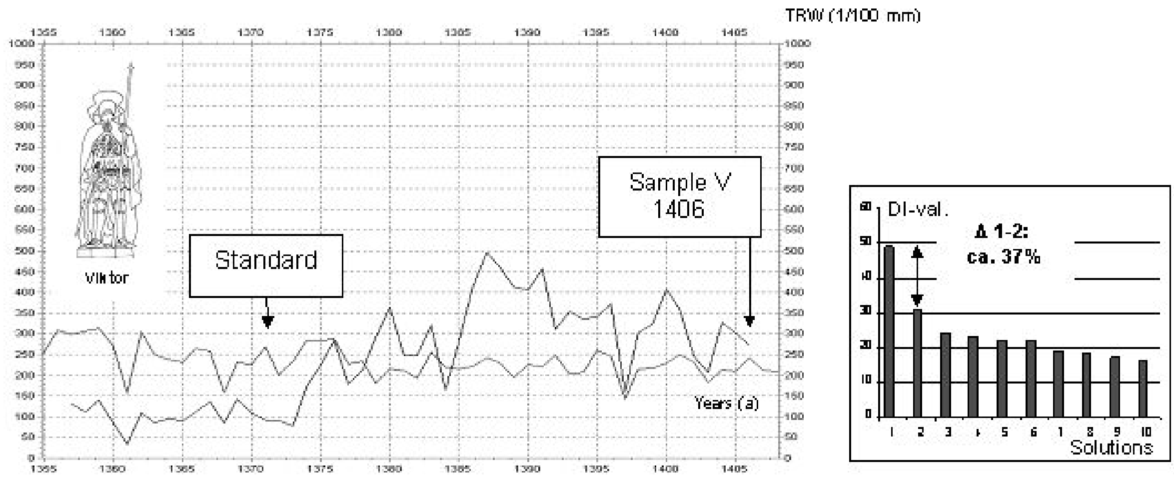

Fig.3: Screen shot (from TSA-programme): Time series "V" with 50 tree-rings could be qualified with 37% of the DI-value in opposite to the wrong solution 2 (1910) and thus be dated statically secured on the correct solution 1 (1406) (diagram right).

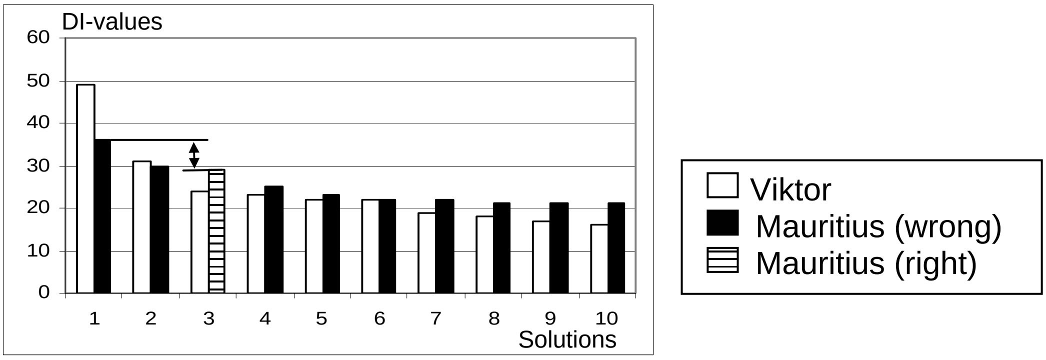

Fig.4: Dating-Index values of ring-width time series for Viktor and Mauritius: The time series of Mauritius with 24 tree-rings could not be dated securely on the basis the univariate dating index (DI) using ring-width. The correct solution 3 (1410) exhibited smaller DI-values than the wrong solution 1 (1792).

The time series of *Mauritius* with 24 tree-rings was not dateable by the ring-width standard chronology. Two wrong solutions showed higher DI-values (Dating-Index cf. Rinn 2003) than the correct solution (see solution No. 3 in Fig. 4). Likewise, the calculations for dating the wood sample from the Albrechtsburg Castle with 36 tree-rings were not successful on the basis of measuring and analysing the ring-width. In the following x-ray densitometrical multivariate dating procedure of both samples, several multivariate time series complexes were formed and analyzed by the standard chronology. The different densitometrical wood density features, e.g. latewood densities, earlywood density, ring widths and wood mass equivalents, furnished variable-specific dating contributions. For a detailed description of the method see König et al. 2005a.

The used MDI-value (Multivariate Dating-Index) is an accumulated reference value for similarities of time series complexes. The MDI-value presents the sum of DI-values of extracted tree-ring parameters by using the principal component analysis (PCA). On the basis of the MDI-values, the Mauritius-sample could be dated to 1410 and the roof truss sample (A) of the Albrechtsburg could be dated to 1816. In the following the multivariate dating procedure will be described by the example of sample A from the Albrechtsburg with 36 tree-rings.

Multivariate analysis and dating:

The time series complex of sample A was cross-correlated with the multivariate standard chronology for spruce (*Picea abies* [L.] Karst.). Aligned to their specific standard chronology, the time series of wood density features contributed more strongly to the dating than the time series of ring-widths (Fig. 5, Fig. 6).

DOI:10.2312/GFZ.b103-08056

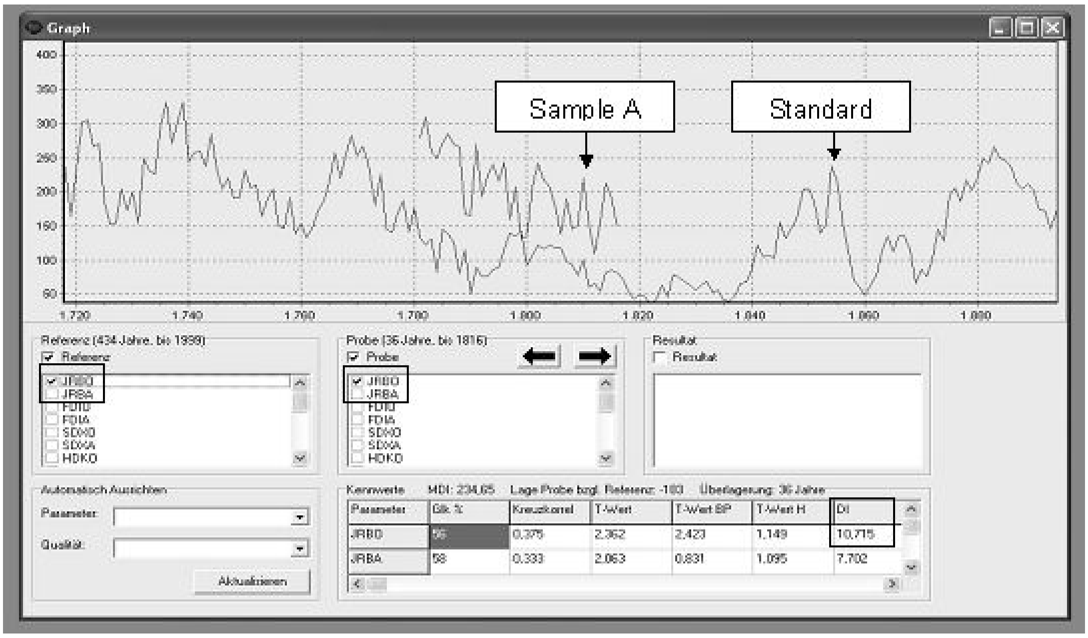

Figure 5: Screen shot of the TreeRingAnalyser: ring-width series (JRBO) of sample A and the multivariate standard-chronology for ring-width (spruce, Saxony); Dating-Index (DI-value): 10.715; Glk = 56%.

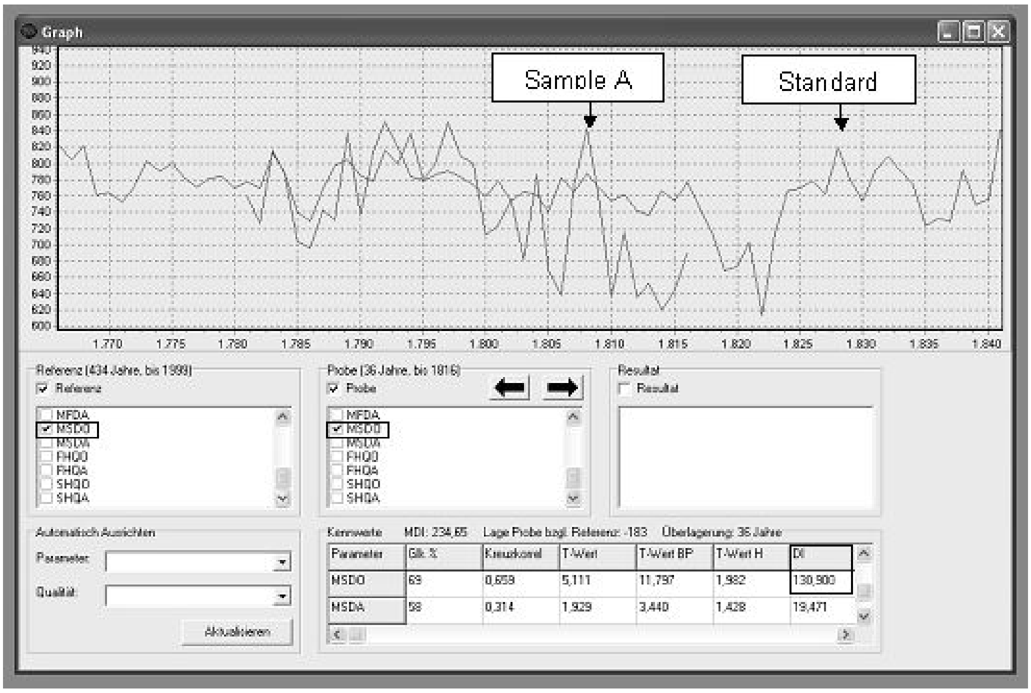

Figure 6: Screen shot of the TreeRingAnalyser: late wood density (MSDO) of sample A and the multivariate standard-chronology for late wood density; Dating-Index (DI-value): 130.9; Glk = 69%.

In summary 10 time series are used for dating during the multivariate dating procedure. According to König et al. (2004), the MDI-value is calculable from univariate partial results (dating indices from the ring-widths parameters (JRBO, JRBA), late wood densities (MSDO, SDXA), mean early wood density (MFDA), proportion of early and late wood (FHPO, FHPA), the accumulated wood masses in early and late wood (FHQO, SHQA) and the wood density contrast (HDKO).

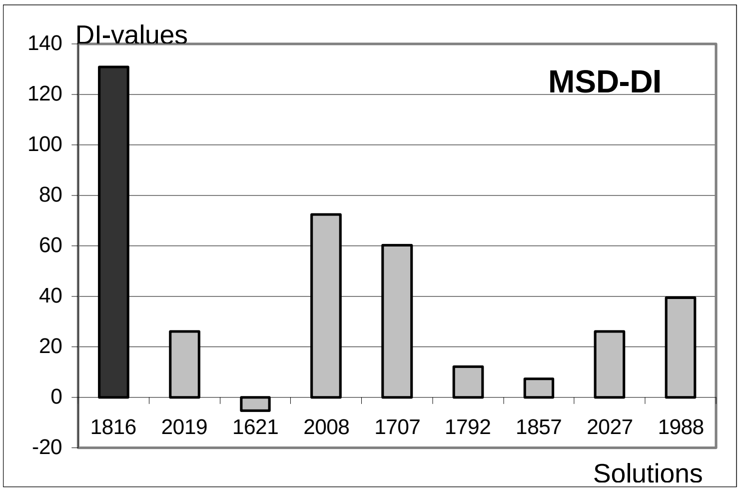

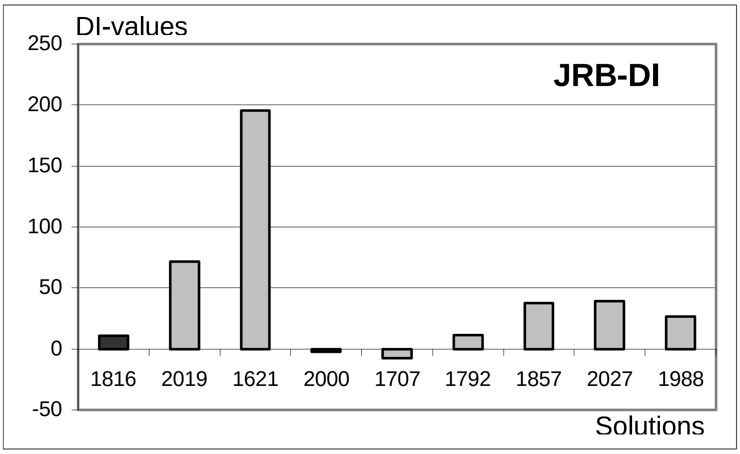

Fig.7: In some cases the ring-width (JRB-DI) does not lead to the correct solution (calendar year 1816) in opposite to the density features e.g. mean late wood density (MSD-DI).

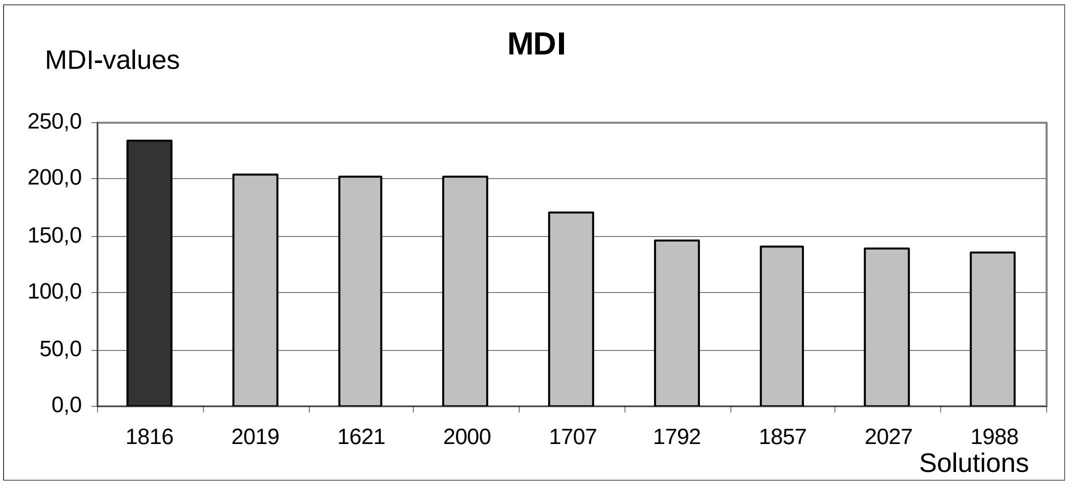

Fig.8: The Multivariate Dating-Index (MDI) as an accumulated number of contributions of ten tree-ring features leads to the correct dating solution for the sample from the Albrechtsburg Castle Meißen (1816).

DOI:10.2312/GFZ.b103-08056

Figure 7 clarifies that positive and negative dating indices can emerge from univariate cross-correlation. The DI-value of the ring-width was significantly lower for the correct solution (1816; DI-value=10.7) than for the wrong solution (1621; DI-value=195.7). The sole application of the univariate method would have led to a wrong dating result. In contrast, the inclusion of the mean late wood densities with a DI-value of 130.9 proved as goal-prominent (DI-values for wrong solutions: 1707: 60.3 and for 2008: 72.4). Yet, only by applying the multivariate method a statistically secured dating was possible. The correct solution (1816) became qualified on the basis of the mean late wood density values (different: 55%) from the wrong solutions (2008). Apart from the wood density characteristics mentioned, 8 further features are evaluated and included in the computation of the MDI-value. This MDI-value for the correct dating solution (1816: MDI-value: 234.7) differed significantly (with 15%) from the wrong solutions (2019: MDI-value: 204.9; 1621: MDI-value: 202.4), (fig.8). The correct dating result of 1816 could be determined and be confirmed with statistic tests (e.g. Wilcoxon-test).

Conclusions

For the dating of spruce samples with less than 50 tree-rings it is necessary to analyze the tracheid structures in detail. The exclusive analysis of the ring widths describes only one part of the year-specific wood density structures of tree-rings. Apart from the minimum, mean and maximum wood density values, also the tree-ring characteristics of the wood mass accumulation in the earlywood and latewood zones contain important information according to tree-ring growth and to climatic conditions of past epochs. That way, characterisation and dating of spruce wood samples are improved.

By the computation of the MDI-value it was possible to date the examined wood samples of the roof truss of the Albrechtsburg Castle. Indeed, the roof truss fell victim to the major fire in 1773 and was rebuilt sometime after 1816. The figures of Victor and Mauritius are based on wooden plates which date back to the early 15th century (1410). Therefore, they must be classified as part of the early history of the Meißen Cathedral.

Particularly in the case of small wood samples with less than 50 tree-rings, the entirety of independent time series of tree-ring features should form a solid basis for their dendrochronological analysis, if a corresponding multivariate standard chronology is available.

References

Cramer, J., Eissing, T. (1996): *Dächer in Thüringen*. Bd. 2, Verlag Ausbildung und Wissen, Bad Homburg, Leipzig, S. 16, 18-19.

Donath, M. (2006): Vom Keller bis zum Dach. Neue Forschungen zur Baugeschichte der Albrechtsburg. Monumenta Misnensia. *Jahrbuch für Dom und Albrechtsburg zu Meißen*. Bd. 05/06. S.146 - 167.

Donath, G. (2007): Aus Ton gebrannt. Tagungsband zum DBU-Projekt. Schirmer-Verlag Lichtenstein. S. 4-11.

König, J., Günther, B. (2007): Dendrochronologische Analysen zur Datierung der Brettstücke unter den Terrakottafiguren im Dom zu Meißen. in: Donath, G. 2007: Aus Ton gebrannt.

Terrakottafiguren im Dom zu Meißen. Tagungsband zum DBU-Projekt. Schirmer-Verlag Lichtenstein. S. 83-90.

König, J., Günther, B., Bues, C.T. (2004): Röntgendensitometrisch multivariate Zeitreihenanalyse. Erarbeitung einer Methode für die Datierung von Holzproben der Baumart Fichte (Picea abies [L.] Karst.) mit geringer Jahrringanzahl. Forstwissenschaftliche Tagung Freising / Weihenstephan. Die Natur als Vorbild, Effiziente Ressourcennutzung, Tagungsband. S. 158.

König, J., Günther, B., Bues, C.T. (2005a): New multivariate cross-correlation analysis. Tree-ring in archaeology, climatology and ecology (TRACE), Association for tree-ring research (ATR), Preceedings of the dendrosymposium 2004, Birmensdorf, Schweiz. S. 159-166.

König, J., Günther, B., Bues, C.T. (2005b): Wie wir das Alter unserer Bauerhäuser bestimmen können – Dendrochronologische Untersuchungen. Mitteilungsblatt des Vereins Ländlicher Bauwerte in Sachsen. Heft 1. S. 12-15.

König, J., Günther, B., Bues, C.T., Gille, C. (2005c): Dendrochronologische Untersuchungen am Dreiseithof Hofefeld 5 in Frauenstein im Osterzgebirge. Mitteilungsblatt des Vereins Ländlicher Bauwerte in Sachsen. Heft 4/5. S. 10-13.

Polge, H. (1970): The use of X-ray densitometric methods in dendrochronology. Tree-ring Bulletin 30. S. 1-10.

Rinn, F. (2003): TSAP – Time Series Analysis and Presentation for WIN. TSAP-WIN Professional Version 0.53. RinnTech, Heidelberg. 25 S.

Schweingruber, F.H. (1980): Dichteschwankungen in Jahrringen von Nadelhölzern in Beziehung zu klimatischökologischen Faktoren. Eidgenössische Anstalt für Forst., Birmensdorf, Berichte: 213. S. 35.

Vohland, P. (2007): Zur Restaurierungsgeschichte und Farbigkeit der Figuren. in: Donath, G. 2007: Aus Ton gebrannt. Terrakottafiguren im Dom zu Meißen. Tagungsband zum DBU-Projekt. Schirmer-Verlag Lichtenstein. S. 64, 69-77.

Fluorescence microscopy utilization for lignin detection in wooden cell walls in spruce. A technical note.

H. Vavrčík, V. Gryc & M. Rybníček
Mendel University of Agriculture and Forestry Brno, Faculty of Forestry and Wood Technology, Department of Wood Science, Zemědělská 1, 613 00 Brno, Czech Republic
Email: vavrcik@mendelu.cz

Introduction

Softwood structure is very simple. It only consists of tracheids (aprox. 90 % of the volume) and parenchyma cells (Panshin & de Zeeuw 1980). Therefore, softwood is very suitable for the xylogenesis (i.e. wood formation process) analysis. There are three zones in a newly forming softwood tree-ring: the radial enlarging zone, the maturation zone and the zone of matured cells (Wodzicki 1971). Tracheids in the radial enlarging zone have cell content, their radial diameters are increasing and their cell walls consist of a middle lamella and a primary cell wall. When they move to the maturation zone their radial diameter remains constant and the process of the secondary thickening (the secondary cell wall formation) starts; the cell wall corners are rounding and the cell walls are gradually lignifying. Meanwhile, the cell content is gradually consumed. In the third zone, the matured cells zone, tracheids have their final cell wall diameter and they may be considered as fully differentiated. In this zone tracheids have no cell content and they are completely dead.

It is necessary to distinguish non-lignified and lignified tracheids to identify the individual zones of a tree-ring. A frequently used method for this purpose is double staining with safranin and fast green (Bamber 1961, Horáček et al. 1999). This method is based on the fact that stained wood cell elements are different in colour of their cell walls. The non-lignified cell walls are green in colour and the lignified ones are red. Subsequently, microscopic wood slices have to be mounted to Canada balsam (or other mounting medium) to make permanent microscopic specimens. The described method of double staining and permanent specimen making is quite difficult and time demanding. Therefore, a new method was suggested as a replacement of double staining. The new method of using fluorescence microscopy is based on autofluorescence of lignin.

Some materials and objects are able to absorb electromagnetic radiation (excitation radiation) and contemporarily emit radiation of different wavelengths. The term used for this phenomenon is photoluminiscence. If the light emission persists for up to a few seconds after the excitation source is withdrawn, the phenomenon is known as phosphorescence. Fluorescence, on the other hand, describes light emission which continues only during the absorption of the excitation light. The time interval between the absorption of excitation radiation and the emission of re-radiated light in fluorescence is of an extraordinarily short duration, usually less than a millionth of a second (Rost 1992).

The main initiator of fluorescence is irradiation of fluorochrome (i.e. material that can emit fluorescence radiation) molecules by specific wavelength electromagnetic radiation. This

DOI:10.2312/GFZ.b103-08056

causes collisions of high-frequency photons and fluorochrome atoms. A fluorochrome molecule absorbs a part of the incident photon energy. If the absorbed energy is sufficient, an electron in the fluorochrome molecule is boosted up to a higher energy level of the excited state, i.e. the electron is excited. The excited electrons may lose some vibrational energy and return to the “lowest excited singlet state”. From the lowest excited singlet state, the electrons “drop back” to the ground state with simultaneous emission of fluorescent light. Light emitted at fluorescence is called fluorescent light (Valeur 2002).

Fluorescence microscopy is an excellent method for the kind of substances that can be forced to emit fluorescence radiation by their own nature (primary fluorescence or autofluorescence) or by staining (secondary fluorescence) with specific fluorescent chemicals – fluorochromes.

The emission spectrum of a fluorochrome is always shifted into longer wavelengths (lower energy) in relation to the absorption spectrum. This shift is called Stoke’s shift (Rost 1992) and it makes it possible to separate the excitation and the emission radiation using optical filters. An optical filter consists of an excitation filter, a dichroic mirror and a barrier filter. The excitation filter only transmits the radiation of specific wavelengths (excitation radiation) to the investigated sample. The barrier filter prevents the excitation radiation to reach the microscope ocular and transmits only a specific part of wavelengths of emitted fluorescent radiation. The dichroic mirror is a specialized filter designed to reflect the excitation radiation and to transmit the radiation emitted by the investigated sample. It is possible to observe the emitted light in the microscope ocular or capture it using a camera.

Besides cellulose, lignin is the most abundant and important polymeric organic substance in wood. Lignin impregnates polysaccharides of wood cell walls. There are chemical bonds between lignin and polysaccharides and together they form lignopolysaccharidic complexes. The lignin amount in wood varies from 20 to 40 % of wood weight in dependence on the species (Fengel & Wegener 1989). Lignin may be considered a native fluorochrome, i.e. a substance that can autofluorescence (Donaldson 2001), and the new method for lignin detection for purposes of distinguishing zones in a newly forming ring is based on this phenomenon.

Material and Methods

40 μm thick microscopic specimens of wood of Norway spruce (*Picea abies* (L.) Karst.) were sectioned on the microtome. Wood samples were taken from 6 trees at the height of 1.3 m from the ground. Both non-permanent specimens (microscopic sections in a drop of water) and permanent specimens (sections mounted in the Canada balsam) were prepared. The number of non-permanent specimens was 84, the number of permanent specimens was 5. A mercury lamp was used as the source of radiation of a wide range of wavelengths (250–700 nm) to induce autofluorescence of lignin. The radiation emitted by the lamp went through an optical filter block. Nikon Optihot-2 microscope with a trinocular was equipped with three Nikon optical filters blocks that were being tested (Tab. 1).

Table 1: Tested Nikon optical filters specifications.

Optical filter block type	G-2A	B-2A	DAPI
EX – Excitation wavelength (nm)	510–560	450–490	340–380
DM – Dichroic mirror – border wavelength (nm)	575	505	400
BA – Barrier filter – minimal wavelength of radiation transmitted to the ocular (nm)	590	520	435–485

PlanFluo 20 and PlanFluo 40 objectives suitable for fluorescence microscopy were used for observations. CCD camera Hitachi HV-C20 was attached to the microscope for digitalization of the observed picture. Image analysis software Lucia G was used for picture processing.
The excitation radiation falls upon the investigated sample through the lens, and the emitted radiation goes through the same lens to the ocular (episcopic fluorescence microscopy).
It was supposed that there was no need of transparent specimens in contrast to fluorescence microscopy with transmitted light. That is why the “non-microscopic” wood samples (10 × 10 × 20 mm) with surface “smoothed” by the microtome were prepared (20 pcs).

Results

There were problems with the microscopic sections mounted in Canada balsam due to its slight fluorescence properties. It made lignin autofluorescence observations impossible. On the other hand, the microscopic sections that were in water only (non-permanent specimens) were suitable for lignin autofluorescence observations.
Each of the available optical filter block was tested for its suitability for fluorescence microscopic observation of the non-permanent specimens. The autofluorescence of lignin occurred at λ_{exc} = 510–560 nm (G-2A filter) and at λ_{exc} = 340–380 nm (DAPI filter). There was no fluorescence light observed at λ_{exc} = 450–490 nm (B-2A filter).
The best image quality was observed at λ_{exc} = 510–560 nm (green light) and the emitted fluorescence light was red (According to printing requirements all pictures were transformed from 24bit mode to greyscale mode. (Fig. 1). But the fading effect (reduction of the emitted light intensity) occurred.

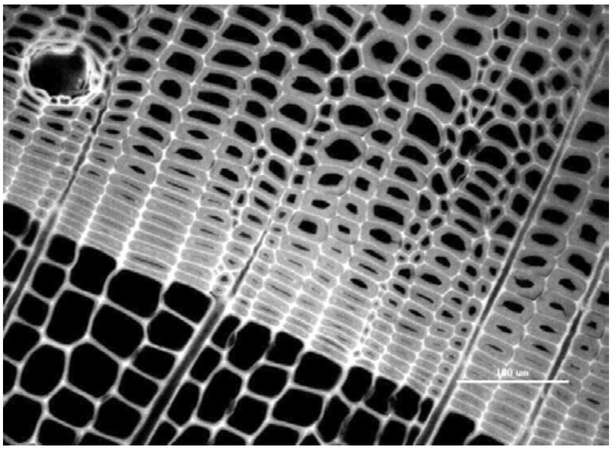

Figure 1: Lignin autofluorescence in Norway spruce at λ_{exc} = 510–560 nm (transformed to greyscale for printing)

When the DAPI filter was used, i.e. λ_{exc} = 340–380 nm (UV-A), the emitted light was blue. The intensity of the emitted light gradually increased.

It was possible to observe gradual lignification of cell walls of anatomical elements in a forming ring thanks to periodically sampled wood samples (Fig. 2). The emitted light indicates the areas of lignin occurrence in the specimens. Other areas of specimens, i.e. areas without lignified cells did not emit any light and they were black in the observed picture.

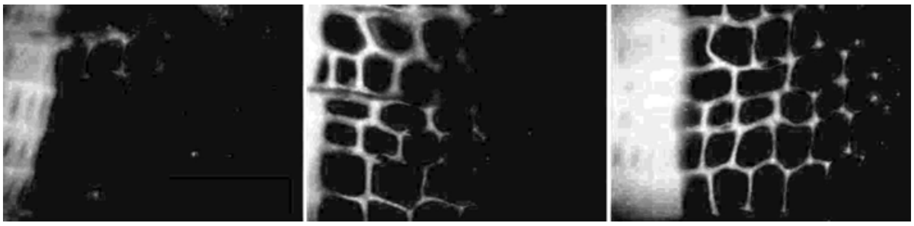

Figure 2: The sample taken on June 2nd (left) – no lignification. The sample taken on June 16th (middle) – two cells of each radial row are lignified, the third and the fourth cells are lignified only in corners. The sample taken on June 30th (right) – at least four cells are lignified. Fluorescence microscopy (transformed to greyscale for printing).

It was found useful to combine a fluorescent picture and a picture acquired by common light microscopic technique for the same observed area of the specimen. Such a kind of picture makes it easy to distinguish the fully lignified, the partly lignified and the non-lignified cell walls. It is supposed that the emitted light intensity is related to lignin concentration in the cell wall. Most lignin concentration was observed in the corners of the middle lamella.

The lignification process began in the cell wall corners in the middle lamella, then it continued in the radial cell walls and finally in the tangential cell walls.

Because of the incident (reflected light or episcopic) illumination principle of used microscopic technique it was not necessary to use thin slices of wood. The picture acquired from the surface of the "non-microscopic" wood sample observation is presented in figure 3.

DOI:10.2312/GFZ.b103-08056

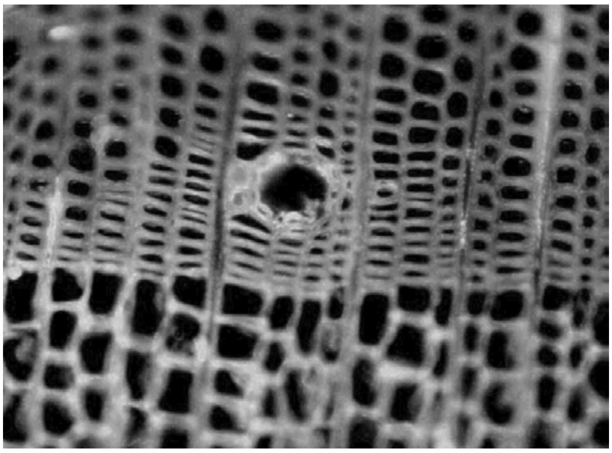

Figure 3: Transverse section surface of non-microscopic sample of wood of Norway spruce. Fluorescence microscopy at λ_{exc} = 340–380 nm (transformed to greyscale for printing).

Discussion

The method of fluorescence microscopy based on lignin autofluorescence was proved as suitable for lignin detection in the cell walls of wood of Norway spruce. In other words, it makes lignin visible. The advantage of this method is that the double staining procedure is not necessary and it does not require samples mounted in Canada balsam. It saves the time needed for specimen preparation. The use of non-permanent specimens is an indisputable advantage. On the other hand, the disadvantages are the necessity to process the image of non-permanent specimens immediately and the impossibility of their storing. However, it is possible to archive all specimens as digital pictures, which eliminates this disadvantage. The combined pictures created as a result of the logical sum of fluorescent and common light pictures can fully substitute pictures acquired by the double staining method.

For lignin, the maximum fluorescence, as measured with a fluorescence spectrophotometer, occurs at λ_{exc} = 335 nm (Kolpak et al. 1983). This wavelength was very close to the excitation wavelengths of the DAPI filter (λ_{exc} = 340–380 nm). Donaldson (2001) observed lignin autofluorescence at λ_{exc} = 530 nm. This wavelength is in the range of excitation wavelengths of the G-2A filter (λ_{exc} = 510–560 nm). Kolpak et al. (1983) reported that no significant fluorescence was observed at λ_{exc} = 633 nm. No such optical filter was available. The lignin autofluorescence that occurred with DAPI and G-2A optical filter blocks is in accordance with the results in the studies mentioned above.

No lignin autofluorescence was achieved using the B-2A optical filter block. It was probably caused by the mercury arc lamp emission spectra. The mercury arc lamp showed very small relative spectral radiation at the wavelength range corresponding to B-2A optical filter excitation wavelengths.

The fading effect occurred at λ_{exc} = 510–560 nm. This effect was described by Rost (1992). On the other hand, the fluorescent light intensity was detected to increase at λ_{exc} = 340–380 nm. This phenomenon was not described in the available studies by other authors. It was probably caused by high energy (short wavelength) of incident radiation, which was able to penetrate deeper, which means it was possible to excite electrons of more molecules.

The result of the observation of lignification is in accordance with the previous studies (Wodzicky 1971, Antonova & Stasova 1997, Horáček et al. 1996); lignification begins in the middle lamella and continues in the radial cell walls and finally in the tangential cell walls.
The quality of the fluorescent picture acquired directly from the surface of non-microscopic piece of wood sample (i. e. without microscopic slices) depends on the quality of the observed sample surface, especially on its flatness. It was found suitable to smooth the surface by a few trims on the microtome.
All experiments were carried out using the wood of Norway spruce but it is supposed that similar results should be obtained even with other European softwood species.

Conclusions

The method for lignin detection using fluorescence microscopy is a full-value replacement of the double staining method. The new method includes a few steps:

1. Sectioning the wood samples on the microtome.
2. Making non-permanent specimens out of microscopic sections.
3. Specimen observation using light microscopy.
4. Digitalisation of the observed specimen area (saving as a picture file).
5. Digitalisation of the same specimen area (without moving) with fluorescence microscopy at λ_{exc} = 510–560 nm (red fluorescence) or at λ_{exc} = 340–380 nm (blue fluorescence).
6. Logical sum of both pictured using image analysis software (e.g. Lucia G).

The method can be recommended for purposes of xylem growth analysis as was described in the Introduction. Lignin autofluorescence was observed at both 340–380 nm and 510–560 nm excitation wavelengths.

Acknowledgements

The project was financially supported by the research plan of LDF MZLU in Brno, MSM 6215648902.

References

Antonova, G.F., Stasova, V.V. (1997): Effects of environmental factors on wood formation in larch (Larix sibirica Ldb.) stems. *Trees* 11: 462–468.

Bamber, R.K. (1961): Staining reaction of the pit membrane of wood cells. *Nature*, Lond. 191: 409–410.

Donaldson, D.A. (2001): Lignification and lignin topochemistry – an ultrastructural view. *Phytochemistry* 57: 859–873. ISSN 0031-9422

Fengel, D., Wegener, G. (1989): Wood Chemistry, Ultrastructue, Reactions. Walter de Gruyter & Co., Berlin. 613 p.

Horáček, P., Šlezingerová, J., Gandelová, L. (1996): Ecophysiology of xylogenesis – interpretation of cambial activity and xylem development. In: *Ecological and physiological* *aspects of xylogenesis in conifers.* Krasnoyarsk: IUFRO S2.01.10.: 143–146. ISSN 1016-3263

Horáček, P., Šlezingerová, J., Gandelová, L. (1999): Effects of environment on the xylogenesis of Norway spruce (Picea abies /L./ Karst.) In: Wimmer, R., Vetter, R. E. (eds.): *Tree ring analysis: biological methodological, and environmental aspects.* CABI International, University Press, Cambridge: 33–53.

Kolpak, F.J., Cietek, D.J., Fookes, W., Cael, J.J. (1983): Analysis of lignin from spent liquors by gel permeation chromatography/low-angle laser light scattering (GPC/LALLS). *Appl Polym Symp* 37: 491–507.

Panshin, A.J., Zeeuw de, C. (1980): Textbook of Wood Technology: Structure, Identification, Properties, and Uses of the Commercial Woods of the United States and Canada. 4th. ed. New York: McGraw-Hill. 722 p. ISBN 0-07-048441-4.

Rost, F.W.D. (1992): Fluorescence Microscopy, Volume I, , Cambridge University Press, Cambridge, United Kingdom, 256 p. ISBN 052123641X.

Valeur, B. (2002): Molecular Fluorescence: Principles and Applications. Wiley-VCH, New York. 387.

Wodzicki, T.J. (1971) Mechanism of xylem differentiation in Pinus silvestris L. *Journal of Experimental Botany*, 22 (72): 670–687. ISSN 0022-0957

DOI:10.2312/GFZ.b103-08056

Mean growth behaviour of forest stands – Methodological aspects from dendrochronology and forest mensuration

W. Beck

Institute for Forest Ecology and Forest Assessment Eberswalde,

Federal Research Centre for Forestry and Forest Products

Email: wbeck@bfh-inst7.fh-eberswalde.de

Situation and Motivation

The development of mean index chronologies is a basic topic of dendrochronolology. Commonly this procedure consists of prewhitening, trend estimation and index calculation of each individual series. Finally, all single index series have to be aggregated to the mean index series. Application of the arithmetic mean may be disadvantageous because all index values have the same weight, and outliers may distort the mean. For this reason so far Tukey's biweight robust mean (Weisstein, 1999-2007) is mostly used for calculation of mean index values. The effect of applying Tukey's biweight motivates the following analyses and alternative proposals. A chronology of common beech from Schleswig-Holstein in northern Germany (Fig. 1) will be used as an example.

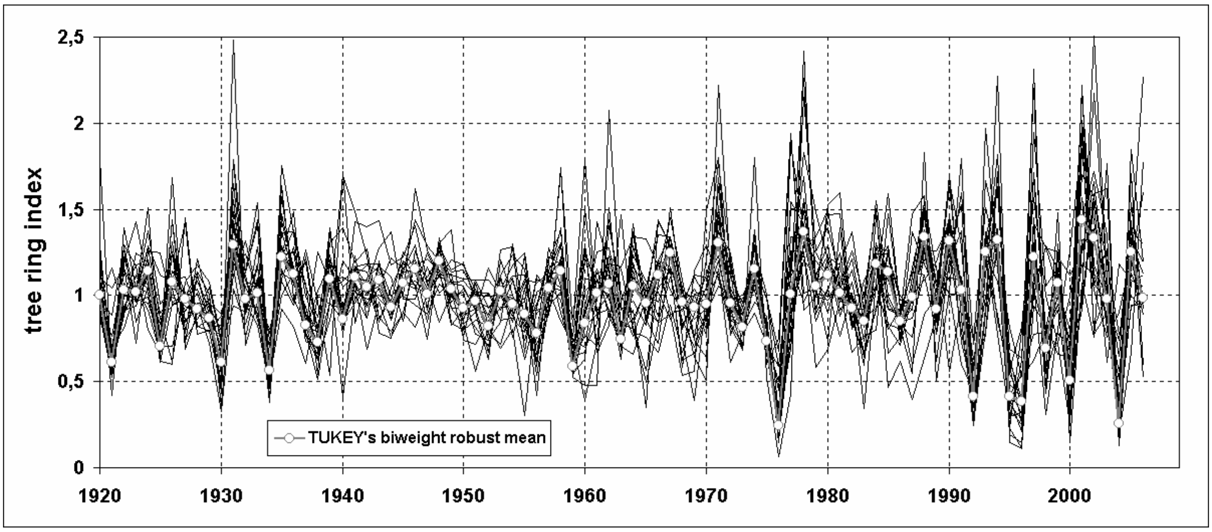

Figure 1: Index chronology Bornhoeved, common beech; 20 dominant sample trees

Tukey's biweight uses a weight function. The absolute weight values of the function increase with growing distance from the mean index, but drop down quickly when the distance from mean exceeds a certain threshold value (Fig. 2). Values beyond these thresholds do not influence the mean, because their weights are close to zero. This basic pattern may be traced at each time step. As additional examples, the years 1960 and 2000 were chosen (Fig. 3 and 4), and the tree numbers of the values are indicated which were excluded by Tukey's biweight from the calculation of the mean. Comparing the figures 2, 3 and 4 (1920, 1960, 2000) it is conspicuous that the tree numbers (individual series) which are excluded from the calculation of the mean calculation by the weight function of Tukey's biweight change from year to year.

DOI:10.2312/GFZ.b103-08056

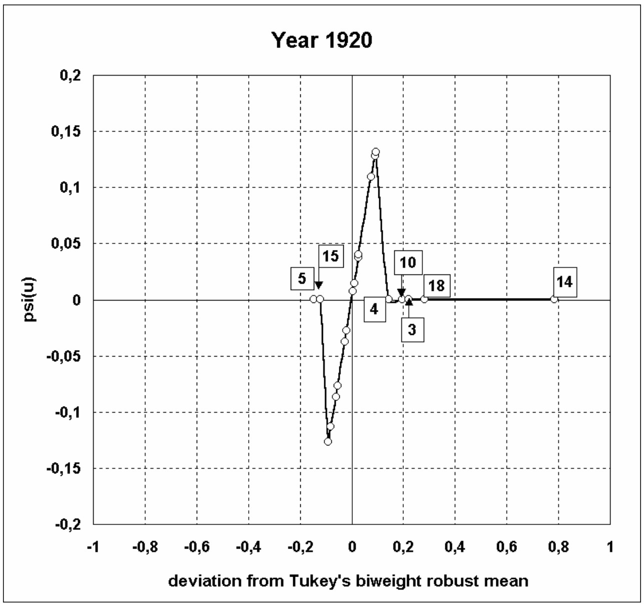

Figure 2: Values of the weight function psi(u) in relation to the deviation of the tree individual index values from the mean; example: year 1920; Numbers of individual series (=sample trees) which do not contribute to the mean index due to their weight values close to zero are indicated with boxes.

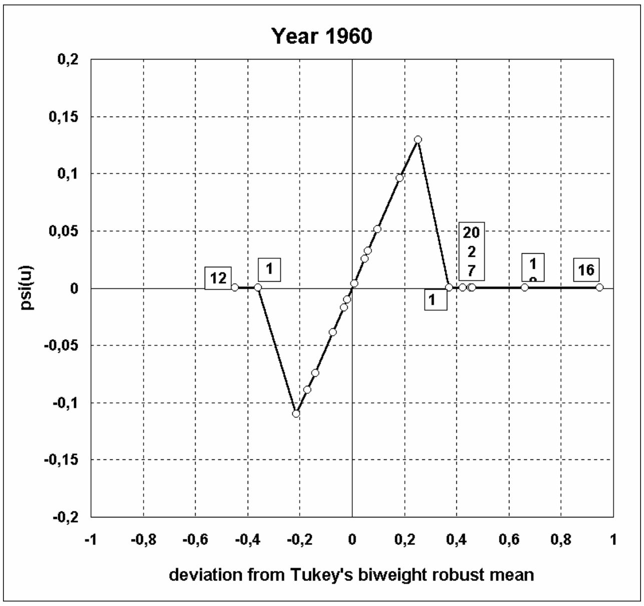

Figure 3: Values of the weight function psi(u) in relation to the deviation of the tree individual series index values from the mean; example: year 1960; Numbers of individual series (=sample trees) which do not contribute to the mean index due to their weight values close to zero are indicated with boxes.

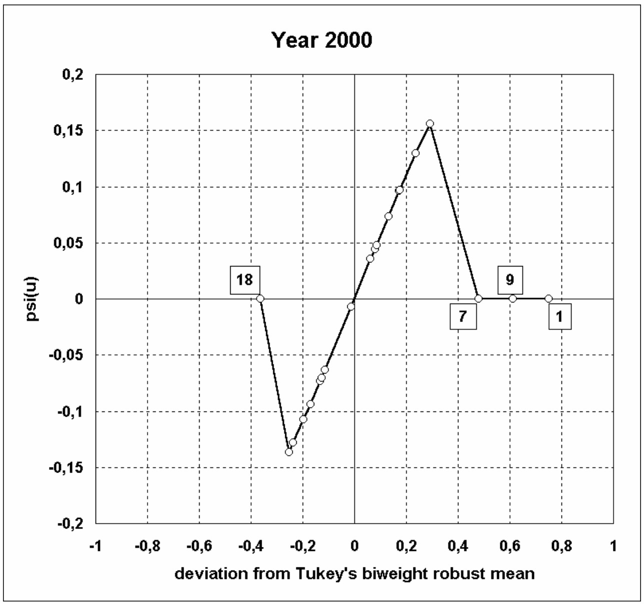

Figure 4: Values of the weight function psi(u) in relation to the deviation of the tree individual series index values from the mean; example: year 2000; Numbers of individual series (=sample trees) which do not contribute to the mean index due to their weight values close to zero are indicated with boxes.

DOI:10.2312/GFZ.b103-08056

This indicates that the same series, which is selected to contribute to the mean index chronology at a certain year, may be rejected at another year. Such effects of a mathematical procedure cause problems concerning its general acceptance. It seems to be necessary to evaluate quality and suitability of each single series with respect to their contribution to the mean index series. Each selected individual series should express the typical behaviour of the investigated tree population.

A first proposal for an alternative approach

A first alternative approach which evaluates single series starts from already prewhitened and detrended individual index series. It includes the following steps:

(1) Calculation of the chronologies‘ signal strength:

$$\hat{S} = \frac{n(n-1)}{2} \cdot \sum_{i<j} cor\left(I^i, I^j\right)$$

and the signal-to-noise ratio: $SNR = \frac{n \cdot r_m}{1 - r_m}$.

(2) Calculation of the signal strength of each series:

$$S_k = \frac{1}{n-1} \cdot \sum_{j \neq k} cor\left(I^k, I^j\right).$$

The signal strength of a single series S_k may be measured as the mean correlation to all other series of the chronology. Therefore S_k may be tested for significance. Series with negative or non-significant S_k are rejected from the chronology building. The procedure returns to step (1) until all remaining series are significant.

(3) Calculation of the mean index chronology according to Neumann (2001):

This calculation is based on the assumption that index series showing more stand-typical patterns have a smaller share of error and thus a higher signal strength than those with stand-untypical patterns. Obviously, it may be concluded that individual index series may be weight by their signal strength for calculation of the mean index chronology:

$$C_t = \frac{1}{\sum_i S_i} \cdot \sum_{i=1}^{n} S_i \cdot I_t^i; \qquad t=1, \ldots, s.$$

For illustrating the effects of this alternative procedure, a chronology of a mature pine stand (Grunewald, Berlin forests; n=30) was chosen (Fig. 5 to 8).

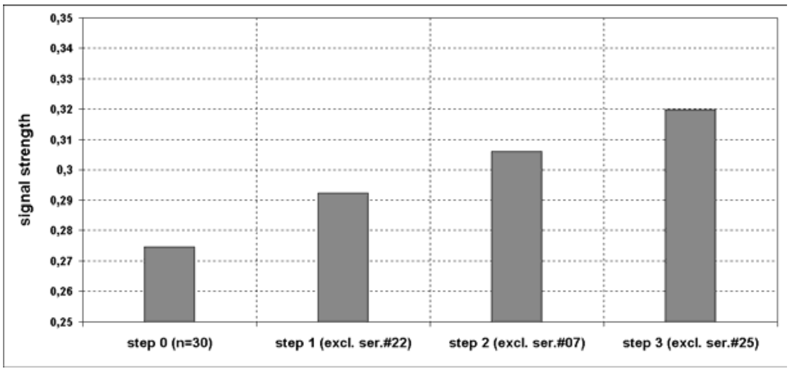

Figure 5: Increase of chronology's signal strength by stepwise exclusion of individual series with non-significant signal strength.

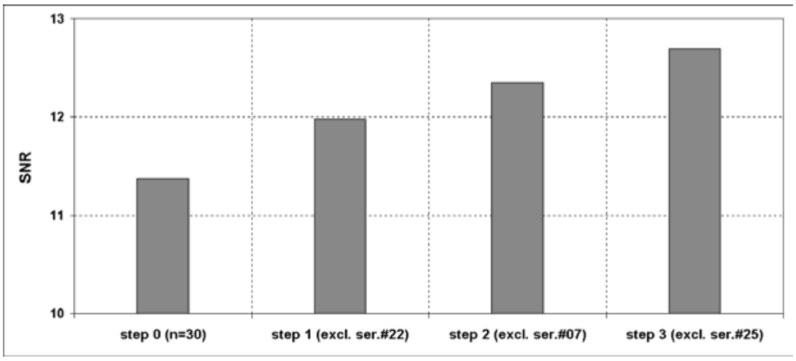

Figure 6: Increase of signal-to-noise ratio.

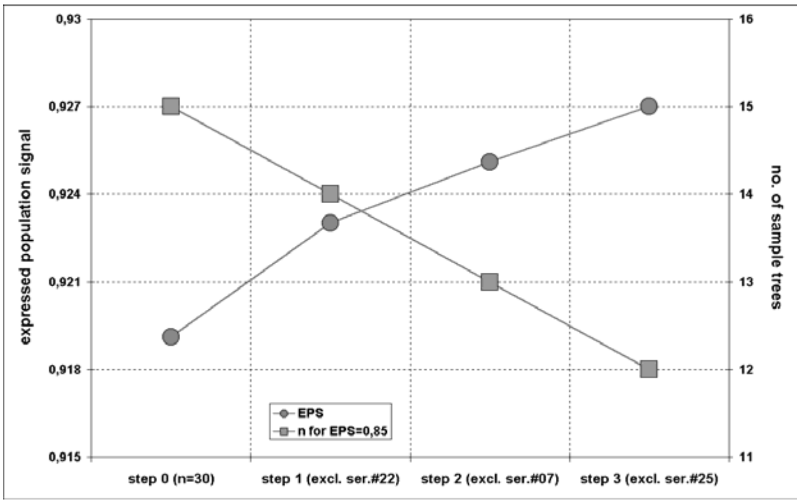

Figure 7: Increase of expressed population signal EPS and decrease of required sample size to get EPS=0,85.

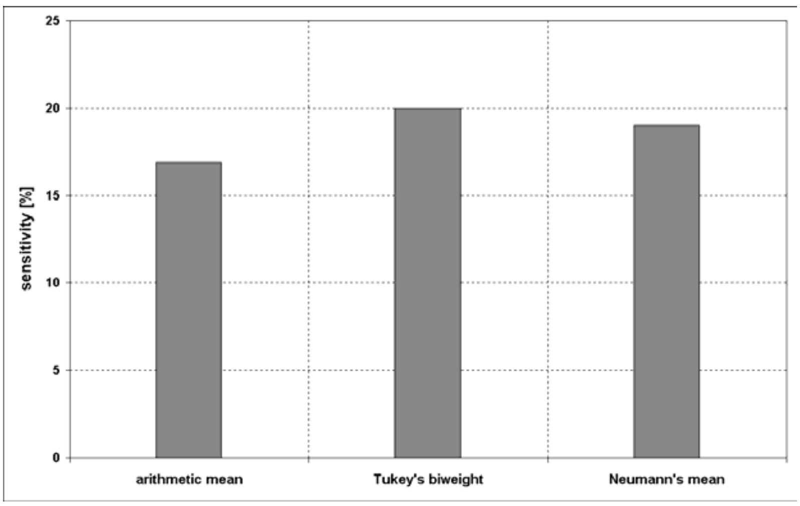

Figure 8: Comparison of mean sensitivity of the mean index series when using different calculations of mean.

Evaluating these results, the following conclusions can be drawn:

i. Identification of series with negative or non-significant mean cross correlation to the other series and their subsequent exclusion from calculation of mean index may improve mean signal strength of the whole chronology.

ii. Simultaneously, SNR and EPS increase and required sample size decreases. The mean sensitivity as a characteristic of the climate impact is higher if the alternative approach together with Neumann's mean is used other than by the application of the arithmetic mean, but sometimes lower than by application of Tukey's biweight. The latter is due to the enhancement of the centre of the actual distribution per year.

iii. The "cleaning" of a noisy chronology by the alternative procedure is done by exclusion of entire series but never by exclusion of index values only at a certain year.

A second proposal to get a stand-typical mean chronology

Taking increment cores to develop mean index chronologies for the investigation of climate growth relationships may be seen as only one special branch of tree ring research. Tree ring series may be used for a more comprehensive growth behaviour analysis of a forest stand if they cover the whole life span of the stand. Growth behaviour analysis aims at the reconstruction of the mean growth course of a stand, represented by the dominant trees, and at the evaluation of their characteristics in the temporal course. Growth courses of individual trees can be compared and evaluated appropriately by their diameter growth course. The measured ring widths have to be cumulated to get the diameter growth course from increment cores. However, we are often faced with the difficulty that the pith of the tree was failed. We do not dispose of measured data of tree's diameter below the place where the first tree ring border is visible. However in many cases a circular arc of the first visible ring can be used to estimate the diameter of the inner part of the stem (Fig. 9).

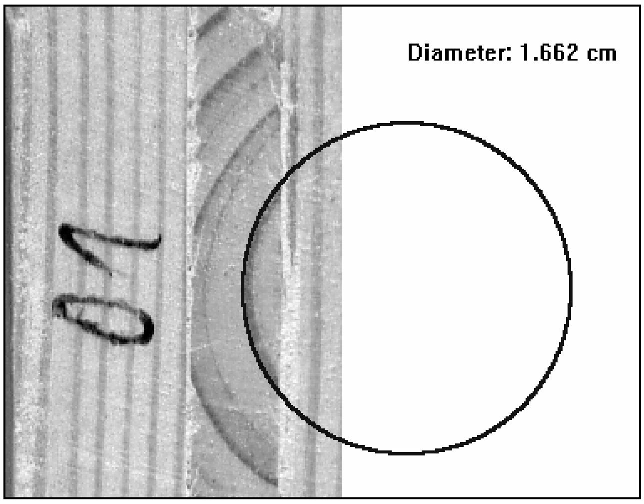

Figure 9: Determination of the inner portion of tree's diameter which was failed while coring; The inner part of the sanded core was scanned. Calculation of the inner diameter is done with the help of a computer program which uses geometrical and graphical methods.

This inner diameter (*ID*) can be used as initial value for the summation of all doubled ring widths to get the stem's diameter without bark. But even if the pith is hit, the summing up will never result in the exact diameter without bark of the tree. This is due to:

i. The shrinkage of the increment core while drying;
ii. The tree ring series obtained by the increment core is only one random realisation of the growth course of the tree. There are theoretically infinite places at breast height of a tree to take increment cores. The extraction of two increment cores in orthogonal position at breast height may not really represent the true shape of the cross section of the tree and therefore the estimation of the radial increment of the tree is hindered. It is strongly recommended to measure exact ring widths (rectangular, i.e. shortest, distances between adjacent ring borders).

The problem may easily be solved by following the assumption that the appropriateness of ring widths within time series is kept independent from the exact place of boring. The diameter of the stem without bark (DBH_{wB}) may be determined from measured values of diameter including bark and withdrawal of double bark thickness obtained from a suitable bark function. If the appropriateness of ring widths (*RW*) within time series is accepted as the most important criterion of growth behaviour, the absolute values may be transformed by correction factors (*CF*) very easily:

$$CF = \frac{DBH_{wB}}{ID + 2 \cdot \sum_{t=1}^{n} RW_t}.$$

In that way one can obtain the chronology of the corrected absolute diameter time series (Fig. 10).

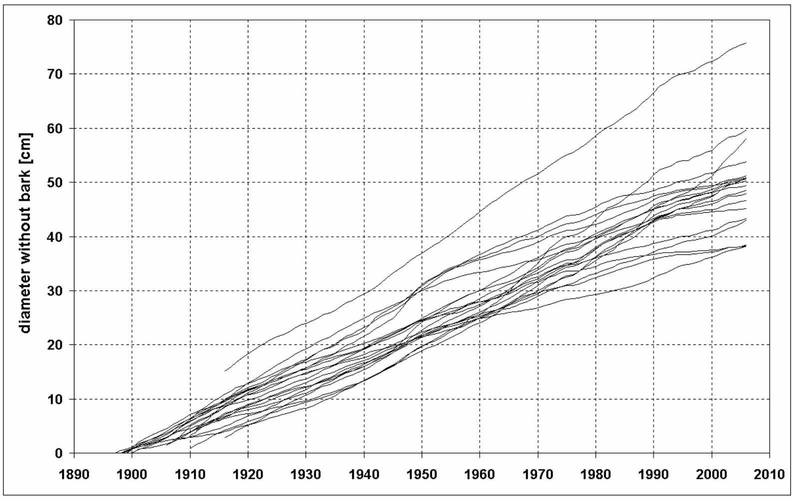

Figure 10: Absolute diameter growth courses of 20 dominant beeches. Identification of outliers concerning growth dynamics is hard to perform.

As an example for illustration of the methodical conclusions the chronology of Bornhoeved (common beech) is used again. By calculation of relative growth courses (all diameter values

DOI:10.2312/GFZ.b103-08056

of a time series are set relative to the final DBH at the end of the series) a better comparison between the series is enabled (Fig. 11).

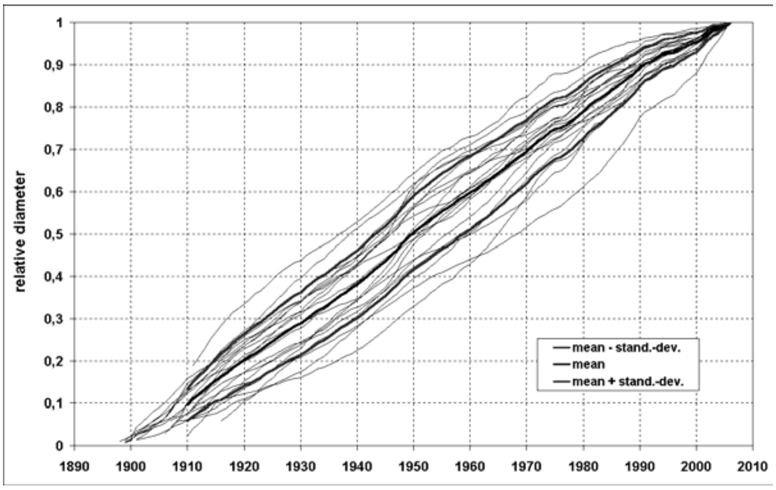

Figure 11: Relative growth courses of the 20 sample trees together with mean +/- standard deviation. Outliers concerning growth dynamics can easily be identified.

Evaluation of the similarities between the series and of the suitability of a individual series using the relation to the stand-typical pattern is eased by the comparison with the mean relative curve and the range between mean +/- standard deviation, respectively. So, outliers concerning stand-typical growth dynamics can be reliably identified and can be excluded from the calculation of the mean curve (Fig. 12).

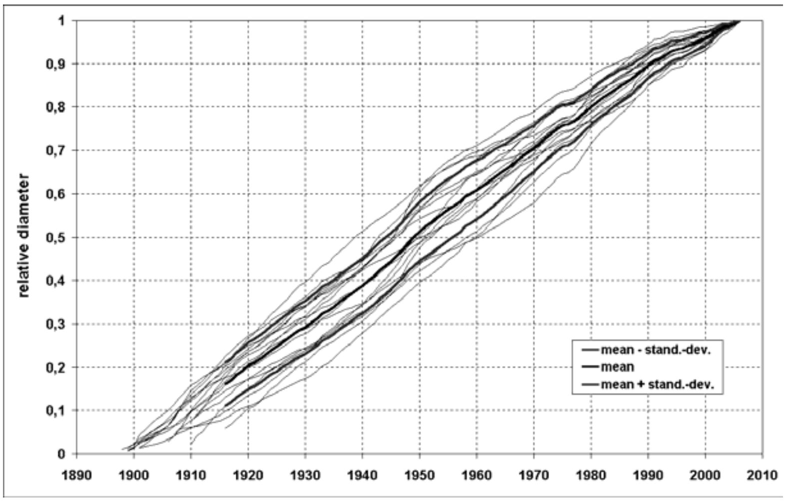

Figure 12: Relative growth courses of 17 sample trees together with mean +/- standard deviation. Sample trees 5, 7 and 19 were excluded as outliers. The stand-typical growth pattern emerges more clearly.

The plot of the included absolute diameter series of the chronology together with the identified outliers (sample trees 5, 7 and 19) shows that these series do not really fit to the common stand-typical growth pattern, especially after 1970 (fig. 13).

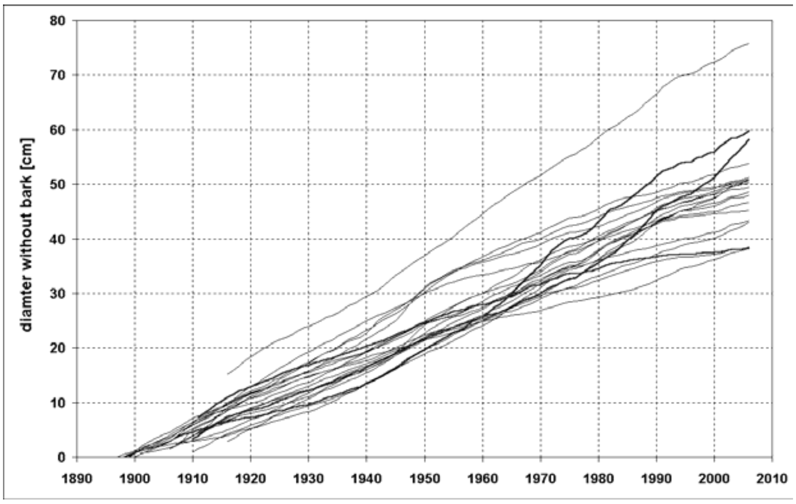

Figure 13: Absolute diameter growth of the included trees of the chronology together with the excluded sample trees 5, 7 and 19 (fat lines).

The remaining steps to get the mean index chronology are easily to perform. The time series of the mean relative diameter growth course forms the basis of the calculation. Mean absolute diameter of all included sample trees is obtained by the calculation of weighted means of the basal areas. Time series of mean diameter DBH_t may be obtained by multiplication of mean relative diameter course with mean absolute diameter. Time series of mean ring width has to be calculated as differences from mean absolute diameter course DBH_t.

$$RW_t = \frac{DBH_t - DBH_{t-1}}{2}\ .$$

Prewhitening, trend estimation, trend elimination and indexation may be done in one of the many known ways, according to the conviction, intention or taste of the dendro-colleague.

Summary

Beginning with the established method of mean index series calculation by Tukey' biweight robust mean, its disadvantages and inconsistency are discussed as well as two alternative procedures are presented.

Statistical analysis of the contribution of a individual series to the mean series and the decision upon its inclusion or exclusion from the mean calculation on the basis of entire series is proved to be an adequate procedure. The weighting of single series by their signal strength to calculate the mean index chronology (Neumann, 2001) seems to be more appropriate than the distance from the centre of the index-distribution at a certain year.

Derivation of the typical stand-wide diameter growth enables a comprehensive growth behaviour analysis. Central to the procedure is the calculation of relative diameter growth courses. By this transformation, outliers can be reliably discovered. From the mean diameter time series one can obtain transformed series of basal area, basal area increment and radial increment. These series may be verified and investigated in many directions such as homogeneity of growth course or structural breaks, autocorrelation of first and higher order, relations between sensitivity and autocorrelation, pointer year analysis and more. Back-

DOI:10.2312/GFZ.b103-08056

transformation to mean ring width series is done by differentiating of mean absolute diameter series. Derivation of mean index series from mean ring width series follows well known procedures which are in common use. All steps are based upon a unified data pool procedure.

References:

Neumann, U. (2001): Zusammenhang von Witterungsgeschehen und Zuwachsverläufen in Fichtenbeständen des Osterzgebirges. Verlag Eugen Ulmer, *Forstwissenschaftliche Beiträge Tharandt*, 193 p.

Weisstein, E. W. (©1999-2007): "Tukey's Biweight." From *MathWorld*--A Wolfram Web Resource. http://mathworld.wolfram.com/TukeysBiweight.html

List of participants

TRACE 2007 — Riga (Latvia) — 3rd – 6th May 2007

DIETER ANHUF
University of Passau, Innstr. 40, 94032 Passau, Germany
Email: anhuf@uni-passau.de

ANNETTE BÄR
Department of Geography, University of Bonn, Meckenheimer Allee 166, 53115 Bonn, Germany
Email: baer@giub.uni-bonn.de

ALEXANDER BAST
Swiss Federal Research Institute WSL, Zürcherstrasse 111, 8903 Birmensdorf, Switzerland
Email: a.bast@uni-wuerzburg.de

ANDREAS BAUEROCHSE
Lower Saxony State Service for Cultural Heritage, Scharnhorststraße 1, 30175 Hannover, Germany
Email: bauerochse@nld.niedersachsen.de

WOLFGANG BECK
Federal Research Centre for Forestry and Forest Products, Alfred-Möller-Straße 1, D-16225 Eberswalde, Germany
Email: wbeck@bfh-inst7.fh-eberswalde.de

ERICA BIGIO
Swiss Federal Research Institute WSL, Zürcherstrasse 111, 8903 Birmensdorf, Switzerland
Email: ericabigio@hotmail.com

SZYMON BIJAK
Department of Dendrometry and Forest Productivity, Faculty of Forestry, Warsaw Agriculture University, Nowoursynowska 159 bud. 34, 02-787 Warszawa, Poland
Email: Szymon.Bijak@wl.sggw.pl

NIELS BLEICHER
Römisch-Germanisches Zentralmuseum Mainz, Ernst-Ludwig Platz 2, 55116 Mainz, Germany
Email: bleicher@holzanalyse.de

STELLA MARYS BOGINO
University of Valladolid, Mayor 97. 3º “D” izquierdo, 34002 Palencia, Spain
Email: sbogino@pvs.uva.es

ANAÏS BOURA
Muséum National d'Histoire Naturelle, Département Histoire de la Terre UMR 5143 Paléobiodiversité et Paléoenvironnement Case Postale 38 Laboratoire de Paléobotanique, 75231 PARIS cedex 5, France
Email: boura@mnhn.fr

OTTO ULRICH BRÄKER
J. Zürrerstr. 9, CH-8915 Hausen a.a., Switzerland
Email: Otto.braeker@datazug.ch

ACHIM BRÄUNING
Institute of Geography, Kochstrasse 4/4, D-91054 Erlangen, Germany
Email: abraeuning@geographie.uni-erlangen.de

MINDAUGAS BRAZAUSKAS
Klaipeda University, Tilzes 13, Klaipeda, Lithuania
Email: vmbrazauskai@takas.lt

MATTHEW BROOKHOUSE
The Australian National University, 48 Linneaus Way, 0200 Canberra, Australia
Email: matthew.brookhouse@anu.edu.au

DOI:10.2312/GFZ.b103-08056

GUNTIS BRŪMELIS
University of Latvia, Faculty of Biology, Kronvalda bulv. 4, LV-1586 Rīga, Latvia
Email: guntis.brumelis@lu.lv

ULF BÜNTGEN
Swiss Federal Research Institute WSL, Zürcherstrasse 111, 8903 Birmensdorf, Switzerland
Email: buentgen@wsl.ch

IRIS BURCHARDT
Department of Geography, University of Erlangen, Kochstrasse 4/4, D-91054 Erlangen, Germany
Email: Iris.burchardt@gmx.de

ROCHELLE CAMPBELL
Swansea University, School of Society and Environment, Geography Department, Singleton Park, SA2 8PP Swansea, United Kingdom
Email: 371431@swansea.ac.uk

ANNA CEDRO
Szczecin University, Waska 13, 71-415 Szczecin, Poland
Email: Anna.Cedro@univ.szczecin.pl

MIREIA CELMA MARTÍNEZ
Universitat autònoma de Barcelona, Departament de Prehistòria, Edifici B, Campus de la UAB, 08193 Bellaterra (Cerdanyola Del Valles), Spain
Email: mireia_celma@hotmail.com

DUNCAN CHRISTIE
Laboratorio de Dendrocronología, Facultad de Ciencias Forestales, Universidad Austral de Chile, Casilla 567, Valdivia, Chile
Email: duncan@sendadarwin.cl

LUCÍA DE SOTO
Área de Botánica. Dpto. Ciencias Agroforestales. E.U.I. Agrarias de Soria, Universidad de Valladolid, Campus de los Pajaritos s/n, 42004 Soria, Spain
Email: luciadesoto@gmail.com

DETLEF DROSIHN
Albert-Ludwigs-University Freiburg, Institute for Forest Growth, Talbachstrasse 3, D-79761 Waldshut-Tiengen, Germany
Email: dedrosi@arcor.de

PHILIPP DUNCKER
Albert-Ludwigs-University Freiburg, Institute for Forest Growth, Talbachstrasse 3, D-79761 Waldshut-Tiengen, Germany
Email: Philipp.duncker@iww.uni-freiburg.de

JAN ECKSTEIN
Albrecht-von-Haller Institute, Dep. of Palynology and Climate Dynamics, Untere Karspuele 2, D-37073 Göttingen, Germany
Email: Jan.Eckstein@biologie.uni-goettingen.de

DIDZIS ELFERTS
University of Latvia, Faculty of Biology, Kronvalda bulv. 4, LV-1586 Rīga, Latvia
Email: didzis.elferts@lu.lv

JAN ESPER
Swiss Federal Research Institute WSL, Zürcherstrasse 111, 8903 Birmensdorf, Switzerland
Email: esper@wsl.ch

ZEXIN FAN
Institute of Geography, Erlangen-Nürnberg University, Kochstr. 4/4, D-90154 Erlangen, Germany
Email: fanzexin@yahoo.com.cn

DAGMAR FRIEDRICHS
Department of Geography, University of Bonn, Meckenheimer Allee 168, 53115 Bonn, Germany
Email: d.friedrichs@giub.uni-bonn.de

DOI:10.2312/GFZ.b103-08056

HOLGER GÄRTNER
Swiss Federal Research Institute WSL, Zürcherstrasse 111, 8903 Birmensdorf, Switzerland
Email: gaertner@wsl.ch

JOZICA GRICAR
Slovenian Forestry Institute, Vecna pot 2, 1000 Ljubljana, Slovenia
Email: jozica.gricar@gozdis.si

JUSSI GRIESSINGER
Friedrich-Alexander-University of Erlangen-Nuremberg, Department of Geography, Kochstrasse 4/4, D-91054 Erlangen, Germany
Email: jgriess@geographie.uni-erlangen.de

VLADIMÍR GRYC
Mendel University of Agriculture and Forestry Brno, Faculty of Forestry and Wood Technology, Department of Wood Science, Zemědělská 3, 613 00 Brno, Czech Republic
Email: gryc@mendelu.cz

BJÖRN GÜNTHER
University of Technology Dresden, Institute of Forest Utilization and Forest Technology, Chair of Forest Utilization, Pienner Straße 19, (Judeich-Bau, 0.09 – 0.11), D-01737 Tharandt, Germany
Email: Guenther.bjoern@gmx.de

ROMAN GUT
Swiss Federal Research Institute WSL, Zürcherstrasse 111, 8903 Birmensdorf, Switzerland
Email: r_gut@cevi.ch

SARAH HANGARTNER
University of Bern, Climate and Environmental Physics, Sidlerstrasse 6, 3012 Bern, Switzerland
Email: shangart@climate.unibe.ch

INGO HEINRICH
Research Centre Jülich, ICG, Wilhelm-Johnen-Str., 52425 Jülich, Germany
Email: i.heinrich@fz-juelich.de

RYSZARD J. KACZKA
University of Silesia, Bedzinska 60, 41-200 Sosnowiec, Poland
Email: kaczka@wnoz.us.edu.pl

RAGNAR KAPAUN
University of Tartu, Faculty of Biology and Geography, Institute of Geography, Kirde 1a-19, Elva, Estonia
Email: rk@ut.ee

JÜRGEN KÖNIG
University of Technology Dresden, Institute of Forest Utilization and Forest Technology, Chair of Forest Utilization, Pienner Straße 19, (Judeich-Bau, 0.09 – 0.11), D-01737 Tharandt, Germany
Email: koenig@forst.tu-dresden.de

MAREK KRĄPIEC
AGH University of Science and Technology, Al. Mickiewicza 30, 30-059 Cracow, Poland
Email: mkrapiec@geol.agh.edu.pl

KRISTEL KUND
University of Tartu, Institute of Geography, Vanemuise 46, 51014 Tartu, Estonia
Email: Krkund@ut.ee

TOMÁŠ KYNCL
DendroLab Brno, Eliášova 37, 616 00 Brno, Czech Republic
Email: kyncl@dendrochronologie.cz

ALAR LÄÄNELAID
University of Tartu, Institute of Geography, Vanemuise 46, 51014 Tartu, Estonia
Email: alar.laanelaid@ut.ee

DOI:10.2312/GFZ.b103-08056

BARBARA LEUSCHNER
DELAG-Dendrochronologisches Labor Göttingen, Rosdorfer Weg 10, 37073 Göttingen, Germany
Email: info@dendro-delag.de

HANNS HUBERT LEUSCHNER
Dep. Palynology and Climate Dynamics, Univ. Goettingen, Wilhelm-Weber-Str. 2, 37073 Göttingen, Germany
Email: hleusch@gwdg.de

TOM LEVANIČ
Slovenian Forestry Institute, Večna pot 2, SI-1000 Ljubljana, Slovenia
Email: Tom.levanic@gozdis.si

HANS LINDERHOLM
Department of Earth Sciences, Göteborg University, Box 460, SE 405 30 Göteborg, Sweden
Email: hansl@gvc.gu.se

ILUTA LŪCE
University of Latvia, Faculty of Biology, Kronvalda bulv. 4, LV-1586 Rīga, Latvia
Email: iluta@lanet.lv

IRENEUSZ MALIK
University of Silesia, Bedzinska 60, 41-200 Sosnowiec, Poland
Email: irekgeo@wp.pl

DARIO MARTIN BENITO
Dep. Sistemas y Recursos Forestales. CIFOR-INIA, Crta. La Coruña km 7.5, 28040 Madrid, Spain
Email: dmartin@inia.es

ROBERTS MATISONS
University of Latvia, Faculty of Biology, Kronvalda bulv. 4, LV-1586 Rīga, Latvia
Email: robism@inbox.lv

KARI MIELIKÄINEN
Finnish Forest Research Institute, Jokiniemenkuja 1, 01370 Vantaa, Finland
Email: kari.mielikainen@metla.fi

BURKHARD NEUWIRTH
Institute of Geography, University of Bonn, Meckenheimer Allee 166, 53115 Bonn, Germany
Email: b.neuwirth@giub.uni-bonn.de

KURT NICOLUSSI
Institute of Geography, University of Innsbruck, Innrain 52, 6020 Innsbruck, Austria
Email: Kurt.Nicolussi@uibk.ac.at

MAGDALENA OPALA
Faculty of Earth Science, University of Silesia, Bedzinska 60, 41-200 Sosnowiec, Poland
Email: magdaopala@hotmail.com

SŁAWOMIRA PAWEŁCZYK
Silesian University of technology, Institute of Physics, Krzywoustego 2, 44 –100 Gliwice, Poland
Email: Slawomira.Pawelczyk@polsl.pl

IONEL POPA
Forest research and management institute, Calea Bucovinei 73BIS, RO725100 Campulung Moldovenesc, Romania
Email: popa.ionel@suceava.astral.ro

EVA PŘEMYSLOVSKÁ
Mendel University of Agriculture and Forestry Brno, Faculty of Forestry and Wood Technology, Department of Wood Science, Zemědělská 3, 613 00 Brno, Czech Republic
Email: premyslo@mendelu.cz

RUTILE PŪKIENĖ
Vytautas Magnus University, Faculty of Natural Sciences, Environmental Research Centre, Z.E.Zilibero 6, LT-46324 Kaunas, Lithuania
Email: r.pukiene@gmf.vdu.lt

DOI:10.2312/GFZ.b103-08056

CHRISTINA REYNOLDS
Paul Scherrer Institut, Laboratory for Atmospheric Chemistry, 5232 Villigen PSI, Switzerland
Email: Christina.Reynolds@psi.ch

MICHAL RYBNÍČEK
Mendel University of Agriculture and Forestry Brno, Faculty of Forestry and Wood Technology, Department of Wood Science, Zemědělská 3, 613 00 Brno, Czech Republic
Email: michalryb@email.cz

INGO SAHLING
Martin-Luther-University Halle-Wittenberg, Institute of Geosciences, Von-Seckendorff-Platz, 6120 Halle, Germany
Email: ingo.sahling@geo.uni-halle.de

GERHARD SCHLESER
FZ Jülich, GFZ Potsdam, D-52425 Jülich, Germany
Email: g.schleser@fz-juelich.de

JOHANNES SCHULTZ
Institute of Geography, University of Bonn, Meckenheimer Allee 166, 53115 Bonn, Germany
Email: schultz@giub.uni-bonn.de

BARBARA SENSULA
Silesian University of Technology, Akademicka 2, 44100 Gliwice, Poland
Email: Barbara.Sensula@polsl.pl

KRISTINA SOHAR
Institute of Geography, University of Tartu, Vanemuise 46, 51014 Tartu, Estonia
Email: kriss8@ut.ee

HEINRICH SPIECKER
Institute for Forest Growth, Tennenbacherstr. 4, 79085 Freiburg, Germany
Email: instww@uni-freiburg.de

NICOLE SUTY
Swedish University of Agricultural Sciences, Dept of Forest Resource Management, 90183 Umeå, Sweden
Email: nicole.suty@resgeom.slu.se

ZANE STRIĶE
University of Latvia, Faculty of Biology, Kronvalda bulv. 4, LV-1586 Rīga, Latvia
Email: zane_strike@inbox.lv

ELISABETH SZYCHOWSKA-KRĄPIEC
AGH University of Science and Technology, Al. Mickiewicza 30, 30-059 Cracow, Poland
Email: szycha@geol.agh.edu.pl

LENKA ŠABATOVÁ
DendroLab Brno, Eliášova 37, 616 00 Brno, Czech Republic
Email: sabatova@brno.npu.cz

MAURI TIMONEN
Finnish Forest Research Institute, Eteläranta 55, 96300 Rovaniemi, Finland
Email: mauri.timonen@metla.fi

ROBERT TOMUSIAK
Faculty of Forestry, Warsaw Agricultural University, Nowoursynowska 159/34, 02-776 Warsaw, Poland
Email: rtomusiak@wl.sggw.pl

KERSTIN TREYDTE
Swiss Federal Research Institute WSL, Zürcherstrasse 111, 8903 Birmensdorf, Switzerland
Email: treydte@wsl.ch

VALERIE TROUET
Swiss Federal Research Institute WSL, Zürcherstrasse 111, 8903 Birmensdorf, Switzerland
Email: trouet@wsl.ch

DOI:10.2312/GFZ.b103-08056

VIVIAN UIBO
University of Tartu Institute of Geography, Vanemuise 46, 51014 Tartu, Estonia
Email: vivian_u@ut.ee

RIK VAN BOGAERT
Ghent University, Krijgslaan 281 S8, 9000 Gent, Belgium
Email: Rik.VanBogaert@UGent.be

HANUŠ VAVRČÍK
Mendel University of Agriculture and Forestry Brno, Faculty of Forestry and Wood Technology, Department of Wood Science, Zemědělská 3, 613 00 Brno, Czech Republic
Email: vavrcik@mendelu.cz

ADOMAS VITAS
Vytautas Magnus University Faculty of Nature Sciences Environmental Research Centre Group of Dendroclimatology and radiometrics, Ž.E. Žilibero 2, LT-46324 Kaunas, Lithuania
Email: a.vitas@gmf.vdu.lt

PETER VON SCHNAKENBURG
Institut für Geographie, Universität Erlangen-Nürnberg, Kochstraße 4/4, 91054 Erlangen, Germany
Email: pvons@web.de

PASCALE WEBER
Swiss Federal Research Institute WSL, Zürcherstrasse 111, 8903 Birmensdorf, Switzerland
Email: pascale.weber@wsl.ch

MARTIN WILMKING
Institute for Botany and Landscape Ecology, University Greifswald, Grimmer Strasse 88, 17487 Greifswald, Germany
Email: wilmking@uni-greifswald.de

VANESSA WINCHESTER
Oxford University Centre for the Environment, South Parks Road, OX1 3QY Oxford, United Kingdom
Email: vanessa.winchester@geog.ox.ac.uk

EWAN WOODLEY
University of Wales Swansea, Singleton Park, SA2 8PP Swansea, United Kingdom
Email: 292870@swan.ac.uk

MĀRIS ZUNDE
Institute of Latvian History at the University of Latvia, Akadēmijas laukums 1, LV-1050 Rīga, Latvia
Email: zunde@lanet.lv

DOI:10.2312/GFZ.b103-08056

Didzis Elferts

Didzis Elferts (1980) studied ecology (dendroecology) at the Faculty of Biology at University of Latvia in Latvia. His master thesis was about climate (temperature and precipitation) influence on the radial growth of Scots pine (Pinus sylvestris) in two territories in Latvia. Now he is working on his Ph.D. on the same theme in the dry forests of Western Latvia. Since 2002 he is working in Faculty of Biology (University of Latvia) – started as assistant in different scientific projects, then worked as ESF project manager, and now he is lecturer of biometry. His main research interests are influence of environmental factors (climate, water level) on the growth of trees and shrubs.

Prof. Dr. Guntis Brūmelis

Prof. Dr. Guntis Brūmelis (1957) studied Botany at the Department of Boatany at University of Toronto in Canada. His Master's thesis was on regeneration of post-logged wetland black spruce stands of the Greater Ontario Clay Belt. Further Doctoral studies were on the the ecophysiology of the feather moss Hylocomium splendens at the Faculty of Biology at the University of Latvia. The focus of current work is on the dendroecology of of natural forest stands to reconstruct past changes in stand structure. Academic duties are teaching ecology, from fundamental principles to multivariate methods of vegetation research, to students at the Faculty of Biology at the University of Latvia.

Dr. Holger Gärtner

Dr. Holger Gärtner (1965) studied Geography and Geology at the University of Heidelberg. At the end of the year 2000 he established the Laboratory of Dendrogeomorphology at the Department of Geosciences, Geography, University of Fribourg in Switzerland. In 2001 he finished his PhD on variations in annual growth rings of roots caused by exposure due to various geomorphic processes. Since 2002 he is working as a research scientist speciallized on wood anatomy and dendrogeomorphology at the Swiss Federal Research Institute WSL, Birmensdorf, Switzerland. He currently is the secretary of the Association of Tree-Ring Research.

Dr. Gerhard Helle

Dr. Gerhard Helle (1966) is head of the stable isotope dendroclimatology group at the Forschungszentrum Jülich GmbH. He studied Geology/Palaeontology at the University in Münster. After working as assistant lecturer at the Chair of Palaeontology he moved to the Forschungszentrum Jülich GmbH participating in the HGF-Strategy-Fonds-Project „KIHZ-Klima in historischen Zeiten bis 10.000 Jahre vor heute". He was co-ordinator of the young researchers network project "TRICE, Tree-Rings, Isotopes, Climate and Environment" funded by the German Federal Ministry for Education and Research (BMBF) within the German Climate Research Programme DEKLIM. Currently his research focuses on climate signal transfer from atmosphere into tree-rings and the related carbon and oxygen isotope transfer in the arboreal system. His special interests are in novel techniques necessary for high resolution intra-annual isotope investigations in tree-rings.

Prof. Dr. G.H. Schleser

Prof. Dr. G.H. Schleser was head of the Institute of Sedimentary Systems at the Forschungszentrum Jülich for many years and retired from this position in August 2005. He studied physics at the Universities of Cologne and Kiel. After three years with the Atomic Energy Establishment at Winfrith Heath, UK, he returned to Germany and received his PhD with distinction from the RWTH Aachen. He has over 25 years of experience in the application of stable isotopes in various fields. This includes work in tree rings, lacustrine sediments, as well as isotope investigations in peat bogs and soils. He participated in numerous projects funded by the EU and the German Science Foundation (DFG) and is Prof. at the University of Cologne where he is still lecturing.

DOI:10.2312/GFZ.b103-08056

Imprint
GeoForschungsZentrum Potsdam
a Helmholtz Centre
Telegrafenberg
D-14473 Potsdam

e-mail:postmaster@gfz-potsdam.de
www:http://www.gfz-potsdam.de

Printed in Potsdam, Germany
April 2008

ISSN 1610-0956

This text is available in electronic form:
http://www.gfz-potsdam.de/bib/zbstr.htm